

**UNDERSTANDING MOLECULAR AND THERMODYNAMIC MISCIBILITY  
OF CARBOHYDRATE BIOPOLYMERS**

by

**DİDEM İÇÖZ**

**A dissertation submitted to the  
Graduate School-New Brunswick  
Rutgers, The State University of New Jersey  
In partial fulfillment of the requirements**

**For the degree of**

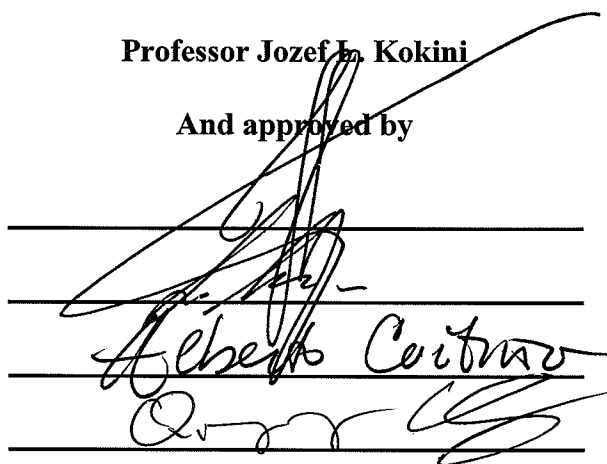
**Doctor of Philosophy**

**Graduate Program in Food Science**

**Written under the direction of**

**Professor Jozef M. Kokini**

**And approved by**



Albert C. Citron  
Jozef M. Kokini

**New Brunswick, New Jersey**

**May, 2008**

## **ABSTRACT OF THE DISSERTATION**

### **Understanding Molecular and Thermodynamic Miscibility of Carbohydrate Biopolymers**

**By DİDEM İÇÖZ**

**Dissertation Director:  
Jozef L. Kokini**

Most food materials are composed of polymeric molecules with different chemistry and properties. Increasing demand for food products with new/improved functionalities require formulations to include/exclude ingredients. Processability, texture, stability and palatability of the food products are greatly influenced by interactions and miscibility/immiscibility between these polymeric components. Molecular and thermodynamic basis of these phenomena are still not well understood and are the focus of scientific debate. A set of quantitative predictive rules are needed to be developed.

The major objective of this dissertation was to fundamentally understand the molecular and thermodynamic basis of miscibility and to develop quantitative miscibility predictions for carbohydrate mixtures. Dextrans (glucose polymers) with different molecular weights ( $M_w$ ) and chemically derivatized forms were used as model

carbohydrate polymers. Thermal analysis on individual and mixtures of standard dextrans showed that physical blend of dextrans was immiscible due to the diffusion barrier, whereas freeze-dried solution of these dextrans was miscible. In the mixtures of chemically derivatized dextrans, thermal analysis showed miscible or immiscible systems depending on the concentration and ionic strength through addition of salt. Systematic differences in the FTIR spectra of miscible systems with different component ratios were assigned to the change in hydrogen-bonding distribution resulting from changes in intra- and inter-molecular interactions, whereas FTIR spectra of immiscible systems didn't show such systematic changes, indicating insufficient hydrogen-bonding to form miscible systems.

In order to quantitatively predict miscibility, first, a methodology was developed to determine solubility parameters of dextrans with different  $M_w$  using their  $T_g$ . Using these solubility parameters, thermodynamic ideas based on the number of configurational arrangements and quantitative measures of dispersive interactions (Flory-Huggins theory) were demonstrated to be insufficient to quantitatively explain the miscibility in carbohydrate systems. This failure was due to the limitation of these ideas in underestimating the effect of specific bonding interactions, including hydrogen-bonds. A more advanced framework, Painter-Coleman association model, quantitatively demonstrated that hydrogen-bonding significantly contributed to predictive miscibility in carbohydrate systems. It was shown that with appropriate approximations it was possible to successfully predict miscibility in dextran systems. The quantitative understanding gained with dextrans was validated on real carbohydrate systems by testing miscibility/immiscibility in inulin-amylopectin systems.

## **ACKNOWLEDGEMENTS**

I would like to express my gratitude to my advisor, Dr. Jozef L. Kokini. He has been an extraordinary advisor throughout the years. He taught me how to come up with ideas that take the scientific knowledge in the field a step further to reach frontier and leading science. His motivation and confidence in me helped me to realize my capabilities to overcome challenges throughout my dissertation. I have also learned a great deal from his experiences and personality. With his patience and continuous support, I was able to find my way with my dissertation.

My thanks also go to my committee members; Drs. Paul Takhistov, Qingrong Huang, Alberto Cuitino and Jerry Scheinbeim for carefully reviewing and providing many valuable comments that improved the contents of this dissertation.

I am also grateful to Dr. Paul Painter from Department of Material Science and Engineering at The Pennsylvania State University for helping me to understand the association model and providing me the MG&PC software that I have used for this dissertation.

I would like to thank my colleagues; Dr. Carmen Moraru for her mentorship at the beginning of my PhD studies; Drs. Erhan Yildiz, Jeanny Zimeri, Robin Connelly to be role models of being great researchers in the lab during the early years of my study; Dr. Hulya Dogan, Bharani Ashokan, Monica Lau, Kiran Vyakaranam, Jigar Rathod, Maureen Evans, Ozlem Kaya, Jarupat Luecha for making the lab an enjoyable place to work through our relaxing conversations without whom surviving this experience would not be easy.

I wish to mention my appreciation to my parents, Emel-Necdet Zincirkiran for their endless support and encouragement during my entire education and finally during my Ph.D. even I had to be thousands of miles away from them for my studies. I would never be who I am without their love and advices. I also would like to thank my in-laws, Icoz's, for their continuous support and belief in me over the years.

Last but definitely not the least, I would like to express my gratitude to my dear husband Dr. Tunc Icoz for all his support throughout the years. He never stopped counseling me through my many emotional strains. I truly appreciate his understanding, patience and devotion to me. This dissertation would not be completed without his continuous moral support.

## **DEDICATION**

To my dear husband Dr. Tunç İçöz

## TABLE OF CONTENTS

<b>ABSTRACT.....</b>	<b>ii</b>
<b>ACKNOWLEDGEMENTS .....</b>	<b>iv</b>
<b>DEDICATION.....</b>	<b>vi</b>
<b>TABLE OF CONTENTS .....</b>	<b>vii</b>
<b>LIST OF TABLES .....</b>	<b>xii</b>
<b>LIST OF FIGURES .....</b>	<b>xiii</b>
<b>1. INTRODUCTION.....</b>	<b>1</b>
<b>1.1. Overview of the Research.....</b>	<b>1</b>
<b>1.2. Objectives of the Research .....</b>	<b>2</b>
<b>2. BACKGROUND .....</b>	<b>4</b>
<b>2.1. Thermodynamics of Mixing in Polymer Systems .....</b>	<b>4</b>
<b>2.2. Flory-Huggins Solution Theory.....</b>	<b>8</b>
2.2.1. Flory-Huggins Interaction Parameter .....	11
2.2.2. Hildebrand Solubility Parameter.....	12
<b>2.3. Painter-Coleman Association Model.....</b>	<b>15</b>
2.3.1. Determination of Non-Hydrogen Bonded Solubility Parameters.....	19
2.3.2. Stoichiometry of Hydrogen Bonding.....	20
2.3.3. Measurement of Hydrogen Bonding Parameters from Infrared Spectroscopy .....	25
2.3.3.1. Determination of Equilibrium Constants for Self-Associating Polymers Containing Hydroxyl Groups.....	25
2.3.3.2. Determination of Equilibrium Constants for Inter-Association.....	32
2.3.4. Determination of Free Energy of Mixing .....	37
2.3.5. Intra-molecular Screening Parameter .....	39
2.3.6. Applications of Painter-Coleman Association Model to Polymer Systems ..	42
<b>2.4. Phase Separation in Polymer Systems .....</b>	<b>46</b>
<b>2.5. Phase Transitions in Polymers.....</b>	<b>48</b>
2.5.1. Glass Transition Temperature ( $T_g$ ) .....	49

2.5.2. Factors Affecting Glass Transition of Polymers.....	50
2.5.2.1. Effect of Molecular Weight on Glass Transition.....	50
2.5.2.2. Effect of Plasticization on Glass Transition.....	52
2.5.2.3. Effect of Copolymerization on Glass Transition .....	55
2.5.2.4. Effect of Chemical Structure on Glass Transition .....	56
2.5.2.5. Effect of Crystallinity on Glass Transition .....	56
2.5.2.6. Effect of Other Factors on Glass Transition .....	57
<b>2.6. Miscibility/Phase Separation in Food Biopolymers.....</b>	<b>57</b>
<b>2.7. Effect of Ionic Strength on Charged Polymers' Miscibility/Immiscibility ...</b>	<b>59</b>
<b>2.8. Determination of Phase Behavior and Miscibility/Immiscibility of Polymers.....</b>	<b>63</b>
2.8.1. Glass Transition Temperature as a Marker of Miscibility in the Solid State determined by Differential Scanning Calorimetry.....	63
2.8.2. Fourier Transform Infrared Spectroscopy to Investigate Specific Bonding Interactions in Polymer Blends.....	66
<b>3. MATERIALS AND METHODS .....</b>	<b>72</b>
<b>3.1. Strategy of the Research.....</b>	<b>72</b>
<b>3.2. Investigation of Miscibility in Dextran Systems with Different <math>M_w</math>.....</b>	<b>76</b>
3.2.1. Materials .....	76
3.2.2. Moisture Sorption Isotherms of Dextrans.....	76
3.2.3. Sample Preparation for Thermal Analysis.....	78
3.2.3.1. Individual Dextrans.....	78
3.2.3.2. Dextran Mixtures .....	78
3.2.4. Measurement of Glass Transition Temperature ( $T_g$ ) by Differential Scanning Calorimetry (DSC).....	79
3.2.5. Steady Shear Rheological Measurements.....	80
<b>3.3. Investigation of the Specific Bonding Interactions and the Possible Mechanism of Miscibility in Dextran Systems .....</b>	<b>81</b>
3.3.1. Materials .....	81
3.3.2. Sample Preparation for DSC and FTIR Spectroscopy Measurements .....	82
3.3.3. Moisture Content of Samples.....	83



3.3.4. Methods of Analysis .....	83
3.3.4.1. Differential Scanning Calorimetry (DSC) .....	83
3.3.4.2. Fourier Transform Infrared (FTIR) Spectroscopy .....	83
<b>3.4. Quantitative Prediction of Miscibility in Carbohydrate Polymer Systems..</b>	<b>84</b>
3.4.1. Determination of Volume Fractions in Dextran Mixtures .....	84
3.4.2. Application of Original Flory-Huggins Theory to Predict Miscibility in Dextran Systems .....	85
3.4.2.1. Determination of Solubility Parameter of Monomeric Unit of Dextran..	85
3.4.2.2. A Predictive Methodology to Determine the Solubility Parameters of Dextrans with Different $M_w$ as a Function of Their Glass Transition Temperatures .....	86
3.4.2.3. Prediction of Thermodynamics of Mixing using Original Flory-Huggins Theory in Dextran Systems.....	94
3.4.3. Application of Painter-Coleman Association Model to Predict Miscibility in Dextran Systems .....	95
3.4.3.1. Approximations Allowing Utilization of the Painter-Coleman Association Model for Carbohydrate Polymers.....	95
3.4.3.2. Association Equilibrium Constants of Dextrans Approximated from Those of the Selected Analogue Compounds .....	98
3.4.3.3. Calculation of Non-hydrogen-bonded Solubility Parameters of Dextrans (Solubility Parameters that Exclude the Effect of Hydrogen Bonding) .....	103
3.4.3.4. Individual Enthalpic and Entropic Contributions of Hydrogen Bonding on Overall Free Energy of Hydrogen Bonding ( $\Delta G_H$ ).....	104
3.4.4. Validation of the Predictive Miscibility Approximations for Dextrans on ‘Real’ Carbohydrate Polymers: Testing Miscibility in Inulin/Amylopectin Systems .....	106
<b>4. RESULTS AND DISCUSSION .....</b>	<b>111</b>
<b>4.1. Investigation of Miscibility in Dextran Systems with Different <math>M_w</math>.....</b>	<b>111</b>
4.1.1. Moisture Sorption Properties of Individual Dextrans.....	111
4.1.2. Effect of $M_w$ on $T_g$ of Pure Dextrans .....	112

4.1.3. Influence of Mixture Preparation Method on Miscibility of Dextran Systems .....	116
4.1.4. Relationship between $T_g$ and Composition of Dextran Systems .....	124
<b>4.2. Investigation of the Specific Bonding Interactions and the Possible Mechanism of Miscibility in Dextran Systems .....</b>	<b>125</b>
4.2.1. Glass Transition Temperature ( $T_g$ ) of Derivatized Dextrans .....	125
4.2.2. Miscibility in Derivatized Dextrans Prepared from Different Polymer Concentrations and Added NaCl .....	127
4.2.3. FTIR Spectroscopy for Miscible/Immiscible Derivatized Dextrans to Probe Specific Bonding Interactions.....	133
<b>4.3. Quantitative Prediction of Miscibility in Carbohydrate Polymer Systems</b>	<b>139</b>
4.3.1. Examination of the Original Flory-Huggins Theory to Predict Miscibility in Dextran Systems .....	139
4.3.2. Application of Painter-Coleman Association Model to Predict Miscibility in Dextran Systems .....	145
4.3.2.1. Effect of Analogue Compound Selected to Approximate Hydrogen Bonding in Carbohydrates on Thermodynamic Calculations of Miscibility .....	146
4.3.2.2. Effect of Relative Values of Self-association and Inter-association Equilibrium Constants on Thermodynamic Calculations of Miscibility .....	153
4.3.2.3. Effect of Selection of the Self-associating Component in the System on Thermodynamic Calculations of Miscibility .....	158
4.3.2.4. Effect of Molecular Weight of Components on Thermodynamic Calculations of Miscibility.....	166
4.3.2.5. Effect of the Value of Intra-molecular Screening Parameter ( $\gamma$ ) on Thermodynamic Calculations of Miscibility .....	171
4.3.2.6. Individual Enthalpic and Entropic Contributions of Hydrogen Bonding on Overall Free Energy of Hydrogen Bonding ( $\Delta G_H$ ).....	180
4.3.3. Validation of the Predictive Miscibility Approximations for Dextrans on ‘Real’ Carbohydrate Polymers: Testing Miscibility in Inulin/Amylopectin Systems .....	186
<b>5. CONCLUSIONS .....</b>	<b>198</b>

<b>6. FUTURE WORK.....</b>	<b>202</b>
<b>APPENDIX A.....</b>	<b>204</b>
<b>APPENDIX B.....</b>	<b>213</b>
<b>APPENDIX C.....</b>	<b>216</b>
<b>APPENDIX D.....</b>	<b>222</b>
<b>APPENDIX E.....</b>	<b>231</b>
<b>APPENDIX F.....</b>	<b>233</b>
<b>REFERENCES.....</b>	<b>237</b>
<b>CURRICULUM VITA.....</b>	<b>248</b>

## LIST OF TABLES

Table 2.1: Molar attraction constants and molar volume of unassociated groups.....	21
Table 2.2: Molar attraction constants and molar volume of weakly associated groups ...	21
Table 3.1: Standard self-association equilibrium constants for hydrogen bond formation of OH group in pentanol, phenol and dimethylphenol .....	99
Table 3.2: Actual self- and inter-association equilibrium constants for hydrogen bond formation of dextran when approximated through hydrogen bond formation of pentanol OH, phenol OH and dimethylphenol OH .....	100
Table 3.3: Non-hydrogen bonded solubility parameters of dextrans with different molecular weights .....	103
Table 3.4: Enthalpy of individual B-B and A-B type hydrogen bond formation of dextran when approximated through hydrogen bonding of pentanol OH, phenol OH and dimethylphenol OH.....	105
Table 4.1: Quantitative glass transition temperature vs. molecular weight correlations for dextrans at various water activities .....	113
Table 4.2: Molecular size characteristics of the dextran blends obtained after solubilization.....	122
Table 4.3: $T_g$ of DS500 and DEAE systems prepared from 30%; 50%; and 70% polymer concentrations with added NaCl of IS=0; IS=1M; and IS=2M .....	128
Table 4.4: Moisture content (% d.b.) of DS500 and DEAE systems prepared from 30%; 50%; and 70% polymer concentrations with added NaCl of IS=0; IS=1M; and IS=2M .....	129

## LIST OF FIGURES

Figure 2.1: Free energy of mixing illustration for conditions of miscibility/immiscibility; (a) completely miscible systems over the entire composition range; (b) partially miscible systems.....	6
Figure 2.2: Illustration of three possible arrangements of different molecules in a volume; (a) Two types of small molecules; (b) A polymer and a small molecule; (c) Two types of polymers.....	7
Figure 2.3: Schematic representation of mixing two molecules of equal size using lattice model.....	8
Figure 2.4: Placement of a polymer on a lattice .....	9
Figure 2.5: Schematic representation of hydrogen bonded structures: (a) Self-association; (b) Inter-association .....	24
Figure 2.6: Schematic representation of self-association of phenol .....	26
Figure 2.7: Infrared spectra of hydroxyl stretching regions of 2-propanol in cyclohexane at 25°C for three different concentrations.....	27
Figure 2.8: Infrared spectra of hydroxyl stretching regions of 2-propanol in cyclohexane for 0.3M concentration at different temperatures .....	28
Figure 2.9: Structure of (a) Repeating unit of poly(hydroxyl ether of bis-phenol A), commonly referred as phenoxy; (b) 2-propanol .....	32
Figure 2.10: Schematic representation of inter-association in phenol/ethylpropionate mixtures.....	33
Figure 2.11: Infrared spectra of carbonyl stretching region of EPh/EIB mixtures of different compositions at 25°C .....	34
Figure 2.12: Structure of (a) Repeating unit of (a) poly(vinylphenol) (PVPh), (b) poly(ethyl methacrylate) (PEMA) .....	37
Figure 2.13: Schematics of intra-molecular screening in long-chain polymers .....	40

Figure 2.14: Fraction of free carbonyl groups in n-butyl methacrylate-co-vinyl phenol (BMAVPh) and styrene-co-2-vinyl pyridine (STVPy) blends as a function of volume fraction of BMAVPh at 150°C .....	43
Figure 2.15: Predicted free energy of mixing for PVPh and different poly(alkyl methacrylate) blends at 150°C using Painter-Coleman association model .....	44
Figure 2.16: Predicted second derivative of free energy of mixing for PVPh and different poly(alkyl methacrylate) blends at 150°C using Painter-Coleman association model .....	45
Figure 2.17: Molecular weight distribution of polymers showing different average molecular weights .....	51
Figure 2.18: A schematic example of the conformation of a polyelectrolyte at decreasing ionic strengths from (a) to (b) to (c).....	59
Figure 2.19: Effect of NaCl on the effective diameter of intra-molecular aggregates of poly(ethylene glycol)-based amphiphilic comb-like polymer at pH 6.2 at polymer concentration of 0.1 wt% .....	62
Figure 2.20: Determination of miscibility/immiscibility using DSC thermograms; (a) $T_g$ s of two individual components; (b) $T_g$ of miscible blend (1 $T_g$ between $T_g$ s of individual components); (c) $T_g$ s of immiscible blends (2 $T_g$ s in the mixture corresponding to $T_g$ s of individual components).....	64
Figure 2.21: DSC rescans of mixed inulin-waxy maize starch systems stored at $a_w=0.33$ for inulin to waxy maize starch ratio of; (a) 3:7; and (b) 6:4.....	65
Figure 2.22: DSC curve obtained with both 7S and 11S enriched soy globulin fractions.....	65
Figure 2.23: FTIR spectra of poly(4-vinylphenol):poly(vinyl acetate) blends; A) 80:20; B) 50:50; C) 20:80; D) 0:100.....	68
Figure 2.24: FTIR spectra for phenolic/PAS blends at room temperature in 1820-1680 $\text{cm}^{-1}$ .....	69
Figure 2.25: FTIR spectra for phenolic/PAS blends at room temperature in 4000-2700 $\text{cm}^{-1}$ .....	70
Figure 3.1: Schematic diagram of the strategy of the research.....	75
Figure 3.2: Molecular structure of dextran .....	77
Figure 3.3: Molecular structure of diethylaminoethyl dextran (DEAE).....	81

Figure 3.4: Molecular structure of dextran sulfate (DS500).....	82
Figure 3.5: Monomer (repeating unit) of dextran .....	85
Figure 3.6: Calculated volume fractions in the system of two dextrans with $M_w=1,000$ and $M_w=2,000,000$ as a function of % w/w ratio ( $m_B$ ) .....	85
Figure 3.7: Calculation of the solubility parameter for monomer of dextran .....	87
Figure 3.8: A second method for calculation of the solubility parameter for monomer of dextran.....	88
Figure 3.9: Variation of cohesive energy density (CED) as a function of number of methacrylate units in poly(methyl methacrylate) .....	91
Figure 3.10: Analogue compounds whose hydrogen bonding was approximated to the hydrogen bonding of dextrans (model carbohydrate polymers) (a) pentanol; (b) phenol; (c) dimethylphenol.....	97
Figure 3.11: Self- and inter-association equilibrium constants as a function of volume fraction for hydrogen bond formation of dextran when approximated through hydrogen bond formation of pentanol OH (a-b); phenol OH (c-d); and dimethylphenol OH (e-f) ( $\gamma=0.00$ for a-c-e; and $\gamma=0.30$ for b-d-f).....	102
Figure 3.12: Monomer (repeating unit) of inulin.....	108
Figure 4.1: Moisture sorption isotherms of pure dextrans with $M_w=970$ ; $M_w=10,800$ ; $M_w=43,000$ ; and $M_w=2,000,000$ .....	112
Figure 4.2: Effect of $M_w$ on $T_g$ of pure dextrans at different water activities.....	113
Figure 4.3: Zero-shear viscosity behavior for 20% and 40% dextran solutions with different molecular weights .....	114
Figure 4.4: Effect of molecular size of polystyrene, polybutadiene, polyisoprene and poly( $\alpha$ -methylstyrene) on glass transition temperature .....	115
Figure 4.5: Influence of mixture preparation method ( $M_w=970/M_w=2,000,000$ ) (50/50); (a) Physical blend of powder dextrans; (b) 30% concentrated, freeze-dried solution of dextrans .....	117
Figure 4.6: 3 <sup>rd</sup> DSC rescan of physical blend of dextran mixture of $M_w=970/M_w=2,000,000$ (50/50) .....	118

Figure 4.7: Thermal behavior of freeze-dried dextran solutions of $M_w=970/M_w=2,000,000$ (50/50): (a) 50% concentrated solutions; (b) 70% concentrated solutions .....	119
Figure 4.8: Conceptual model of the mixed dextran systems; (A) Without prior solubilization; (B) With prior solubilization.....	120
Figure 4.9: Effect of dextran with $M_w=970$ on the $T_g$ of 30% concentrated, freeze-dried solutions of dextran mixtures. The numbers indicate the $M_w=970/M_w=2,000,000$ ratio (w/w, d.b.).....	121
Figure 4.10: Effect of $M_n$ on $T_g$ of the 30% concentrated, freeze-dried solutions of dextran mixtures.....	123
Figure 4.11: Comparison of $T_g$ predictions by Couchman-Karas equation with experimental $T_g$ values for 30% concentrated, freeze-dried solutions of dextran mixtures .....	125
Figure 4.12: DSC thermograms of DEAE and DS500 prepared from 30% polymer concentrated solutions in the absence of NaCl [IS(NaCl)=0].....	127
Figure 4.13: Single $T_g$ in 50/50 ratio of DS500+DEAE prepared from 30% polymer concentrated solutions in the absence of NaCl [IS(NaCl)=0].....	130
Figure 4.14: Two $T_g$ s in 50/50 ratio of DS500+DEAE prepared from 30% polymer concentrated solutions with IS(NaCl)=1M .....	132
Figure 4.15: Hydroxyl stretching regions of FTIR spectra for DS500+DEAE blends prepared from 30% polymer concentration in the absence of NaCl [IS(NaCl)=0] .....	135
Figure 4.16: Schematics of possible hydrogen bonding between DS500 and DEAE ....	135
Figure 4.17: C-OH stretching region of FTIR spectra for DS500+DEAE blends prepared from 30% polymer concentration in the absence of NaCl [IS(NaCl)=0] .....	137
Figure 4.18: Hydroxyl stretching regions of FTIR spectra for DS500+DEAE blends prepared from 30% polymer concentration with IS(NaCl)=1M.....	138
Figure 4.19: C-OH stretching region of FTIR spectra for DS500+DEAE blends prepared from 30% polymer concentration with IS(NaCl)=1M.....	138
Figure 4.20: Flory-Huggins miscibility predictions for two dextrans with $M_w=1,000$ and $M_w=2,000,000$ at 25°C; (a) Free energy ( $\Delta G_{mix}$ ), enthalpy ( $\Delta H_{mix}$ ), and entropy ( $-T\Delta S_{mix}$ ) of mixing; (b) 2 <sup>nd</sup> derivative of free energy of mixing .....	142



Figure 4.21: Flory-Huggins miscibility predictions for two dextrans with  $M_w=1,000$  and  $M_w=2,000,000$  at  $25^\circ\text{C}$ ; (a) Free energy ( $\Delta G_{\text{mix}}$ ), enthalpy ( $\Delta H_{\text{mix}}$ ), and entropy ( $-T\Delta S_{\text{mix}}$ ) of mixing; (b)  $2^{\text{nd}}$  derivative of free energy of mixing ..... 143

Figure 4.22: Predicted miscibility of two dextrans with  $M_w=1,000$  and  $M_w=2,000,000$  at  $25^\circ\text{C}$  when H-bonding of pentanol OH was used to simulate H-bonding in dextrans; (a) Free energy of mixing; (b)  $2^{\text{nd}}$  derivative of free energy of mixing [ $\gamma=0.30$ ] ..... 148

Figure 4.23: Predicted miscibility of two dextrans with  $M_w=1,000$  and  $M_w=2,000,000$  at  $25^\circ\text{C}$  when H-bonding of phenol OH was used to simulate H-bonding in dextrans; (a) Free energy of mixing; (b)  $2^{\text{nd}}$  derivative of free energy of mixing [ $\gamma=0.30$ ] ..... 149

Figure 4.24: Predicted miscibility of two dextrans with  $M_w=1,000$  and  $M_w=2,000,000$  at  $25^\circ\text{C}$  when H-bonding of dimethylphenol OH was used to simulate H-bonding in dextrans; (a) Free energy of mixing; (b)  $2^{\text{nd}}$  derivative of free energy of mixing [ $\gamma=0.30$ ] ..... 150

Figure 4.25: Entropic, enthalpic, and H-bonding contributions to the total free energy of mixing two dextrans with  $M_w=1,000$  and  $M_w=2,000,000$  at  $25^\circ\text{C}$  when H-bonding of; (a) pentanol OH; (b) phenol OH; (c) dimethylphenol OH was used to simulate H-bonding in dextrans [ $\gamma=0.30$ ] ..... 152

Figure 4.26: Effect of the value of inter-association equilibrium constant ( $K_A$ ) relative to self-association equilibrium constants ( $K_2$  and  $K_B$ ) on; (a) H-bonding contribution; (b) total free energy of mixing two dextrans with  $M_w=1,000$  and  $M_w=2,000,000$  at  $25^\circ\text{C}$  [H-bonding of pentanol OH was approximated for H-bonding in dextrans; and  $\gamma=0.30$ ].... 155

Figure 4.27: Effect of the value of inter-association equilibrium constant ( $K_A$ ) relative to self-association equilibrium constants ( $K_2$  and  $K_B$ ) on; (a) H-bonding contribution; (b) total free energy of mixing two dextrans with  $M_w=1,000$  and  $M_w=2,000,000$  at  $25^\circ\text{C}$  [H-bonding of phenol OH was approximated for H-bonding in dextrans; and  $\gamma=0.30$ ] ..... 156

Figure 4.28: Effect of the value of inter-association equilibrium constant ( $K_A$ ) relative to self-association equilibrium constants ( $K_2$  and  $K_B$ ) on; (a) H-bonding contribution; (b) Total free energy of mixing two dextrans with  $M_w=1,000$  and  $M_w=2,000,000$  at  $25^\circ\text{C}$  [H-bonding of dimethylphenol OH was approximated for H-bonding in dextrans; and  $\gamma=0.30$ ] ..... 157

Figure 4.29: Predicted miscibility [ (a) free energy and (b)  $2^{\text{nd}}$  derivative of free energy of mixing ] of two dextrans with  $M_w=1,000$  and  $M_w=2,000,000$  at  $25^\circ\text{C}$  when dextran with  $M_w=2,000,000$  was selected as the self-associating component [H-bonding of pentanol OH was approximated for H-bonding in dextrans; and  $\gamma=0.30$ ] ..... 160

Figure 4.30: Predicted miscibility [ (a) free energy and (b)  $2^{\text{nd}}$  derivative of free energy of mixing ] of two dextrans with  $M_w=1,000$  and  $M_w=2,000,000$  at  $25^\circ\text{C}$  when dextran with

$M_w=2,000,000$  was selected as the self-associating component [H-bonding of phenol OH was approximated for H-bonding in dextrans; and  $\gamma=0.30$ ]..... 161

Figure 4.31: Predicted miscibility [ (a) free energy and (b) 2<sup>nd</sup> derivative of free energy of mixing) ] of two dextrans with  $M_w=1,000$  and  $M_w=2,000,000$  at 25°C when dextran with  $M_w=2,000,000$  was selected as the self-associating component [H-bonding of dimethylphenol OH was approximated for H-bonding in dextrans; and  $\gamma=0.30$ ]..... 162

Figure 4.32: Entropic, enthalpic, and H-bonding contributions to the total free energy of mixing two dextrans with  $M_w=1,000$  and  $M_w=2,000,000$  at 25°C when dextran with  $M_w=2,000,000$  was selected as the self-associating component [H-bonding of; (a) pentanol OH; (b) phenol OH; (c) dimethylphenol OH was approximated for H-bonding in dextrans; and  $\gamma=0.30$ ]..... 166

Figure 4.33: Effect of component molecular weight on entropic, enthalpic, and H-bonding contributions to the total free energy of mixing two dextrans at 25°C; Systems of (a)  $M_w=5,000$  and  $M_w=2,000,000$ ; (b)  $M_w=10,000$  and  $M_w=2,000,000$  [H-bonding of pentanol OH was approximated for H-bonding in dextrans; and  $\gamma=0.30$ ]..... 168

Figure 4.34: Effect of component molecular weight on entropic, enthalpic, and H-bonding contributions to the total free energy of mixing two dextrans at 25°C; Systems of (a)  $M_w=5,000$  and  $M_w=2,000,000$ ; (b)  $M_w=10,000$  and  $M_w=2,000,000$  [H-bonding of phenol OH was approximated for H-bonding in dextrans; and  $\gamma=0.30$ ]..... 169

Figure 4.35: Effect of component molecular weight on entropic, enthalpic, and H-bonding contributions to the total free energy of mixing two dextrans at 25°C; Systems of (a)  $M_w=5,000$  and  $M_w=2,000,000$ ; (b)  $M_w=10,000$  and  $M_w=2,000,000$  [H-bonding of dimethylphenol OH was approximated for H-bonding in dextrans; and  $\gamma=0.30$ ]..... 170

Figure 4.36: Predicted miscibility [ (a) Free energy of mixing; (b) 2<sup>nd</sup> derivative of free energy of mixing) ] of two dextrans with  $M_w=1,000$  and  $M_w=2,000,000$  at 25°C when  $\gamma=0.00$  [H-bonding of pentanol OH was approximated for H-bonding in dextrans]..... 173

Figure 4.37: Predicted miscibility [ (a) Free energy of mixing; (b) 2<sup>nd</sup> derivative of free energy of mixing) ] of two dextrans with  $M_w=1,000$  and  $M_w=2,000,000$  at 25°C when  $\gamma=0.00$  [H-bonding of phenol OH was approximated for H-bonding in dextrans]..... 174

Figure 4.38: Predicted miscibility [ (a) Free energy of mixing; (b) 2<sup>nd</sup> derivative of free energy of mixing) ] of two dextrans with  $M_w=1,000$  and  $M_w=2,000,000$  at 25°C when  $\gamma=0.00$  [H-bonding of dimethylphenol OH was approximated for H-bonding in dextrans]..... 175

Figure 4.39: Entropic, enthalpic, and H-bonding contributions to the total free energy of mixing two dextrans with  $M_w=1,000$  and  $M_w=2,000,000$  at 25°C when  $\gamma=0.00$  [H-

bonding of; (a) pentanol OH; (b) phenol OH; (c) dimethylphenol OH was approximated for H-bonding in dextrans]..... 177

Figure 4.40: Entropic, enthalpic, and H-bonding contributions to the total free energy of mixing two dextrans with  $M_w=1,000$  and  $M_w=2,000,000$  at  $25^\circ\text{C}$  when; (a)  $\gamma=0.50$ ; (b)  $\gamma=0.70$ ; (c)  $\gamma=0.90$  [H-bonding of pentanol OH was approximated for H-bonding in dextrans]..... 179

Figure 4.41: Individual contributions to the overall free energy of mixing, including enthalpy and entropy of H-bonding when (a) pentanol OH; (b) phenol OH; (c) dimethylphenol OH was used as the model analogue compound for H-bonding in dextran systems of  $M_w=1,000+M_w=2,000,000$  at  $25^\circ\text{C}$  [ $\gamma=0.30$ ] ..... 181

Figure 4.42: Enthalpy and entropy of H-bonding; and overall free energy of H-bonding when (a) pentanol OH; (b) phenol OH; (c) dimethylphenol OH was used as the model analogue compound for H-bonding in dextran systems of  $M_w=1,000+M_w=2,000,000$  at  $25^\circ\text{C}$  [ $\gamma=0.30$ ]..... 183

Figure 4.43: Comparison of; (a) enthalpy of H-bonding; (b) entropy of H-bonding; (c) overall free energy of H-bonding between pentanol OH, phenol OH and dimethylphenol OH as model analogues for H-bonding in dextran systems of  $M_w=1,000+M_w=2,000,000$  at  $25^\circ\text{C}$  [ $\gamma=0.30$ ]..... 186

Figure 4.44: Predicted miscibility of inulin and amylopectin at  $25^\circ\text{C}$  when H-bonding of pentanol OH was approximated for H-bonding in carbohydrates; (a) Entropic, enthalpic, and H-bonding contributions to the total free energy of mixing; (b)  $2^{\text{nd}}$  derivative of free energy of mixing [ $\gamma=0.30$ ] ..... 189

Figure 4.45: DSC rescans of mixed inulin-amylopectin systems stored at  $a_w = 0.33$  for inulin to amylopectin ratio of; (a) 30:70; and (b) 60:40 (% , d.b.) ..... 190

Figure 4.46: Two glass transition temperatures in mixed samples containing inulin to amylopectin ratio of (a) 30:70 and (b) 60:40 (% , d.b.) ..... 191

Figure 4.47: Predicted miscibility of inulin and amylopectin at  $25^\circ\text{C}$  when H-bonding of (a-b) phenol OH; (c-d) dimethylphenol OH was approximated for H-bonding in carbohydrates [ (a-c) Entropic, enthalpic, and H-bonding contributions to the total free energy of mixing; (b-d)  $2^{\text{nd}}$  derivative of free energy of mixing; and  $\gamma=0.30$  ] ..... 193

Figure 4.48: Predicted miscibility [ (a) Entropic, enthalpic, and H-bonding contributions to the total free energy of mixing; (b)  $2^{\text{nd}}$  derivative of free energy of mixing) ] of inulin and amylopectin at  $25^\circ\text{C}$  when amylopectin was selected as the self-associating component [H-bonding of pentanol OH was approximated for H-bonding in carbohydrates; and  $\gamma=0.30$ ] ..... 194

Figure 4.49: Predicted miscibility [ (a) Entropic, enthalpic, and H-bonding contributions to the total free energy of mixing and (b) 2<sup>nd</sup> derivative of free energy of mixing ] of inulin and amylopectin at 25°C when  $\gamma=0.00$  [H-bonding of pentanol OH was approximated for H-bonding in carbohydrates]..... 195

Figure 4.50: Effect of the value of inter-association equilibrium constant ( $K_A$ ) relative to self-association equilibrium constants ( $K_2$  and  $K_B$ ) on; (a) H-bonding contribution; (b) Total free energy of mixing; (c) 2<sup>nd</sup> derivative of free energy of mixing inulin and amylopectin at 25°C [H-bonding of pentanol OH was approximated for H-bonding in carbohydrates; and  $\gamma=0.30$ ]..... 197

Figure A.E: Screen snapshot of the software..... 232

## 1. INTRODUCTION

### 1.1. Overview of the Research

Food materials are composed of multiple polymer molecules with different chemistry and properties, such as carbohydrates, proteins and lipids. Increasing demand for new food formulations, with reduced carbohydrate or fat content and added nutraceutical compounds to deliver healthier foods, require formulating food products to include or exclude various ingredients. The alternate ingredients with new and improved functionalities to satisfy the consumer should successfully replace commonly used ingredients. Ingredient compatibility (or incompatibility) is critical to control the processability, texture, palatability and stability of the final new and improved food products. There is a need to understand conditions that favor miscibility/compatibility of food biopolymers with each other in order to deliver successful food applications. Developing *a priori* thermodynamic rules for molecular miscibility will enable prediction of how a set of selected ingredients will result in the stability needed in the final food products, which in turn affects quality as well.

Molecular incompatibility in carbohydrate-protein systems manifests itself in phase separation. This is mainly due to the molecular size and hydrophilicity/hydrophobicity differences resulting from very different macromolecular chemistry, molecular conformation and affinity for water (Tolstoguzov, 1991, 1998, 2000b, 2003; Michon et al., 1995; Grinberg and Tolstoguzov, 1997; Moraru et al., 2002). Incompatibility and immiscibility also occurs in carbohydrate-carbohydrate mixtures

(Kalichevsky and Ring, 1987; German et al., 1992; Garnier et al., 1995; Ahmad and Williams, 2001; Zimeri and Kokini, 2002, 2003a, 2003b, 2003c). Most of the existing studies refer to mixtures of carbohydrates with significant differences in chemical structure and composition. The molecular and thermodynamic bases of these phenomena are still not well understood and are the focus of scientific debate. *A set of quantitative predictive rules need to be developed to help the field.*

## **1.2. Objectives of the Research**

The overall objective of this dissertation is to fundamentally understand the molecular and thermodynamic basis for miscibility in carbohydrate polymers. It is hypothesized that the fundamental understanding of the interactions between polymeric molecules and development of quantitative predictive rules using advanced thermodynamic models would be a step forward in helping to choose which ingredients in a food formulation would form the desired miscible/immiscible systems on a predictive basis. This would speed up ingredient replacement strategies and overall product development process. This dissertation focuses on the following specific objectives:

- The role of method of preparation, molecular size and incremental changes in chemical structure on the boundaries of molecular miscibility was investigated using dextran systems of different molecular weights and chemically derivatized forms as structurally compatible model systems for food carbohydrate polymers.

- Quantitative predictions for molecular miscibility in dextran systems were developed starting from the chemical structure of the molecules utilizing an advanced theoretical thermodynamic model for the mixing of polymer blends.

- The quantitative understanding gained with dextrans was then validated on a real carbohydrate system by testing miscibility/immiscibility in inulin/amylopectin systems.

## 2. BACKGROUND

### 2.1. Thermodynamics of Mixing in Polymer Systems

The first condition for miscibility of one component in another is obtaining a negative change in the free energy of mixing (Equation 2.1) (Coleman et al., 1991; Painter and Coleman, 1997; Sperling, 2001; Coleman and Painter, 2006), where the change in free energy of mixing is related to enthalpic and entropic contributions (Equation 2.2).

$$\Delta G_{\text{mix}} < 0 \quad (2.1)$$

$$\Delta G_{\text{mix}} = \Delta H_{\text{mix}} - T \cdot \Delta S_{\text{mix}} \quad (2.2)$$

$\Delta G_{\text{mix}}$  is the Gibbs' free energy of mixing;  $\Delta H_{\text{mix}}$  is the enthalpy of mixing;  $\Delta S_{\text{mix}}$  is the entropy of mixing; and  $T$  is the absolute temperature. A negative value of  $\Delta G_{\text{mix}}$  shows that the solution process is spontaneous.  $\Delta S_{\text{mix}}$  arises from the number of possible configurations of solute in solution (also called combinatorial entropy) (Painter and Coleman, 1997).  $\Delta S_{\text{mix}}$  is always positive since entropy increases upon mixing, due to increase in randomness. Therefore, the sign of  $\Delta G_{\text{mix}}$  depends on the magnitude and sign of  $\Delta H_{\text{mix}}$  (Sperling, 2001), which arises mainly from the dispersive interactions between the monomeric units (Painter and Coleman, 1997).

The second condition required for miscibility is to have a positive second derivative of  $\Delta G_{\text{mix}}$  (Coleman et al., 1991; Coleman and Painter, 2006) as;

$$\frac{\partial^2 \Delta G_{\text{mix}}}{\partial \Phi_A^2} > 0 \quad (2.3)$$



If the negative valued  $\Delta G_{\text{mix}}$  as a function of composition plots are concave upwards for all compositions (Figure 2.1a), then the components of the mixture are miscible in all proportions. Any point on this curve shown in Figure 2.1a (for example; point Q) has lower free energy than any two phase system of the same overall composition. In a hypothetical phase separated mixture shown by points  $P_1$  and  $P_2$ , the sum of their composition weighted free energy is given by  $Q^*$  and  $Q^*$  has a higher free energy than a miscible mixture, Q (Coleman et al., 1991). These types of plots give positive second derivative of  $\Delta G_{\text{mix}}$  over the entire composition range. On the other hand, if the negative valued  $\Delta G_{\text{mix}}$  vs. composition plots show portions that are concave downwards (Figure 2.1b), then the blend components are not miscible in that specific composition range although the  $\Delta G_{\text{mix}}$  is negative (Coleman et al., 1991). The free energy of the phase separated system with compositions  $B_1$  and  $B_2$ , which are the contact of double tangent to the free energy curve, is lower (Figure 2.1b). The portions of the free energy curve between  $B_1$  and the point of reflection,  $S_1$ , and similarly between  $B_2$  and  $S_2$ , are still concave upward. This means that mixtures with the compositions between these points are stable against phase separation, but not stable against phase separation at compositions  $B_1$  and  $B_2$  (Figure 2.1b). These are called metastable mixtures. In Figure 2.1b, the free energy curve between  $S_1$  and  $S_2$  are concave downwards, they are unstable and phase separation is spontaneous (Coleman et al., 1991). As a summary, it is important to consider both the  $\Delta G_{\text{mix}}$  and the second derivative of  $\Delta G_{\text{mix}}$  to decide if the blend components are miscible or not.

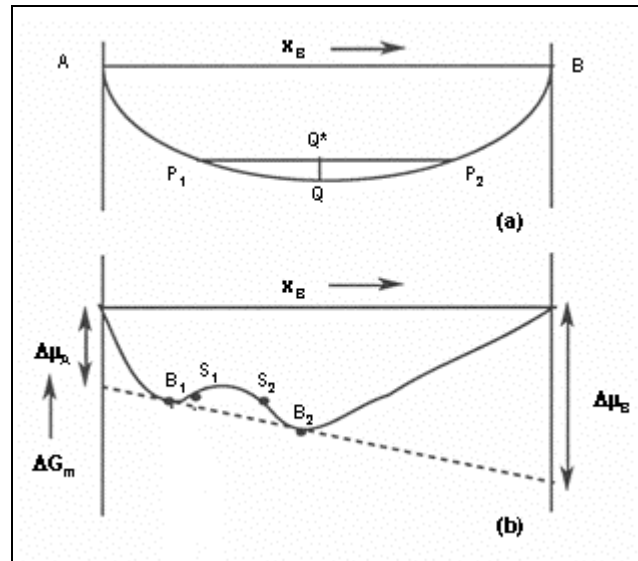


Figure 2.1: Free energy of mixing illustration for conditions of miscibility/immiscibility; (a) completely miscible systems over the entire composition range; (b) partially miscible systems (Coleman et al., 1991)

When two types of small molecules are considered in a mixture (Figure 2.2a), the molecules can rearrange themselves in the available volume in many ways. Therefore, the randomness in the system and the entropy of mixing is very high. When one of the small molecules is replaced with a polymer molecule (Figure 2.2b), the number of configurational arrangements becomes more limited; the randomness in the system and entropy of mixing decreases significantly, as compared to the system of two small molecules. Furthermore, if there are two types of polymers present in the system (Figure 2.2c), then the order in the system increases, the randomness and entropy of mixing decreases even more (Sperling, 2001).

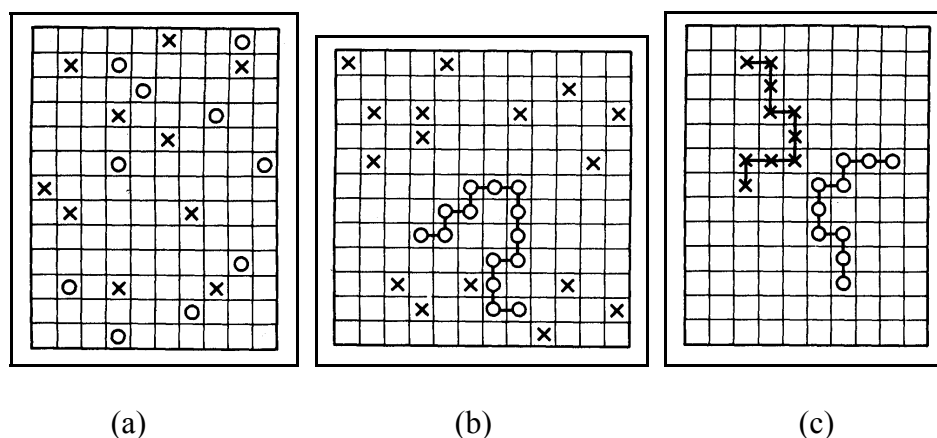


Figure 2.2: Illustration of three possible arrangements of different molecules in a volume; (a) Two types of small molecules; (b) A polymer and a small molecule; (c) Two types of polymers (Sperling, 2001)

In statistical thermodynamics of mixing, entropy of mixing can be determined by obtaining a quantitative measure of the number of possible arrangements of the molecules in the system (Sperling, 2001). A simple method for counting the possible configurations is the use of a lattice model. In the lattice model, the molecules are placed on a lattice as black and white balls, as shown in Figure 2.3 (Painter and Coleman, 1997). A simplification in the lattice model is to assume that the energy of interactions between any molecules is an average energy over all possible configurations. This simplification is called mean field approximation. Each molecule is assumed to move in a potential field, experiencing intermolecular forces, which is unaffected by local variation in composition, so it is an average over all possible configurations (Painter and Coleman, 1997). In other words, random mixing is assumed and this assumption is valid as long as the interactions between the molecules are weak, so the motion due to thermal energy keeps the system random (Painter and Coleman, 1997).

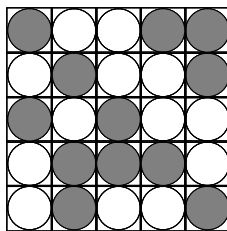


Figure 2.3: Schematic representation of mixing two molecules of equal size using lattice model

## 2.2. Flory-Huggins Solution Theory

The simplest thermodynamic equation for mixing polymer systems is given by the Flory-Huggins solution theory (Flory, 1952). The Flory-Huggins theory is a lattice model derived for small molecules and it assumes that each molecule occupies one site on the lattice (Figure 2.3). The theory assumes random distribution of the segments (Flory, 1952; Painter and Coleman, 1997; Viswanathan and Dadmun, 2002). This assumption may not hold when there are strong polar forces or specific interactions such as hydrogen bonding, between the components of the blends due to the fact that strong intermolecular interactions limit the mobility of the chains and force the chains into non-random configurations (Coleman et al., 1991; Viswanathan and Dadmun, 2002). The theory also assumes no free volume in the system (all lattice sites are occupied) and the volume change upon mixing is negligible (Flory, 1952; Painter and Coleman, 1997).

The original Flory-Huggins theory is expanded for polymer systems, assuming that the polymer is a flexible chain composed of a series of connected monomers (repeating units) and each monomer occupies one lattice site, which is also equal in size (volume) to a solvent molecule (Painter and Coleman, 1997; Madkour, 2001; Patnaik and

Pachter, 2002). Accordingly, the polymer is placed on the lattice as shown in Figure 2.4, occupying lattice sites next to each other.

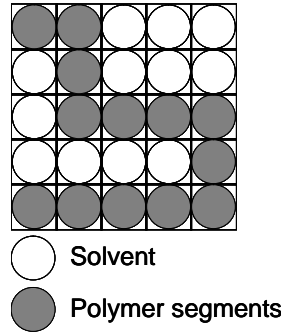


Figure 2.4: Placement of a polymer on a lattice

The general expression of Flory-Huggins theory for free energy of mixing (applicable both for polymer-solvent and polymer-polymer systems) is given as;

$$\left[ \frac{\Delta G_{\text{mix}}}{R.T} \right]^* \left[ \frac{V_r}{V} \right] = \frac{\Phi_A}{M_A} \cdot \ln \Phi_A + \frac{\Phi_B}{M_B} \cdot \ln \Phi_B + \chi_{AB} \cdot \Phi_A \cdot \Phi_B \quad (2.4)$$

where  $\Phi$  is the volume fraction of each component;  $M$  is the number of polymerized segments;  $\chi$  is the Flory-Huggins interaction parameter;  $V_r$  is the reference volume;  $V$  is the total molar volume of the system; and subscripts A and B refer to the two components in the mixture (Painter and Coleman, 1997; Madkour, 2001; Kuo and Chang, 2002; Patnaik and Pachter, 2002; Viswanathan and Dadmun, 2002). Equation 2.4 can also be written in terms of free energy of mixing per mole of lattice sites, paying attention to the reference volume, as;

$$\left[ \frac{\Delta G_{\text{mix}}}{R.T} \right] = \frac{\Phi_A}{M_A} \cdot \ln \Phi_A + \frac{\Phi_B}{M_B} \cdot \ln \Phi_B + \chi_{AB} \cdot \Phi_A \cdot \Phi_B \quad (2.5)$$

The first two terms on the right-hand side in Equation 2.5 corresponds to the combinatorial entropy contribution, which is always negative, since the natural logarithm of volume fraction (a number smaller than 1) is always negative. These terms are always favorable, but in polymer mixtures (i.e. large values of  $M$ ) are usually very small. The third term on the right-hand side of Equation 2.5 corresponds to the enthalpy of mixing representing physical forces between the components (Painter and Coleman, 1997; Madkour, 2001; Sperling, 2001; Kuo and Chang, 2002; Patnaik and Pachter, 2002; Viswanathan and Dadmun, 2002). It should be noted that the free energy of mixing described in Equation 2.5 is written for a system that has two components. For instance, in a systems of three components, Equation 2.5 should include the respective terms for the entropic contribution of the third component and the non-specific interactions between 1<sup>st</sup> and 3<sup>rd</sup>, and 2<sup>nd</sup> and 3<sup>rd</sup> components.

The selection of the reference volume,  $V_r$ , on a lattice, which in general corresponds to the volume of each lattice site, is critical, as it is a determinant factor for the selection of  $M$  in Equation 2.5. If components A and B are small molecules of equal size, then  $V_r = V_A = V_B$  and  $M_A = M_B = 1$ . If component A is a solvent and component B is a polymer, then  $V_r = V_A$ , where  $V_A$  is the volume of the solvent that is equal to the volume of each polymer segment. In this case,  $M_A = 1$  and  $M_B \gg 1$ . If both components A and B are polymers, then  $V_r$  is chosen as the volume of the monomeric unit of one of the components and  $M_A$  and  $M_B$  will be large (Painter and Coleman, 1997).

Volume fractions ( $\Phi$ ) in Equation 2.5 are defined as;

$$\Phi_A = \frac{n_A \cdot M_A}{n_A \cdot M_A + n_B \cdot M_B}, \quad \Phi_B = \frac{n_B \cdot M_B}{n_A \cdot M_A + n_B \cdot M_B} \quad (2.6)$$

where  $n_A$  and  $n_B$  are the moles of polymers in the mixture;  $M_A$  and  $M_B$  are the number of segments in each polymer chain (Painter and Coleman, 1997). Since  $\Phi$  is the volume fraction of components,  $\Phi_A + \Phi_B = 1$ .

### 2.2.1. Flory-Huggins Interaction Parameter

A key term that needs attention in Equation 2.5 is the Flory-Huggins interaction parameter ( $\chi$ ) (Flory, 1952).  $\chi$  is used to characterize interactions in mixtures of small molecules, in polymer solutions (polymer-solvent systems) and polymer blends (polymer-polymer systems). It is a dimensionless number and is related to Hildebrand's widely used solubility parameters ( $\delta$ ) (Hildebrand and Scott, 1950) as;

$$\chi_{AB} = \frac{V_r}{R.T} (\delta_A - \delta_B)^2 \quad (2.7)$$

where  $V_r$  is the reference volume;  $\delta_A$  and  $\delta_B$  are the solubility parameters of each component;  $R$  is the universal gas constant; and  $T$  is the absolute temperature. Equation 2.7 has been shown not to work well for the polymer-solvent systems. The comparison of theoretical calculations and experimental results for various polymer solutions suggests that adding a fudge factor of 0.34 (sometimes called the lattice constant of entropic origin associated with free volume) to the right hand side of Equation 2.7 is more appropriate (Painter and Coleman, 1997; Sperling, 2001). The most likely origin of this correction term lay in the so-called free volume effects that are neglected by Flory-Huggins theory. In the liquid state, the motion and vibrations of the molecules leads to density fluctuations, leading to free volume. The free volume associated with a low molecular weight liquid is usually larger than that of a polymer, so that in mixtures of a polymer and

a solvent there is a mismatch of free volumes. This leads to the additional fudge factor added to Equation 2.7. Since  $\chi$  is proportional to the square of the difference between the solubility parameters of the blend components  $[(\delta_A - \delta_B)^2]$ , enthalpy term in Equation 2.5 is always positive, opposing mixing, resulting in phase separation in many cases (Coleman et al., 1991; Madkour, 2001; Kuo and Chang, 2002; Viswanathan and Dadmun, 2002).

### 2.2.2. Hildebrand Solubility Parameter

Solubility parameter of a material with physical, dispersive interactions (Hildebrand and Scott, 1950) is defined as;

$$\delta = \left( \frac{E_{\text{coh}}}{V_m} \right)^{1/2} \quad (2.8)$$

where  $E_{\text{coh}}$  is the energy of vaporization at zero pressure, known as the cohesive energy; and  $V_m$  is the molar volume. Cohesive energy corresponds to the total attractive forces in a condensed state material. Molecules that are highly attracted to one another have high cohesion and high solubility parameters; and materials that have high solubility parameters require more energy for dispersion than materials with low solubility parameters (Olabisi et al., 1979).

Cohesive energy per molar volume ( $E_{\text{coh}}/V_m$ ) is called the cohesive energy density (CED) and it is related to the energy required to break all intermolecular physical links in the unit volume (Greenhalgh et al., 1999). When two components have similar CED values, they are likely to be soluble in each other as the interactions in one component would be similar to those in the other component. The overall energy needed to facilitate



mixing of the components would be small, because the energy required to break the interactions within the components would be equally compensated by the energy released due to formation of interactions between unlike molecules (Greenhalgh et al., 1999). Moreover, two materials with very similar CED values approximately makes the enthalpy term in Equation 2.5 zero, minimizing the opposing effect to mixing.

Solubility parameters ( $\delta$ ) of polymers can not be directly determined from their energy of vaporization, because polymers can not be evaporated by heating as they decompose below their theoretical vaporization temperature. One way of determining solubility parameter of a polymer is through predictions using group contribution methods based on the chemical structure of the monomeric unit of the polymer (Van Krevelen and Hoftyzer, 1976; Coleman et al., 1991; Painter and Coleman, 1997; Sperling, 2001). The cohesive energies and molar volumes of chemical groups that conform the molecule are additive and  $\delta$  can be calculated as;

$$\delta = \left( \frac{\sum E_{\text{coh}}}{\sum V_{\text{m}}} \right)^{1/2} \quad (2.9)$$

following Equation 2.8, where  $\sum E_{\text{coh}}$  is the sum of the cohesive energies; and  $\sum V_{\text{m}}$  is the sum of the molar volumes of all chemical groups in the structure of the monomeric unit. It should be noted that calculation of  $\delta$  using Equation 2.9 give the overall cohesive energy in the materials and do not give specific information on the relative strengths of the forces in a system, such as hydrogen bonding (Greenhalgh et al., 1999).

A refined approach to determine solubility parameters for polymers where cohesive energy is dependent not only on the dispersion forces but also on interactions between polar groups and on hydrogen bonding is to divide  $\delta$  into its dispersive ( $\delta_{\text{d}}$ ),

polar ( $\delta_p$ ) and hydrogen bonding ( $\delta_h$ ) contributions and calculated as (Van Krevelen and Hoftyzer, 1976);

$$\delta^2 = \delta_d^2 + \delta_p^2 + \delta_h^2 \quad (2.10)$$

where

$$\delta_d = \frac{\sum F_{di}}{V_m}, \quad \delta_p = \frac{(\sum F_{pi}^2)^{1/2}}{V_m}, \quad \delta_h = \left( \frac{\sum E_{hi}}{V_m} \right)^{1/2} \quad (2.11)$$

However, it should be noted that the interaction of different structural groups in producing overall polar and hydrogen-bonding properties is very complicated that it does not obey simple predictive rules, as presented in Equations 2.10-2.11. So, this refined approach of determining solubility parameters still provides very rough estimates for structures with polar or hydrogen bonding capabilities. Moreover, the available data for  $F_{di}$ ,  $F_{pi}$  and  $E_{hi}$  (Equation 2.11) for calculation of Equation 2.10 is very limited for different atomic groups compared to the  $E_{coh}$  in Equation 2.9 (Van Krevelen and Hoftyzer, 1976).

A limitation of determining solubility parameter of a polymer using either Equation 2.9 or Equation 2.10 is that the calculation of  $\delta$  based on the chemical groups on the monomeric unit of the polymer does not take into account the effect of molecular weight ( $M_w$ ) and chain conformation, including branching and linkages between monomer units (Olabisi et al., 1979; Patnaik and Pachter, 2002), which are important factors for solubility of one polymer in a solvent or for miscibility with another polymer. For example, according to  $\delta$  calculation using Equation 2.9 or Equation 2.10, two polymers with different  $M_w$  (i.e. a glucose polymer with small or large  $M_w$ ) or two polymers that are composed of only one type of monomers (i.e. amylose and

amylopectin) would be predicted to have the exact same solubility parameters. More accurate predictions of solubility parameters for polymers should take these factors into account which would provide better miscibility predictions in polymer blends.

### **2.3. Painter-Coleman Association Model**

The major assumption of the original Flory-Huggins theory is that the two polymers mix randomly. However, this assumption does not hold when there are strong polar forces or specific interactions, such as hydrogen bonding, between the components of the blends (Coleman and Painter, 1995; Painter and Coleman, 1997; Viswanathan and Dadmun, 2002). The hydrogen bonded species (intra- or inter-molecular) is not random, so the enthalpic term in Equation 2.5 would take a much more complex composition dependence than its simple form in Equation 2.5 ( $\Phi_A \cdot \Phi_B \cdot \chi_{AB}$ ). Moreover, the formation of hydrogen bonds would bring favorable change in enthalpy, but also impose constraints on orientational and translational degrees of freedom which affect the entropy change on mixing (Coleman et al., 1991; Coleman and Painter, 1995, 2006; Viswanathan and Dadmun, 2002).

The extent of inter-molecular hydrogen bonding between two polymers depends on many parameters. If one or both of the polymers have intra-molecular hydrogen bonding in pure state, also called “self-association”, then the number of possible inter-molecular hydrogen bonding will be limited (Viswanathan and Dadmun, 2002). Another important factor is that a flexible chain can bend back upon itself to avoid inter-molecular interactions, called intra-molecular screening (Painter et al., 1997a, 1997b; Coleman et al., 1999; Viswanathan and Dadmun, 2002). The accessibility of the functional groups

that can form inter-molecular interactions is another determinant factor for the extent of the inter-molecular hydrogen bonding. For instance, increasing spacing between functional groups on a chain increases the amount of inter-molecular hydrogen bonding, where the optimum spacing is system dependent (Coleman et al., 1996; Viswanathan and Dadmun, 2002). Steric crowding of hydrogen-bonded groups, due to limited spacing between the functional groups, also affects the extent of inter-molecular interactions between the polymer chains (Pehlert et al., 1998; Viswanathan and Dadmun, 2002).

Painter-Coleman group (Coleman et al., 1991; Coleman and Painter, 1995, 2006) have developed an association model approach for the thermodynamics of mixing of two polymers that have strong hydrogen bonding capabilities and suggested adding a free energy of hydrogen bond formation term into the Flory-Huggins expression in Equation 2.5 as;

$$\frac{\Delta G_{\text{mix}}}{R.T} = \frac{\Phi_A}{M_A} \cdot \ln \Phi_A + \frac{\Phi_B}{M_B} \cdot \ln \Phi_B + \chi_{AB} \cdot \Phi_A \cdot \Phi_B + \frac{\Delta G_H}{R.T} \quad (2.12)$$

where  $\Delta G_H$  is a free energy term that imposes the constraints due to hydrogen bonding and represents chemical forces that have favorable, negative valued contribution to the free energy of mixing. According to the association model, non-specific interactions should be handled by solubility parameters calculated from groups contributions that are designed to exclude the association effects and the effect of specific interactions, such as hydrogen bonds, are only included in  $\Delta G_H$  term (Coleman et al., 1991; Coleman and Painter, 1995).

In Equation 2.12, the first two terms in the right-hand side  $[(\Phi_A / M_A) \cdot \ln \Phi_A + (\Phi_B / M_B) \cdot \ln \Phi_B]$  represents the combinatorial entropy, which have

favorable negative contribution to the free energy of mixing because logarithms of fractions are always negative; however this is a very small contribution for high molecular weight polymer blends (Coleman et al., 1991; Coleman and Painter, 1995). Therefore, in very high molecular weight polymer blends, miscibility would depend on the balance between the contributions from the third and fourth terms in Equation 2.12. The third term in Equation 2.12  $[\chi_{AB} \cdot \Phi_A \cdot \Phi_B]$  represents the weak, dispersive forces which have unfavorable positive contribution to the free energy of mixing since it is calculated using the square of the difference of the solubility parameters of the components in the mixture. One important point is that the solubility parameters in Painter-Coleman association model are to be calculated in a way to exclude contributions from strong interactions because strong interactions are handled in the last term of Equation 2.12. The main reason for separating the contributions from weak and strong interactions is mainly due to the fact that these interactions have different composition and temperature dependencies (Coleman et al., 1991; Coleman and Painter, 1995). The last term in Equation 2.12  $[\Delta G_H / R.T]$  represents the chemical forces, which would provide favorable negative contribution to the free energy of mixing.

The most extensively studied mixtures in the Painter-Coleman association model are mixtures where the first component self-associates (i.e. has functional groups, such as  $-OH$ , that can form hydrogen bonds with one another in the pure state), while the second component does not self-associate, but has a functional group that can form hydrogen bonds with the first component. When a self-associating polymer is mixed with a non-self-associating polymer, free energy can be gained from the balance between breaking hydrogen bonds between “like” molecules and forming hydrogen bonds between “unlike”

ones (Coleman et al., 1991). Painter-Coleman model assumes that there will be a negative contribution from hydrogen bonding, because the effect of H-bonds on the miscibility of two polymers with hydrogen bonding capabilities arises from the possible specific inter-molecular interactions between components. If the two polymers can make hydrogen bonds with each other, there is a very good chance that they will form miscible blends, although it does not guarantee that a miscible system will form, because free energy of mixing also depends on enthalpy and entropy of mixing. But as will be discussed later, inter-association is not the only factor that determines the hydrogen bonding contribution, because self-association of one of the polymers also results in competition for the available H-bonding sites and the overall hydrogen bonding contribution depends of the inter-association vs. self-association.

Hydrogen bonds are in a dynamic equilibrium state and exist as distribution of non-hydrogen-bonded ('free') and hydrogen-bonded species at any instant at a given temperature (Coleman and Painter, 1995). Accordingly, the free energy of hydrogen bond formation in the mixture can be described as;

$$\frac{\Delta G_H^*}{R.T} = n_A \ln \frac{\Phi_{A_l}}{\Phi_A} + n_B \ln \frac{\Phi_{B_l}}{\Phi_B} + n_{BB}^h + n_{AB}^h \quad (2.13)$$

where  $n_A$ ,  $n_B$  are the number of A and B type segments;  $\Phi_{A_l}/\Phi_A$ ,  $\Phi_{B_l}/\Phi_B$  are the fractions of 'free' (non-hydrogen-bonded) A and B segments; and  $n_{BB}^h$ ,  $n_{AB}^h$  are the number of B--B and A--B hydrogen bonds, respectively. This equation only contains terms that describe the free energy of hydrogen bonded species with one another when A and B are mixed. Similar equations for the free energy of hydrogen bonding in the pure component ( $\Delta G_H^0/RT$ ) is needed to be subtracted from Equation 2.13 to get the final contribution of hydrogen bonding to the free energy of mixing ( $\Delta G_H/RT$ ). This other

equation will only contain the terms of B in pure state. Then, the overall contribution of hydrogen bonding will depend on the balance between breaking/forming of hydrogen bonds in the pure B and in the mixture of A and B. In other words, it would not be practical to make comments on the sign of free energy of hydrogen bonding term without knowing the balance between breaking/forming of hydrogen bonds in the pure B and in the mixture of A and B. The fraction of ‘free’ and hydrogen-bonded groups is determined as a function of self- and inter-association equilibrium constants that are determined through systematically designed infrared spectroscopy measurements (Coleman et al., 1991; Coleman and Painter, 1995, 2006).

One significant factor that affects the magnitude of  $\Delta G_H$  is the relative magnitudes of self-association vs. inter-association. In general, if inter-association between two different components is more favorable than self-association within the pure components, then this trend is favorable for miscibility. The magnitude of  $\Delta G_H$  also depends on the number of specific interaction sites per unit volume of the blend. For example, if the number of specific interaction sites per unit volume is decreased in a system, this would result in lower  $\Delta G_H$  in the system compared to the original state (Coleman et al., 1991; Coleman and Painter, 1995).

### 2.3.1. Determination of Non-Hydrogen Bonded Solubility Parameters

According to the Painter-Coleman association model, only dispersive forces (forces pushing the two polymers apart, which is unfavorable for obtaining a miscible blend) should be included in  $\chi_{AB} \cdot \Phi_A \cdot \Phi_B$  term of Equation 2.12 as the effect of any specific interactions (particularly hydrogen bonding) are included in  $\Delta G_H / R.T$  term of

Equation 2.12 (Coleman et al., 1991; Coleman and Painter, 1995). Solubility parameters can be determined from group contributions in a similar way to Equation 2.9 and Equation 2.10 as;

$$\delta = \frac{\sum F_i}{V} \quad (2.14)$$

where  $F$  is the molar attraction constants; and  $V$  is the molar volume of the molecule. Painter-Coleman group (Coleman et al., 1990) has chosen 210 specific compounds that contain no known groups that strongly self-associate in order to determine the molar attraction constants that exclude hydrogen bonding effects. Table 2.1 and Table 2.2 show the molar attraction constants and molar volume of different groups that do not self-associate and that can weakly associate, respectively. As a summary, the third term on the right-hand side of Equation 2.12 is calculated from solubility parameters excluding the effect of specific interactions between components and still has unfavorable, positive valued contribution to the free energy of mixing because it is calculated from the square of the difference between the solubility parameters of the components as in Equation 2.7.

### 2.3.2. Stoichiometry of Hydrogen Bonding

According to the definition by Pauling (1960), a hydrogen bond is formed under certain circumstances, where a hydrogen atom that is already bonded to an atom is attracted to another atom by rather strong forces (eg. —O—H---O—H). The strength of a hydrogen bond is of the order of 1-10 kcal/mole, whereas that of a covalent bond is 50 kcal/mole and that of the dispersive forces (Van der Waals) is 0.2 kcal/mole (Coleman et al., 1991).



Table 2.1: Molar attraction constants and molar volume of unassociated groups (Coleman et al., 1991)

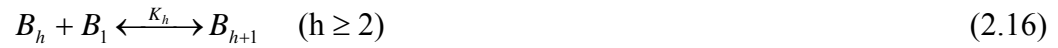
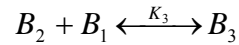
GROUP	V (cm <sup>3</sup> /mole)	F (cal.cm <sup>3</sup> ) <sup>0.5</sup> /mole
-CH <sub>3</sub>	31.8	218
-CH <sub>2</sub> -	16.5	132
>CH-	1.9	23
>CH<	-14.5	-97
C <sub>6</sub> H <sub>3</sub>	41.4	562
C <sub>6</sub> H <sub>4</sub>	58.8	652
C <sub>6</sub> H <sub>5</sub>	75.5	735
CH <sub>2</sub> =	29.7	203
-CH=	13.7	113
>C=	-2.4	18
-OCO-	19.6	298
-CO-	10.7	262
-O-	5.1	95
>N-	-5.0	-3

Table 2.2: Molar attraction constants and molar volume of weakly associated groups (Coleman et al., 1991)

GROUP	V (cm <sup>3</sup> /mole)	F (cal.cm <sup>3</sup> ) <sup>0.5</sup> /mole
-Cl	23.9	264
-CN	23.6	426
-NH <sub>2</sub>	18.6	275
>NH	8.5	143

A simple example to illustrate the Painter-Coleman association model is to consider that one of the components is a small, non-polymeric molecule with only one functional group capable of hydrogen bonding. This molecule labeled as 'B' can self-associate in the pure state through hydrogen bonding (Figure 2.5a). The monomer (repeating unit) of B molecules is represented by B<sub>1</sub>. Two monomers of B form a dimer,

which is represented by  $B_2$ , where  $K_2$  is the equilibrium constant describing formation of dimers (Equation 2.15).  $B_2$  and another  $B_1$  form a trimer ( $B_3$ ), and  $K_3$  is the equilibrium constant describing formation of trimer (Equation 2.16). Similarly,  $B_h$  is the  $h^{\text{th}}$  order multimer of B molecules ( $h$  monomers forming a  $h$ -mer), where  $K_h$  is the equilibrium constant describing formation of  $h$ -mers (Equation 2.16) (Coleman et al., 1991; Coleman and Painter, 1995). At equilibrium, the formation of dimer and subsequent multimer (trimer,...,h-mer) formation is written as;



$K_2$  and subsequent multimer formation equilibrium constants ( $K_3, \dots, K_h$ ) are given as;

$$K_2 = \frac{\Phi_{B_2}}{2 \cdot \Phi_{B_1}^2} \quad (2.17)$$

$$K_3 = \frac{\Phi_{B_3}}{\Phi_{B_2} \cdot \Phi_{B_1}} \cdot \frac{2}{3}$$



$$K_h = \frac{\Phi_{B_{h+1}}}{\Phi_{B_h} \cdot \Phi_{B_1}} \cdot \frac{h}{h+1} \quad (2.18)$$

where  $\Phi_{B_1}$  is the volume fraction of monomers (non-hydrogen bonded groups);  $h$  is the number of mers (monomers);  $\Phi_{B_2}$ ,  $\Phi_{B_3}$ ,  $\Phi_{B_h}$  and  $\Phi_{B_{h+1}}$  are the volume fractions of the

chains with 2, 3, h and h+1 mers, respectively. It has been shown that for molecules that self-associate, the equilibrium constant describing the dimer formation ( $K_2$ ) should be different from that describing subsequent h-mer formation ( $K_3, \dots, K_h$ ). However, subsequent multimer formation can be represented by one equilibrium constant,  $K_B$  ( $K_3 = \dots = K_h = K_B$ ). As a result only two equilibrium constants describing self-association is sufficient to describe the overall self-association of molecules with hydroxyl groups,  $K_2$  and  $K_B$  (Coleman et al., 1991; Coleman and Painter, 1995).

Molecules of ‘B’ are mixed with molecules of ‘A’, where ‘A’ is also non-polymeric and do not self-associate in pure state, but has a functional group that is an “acceptor” for the proton “donor” of the OH group in molecule ‘B’ (Figure 2.5b) (Coleman et al., 1991; Coleman and Painter, 1995). At equilibrium;



where  $A_1$  is the monomer of A that has the functional group that can make hydrogen bond with B molecules;  $B_h A$  represents the inter-associated B and A molecules; and  $K_A$  is the equilibrium constant of inter-association, which is given as;

$$K_A = \frac{\Phi_{B_h A}}{\Phi_{B_h} \cdot \Phi_{A_1}} \cdot \frac{h \cdot r}{h + r} \quad (2.20)$$

where  $\Phi_{A_1}$  is the volume fraction of ‘A’ molecules that are not hydrogen bonded;  $\Phi_{B_h A}$  is the volume fraction of inter-associated molecules; and r is the ratio of molar volume of molecules ‘A’ to ‘B’ ( $V_A/V_B$ ). The system is assumed to be incompressible so that the complications by equation of state effects are neglected (Coleman et al., 1991; Coleman and Painter, 1995).

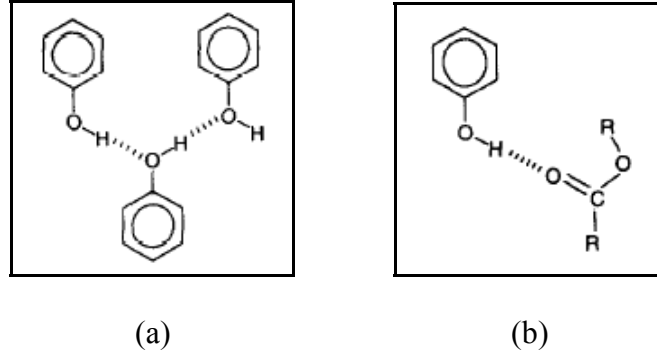


Figure 2.5: Schematic representation of hydrogen bonded structures: (a) Self-association; (b) Inter-association (Coleman and Painter, 1995)

The total volume fraction of all ‘B’ units (self-associating molecule) ( $\Phi_B$ ) is (Coleman et al., 1991);

$$\Phi_B = \Phi_{B1} + \sum_{h=2}^{\infty} \Phi_{Bh} + \sum_{h=1}^{\infty} \Phi_{BhA} \cdot \left( \frac{h}{h+r} \right) \quad (2.21)$$

Using the stoichiometric relationships obtained from materials balance for the formation of dimers, and multimers;

$$\sum_{h=2}^{\infty} \Phi_{Bh} = -\frac{K_2}{K_B} \cdot \Phi_{B1} + \frac{K_2}{K_B} \cdot \Phi_{B1} \cdot \left[ \frac{1}{(1 - K_B \cdot \Phi_{B1})^2} \right] \quad (2.22)$$

and

$$\sum_{h=1}^{\infty} \Phi_{BhA} \cdot \left( \frac{h}{h+r} \right) = \frac{K_A \cdot \Phi_{A1}}{r} \cdot \left[ \Phi_{B1} + \sum_{h=2}^{\infty} \Phi_{Bh} \right] \quad (2.23)$$

Substituting Equation 2.22 and Equation 2.23 into Equation 2.21 results in (Coleman et al., 1991);

$$\Phi_B = \Phi_{B1} \cdot \left[ \left( 1 - \frac{K_2}{K_B} \right) + \frac{K_2}{K_B} \cdot \left( \frac{1}{(1 - K_B \cdot \Phi_{B1})^2} \right) \right] \cdot \left[ 1 + \frac{K_A \cdot \Phi_{A1}}{r} \right] \quad (2.24)$$

Similarly, the total volume fraction for ‘A’ units ( $\Phi_A$ ) is (Coleman et al., 1991);

$$\Phi_A = \Phi_{A1} + \sum_{h=1}^{\infty} \Phi_{BhA} \cdot \left( \frac{r}{h+r} \right) \quad (2.25)$$

and making the necessary substitutions, Equation 2.26 can be obtained (Coleman et al., 1991).

$$\Phi_A = \Phi_{A1} + K_A \cdot \Phi_{A1} \cdot \Phi_{B1} \cdot \left[ \left( 1 - \frac{K_2}{K_B} \right) + \frac{K_2}{K_B} \cdot \left( \frac{1}{(1 - K_B \cdot \Phi_{B1})} \right) \right] \quad (2.26)$$

### 2.3.3. Measurement of Hydrogen Bonding Parameters from Infrared Spectroscopy

#### 2.3.3.1. Determination of Equilibrium Constants for Self-Associating Polymers Containing Hydroxyl Groups

Molecules containing hydroxyl groups, such as phenol, can self-associate in the condensed state through formation of hydrogen bonds between hydroxyl groups forming dimers and higher multimers (Figure 2.6). Hydrogen bonds are dynamic in nature, so they continuously break and reform by the thermal motion. At any instant, there exists a number of free (non-hydrogen bonded) monomers, hydrogen bonded dimers and multimers (Coleman et al., 1991; Coleman and Painter, 1995).

Changes in temperature and concentration are two factors that affect the distribution of monomers, dimers and multimers. As an example, Figure 2.7 and Figure 2.8 show infrared spectra of the hydroxyl stretching region of 2-propanol in cyclohexane, at 25°C for three different concentrations and at different temperatures for 0.3M, respectively. 2-propanol is a low molecular weight molecule that can self-associate. Cyclohexane is an inert solvent that does not interact favorably through strong dipole/dipole interactions or hydrogen bonds (Coleman and Painter, 1995), which means that there is only self-association of 2-propanol in this system and there isn't any inter-

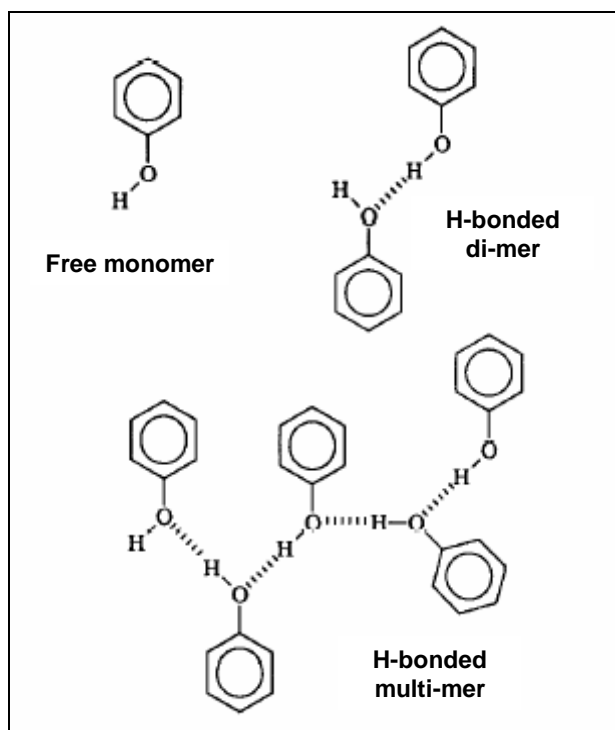


Figure 2.6: Schematic representation of self-association of phenol (Coleman and Painter, 1995)

association between 2-propanol and cyclohexane. In Figure 2.7 and Figure 2.8, bands at  $3630$ ,  $3530$  and  $3350\text{cm}^{-1}$  are assigned to non-hydrogen bonded hydroxyl groups, hydrogen bonded dimers and hydrogen bonded multimers, respectively (Coleman and Painter, 1995). In Figure 2.7, at low concentration of 2-propanol ( $0.02\text{M}$ ), the majority of 2-propanol is in monomeric form, represented by the large peak at  $3630\text{cm}^{-1}$  on the IR spectra. As the concentration is increased from  $0.02\text{M}$  to  $0.09\text{M}$ , the intensity of the monomer peak at  $3630\text{cm}^{-1}$  decreases and two peaks at  $3530$  and  $3350\text{cm}^{-1}$  start to appear, representing that the monomers start to form dimers and multimers at higher concentrations. As the concentration is further increased to  $0.3\text{M}$ , then the intensity of the monomer peak at  $3630\text{cm}^{-1}$  decreases even more and the intensity of the peaks

representing dimer and multimer formation at  $3530$  and  $3350\text{cm}^{-1}$  increases even more. This shows the change in the monomer-dimer-multimer formation of a self-association molecule in an inert solvent as the concentration changes. Figure 2.8 shows the similar changes as a function of temperature. As the temperature is decreased, the monomers of 2-propanol forms dimers and multimers, therefore the intensity of the peak at  $3630\text{cm}^{-1}$  decreases, whereas the intensity of the peaks at  $3530$  and  $3350\text{cm}^{-1}$  increases at lower temperatures. This information from infrared studies is the basis for determination of equilibrium constants and enthalpies of hydrogen bond formation for self-association of low molecular weight molecules (Coleman et al., 1991; Coleman and Painter, 1995).

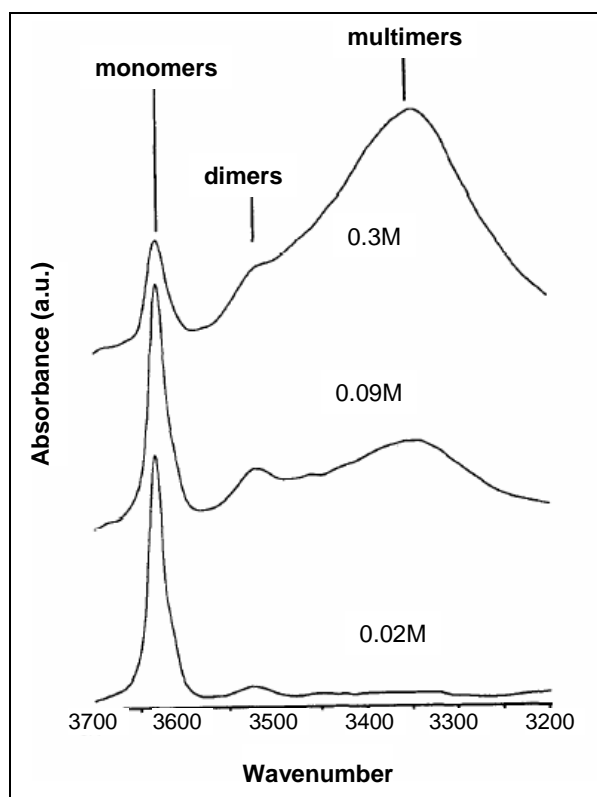


Figure 2.7: Infrared spectra of hydroxyl stretching regions of 2-propanol in cyclohexane at  $25^{\circ}\text{C}$  for three different concentrations (Coleman and Painter, 1995)

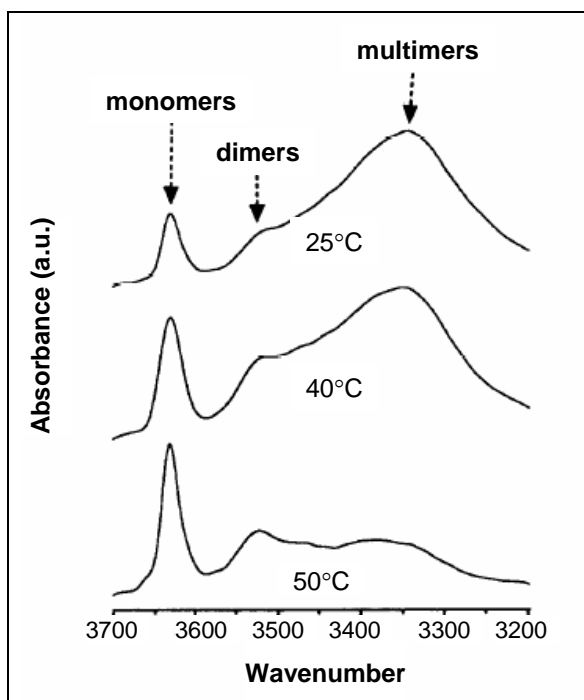


Figure 2.8: Infrared spectra of hydroxyl stretching regions of 2-propanol in cyclohexane for 0.3M concentration at different temperatures (Coleman and Painter, 1995)

Quantitative measure of fraction of free monomers in dilute solutions of known concentrations is needed in order to calculate the self-association equilibrium constants. The intensity of the free hydroxyl band is assumed to be a quantitative measure of monomers, such that it has no contribution from free hydroxyl end groups. According to the Beer-Lambert law, the absorbance (intensity of the isolated hydroxyl band) ( $I$ ), is related to absorptivity coefficient ( $\epsilon$ ), the concentration ( $c$ ) and the path length ( $l$ ) in the form of; (Coleman and Painter, 1995)

$$I = \epsilon \cdot l \cdot c \quad (2.27)$$

Absorptivity coefficient ( $\epsilon$ ) can be determined from a plot of ( $I / c \cdot l$ ) vs.  $c$  as;

$$\left. \frac{I}{c \cdot l} \right|_{\lim c \rightarrow 0} = \epsilon \quad (2.28)$$



where  $I$  is the experimentally measured absorptivity of monomers (intensity of the monomer band) at different concentrations from the IR spectra. Experimental fraction of free monomers ( $f_m^{OH}$ ) at any given concentration is then given by;

$$f_m^{OH} = \frac{I}{I_0} \quad (2.29)$$

where  $I_0$  is the calculated intensity using Equation 2.27 at any given concentration.

An iterative least square fitting procedure developed by Coleman et al. (1991) is used to obtain the best fit of Equation 2.30 to experimental data at various compositions. Equation 2.30 relates fraction of free monomers ( $f_m^{OH}$ ) to dimensionless equilibrium constants ( $K_2$  and  $K_B$ ) as follows;

$$f_m^{OH} = \frac{\Phi_{B1}}{\Phi_B} = \left[ \left( 1 - \frac{K_2}{K_B} \right) + \frac{K_2}{K_B} \cdot \left( \frac{1}{(1 - K_B \cdot \Phi_{B1})^2} \right) \right]^{-1} \quad (2.30)$$

where  $\Phi_B$  is the total volume fraction of 'B' molecules (calculated from Equation 2.6); and  $\Phi_{B1}$  is the volume fraction of non-hydrogen bonded (free) 'B' (calculated from combining Equation 2.29 and left-hand side of Equation 2.30). This least square fitting procedure uses Equation 2.30 at different concentrations; At each concentration, there is a specific  $\Phi_{B1}$  and  $f_m^{OH}$  value (Equation 2.29), and these concentration dependent  $\Phi_{B1}$  and  $f_m^{OH}$  are inserted in Equation 2.30 to form a series of equations. Using these equations, the least square fitting procedure enables the best fit of Equation 2.30 that leads to the determination of the two unknowns,  $K_2$  and  $K_B$ .

For different temperatures, the above procedure can be repeated to find equilibrium constants,  $K_2$  and  $K_B$ , at any temperature. Then, the  $K_2$  and  $K_B$  values at different temperatures are used to calculate the enthalpies of hydrogen bond formation,

$H_2$  and  $H_B$ , from the slope of  $\ln K_{(2 \text{ and } B)}$  vs.  $1/T$  plots (Coleman et al., 1991; Coleman and Painter, 1995)  $\{H = (-)(\text{slope})(R)\}$ , since  $\frac{\partial(\ln K)}{\partial(1/T)} = -H/R$ , where  $R$  is the gas constant}.

However, self-association equilibrium constants of polymers that contain hydroxyl groups can not be determined in the same way as the low molecular weight molecules described above, because these polymers are not soluble in inert solvents, such as linear or cyclic hydrocarbons. They can be soluble in polar solvents, but in these systems there are specific interactions between polymer and solvent (Coleman et al., 1991; Coleman and Painter, 1995). These systems will not be suitable just to determine the self-association of the polymer. In other words, an inert solvent needs to be used to characterize the self-association of the hydrogen bonding polymer but there isn't any inert solvent systems in which the self-association of a hydrogen bond forming polymer molecule can be characterized. One can not use a good solvent in this case, because then there will be specific interactions between the polymer and the good solvent. There will be competition between the polymer itself and solvent for the available hydrogen bonding sites on the polymer, and this will not enable the characterization of true self-association.

Because of the explanations above, a practical assumption is that  $K_2$  and  $K_B$  of polymers containing hydroxyl groups are the same as those obtained from appropriate model compounds. By "appropriate", we mean model compounds that have hydroxyl groups with similar chemical environments to the repeating unit of the polymer in interest. For instance, for poly(vinyl phenol), phenol is a good analogue compound; or for poly(2,6-diisopropyl styrene), 2,6-diisopropyl phenol is a good analogue. For this approach, it is assumed that there are no steric or electronic effects on going from the low

molecular weight model to the polymer; equilibrium constant is independent of molecular weight of the polymer chain; and the polymer chain is flexible enough so that the occurrence of hydrogen bonds are natural (Coleman et al., 1991). One adjustment that is needed to be done while using this approach is to scale the equilibrium constant to molar volume of the specific repeat unit of the polymer as;

$$K_i^{\text{polymer}} = \frac{V_{\text{model}}}{V_{\text{repeat unit of polymer}}} \cdot K_i^{\text{model}} \quad (2.31)$$

where  $V_{\text{model}}$  is the molar volume of the analogue;  $V_{\text{repeat unit of polymer}}$  is the molar volume of the monomer of the polymer in interest;  $K_i^{\text{model}}$  is the equilibrium constant for self-association of the model analogue compound; and  $K_i^{\text{polymer}}$  is the equilibrium constant for self-association of the polymer in interest (Coleman et al., 1991; Coleman and Painter, 1995).

As an example, self-association equilibrium constant for poly(hydroxyl ether of *bis*-phenol A), commonly referred as phenoxy, with the repeating unit shown in Figure 2.9a, can be determined from that of 2-propanol (Figure 2.9b) as the model analogue compound. The molar volume of the phenoxy repeat is 222.6cm<sup>3</sup>/mol. Self-association equilibrium constants of 2-propanol, determined from the least square fit of Equation 2.30, is given as  $K_2=34.8$ ;  $K_B=57.6$ . The molar volume of 2-propanol is  $V_B=76.6\text{cm}^3/\text{mol}$ . For phenoxy, self-association equilibrium constants determined for 2-propanol ( $K_2=34.8$ ;  $K_B=57.6$ ;  $V_B=76.6\text{cm}^3/\text{mol}$ ) can be transferred to the phenoxy repeat unit using Equation 2.31. Then,  $K_2$  and  $K_B$  for phenoxy can be calculated as  $K_2=76.6/222.6 \times 34.8=12$  and  $K_B=76.6/222.6 \times 57.6=19.8$ , respectively (Coleman and Painter, 1995).

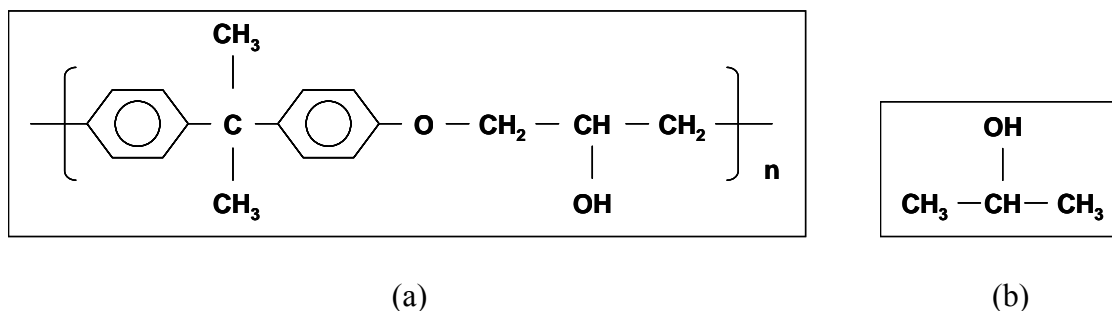


Figure 2.9: Structure of (a) Repeating unit of poly(hydroxyl ether of bis-phenol A), commonly referred as phenoxy; (b) 2-propanol

### 2.3.3.2. Determination of Equilibrium Constants for Inter-Association

Inter-association represents the hydrogen bonding between two different functional groups, which is in principle favorable to mixing of two polymers. Figure 2.10 shows a schematic example of inter-association between phenol and ethylpropionate, two low molecular weight models, where inter-association occurs between hydroxyl group of phenol and carbonyl group of ethylpropionate. The distribution of all species, including free monomers of phenol, inter-associated phenol monomer and ester carbonyl of ethylpropionate and inter-associated phenol multimers and ester carbonyl (Figure 2.10), depends on the composition of the mixture, temperature and equilibrium constants describing self-association and inter-association (Coleman et al., 1991; Coleman and Painter, 1995).

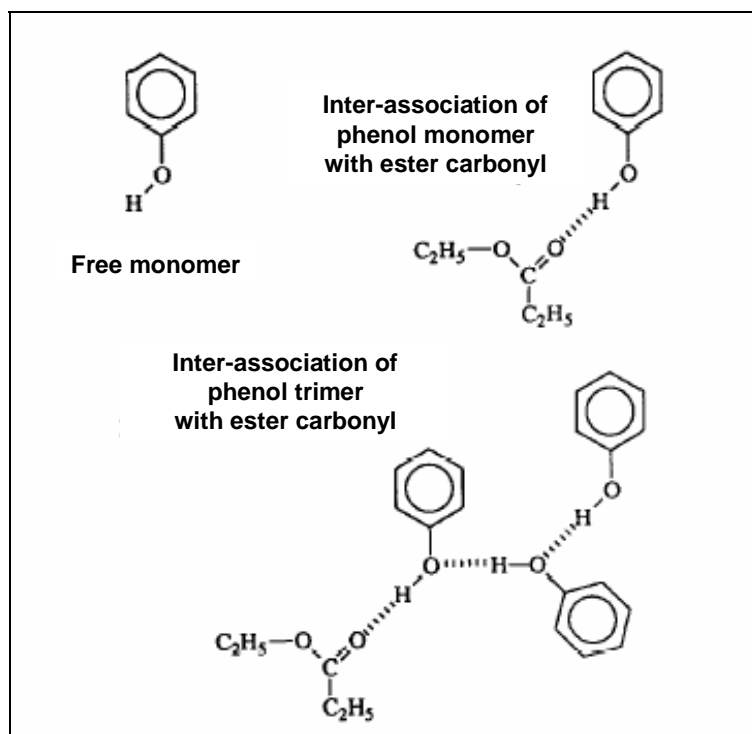


Figure 2.10: Schematic representation of inter-association in phenol/ethylpropionate mixtures (Coleman and Painter, 1995)

Equilibrium constants describing inter-association ( $K_A$ ) can not be calculated independent of self-association equilibrium constants ( $K_2$  and  $K_B$ ). In other words,  $K_2$  and  $K_B$  need to be known in order to calculate  $K_A$ . Section 2.3.3.1 has covered the determination of  $K_2$  and  $K_B$ , two necessary self-association equilibrium constants. Once the self-association of the hydrogen bonding molecule is characterized in an inert solvent, then the inter-association of the self-associating molecule with another hydrogen bonding molecule can be determined. In most cases, when dealing with carbonyl containing compounds, equilibrium constant for inter-association of low molecular weight mixtures can be determined using the carbonyl stretching regions of the infrared spectra. As an example, Figure 2.11 shows the infrared spectra of carbonyl stretching region of ethyl

phenol (EPh)/ethyl isobutyrate (EIB) mixtures as a function of composition (Coleman and Painter, 1995).

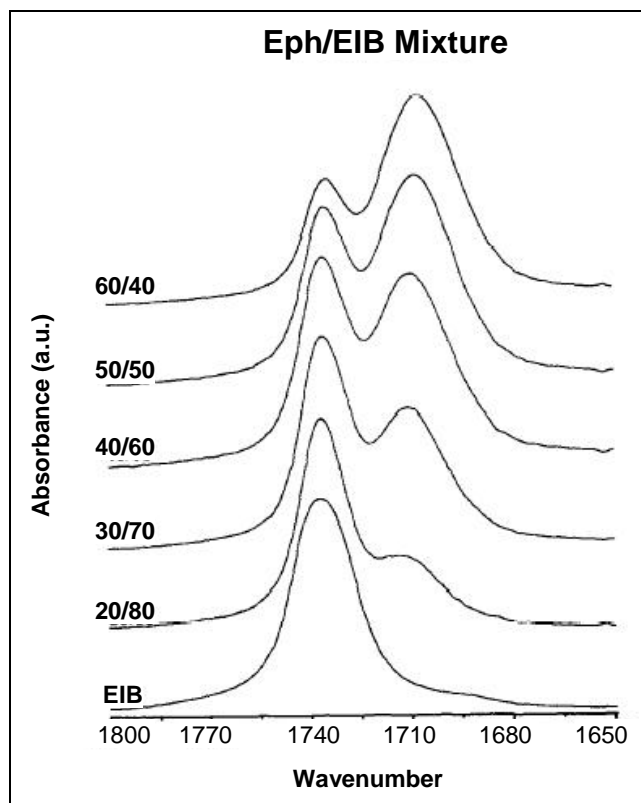


Figure 2.11: Infrared spectra of carbonyl stretching region of EPh/EIB mixtures of different compositions at 25°C (Coleman and Painter, 1995)

In Figure 2.11, carbonyl stretching region of the infrared spectra show two bands at 1736 and 1707cm<sup>-1</sup> that are assigned to free and hydrogen bonded carbonyl groups, respectively. The pure EIB shows a large band at 1736cm<sup>-1</sup>, representing the free carbonyl groups of EIB; and the intensity of this band decreases as EPh is introduced into the system, because the free carbonyl groups are involved in hydrogen bonding with EPh. Moreover, a band at around 1707cm<sup>-1</sup> starts to appear and its intensity increases as the

composition of EPh increases, because as more EPh is introduced to the system, the free carbonyl groups on EIB are involved in hydrogen bonding with EPh.

The fraction of free carbonyl groups ( $f_F^{C=0}$ ) is determined using the relative absorption coefficients and the relative intensities of the two bands from the IR spectra (Coleman and Painter, 1995), similar to the procedure described in Section 2.3.3.1 with equations similar to Equations 2.28-2.29.  $f_F^{C=0}$  is related to the equilibrium constants as;

$$f_F^{C=0} = \frac{\Phi_{A1}}{\Phi_A} = \frac{1}{\left\{ 1 + K_A \cdot \Phi_{B1} \cdot \left[ (1 - K_2 / K_B) + (K_2 / K_B) \cdot \left( \frac{1}{1 - K_B \cdot \Phi_{B1}} \right) \right] \right\}} \quad (2.32)$$

where  $\Phi_A$  is the total volume fraction of 'A';  $\Phi_{A1}$  and  $\Phi_{B1}$  are the volume fractions of non-hydrogen bonded 'A' and 'B' species in the blend. Similar to the procedure outlined in Section 2.3.3.1, at each composition ratio of A and B, there is a specific  $f_F^{C=0}$ , determined from the intensity of the free carbonyl group band. These values of  $f_F^{C=0}$  are then inserted in Equation 2.32, forming a system of equations with two unknowns,  $K_A$  and  $\Phi_{B1}$ . Recall that  $K_2$  and  $K_B$  are already determined at this point, as described in Section 2.3.3.1. Using these equations, the least square fitting procedure can be employed to determine the unknowns, including  $K_A$ . Direct transfer or scale of inter-association equilibrium constants determined from low molecular weight models into those for polymers is not possible and the fraction of hydrogen bonds between unlike groups in polymer blends of same molar concentration of the functional groups is significantly overestimated by equilibrium constants of low molecular weight analogues possible due to polymer chain connectivity and compositional heterogeneity (Coleman and Painter, 1995). But practically, inter-association equilibrium constants of polymers can be determined directly from infrared spectroscopy experiments, where the non-self-

associating polymer has a carbonyl group that can be used as a probe of the distribution of hydrogen bonded species, since carbonyl stretching vibrations has been proven to be an excellent indicator of molecular interactions for a number of polymers (Coleman and Painter, 1990, 1995; Coleman et al., 1991; Kuo and Chang, 2001, 2002; Hartikainen et al., 2004). When the infrared spectra of the polymers rather than low molecular weight models are used to determine the inter-association equilibrium constants, it is not necessary to account for the influence of chain connectivity and chain stiffness, since the experimentally determined fraction of hydrogen bonded species already includes these effects, because the polymer itself is being used in the IR spectroscopy (Coleman et al., 1991).

As an example, inter-association equilibrium constant of poly(vinylphenol) (PVPh), polymer containing hydroxyl group, and poly(ethyl methacrylate) (PEMA), polymer containing carbonyl group, (Figure 2.12), is directly determined from the IR spectra of the carbonyl stretching regions of the blend using the least-square fit of Equation 2.32 and is determined as  $K_A=37.1$  at 25°C (Coleman et al., 1991).

As an overall summary, miscibility predictions hydrogen bonded polymer blends can be determined using self-association equilibrium constants of low molecular weight model compounds (as in example in Figure 2.9) and inter-association equilibrium constants of polymer blends that are directly obtained from infrared measurements on miscible polymer blends (as in example in Figure 2.12) (Coleman et al., 1991; Coleman and Painter, 1995).



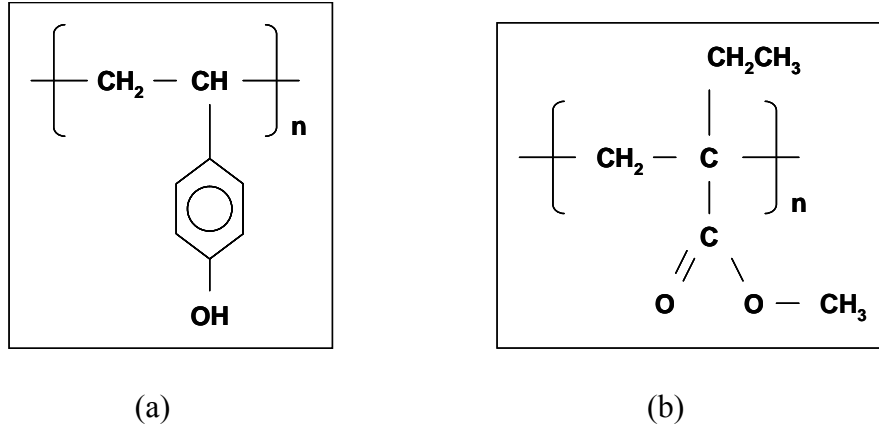


Figure 2.12: Structure of (a) Repeating unit of (a) poly(vinylphenol) (PVPh), (b) poly(ethyl methacrylate) (PEMA)

#### 2.3.4. Determination of Free Energy of Mixing

According to the association model, hydrogen bonds are in a dynamic equilibrium state and exist as distribution of non hydrogen-bonded and hydrogen-bonded species at any instant at a given temperature (Coleman et al., 1991; Coleman and Painter, 1995).

Free energy of mixing per mole of lattice site is given by;

$$\begin{aligned}
 \frac{\Delta G_{\text{mix}}}{R.T} = & \left[ \frac{\Phi_A}{M_A} \cdot \ln \Phi_A + \frac{\Phi_B}{M_B} \cdot \ln \Phi_B + \Phi_A \cdot \Phi_B \cdot \chi_{AB} \right] \\
 & + \left[ \Phi_B \cdot \ln \left( \frac{\Phi_{B1}}{\Phi_{B1}^0} \right) + \frac{\Phi_A}{r} \cdot \ln \Phi_{A1} + \Phi_B \cdot \left[ \left( \frac{\Gamma_1^0}{\Gamma_2^0} \right) - \left( \frac{\Gamma_1}{\Gamma_2} \right) \right] \right] \\
 & + \left[ \Phi_B \cdot \left( \frac{\Gamma_1}{\Gamma_2} \right) \cdot \left( \frac{X}{1+X} \right) \right] \\
 & - \left[ \Phi_B \cdot \ln \Phi_B + \frac{\Phi_A}{r} \cdot \ln \Phi_A \right]
 \end{aligned} \tag{2.33}$$

where

$$\Gamma_1 = \left(1 - \frac{K_2}{K_B}\right) + \frac{K_2}{K_B} \cdot \left[ \frac{1}{(1 - K_B \cdot \Phi_{B1})} \right] \quad (2.34)$$

$$\Gamma_2 = \left(1 - \frac{K_2}{K_B}\right) + \frac{K_2}{K_B} \cdot \left[ \frac{1}{(1 - K_B \cdot \Phi_{B1})^2} \right] \quad (2.35)$$

$$X = \frac{K_A \cdot \Phi_{A1}}{r} \quad (2.36)$$

$$\Gamma_1^0 = \left(1 - \frac{K_2}{K_B}\right) + \frac{K_2}{K_B} \cdot \left[ \frac{1}{(1 - K_B \cdot \Phi_{B1}^0)} \right] \quad (2.37)$$

$$\Gamma_2^0 = \left(1 - \frac{K_2}{K_B}\right) + \frac{K_2}{K_B} \cdot \left[ \frac{1}{(1 - K_B \cdot \Phi_{B1}^0)^2} \right] \quad (2.38)$$

where  $\Phi_B$  is the total volume fraction of ‘B’ molecules;  $\Phi_A$  is the total volume fraction of ‘A’ molecules;  $\Phi_{B1}$  is the volume fraction of monomers of ‘B’;  $\Phi_{B1}^0$  is the volume fraction of monomers in pure ‘B’;  $\Phi_{A1}$  is the volume fraction of non-hydrogen bonded species of ‘A’;  $r$  is the ratio of molar volume of molecules ‘A’ and ‘B’ ( $V_A/V_B$ );  $K_A$  is the equilibrium constant for formation of a hydrogen bond between ‘A’ and ‘B’ units;  $K_2$  and  $K_B$  are the equilibrium constants for formation of hydrogen bonds between ‘B’ units (dimer and multi-mer formation, respectively) (Coleman et al., 1991; Coleman and Painter, 1995). In Equation 2.33, free energy of mixing is represented by 3 terms expressed in each bracket:

1. The first term is the original Flory-Huggins equation for mixing polymers.
2. The second term is the expression equal to the change in free energy that would occur as a result of the change in hydrogen bonding upon mixing if the segments were not connected to form covalent chains. The distribution of hydrogen bond is defined as that actually found in the polymer, not that which might occur in an equivalent mixture of

monomer analogues. This part of the equation is derived using the difference between the contribution of hydrogen bonding in the mixture of A+B and in pure B on free energy of mixing.

3. A correction term for the fact that the second term not only gives the free energy change associated with the changing pattern of hydrogen bonding, but also has excess combinatorial entropy of mixing contribution. This term is the entropy of mixing that would be obtained by mixing non-covalently bonded 'B' segments with 'A' units if there were no change in hydrogen bonding upon mixing, in other words, if the distribution of hydrogen bonds remained the same as that found in pure 'B'. This last term is called the excess combinatorial entropy.

### **2.3.5. Intra-molecular Screening Parameter**

Painter-Coleman group have shown that “intra-molecular screening” is a significant effect in miscibility predictions (Painter et al., 1997a, 1997b; Coleman et al., 1999; Coleman and Painter, 2006). Screening is a consequence of chain connectivity in polymers that disables hydrogen bonding functional groups: The covalent linkages between the polymer segments result in an increase in the number of same-chain contacts over that calculated on the basis of a simpler random mixing of segments, because the chain can bend back upon itself both locally and through long-range effects, which may disable hydrogen bonding functional groups and consequently decrease the number of possible inter-molecular interactions (Figure 2.13) (Coleman and Painter, 2006).

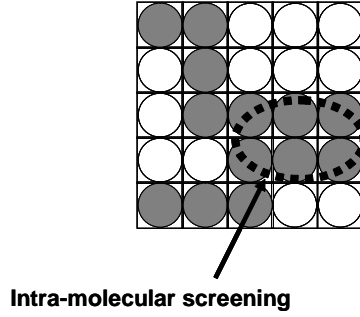


Figure 2.13: Schematics of intra-molecular screening in long-chain polymers

The association model in Equation 2.12 is modified by Painter-Coleman group to include this effect as;

$$\frac{\Delta G_{mix}}{RT} = \frac{\Phi_A}{M_A} \cdot \ln \Phi_A + \frac{\Phi_B}{M_B} \cdot \ln \Phi_B + \chi_{AB} \cdot \Phi_A \cdot \Phi_B \cdot \underline{(1-\gamma)} + \frac{\Delta G_H}{RT} \quad (2.39)$$

where  $\gamma$  is intra-molecular screening parameter and defined as the fraction of same chain contacts that originate from polymer chain bending back upon itself through local and long-range connectivity effects. It should be emphasized that incorporating the intra-molecular screening parameter ( $\gamma$ ) not only modifies the enthalpic term (3<sup>rd</sup> term on right hand side) in Equation 2.12, but also modifies the free energy of hydrogen bonding term ( $\Delta G_H/RT$ ) implicitly through the modification of self- and inter-association equilibrium constants (Coleman and Painter, 2006). In other words,  $\Delta G_H/RT$  in Equation 2.39 is different than that in Equation 2.12. Self- and inter-association equilibrium constants are modified as a function of intra-molecular screening parameter as;

$$K_{2B} = K_2 \cdot \left[ \frac{\gamma + (1-\gamma) \cdot \Phi_B}{\Phi_B} \right] \quad (2.40)$$

$$K_{BB} = K_B \cdot \left[ \frac{\gamma + (1-\gamma) \cdot \Phi_B}{\Phi_B} \right] \quad (2.41)$$

$$K_{AB} = K_A \cdot (1 - \gamma) \quad (2.42)$$

Where  $K_{2B}$  and  $K_{BB}$  are the modified self-association equilibrium constants for di-mer and multi-mer formation, respectively; and  $K_{AB}$  is the modified inter-association equilibrium constant, all involving the intra-molecular screening effect. It should be noted that  $K_{2B}$  and  $K_{BB}$  are a function of volume fraction of components, whereas  $K_{AB}$  is volume fraction independent. Moreover, the  $K_{2B}$  and  $K_{BB}$  values would be larger than  $K_2$  and  $K_B$ , respectively, whereas  $K_{AB}$  value would be smaller than  $K_A$ , due to the intra-molecular screening effect. During intra-molecular screening, the chain can bend back upon itself both locally and through long-range effects, which may disable hydrogen bonding functional groups to the other polymer in the blend, and consequently decrease the number of possible inter-molecular interactions (Figure 2.13) (Coleman and Painter, 2006). For instance, let's assume that  $K_B=50$ ; volume fraction is  $\Phi_B=0.1$ ; and  $\gamma=0.30$ . Then,  $K_{BB}$  will be calculated as 185 using Equation 2.41. Similarly, if  $K_A=120$ ,  $K_{AB}$  will be calculated as 84 using Equation 2.42. So, as can be seen in this calculation, in the absence of intra-molecular screening,  $K_A$  is higher than  $K_B$ , which indicates that inter-association between two polymers is more favorable than self-association of polymer B. When screening is taken into account,  $K_{BB}$  increases whereas  $K_{AB}$  decreases. This indicates that when screening is taken into account, the favorability of inter-molecular interactions decreases and the self-association of polymer B increases, which would be unfavorable effect for miscibility of polymers A and B. However, it should be remembered that inclusion of screening effects also modifies the enthalpy of mixing term ( $\chi_{AB} \cdot \Phi_A \cdot \Phi_B \cdot (1 - \gamma)$ ) in Equation 2.39. This term would get a lower positive value, so the

free energy of hydrogen bonding term in Equation 2.39 would need to overcome a lower positive valued term.

Since it has been shown that intra-molecular screening has a significant effect for miscibility (Painter et al., 1997a, 1997b; Coleman et al., 1999; Coleman and Painter, 2006), it should be taken into account that would provide a more realistic miscibility prediction. Painter-Coleman group have looked into a series of  $\gamma$  values. They have compared the experimental fraction of free carbonyl groups ( $f_F^{C=O}$ ) directly determined from IR experiments using the intensity of free carbonyl bands (similar to Equation 2.29) with the best predictive fit of Equation 2.32 for various synthetic polymers. An example is given in Figure 2.14 that shows the experimental results of the fraction of free carbonyl groups plotted as a function of blend composition for n-butyl methacrylate-co-vinyl phenol (BMAVPh) and styrene-co-2-vinyl pyridine (STVPy). Theoretical curves using varying values of  $\gamma$  are also displayed. Clearly, a model where  $\gamma=0$  is not capable of reproducing the experimental data, whereas values of  $\gamma$  between 0.25 and 0.35 gives the best comparison with the experimental results (Figure 2.14) (Coleman et al., 1998; Coleman and Painter, 2006) and an average value of  $\gamma=0.30$  is being accepted for most polymer systems.

### 2.3.6. Applications of Painter-Coleman Association Model to Polymer Systems

The Painter-Coleman association model has been successfully applied for the prediction of miscibility in a wide-range of synthetic polymer systems where miscibility is strongly affected by hydrogen bonding interactions (Coleman et al., 1991; Coleman and Painter, 1995, 2006; Kuo and Chang, 2001, 2002; He et al., 2004). The researchers

have developed a software, called “Miscibility Software and Phase Calculator” (Coleman et al., 1991) for calculations of miscibility between various polymer systems.

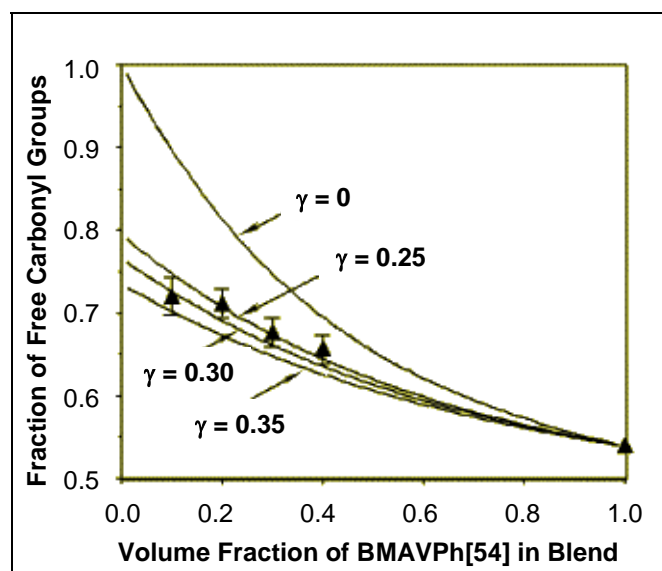


Figure 2.14: Fraction of free carbonyl groups in n-butyl methacrylate-co-vinyl phenol (BMAVPh) and styrene-co-2-vinyl pyridine (STVPy) blends as a function of volume fraction of BMAVPh at 150°C (Coleman et al., 1998)

As an example for the application of Painter-Coleman association model, free energy of mixing and second derivative of free energy of mixing for poly(vinyl phenol) (PVPh) (a self-associating polymer that can form hydrogen bonds in pure state) and poly(alkyl methacrylate) (do not self-associate, but have a functional group that can form hydrogen bonds with PVPh) blends at 150°C are shown in Figure 2.15 and Figure 2.16, respectively. For these systems, all calculations are performed using “Miscibility Software and Phase Calculator” (Coleman et al., 1991). Non-hydrogen bonded solubility parameters are calculated, as described in Section 2.3.1. Infrared studies of phenol, low

molecular weight analogue, is used to obtain  $K_2$  and  $K_B$  of PVPh, which are determined as 21.0 and 66.8, respectively, as described in Section 2.3.3.1. Infrared studies of mixture systems are used to determine  $K_A$  as 37.1 (Coleman et al., 1991), as described in Section 2.3.3.2. Negative free energy and positive second derivative of free energy over the entire composition range is only obtained for PVPh+PMMA and PVPh+PEMA blends, showing that these systems are miscible; PVPh+POMA and PVPh+PHMA blends are predicted to be immiscible; and PVPh+PBMA blends are predicted to be at the edge of miscibility, but still phase-separated at the selected temperature (Coleman et al., 1991).

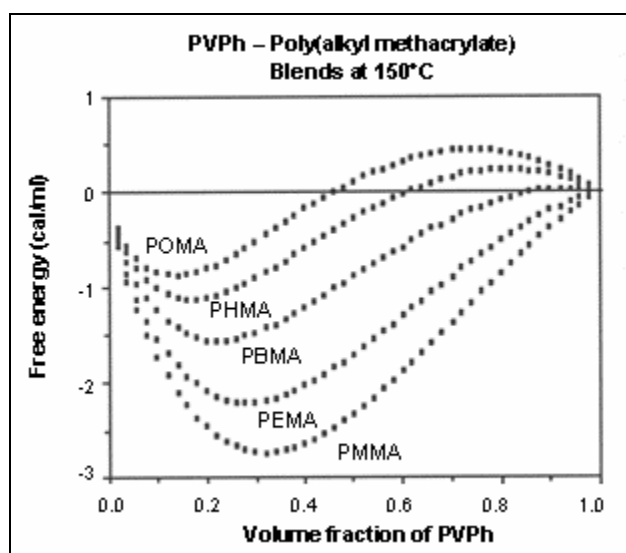


Figure 2.15: Predicted free energy of mixing for PVPh and different poly(alkyl methacrylate) blends at 150°C using Painter-Coleman association model (Coleman et al., 1991)



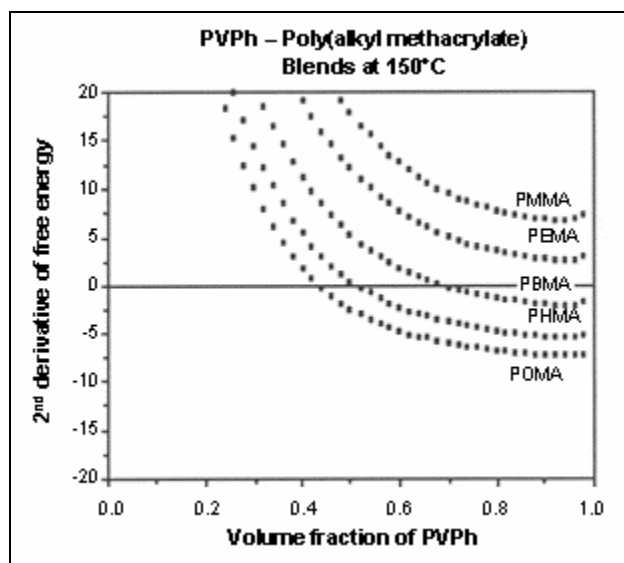


Figure 2.16: Predicted second derivative of free energy of mixing for PVPh and different poly(alkyl methacrylate) blends at 150°C using Painter-Coleman association model (Coleman et al., 1991)

Understanding how these theories apply to food carbohydrate polymers and their use/modification to develop tools to predict miscibility/immiscibility will advance the state-of-art in food polymer science. However, the applicability of the Painter-Coleman hydrogen bonding association model for carbohydrate systems is still limited. Because the model is designed in such a way that the repeating unit of the 1<sup>st</sup> polymer has a functional group, such as OH, that can self-associate, and the repeating unit of the 2<sup>nd</sup> polymer has one functional group that can form H-bond with the first polymer. If there are multiple or different types of functional groups on the repeating unit of the polymer blend components, as in the case of most carbohydrate polymers; (for example, biopolymers with glucose repeating unit, such as dextran, amylopectin etc.) or if both components self-associate in the pure state (which also describes the behavior in many

carbohydrate polymers), then the calculation of hydrogen bonding contribution to the free energy becomes more complicated (Coleman and Painter, 1995), and the association model can only offer a crude approximation to predict miscibility in such systems. New thermodynamic models which build on the Painter Coleman model are needed that can account for the structural complexities of carbohydrates, including the presence of multiple hydrogen bonding groups which result in multiple and more intricate self-association. However, in order to bring the capabilities of this model to food polymer science and to demonstrate the importance of hydrogen bonding contributions to predict miscibility, some approximate calculations can be made in order to show the use of the association model to improve the prediction of miscibility in carbohydrate systems relative to the Flory Huggins theory. Any progress with carbohydrate polymers would be a step forward towards choosing which ingredients in a food formulation would form the desired miscible/immiscible systems on a predictive basis and will offer product development rules which will increase the utilization of alternative agricultural ingredients in novel food products.

#### **2.4. Phase Separation in Polymer Systems**

When there are two polymers in a common solvent (mixing two polymer solutions), there are three possibilities in terms of phase behavior:

*a) Segregative phase separation* is caused by repulsive forces between the polymers that push the polymers apart, which induce separation of these polymers in different phases. In other words, two different phases are formed; one with polymer1-solvent and the other with polymer2-solvent. This is a phase separated 3 component system. This is usually

observed for uncharged polymers or polyelectrolytes with charges of equal sign and similar charge density (Albertson, 1986; Thuresson et al., 1996).

*b) Complex coacervation (Associative phase separation)* leads to the formation of complex capsules caused by attractive forces between polymers, which favor local separation but nano/micro scale association of the polymers in a common phase. Two different phases are formed; the two polymers associate to form a network in a single phase and the solvent forms the other phase. So, this is still a phase separated 3 component system, the two polymers are phase separated from the solvent. This is usually seen for mixtures of oppositely charged polyelectrolytes (Albertson, 1986; Thuresson et al., 1996).

*c) Compatibility* leads to miscibility of the polymers. In this case, there are no attractive or repulsive forces between the polymers, which result in a homogeneous, single phase with two polymers and the solvent (Albertson, 1986).

Phase separation in miscible polymer blends usually occurs when there is a variation in temperature, pressure and/or composition in the system affecting the entropy and enthalpy of mixing significantly (Olabisi et al., 1979). Increasing entropy which results in more randomness of the macromolecules enhances mixing. Lack of resistance which is acceptance of energy giving a negative heat of mixing also enhances mixing. The combination results in negative free energy leading to spontaneous mixing and miscibility.

## 2.5. Phase Transitions in Polymers

The physical states of low molecular weight materials are well known; solid (crystalline), liquid and gaseous. Melting and boiling are two first-order transitions that separate the states of these materials. However, for high-molecular weight polymers, there is no vaporization to a gaseous state and they decompose before their boiling point can be reached. Moreover, many polymers do not crystallize at all, but form glasses at low temperatures and viscous liquids at higher temperatures. The transition that separates glassy state from viscous liquid state is called the glass-rubber transition. Glass-rubber transition (also called glass transition) is a second-order transition at slow rates of heating and cooling (Sperling, 2001). An amorphous polymer can behave as a glassy-brittle solid, an elastic rubber or a viscous liquid depending on the temperature and the time scale of the measurements (Aklonis and MacKnight, 1983; Sperling, 2001).

In food systems, phase transitions have significant importance, since transitions during processing, storage and consumption affect the quality, stability and in turn consumer acceptance of the final food products. Phase transitions in foods are generally the result of a change in composition, temperature, solvent environment (ex: water activity in foods) or pressure. The principal components of food systems are carbohydrates, proteins and lipids and the presence of these components in their thermodynamically stable equilibrium state controls the stability and shelf-life of food products. Food materials often exist in a non-equilibrium state, which can exhibit time-dependent changes (Roos, 1995). Understanding the phase behavior and thermodynamics of phase transition in foods as a function of temperature, water content and pressure is important for better control of processing conditions and the changes during storage and

consumption. Among diagnostic tools for phase behavior and phase separation, the glass transition plays an important role.

### **2.5.1. Glass Transition Temperature ( $T_g$ )**

The bulk state of polymers may include both amorphous and crystalline states. Amorphous polymers do not contain crystalline regions, whereas crystalline polymers generally contain amorphous regions, which make them ‘semi-crystalline materials’ (Sperling, 2001). Amorphous materials contain excess free energy and entropy when compared to their crystalline counterparts at the same temperature and pressure conditions. Below their melting point, the physical state of amorphous materials is a thermodynamically non-equilibrium state. Therefore, many properties of amorphous materials are functions of temperature and time; and these properties impact shelf-life since they are not stable (Roos, 1995).

Every amorphous polymer has a glass transition region, characterized by a “glass transition temperature” ( $T_g$ ). Below  $T_g$ , thermal motions in the material cease; long-range rotational and translational motions stop (Ferry, 1980; Sperling, 2001). The glass transition is the temperature at which segmental motion of macromolecules are activated, including motion of its chains, chain-segments, torsions of end-chain fragments and side groups, rotational isomerizations and transformation from one stable conformation to another (Tolstoguzov, 2000a). Below  $T_g$ , the material is in its glassy, rigid state and has a high internal viscosity with negligible molecular mobility and diffusion. Above  $T_g$ , the material is in its rubbery, softer state with lower viscosity and higher mobility.  $T_g$  depends on various factors, such as molecular weight, chemical structure, presence of

plasticizers and copolymers, ratio of amorphous and crystalline regions, degree of cross-linking and pressure.

The glass transition in a food system occurs due to: 1) rapid cooling (below  $T_g$ ); 2) removal of water and/or other plasticizers by drying, for instance; and 3) aggregation (self-concentration) of structure forming biopolymers, such as during re-folding and/or association of denatured proteins, gelation of proteins and polysaccharides (Tolstoguzov, 2000b). Determination of glass transition in food materials is of great importance since it has significant effects on processing and storage conditions of the amorphous foods, which in turn affects the final structure and stability of the food products. For example, physical/textural properties in foods, such as stickiness, viscosity, crispness or crunchiness are affected at glass transition. The change in the molecular mobility at the glass transition also affects diffusion (Yildiz and Kokini, 2001, 2003; Ribeiro et al., 2003), and the rate of various desirable or undesirable changes in foods, such as oxidation, crystallization, browning reactions and enzymatic reactions.

## **2.5.2. Factors Affecting Glass Transition of Polymers**

### **2.5.2.1. Effect of Molecular Weight on Glass Transition**

Molecular weight and molecular weight distribution of polymers can be characterized by the number-average molecular weight ( $M_n$ ); the weight-average molecular weight ( $M_w$ ); the z-average molecular weight ( $M_z$ ); and the viscosity-average molecular weight ( $M_v$ ), which are defined below;

$$M_n = \frac{\sum_i N_i \cdot M_i}{\sum_i N_i} = \frac{\sum_i w_i}{\sum_i \frac{w_i}{M_i}} \quad (2.43)$$

$$M_w = \frac{\sum_i N_i \cdot M_i^2}{\sum_i N_i \cdot M_i} = \frac{\sum_i w_i \cdot M_i}{\sum_i w_i} \quad (2.44)$$

$$M_z = \frac{\sum_i N_i \cdot M_i^3}{\sum_i N_i \cdot M_i^2} = \frac{\sum_i w_i \cdot M_i^2}{\sum_i w_i \cdot M_i} \quad (2.45)$$

$$M_v = \left[ \frac{\sum_i N_i \cdot M_i^{1+a}}{\sum_i N_i \cdot M_i} \right]^{1/a} \quad (2.46)$$

where  $N_i$  is the number of specie  $i$ ;  $M_i$  is the molecular weight of specie  $i$ ;  $w_i$  is the weight fraction of specie  $i$ ; and  $a$  is a polymer dependent constant ranging from 0.5 to 0.8. Polydispersity index (PDI) is defined as  $M_w/M_n$ , which is a measure of the molecular weight distribution of the polymer. For a random molecular weight distribution;  $M_n:M_w:M_z = 1:2:3$  (Sperling, 2001). Figure 2.17 illustrates a simple diagram for molecular weight distribution of polymers with various average molecular weights.

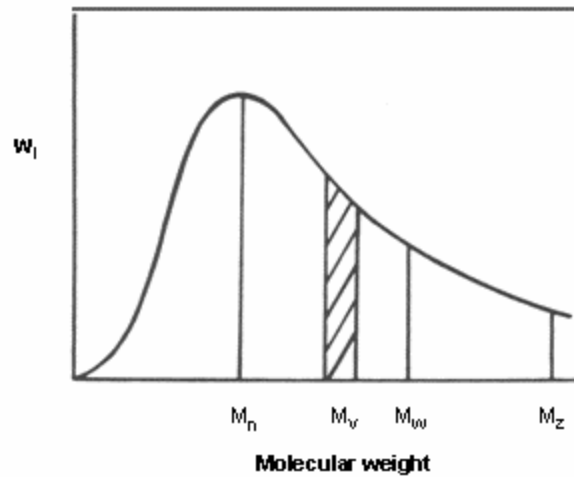


Figure 2.17: Molecular weight distribution of polymers showing different average molecular weights (Sperling, 2001)

Most thermodynamic properties of polymers depend on their number-average molecular weight (Van Krevelen and Hoftyzer, 1976; Aklonis and MacKnight, 1983; Billmeyer, 1984; Furuya et al., 1995; Gabarra and Hartel, 1998). For linear polymers, the general relationship between molecular weight and glass transition temperature is described as (Fox and Flory, 1950);

$$T_g = T_{g,\infty} - \frac{A}{M} \quad (2.47)$$

where  $T_{g,\infty}$  is the glass transition temperature at infinite molecular weight;  $M$  is the molecular weight; and  $A$  is a polymer dependent constant. Equation 2.47 indicates that glass transition temperature increases with molecular weight (Aklonis and MacKnight, 1983; Slade and Levine, 1991a; Ruan et al., 1999; Sperling, 2001; Gropper et al., 2002), which is a consequence of the decrease in free volume with increasing molecular weight, caused by the increased number of connected monomer units in the system and decreased number of end groups (Aklonis and MacKnight, 1983; Sperling, 2001). At very high molecular weights, the concentration of chain ends is negligible, which results in the glass transition temperature to be independent of molecular weight (Aklonis and MacKnight, 1983; Slade and Levine, 1991b).

#### **2.5.2.2. Effect of Plasticization on Glass Transition**

A plasticizer is usually a small, non-volatile molecule added to polymers to increase mobility and to soften them by lowering their glass transition temperature. In the case of semi-crystalline polymers, the plasticizer softens the polymers by reducing their crystallinity or melting temperature (Ferry, 1980; Sperling, 2001). They are compatible



and therefore dissolve in the polymer and serve to separate the polymer chains from each other. The flexibility, ductility and extensibility of the polymer increase by the effect of plasticizers (Ferry, 1980; Sears and Darby, 1982). Plasticizers also decrease the mechanical resistance of the polymers (Sears and Darby, 1982).

Plasticization occurs as a result of several steps: The plasticizer wets the polymer surface and is adsorbed by the surface followed by diffusion toward the interior of the polymer. Solvation and/or penetration take place toward the surface and finally dissolution in the amorphous regions occurs (Sears and Darby, 1982). According to Slade and Levine (1993), solvents that have high compatibility/miscibility with the polymer at all proportions can be considered as a plasticizer. On the other hand, all plasticizer are not necessarily solvents for the polymer. For example, water is a plasticizer for zein (the corn protein) (Madeka and Kokini, 1994), but zein is insoluble in water (Fu et al., 1999).

Free volume theory, lubricity theory and gel theory are three common theories to explain plasticization. Gel theory states that plasticizers disrupt hydrogen bonding and van der Waals interactions between polymer chains (Gioia and Guilbert, 1999). According to lubrication theory, the plasticizers serve as lubricant and facilitate the movement of macromolecules relative to each other (Gioia and Guilbert, 1999). Free volume theory provides the most accepted explanation for plasticization as follows: Small molecules having larger chain end to backbone ratio has larger free volume. Therefore, addition of these molecules into the polymer increases the free volume (Ferry, 1980; Sears and Darby, 1982; Aklonis and MacKnight, 1983). At a given temperature, the plasticized polymer has more free volume than the unplasticized polymer if additivity

of the free volume is assumed. More free volume loosens the local structure, resulting in reduced glass transition temperatures and increased softening (Kelley and Bueche, 1961).

Water is shown to be one of the common plasticizers in biopolymer systems. Plasticization by water affects the thermo-mechanical, viscoelastic and diffusion related properties of amorphous and semi-crystalline biopolymers (Slade and Levine, 1991a; Slade et al., 1993). Effect of water as a plasticizer has been shown in many food polymers, including elastin (Kakivaya and Hove, 1975; Hove and Hove, 1978); gelatin (Marshall and Petrie, 1980; Reutner et al., 1985; Slade et al., 1989); collagen (Batzer and Kriebich, 1981; Levine and Slade, 1987); gluten (Hoseney et al., 1986); 7S and 11S fractions of soy protein (Morales-Diaz and Kokini, 1997); glutenin (Cocero and Kokini, 1991); gliadin (De Graaf et al., 1993; Madeka and Kokini, 1994); zein (Madeka and Kokini, 1996); agar and carrageenan (Mitsuiki et al., 1998); starch (Biliaderis, 1991; Kalichevsky et al., 1992; Zimeri and Kokini, 2003a); inulin (Zimeri and Kokini, 2002).

Glass transition temperature of biopolymer-water systems can be predicted based on the  $T_g$  of individual components and the composition of the mixture using Gordon-Taylor equation (Gordon and Taylor, 1952);

$$T_g = \frac{w_1 T_{g1} + k w_2 T_{g2}}{w_1 + k w_2} \quad (2.48)$$

where  $w_i$  is the weight fraction of the components;  $T_{gi}$  is the glass transition temperature of the components; and  $k$  is a constant which is determined from experimental data for  $T_g$  at different water contents. Gordon-Taylor equation has been successfully used to study water plasticization of several food components, including carbohydrates and proteins, such as maltodextrin-sucrose mixtures (Roos and Karel, 1991); amorphous corn starch (Jouppila and Roos, 1997); 7S and 11S fractions of soy protein (Morales-Diaz and

Kokini, 1997); glutenin (Cocero and Kokini, 1991); starch (Kalichevsky et al., 1992; Zimeri and Kokini, 2003a); inulin (Zimeri and Kokini, 2002).

### 2.5.2.3. Effect of Copolymerization on Glass Transition

Addition of a second monomeric component may be in the form of copolymerization or formation of a blend of polymers. According to Couchman and Karasz (1978),  $T_g$  of binary blends of miscible polymers can be predicted by an equation (Equation 2.49) similar to the Gordon-Taylor equation for polymer-water systems (Equation 2.48), where  $k$  is an empirical constant which can be determined as;

$$k = \frac{\Delta C_{P1}}{\Delta C_{P2}} \quad (2.49)$$

The Gordon-Taylor equation is restricted only for binary mixtures of the polymer and water, whereas Couchman-Karasz equation can be applied for miscible mixtures with more than two components as;

$$T_g = \frac{w_1 \Delta C_{P1} T_{g1} + w_2 \Delta C_{P2} T_{g2} + w_3 \Delta C_{P3} T_{g3}}{w_1 \Delta C_{P1} + w_2 \Delta C_{P2} + w_3 \Delta C_{P3}} \quad (2.50)$$

Application of Equation 2.50 to food materials with high glass transition temperature, such as proteins and starch, is difficult due to thermal decomposition of the anhydrous biopolymer at high temperatures. Moreover, determination of  $\Delta C_P$  also gets difficult at lower water contents since the glass transition range often broadens and the  $\Delta C_P$  decreases with decreasing water content (Roos, 1995).

#### **2.5.2.4. Effect of Chemical Structure on Glass Transition**

Molecular structure of polymers affects their glass transition temperatures by either enhancing or restricting their molecular motion. Steric hindrance introduced by the presence of substituents on the chain backbone or the barrier to internal rotation are two factors that affect the mobility of a chain (Aklonis and MacKnight, 1983). In general, as the energy required for the onset of molecular motion increases, the glass transition temperature increases. For example, increase in intermolecular forces, intra-chain steric hindrances and presence/addition of bulky, stiff side chains increase  $T_g$  of the system. On the other hand, in-chain groups such as double bonds and ether linkages that promote flexibility of the molecules and presence/addition of flexible side groups decrease  $T_g$  of the systems (Sperling, 2001).

#### **2.5.2.5. Effect of Crystallinity on Glass Transition**

Although glass transition is a property of amorphous polymers, semi-crystalline polymers may also exhibit a glass transition through their amorphous portions. The molecular motion restricted by the presence of crystallites, increases the  $T_g$ . For highly crystalline polymers,  $T_g$  may be masked, since  $T_g$  is always lower than the melting temperature ( $T_m$ ) of the polymer. Many semi-crystalline polymers have two  $T_g$ s; the lower one corresponding to the completely amorphous regions and the higher one that occurs in semi-crystalline part and varies with the extent of crystallinity (Sperling, 2001).

#### **2.5.2.6. Effect of Other Factors on Glass Transition**

The effect of cross-linking and pressure on the glass transition temperature can be explained by the free volume theory of the glass transition. Increasing number of cross-links or pressure decreases the total volume which also decreases the available free volume and in turn results in increase of  $T_g$  (Mansfield, 1993; Sperling, 2001).

### **2.6. Miscibility/Phase Separation in Food Biopolymers**

Many carbohydrate-protein systems phase separate, because there are significant differences in their hydrophilicity/hydrophobicity resulting from very different macromolecular chemistry, molecular conformation and affinity for water (Tolstoguzov, 1991, 1998, 2000b, 2003; Michon et al., 1995; Grinberg and Tolstoguzov, 1997; Moraru et al., 2002). Phase separation in carbohydrate-carbohydrate systems has also been observed even though the components are chemically closer to each other. Kalichevsky and Ring (1987) showed that phase separation occurred even in moderately concentrated (6%) solutions of amylose and amylopectin, due to the large difference in molecular weight between components. Their findings were confirmed by German et al. (1992), who concluded that phase separation occurred due to precipitation of amylopectin, which captures a lot of the solvent and facilitated the aggregation of amylose by making less solvent available for amylose. These results need better mechanistic understanding.

Even small differences in chemical structures lead to phase separation. Dextran and locust bean gum (LBG) phase separate in aqueous solution at 20°C and form an LBG-rich gel in the upper phase, and a liquid lower phase that contains only dextran (Garnier et al., 1995). Phase separation was also observed in LBG/starch and guar

gum/starch mixtures of different concentrations (Ahmad and Williams, 2001), particularly for higher molecular weights of LBG. These studies are elegant experimental investigations and refrain from engaging in mechanistic explanations.

Mixtures of inulin, a fructo-oligosaccharide, and amylopectin have been shown to be immiscible at low moisture contents (Zimeri and Kokini, 2002, 2003a, 2003b, 2003c). At high moisture contents, two phases with completely different morphologies were found to co-exist and the mechanism of phase separation was determined to be that of nucleation and growth of inulin crystallites resulting from strong attractive forces between inulin molecules (Zimeri and Kokini, 2002, 2003a, 2003b, 2003c).

Concentrated solutions of dextran with molecular weight of 472,000 and amylose were immiscible as well (Kalicevsky et al., 1986). The dextran concentration affected the mechanical behavior of amylose gels: at dextran concentrations lower than 3%, the modulus of the gels increased with increasing dextran concentrations, and at dextran concentrations higher than 3%, segregation of dextran-rich droplets and immiscibility resulted in decrease of firmness of amylose gels (Kalicevsky et al., 1986).

Phase separation was also reported for mixtures of guar-amylopectin (Closs et al., 1999), dextran-agarose (Medin and Janson, 1993), gelatin-iota carrageenan (Michon et al., 1995), starch-glycerol (Forssell et al., 1997), sucrose-globular proteins (Antipova and Semenova, 1995), and starch-sorbitol (Gaudin et al., 1999). It should be noted that none of the studies have been able to quantitatively predict the observed phenomena. There is a massive gap between experimental results and a quantitative framework leading to a useful predictive tool.

## 2.7. Effect of Ionic Strength on Charged Polymers' Miscibility/Immiscibility

Electrostatic interactions are important in systems that contain electrically charged particles. Solution properties of polymer electrolytes (polyelectrolytes) differ considerably from those of uncharged polymers. Strong repulsion between similarly charged monomers results in polyelectrolytes' tendency to be highly swollen and stretched (Figure 2.18c) (Walstra, 2003). These polyelectrolytes can even be dissolved in solvents that are considered poor for the polymer backbone (Shinoda, 1978; Dobrynin et al., 1996; Jousset et al., 1998; Lauten and Nystrom, 2000).

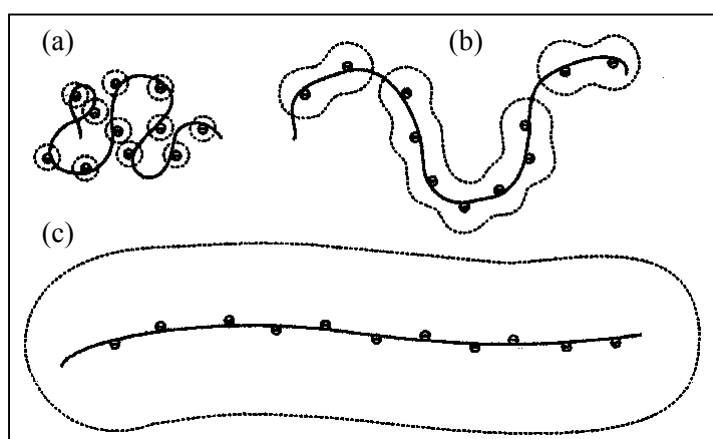


Figure 2.18: A schematic example of the conformation of a polyelectrolyte at decreasing ionic strengths from (a) to (b) to (c) (Walstra, 2003)

Electrostatic interactions can be screened by the addition of salt to the aqueous solution of charged polymer molecules (Demetriades and McClements, 1998; Lauten and Nystrom, 2000; Basak et al., 2003; Hellebust et al., 2004). A charged polymer can be assumed to behave as a soft sphere with an approximate effective radius ( $R_{\text{eff}}$ ), which is

the sum of hydrodynamic radius of gyration ( $R_g$ ) and Debye screening length ( $\kappa^{-1}$ ) (Tadros, 1996).

$$R_{\text{eff}} = R_g + \kappa^{-1} \quad (2.51)$$

$R_g$  is defined as the mean square distance away from the center of gravity of the molecule and for a random coil polymer, it is defined as;

$$R_g = \frac{r^2}{6} \quad (2.52)$$

where  $r$  is the end-to-end distance of the polymer chain (Sperling, 2001).  $\kappa^{-1}$  in Equation 2.51 is the thickness of electric double layer resulting from the screening effect of the ions, corresponding to the distance from the charged surface of the spherical molecule where electric potential falls  $1/e$  of its value at the surface of the charged molecule (dotted lines in Figure 2.18) (Walstra, 2003). For water at room temperature,  $\kappa^{-1}$  is given as;

$$\kappa^{-1} = (3.2) \cdot I^{-1/2} \quad (2.53)$$

where  $I$  (mol/L) is the ionic strength; and  $\kappa^{-1}$  is in nm (Walstra, 2003). Addition of an electrolyte, such as salt, increases the ionic strength and results in decrease of effective radius in Equation 2.51 (Russel, 1991), because the increase in ionic strength reduces  $\kappa^{-1}$  (Equation 2.53) and electrostatic screening reduces the repulsion of the charged groups along the polymer chain, resulting in decrease of  $R_g$  (Demetriades and McClements, 1998).

As a summary, in the absence of electrostatic screening (in other words, in the absence of an electrolyte, such as salt), strong repulsion between similarly charged monomers in a polyelectrolyte results in a highly swollen and stretched conformation



with higher radius of gyration (Figure 2.18c). On the other hand, upon addition of an electrolyte, such as salt, the repulsion of the charged groups decreases, and the molecule assumes a conformation shown in Figure 2.18a with lower radius of gyration. Due to electrostatic screening effects in the presence of an electrolyte, flexibility of the polyelectrolyte increases favoring intra-molecular interactions, and leads to more compact and less expanded structure that occupies less volume (Basak et al., 2003), as also shown in Figure 2.18.

Effect of ionic strength in an aqueous medium on the phase behavior of polyelectrolytes has been studied using several polymer systems. For example, addition of salt resulted in contraction of the polymer backbone and reduction in hydrodynamic size of the aggregates obtained from poly(ethylene glycol)-based amphiphilic comb-like polymers (Basak et al., 2003). This was shown by the decrease in effective diameter of the intra-molecular aggregates, indicating more compact structure with the addition of salt (Figure 2.19). This result confirms that the addition of salt screens the electrostatic repulsion of the charged polymer backbone, increasing its flexibility and favoring the intra-molecular aggregates (Basak et al., 2003).

Ionic strength affects the phase behavior of blends of polycations and/or polyanions, as well. For example, mixtures of dextran sulphate sodium salt (an anionic polymer) and tetradecyltrimethylammonium bromide (a cationic surfactant) in aqueous solution showed both associative and/or segregative phase separation depending on ionic strength of the solvent (Hellebust et al., 2004). Here, associative phase separation is the case where the two polymers form a network and form one phase whereas the solvent forms the other phase. So, this is still a phase separated 3 component system, the two

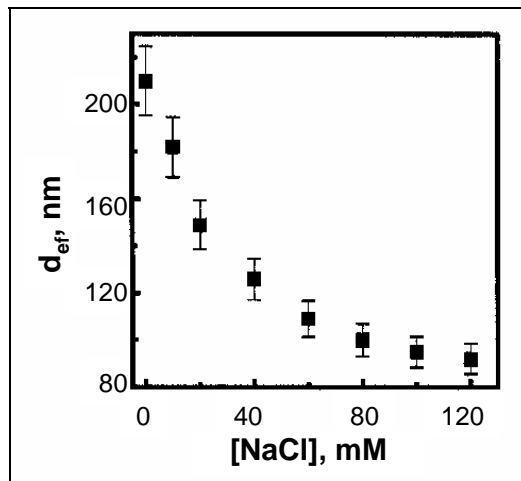


Figure 2.19: Effect of NaCl on the effective diameter of intra-molecular aggregates of poly(ethylene glycol)-based amphiphilic comb-like polymer at pH 6.2 at polymer concentration of 0.1 wt% (Basak et al., 2003)

polymers are phase separated from the solvent. Segregative phase separation is the case where the two polymers are separated in the common solvent, forming polymer1-solvent and polymer2-solvent phases. This also is a phase separated 3 component system. According to Hellebust et al., 2004, at high ionic strengths, electrostatic attraction between oppositely charged polymers (dextran sulphate sodium salt (an anionic polymer) and tetradecyltrimethylammonium bromide (a cationic surfactant) in aqueous solution) was screened, reducing the associative separation and increasing the segregative separation (Hellebust et al., 2004; Hellebust et al., 2003).

## **2.8. Determination of Phase Behavior and Miscibility/Immiscibility of Polymers**

### **2.8.1. Glass Transition Temperature as a Marker of Miscibility in the Solid State determined by Differential Scanning Calorimetry**

Differential Scanning Calorimetry (DSC) is one of the most commonly used thermal methods to establish miscibility/immiscibility in polymer blends. DSC measures the enthalpy (H) change with respect to temperature (T), which gives the heat capacity ( $C_p$ ) at constant pressure  $[(\partial H/\partial T)_P = C_p]$ . At  $T_g$ , an amorphous polymer goes through a step change in the magnitude of  $C_p$  with temperature. As a result,  $T_g$  is identified as the midpoint of step change in heat flow on DSC thermograms (Figure 2.20a).

Using DSC, miscibility/immiscibility in polymer blends is determined through measurement of  $T_g$  of the components (Figure 2.20a) versus that of blends (Figure 2.20b and Figure 2.20c). Perfectly miscible polymer mixtures exhibit a single  $T_g$  located between the  $T_g$ s of the individual components with a sharpness of transition similar to that of the components (Figure 2.20b). In the case of partial miscibility, broadening of the transition occurs. On the other hand, immiscible blends show multiple  $T_g$ s, corresponding to the  $T_g$  of each component in the mixture (Figure 2.20c) (Cascone et al., 1997; Morales-Diaz and Kokini, 1997, 1998; Shamblin et al., 1998; Tolstoguzov, 2000a; Sperling, 2001; Zimeri and Kokini, 2003a; Hartikainen et al., 2004).

DSC has been successfully used to show phase behavior in biopolymer blends, such as fructose-amylopectin blends (Kalichevsky and Blanshard, 1993); in 7S and 11S soy globulins (Morales-Diaz and Kokini, 1997); in starch-meat extrudates (Moraru et al., 2002); in inulin-amylopectin mixtures (Zimeri and Kokini, 2003a). For instance, in

Figure 2.21, two separate  $T_g$ s are shown in mixed inulin-waxy maize starch systems, indicating immiscible systems (Zimeri and Kokini, 2003a).

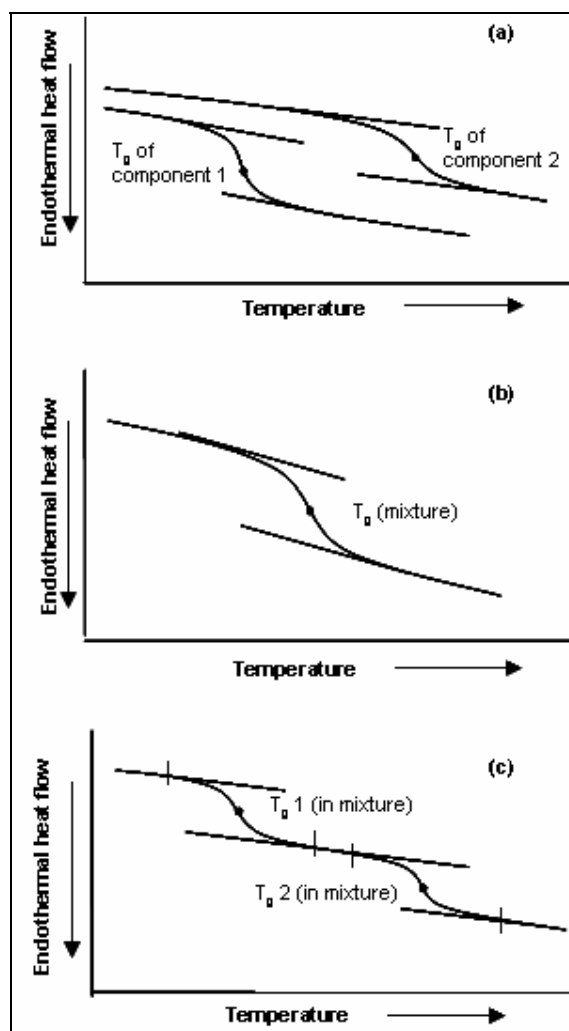


Figure 2.20: Determination of miscibility/immiscibility using DSC thermograms; (a)  $T_g$ s of two individual components; (b)  $T_g$  of miscible blend (1  $T_g$  between  $T_g$ s of individual components); (c)  $T_g$ s of immiscible blends (2  $T_g$ s in the mixture corresponding to  $T_g$ s of individual components)

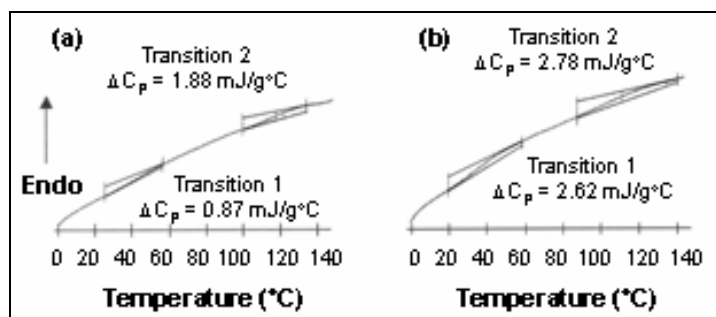


Figure 2.21: DSC rescans of mixed inulin-waxy maize starch systems stored at  $a_w=0.33$  for inulin to waxy maize starch ratio of; (a) 3:7; and (b) 6:4 (Zimeri and Kokini, 2003a)

Figure 2.22 shows another example of a 2- $T_g$  system. DSC thermogram of soy protein shows two individual  $T_g$ s; the higher  $T_g$  for the higher  $M_w$  component (11S globulin) and the lower  $T_g$  for the lower  $M_w$  component (7S globulin) (Morales-Diaz and Kokini, 1998).

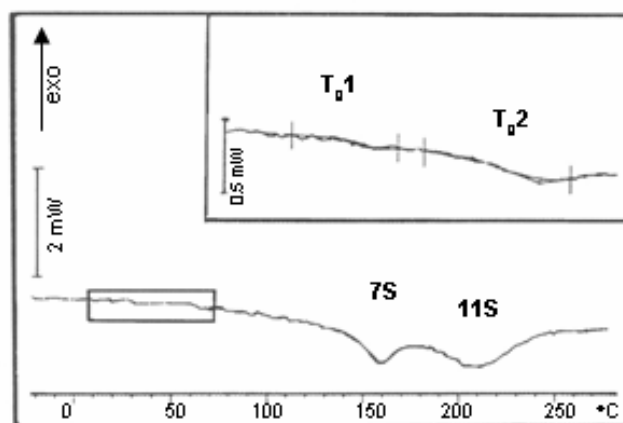


Figure 2.22: DSC curve obtained with both 7S and 11S enriched soy globulin fractions (Morales-Diaz and Kokini, 1997)

Kuo and Chang (2002) have also shown a single  $T_g$  behavior for phenolic resin/poly(acetoxystyrene) blends at various compositions, demonstrating that these are macroscopically miscible blends. Similarly, DSC thermogram of polyamide 66 and phenol formaldehyde resin blends at different compositions showed a single  $T_g$ , indicating that the components were miscible at different ratios of components (Hartikainen et al., 2004). Both these authors have shown that the hydrogen bonding between the two polymers is the reason for the experimentally observed miscibility, which will be further discussed in the following section.

### **2.8.2. Fourier Transform Infrared Spectroscopy to Investigate Specific Bonding Interactions in Polymer Blends**

Infrared spectroscopy is one of the many techniques that have been applied to study molecular interactions in polymer blends. Infrared spectra are obtained by passing infrared radiation through the sample of interest and observing the wavelength of absorption peaks. These peaks are formed by the absorption of the electromagnetic radiation and its conversion into specific molecular motions, such as C-H stretching, O-H stretching etc. (Sperling, 2001).

When two polymers are in separate and distinct phases (complete immiscible systems), it can be assumed that one polymer is isolated from the other and does not see or interfere with the other in IR spectral terms. In that case, the spectrum of the blend reflects the appropriate addition of the spectrum of the two individual components similar to two  $T_g$ s in the case of DSC. In the case of miscible or partially miscible polymer blends, the IR spectrum would show a composite of bands of the original IR spectrum of

the pure components and sometimes some additional spectra as well. These additional spectra, such as disappearance of component bands and/or shifts in component bands depending on the nature, relative strength and number of inter-molecular interactions between the polymeric components, occur as the results of miscibility (Coleman and Painter, 1990; Chalmers and Everall, 1993; Dong and Ozaki, 1997).

Fourier Transform Infrared (FTIR) spectroscopy provides a very sensitive way to monitor the changes in molecular interactions in a blend (Kolhe and Kannan, 2003). The sensitivity of FTIR spectroscopy to intermolecular interactions can be illustrated in Figure 2.23 for poly(vinyl acetate) and miscible blends at different ratios of poly(vinyl acetate) and poly(4-vinylphenol) (Coleman and Painter, 1990). In the IR spectrum, the carbonyl-stretching region of poly(vinyl acetate) and miscible blends of poly(vinyl acetate) and poly(4-vinylphenol) shows that the band at  $1739\text{cm}^{-1}$  was attributed to free poly(vinyl acetate) carbonyl groups (non hydrogen-bonded). As ratio of poly(4-vinylphenol) increased in the blend, a band at  $1714\text{cm}^{-1}$  started to appear and its intensity increased at higher poly(4-vinylphenol) ratios. This band at  $1714\text{cm}^{-1}$  was the representative of poly(vinyl acetate) carbonyl groups hydrogen-bonded to the phenolic hydroxyl group of poly(4-vinylphenol), indicating mixing at the molecular level (Coleman and Painter, 1990).

Kuo and Chang (2002) investigated the miscibility behavior and specific interactions in phenolic resin ( $M_w=1,200$ ) and poly(acetoxystyrene) (PAS) ( $M_w=35,000$ ) blends using DSC and FTIR. DSC results showed a single  $T_g$  over the entire composition range, indication fully miscible blends. In FTIR experiments, from carbonyl stretching frequencies ( $1820\text{-}1680\text{cm}^{-1}$ ), band at  $1760\text{cm}^{-1}$  was assigned to free carbonyl groups,

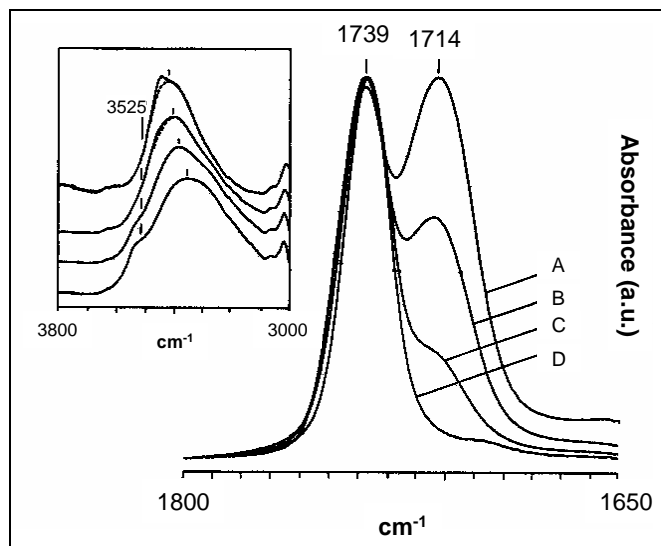


Figure 2.23: FTIR spectra of poly(4-vinylphenol):poly(vinyl acetate) blends; A) 80:20; B) 50:50; C) 20:80; D) 0:100 (Coleman and Painter, 1990)

whereas band at  $1730\text{cm}^{-1}$  was assigned to hydrogen-bonded carbonyl groups (Figure 2.24). The increase in the band at  $1730\text{cm}^{-1}$  with phenolic content indicated hydrogen bonding between carbonyl group of PAS and hydroxyl group of phenolic resin (Figure 2.24) (Kuo and Chang, 2002).

According to Kuo and Chang (2002), from hydroxyl stretching frequencies ( $4000\text{--}2700\text{cm}^{-1}$ ), pure phenolic resin had a broad band at  $3350\text{cm}^{-1}$ , which was due to large number of hydrogen-bonded hydroxyl groups, and a narrow band at  $3525\text{cm}^{-1}$ , which was assigned to the free hydroxyl group (Figure 2.25). The band at  $3525\text{cm}^{-1}$  decreased with PAS content and the band at  $3350\text{cm}^{-1}$  shifted to  $3384\text{cm}^{-1}$  with increasing PAS content, indicating the switch from hydroxyl-hydroxyl bond to hydroxyl-carbonyl bond (Figure 2.25). This shows once more that when phenolic resin, self-associating polymer, was mixed with PAS, the carbonyl containing polymer, hydrogen bonds were formed between the polymers through hydroxyl groups of phenolic resin and carbonyl groups of the PAS.



As a summary, carbonyl and hydroxyl stretching frequencies in the FTIR spectra of the blends (Figure 2.24 and Figure 2.25) has shown that the miscibility, determined by 1  $T_g$  behavior in blends, was due to the formation of intermolecular hydrogen bonding between the hydroxyl group of the phenolic resin and the carbonyl group of PAS (Figure 2.24 and Figure 2.25) (Kuo and Chang, 2002).

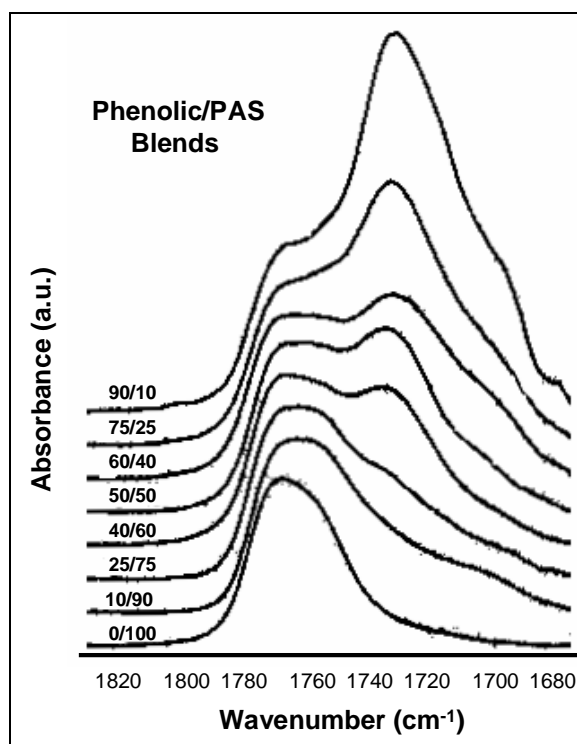


Figure 2.24: FTIR spectra for phenolic/PAS blends at room temperature in 1820-1680 $\text{cm}^{-1}$  (Kuo and Chang, 2002)

Using FTIR, Hartikainen et al. (2004) have shown that the carbonyl oxygen of N-methylacetamide (NMA), as a proton acceptor, hydrogen bonded with the hydroxyl

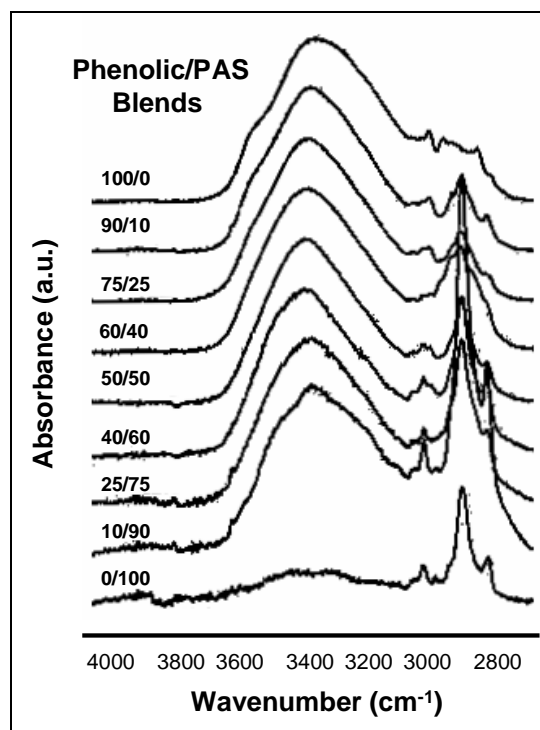


Figure 2.25: FTIR spectra for phenolic/PAS blends at room temperature in 4000-2700 $\text{cm}^{-1}$  (Kuo and Chang, 2002)

group of phenol, as a proton donor. This was determined by a shoulder formed at 3420 $\text{cm}^{-1}$ , which the researchers assigned to the O-H stretching vibrations of phenol hydrogen-bonded with NMA. In the same study, DSC analysis showed a single  $T_g$  for all blends, implying miscibility. Combining DSC with FTIR gave very convincing and powerful diagnostic information to demonstrate miscibility between the two polymers and the mechanism of miscibility through hydrogen bonding (Hartikainen et al., 2004).

Hydroxyl and carbonyl stretching regions of FTIR spectra clearly gives very sensitive information on specific bonding interactions in polymer blends with hydroxyl and carbonyl groups, which in turn results in miscibility, partial miscibility or complete immiscibility between the blend components. The use of FTIR to investigate interactions,

specifically hydrogen bonding interactions, in synthetic polymers is quite common as illustrates above (Coleman and Painter, 1990, 2006; Coleman et al., 1991; Kuo and Chang, 2001, 2002; Kolhe and Kannan, 2003; Hartikainen et al., 2004). In most of these studies, one of the components has one hydroxyl group in its monomeric unit that gives signature information in the hydroxyl stretching regions, whereas the other component in the mixture has a different group (a carbonyl group) that can make hydrogen bonding with the hydroxyl group of the first component. Therefore, carbonyl stretching regions together with hydroxyl stretching regions of the FTIR spectra of the components and the blends enable significant information about the specific bonding interactions in these systems. On the other hand, the application of the FTIR spectroscopy to carbohydrate polymers to study specific interactions that affect miscibility is more complex due to the multiple hydrogen bonding groups present in the monomeric unit of carbohydrates, such as glucose. Moreover, most carbohydrates are polymers of simple sugars that do not have any carbonyl groups which would make the IR spectra interpretation easier. An application of FTIR spectroscopy to investigate specific bonding interaction in carbohydrate blends would lead to understanding the possible mechanism of miscibility in these systems. Icoz and Kokini (2007a) provide an example of the use of FTIR spectroscopy coupled with DSC to determine miscibility and the possible mechanism of miscibility on dextran blends, which is one of its kind in the literature to date.

### 3. MATERIALS AND METHODS

#### 3.1. Strategy of the Research

This study mainly consists of two parts:

**Part A)** In the first part, standard dextrans with different molecular weights and chemically derivatized dextrans were used to study carbohydrate-carbohydrate interactions. Dextrans are excellent simple model systems for glucose based carbohydrates, such as starch. The commercial availability of different specific molecular weights and chemically derivatized forms of dextran make it possible to investigate how small changes in the molecular structure, polymer concentration and ionic strength in simple dextran systems affect miscibility in relation to carbohydrate polymers. Standard dextrans that have the same repeating unit chemistry with different molecular weights served as the initial model with chemically identical repeating units, which were tested as possibly compatible systems. The first question to be investigated was: “Are there barriers to miscibility of dextrans with different molecular weights?” In order to characterize the phase behavior of each dextran system as a basis for molecular compatibility/incompatibility, the glass transition temperature ( $T_g$ ) and moisture sorption properties of standard dextrans with different molecular weights were obtained. The factors that had impact on the phase behavior of dextran systems, such as effect of method of mixture preparation; the influence of low molecular weight dextrans on the glass transition temperature of the mixed systems; and the effect of polymer concentration on miscibility of the mixtures were studied.

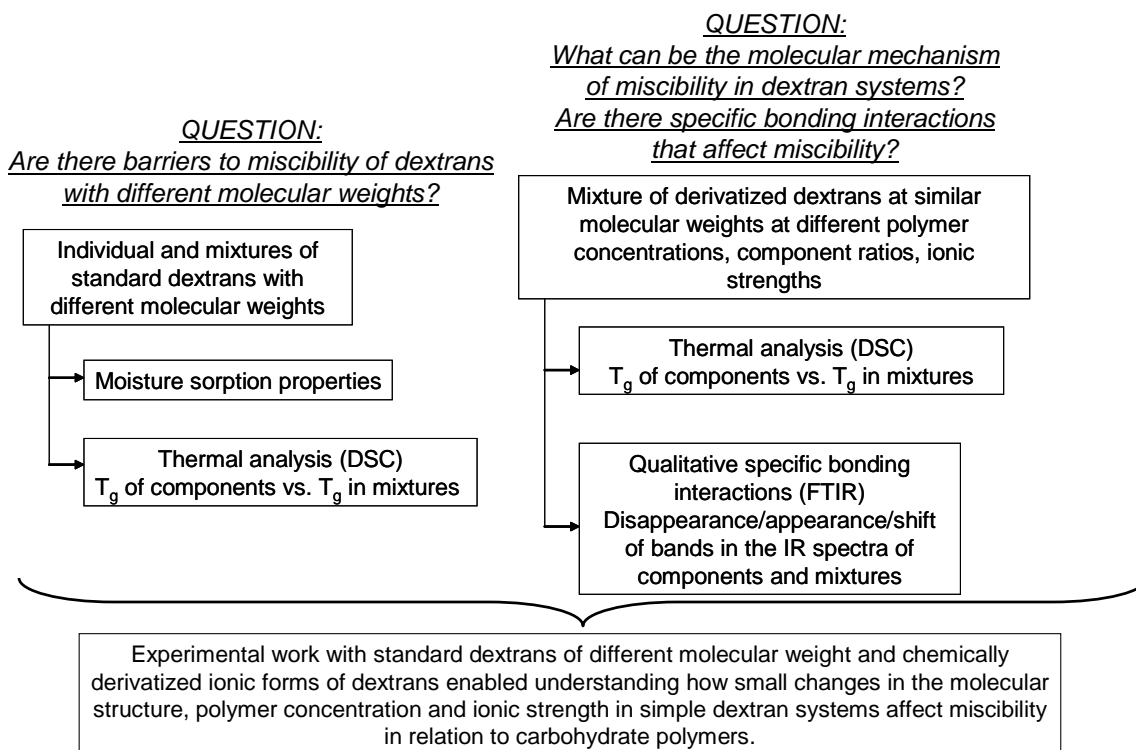
The next question to be investigated was; “What is the molecular mechanism of miscibility in dextran systems?” and “Are there specific bonding interactions that affect miscibility?” To find answers for these questions, commercially available chemically derivatized dextrans [DEAE (diethylaminoethyl dextran) and DS500 (dextran sulfate), both produced from the standard dextran with  $M_w=500,000$ ] were used. The systems were prepared at different concentrations and added salt (NaCl) and were investigated for their thermal behavior (through determination of  $T_g$ ) and specific binding interactions (using FTIR spectroscopy). These dextrans were chosen among other dextrans, because they had significant differences in their repeating units so that the specific interactions could be monitored by FTIR spectroscopy.

**Part B)** The second part consists of quantitative prediction of miscibility in carbohydrate systems. The specific question to be investigated was: “Can we quantitatively predict miscibility/immiscibility in carbohydrate biopolymers using thermodynamic rules of mixing which have been designed to account for the properties of hydrogen bonded food biopolymers?” The investigation involved application and examination of state of the art theoretical thermodynamic models for suitability to predict miscibility in dextran systems in relation to carbohydrate polymers. A predictive methodology to determine solubility parameters of dextrans with different molecular weights using their glass transition temperature was presented. Theoretical ideas based on the role of the number of configurational arrangements and quantitative measures based on dispersive interactions (Flory-Huggins theory) were investigated for its ability to quantitatively explain the miscibility in dextran systems. Since most carbohydrate polymers have structural groups that can form a large number of hydrogen bonds,

prediction of their molecular mixing was shown to require advanced models which are able to include the role of hydrogen bonds in affecting miscibility. One such quantitative framework is the Painter-Coleman association model, which builds on the conformational and configurational theories advanced by Flory-Huggins by adding a component that accounts for hydrogen bonding interactions. This advanced theoretical model was used to predict miscibility in dextran systems. Finally, the understanding gained with dextran systems was extended to real carbohydrate mixtures to test miscibility in a case study of inulin-amylopectin mixtures.

Figure 3.1 shows the schematic diagram for the strategy of the research.

## PART A



## PART B

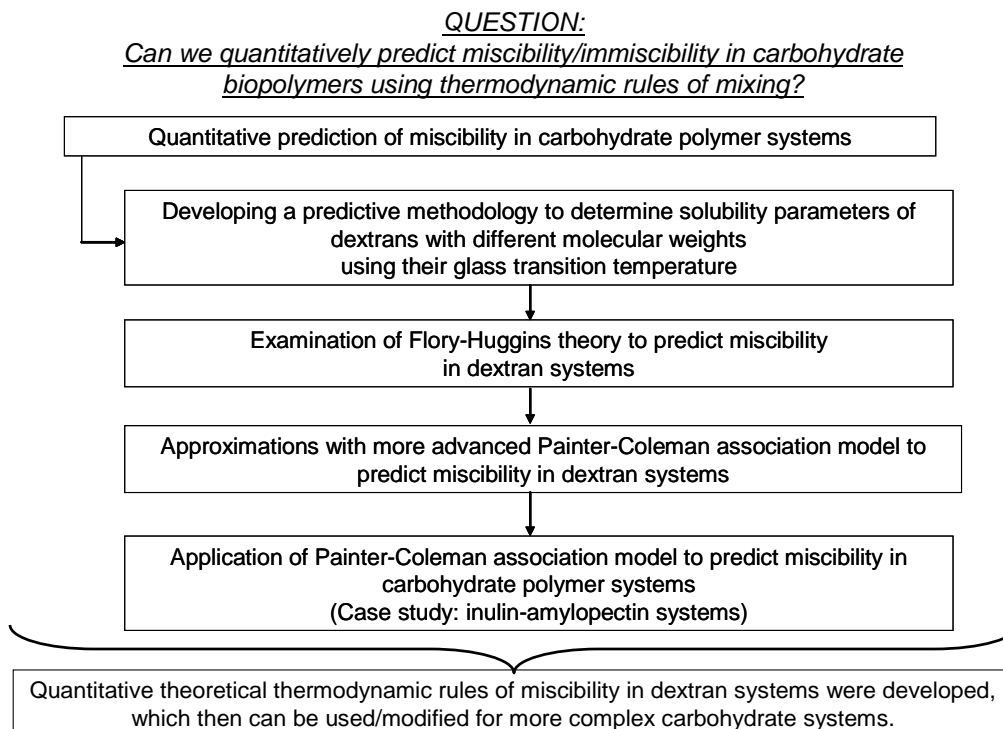


Figure 3.1: Schematic diagram of the strategy of the research

### 3.2. Investigation of Miscibility in Dextran Systems with Different $M_w$

#### 3.2.1. Materials

Seven dextrans with weight-average molecular weights of 970 (lot no: 289350); 5,200 (lot no: 288649); 10,800 (lot no: 291111); 43,000 (lot no: 285740); 67,200 (lot no: 279504); 482,000 (lot no: 286753) and 2,000,000 (lot no: 285645) (Amersham Biosciences, Piscataway, NJ) were used.

Dextrans are high molecular weight polymers of glucose (Figure 3.2) obtained by the fermentation of sucrose with the bacterium *Leuconostoc mesenteroides*, strain B512. About 95% of the linkages in dextran are  $\alpha$ -D-(1-6), while the other 5% of linkages are  $\alpha$ -D-(1-3), and account for branching (Ioan et al., 2000). Dextrans behave as flexible, slightly branched random coil polysaccharides rather than ideal random coils in dilute solutions (Tvaroska et al., 1978; Nordmeier, 1993) and are highly soluble in water at room temperature (Blondiaux et al., 2001; Walsh et al., 2003). They are excellent model systems for food carbohydrate polymers as their molecular structures are similar and they are readily available in a wide range of molecular weights and some chemically derivatized forms. They also provide the precise and thorough characterization needed to quantitatively test thermodynamic principles and conduct meaningful interpretable experiments.

#### 3.2.2. Moisture Sorption Isotherms of Dextrans

Pure dextran samples were equilibrated at room temperature, at six water activity ( $a_w$ ) values: 0.00; 0.12; 0.33; 0.52; 0.75; and 0.93, over  $P_2O_5$  ( $a_w=0.00$ ) and saturated



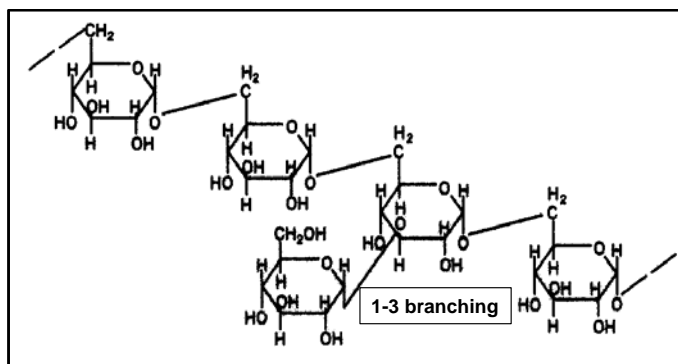


Figure 3.2: Molecular structure of dextran

solutions of the following salts: LiCl; MgCl<sub>2</sub>; Mg(NO<sub>3</sub>)<sub>2</sub>; NaCl and KNO<sub>3</sub>, respectively (Nyqvist, 1983). Moisture contents were measured using the AOAC method 950.46 (air-drying at 103°C, 16-18h), using a Thermolyne 9000 air-drying oven (Dubuque, IA). The water activity of each sample was measured using an Aqualab hygrometer (Decagon Devices Inc., Pullman, WA). Four replicate measurements were performed for each analysis.

The moisture sorption isotherms were built by plotting equilibrium moisture content vs.  $a_w$ . The data were fitted to the Guggenheim-Anderson-DeBoer (GAB) model (Equation 3.1), which is given as;

$$\frac{M}{M_0} = \frac{C_G k a_w}{(1 - k a_w)(1 - k a_w + C_G k a_w)} \quad (3.1)$$

where  $M$  is the equilibrium moisture content (dry basis);  $M_0$  is the monolayer moisture content;  $C_G$  is the Guggenheim constant; and  $k$  is a factor correcting properties of the multilayer with respect to the bulk liquid (Singh and Heldman, 1993; Bell and Labuza, 2000).

In order to fit the experimental data to the GAB model, Equation 3.1 was rewritten in the form of a second-order polynomial as;

$$\frac{a_w}{M} = \alpha a_w^2 + \beta a_w + \gamma \quad (3.2)$$

$$\text{where } \alpha = \frac{k}{M_0} \left[ \frac{1}{C_G} - 1 \right], \beta = \frac{1}{M_0} \left[ 1 - \frac{2}{C_G} \right] \text{ and } \gamma = \frac{1}{C_G k M_0} \quad (3.3)$$

The experimental water activity and equilibrium moisture content data were plotted using Equation 3.2. From the second-order regression line;  $\alpha$ ,  $\beta$ , and  $\gamma$  were calculated from which  $k$ ,  $M_0$  and  $C_G$  were determined (Singh and Heldman, 1993; Bell and Labuza, 2000). The details of the calculations are shown in Appendix A.

### 3.2.3. Sample Preparation for Thermal Analysis

#### 3.2.3.1. Individual Dextrans

All dextrans were used in pure powder form, as purchased from the manufacturer. The samples were equilibrated at the same  $a_w$  values as in Section 3.2.2 at room temperature in desiccators over  $P_2O_5$  and saturated salt solutions. After equilibration,  $20 \pm 2$  mg of dextran sample was weighed into hermetic, stainless steel, medium pressure DSC crucibles (Mettler Instrument Inc., Highstown, NJ). Then, the crucibles were sealed immediately.

#### 3.2.3.2. Dextran Mixtures

##### *a) Mixtures Formed by Physical Mixing of Dextran Powders:*

After equilibration at  $a_w=0.33$ , pure dextran powders with  $M_w=970$  and  $M_w=2,000,000$  were hand-mixed in equal amounts.  $20 \pm 2$  mg of this dextran mixture were

weighed into DSC crucibles and the crucibles were sealed immediately. The same procedure was followed for obtaining mixtures of dextrans with  $M_w=5,200$  and  $M_w=2,000,000$  at the same water activity ( $a_w=0.33$ ).

***b) Mixtures Obtained by Preliminary Solubilization of Dextrans:***

30% (w/w) (w.b.) polymer concentrated solutions of dextrans with  $M_w=970$  and  $M_w=2,000,000$  were prepared and then mixed in w/w (d.b.) ratios of 50/50; 40/60; 30/70; 20/80 and 10/90, respectively, by hand-mixing at room temperature. All the solutions were freeze-dried for 36 hours in a bench top freeze dryer (The Virtis Company Inc., Gardiner, NY). The freeze-dried samples were ground at room temperature using a mortar and a pestle. The dry powders were then equilibrated at  $a_w=0.33$ . The same procedure was followed for preparing mixtures of dextrans with  $M_w=5,200/M_w=2,000,000$  and  $M_w=10,800/M_w=2,000,000$ . From equilibrated mixtures,  $20\pm 2\text{mg}$  was weighed into DSC crucibles and the crucibles were sealed immediately.

In addition to 30% (w/w) (w.b.) polymer concentrated solution of dextrans with  $M_w=970/M_w=2,000,000$ ; 50% and 70% (w/w) (w.b.) solutions of the same dextrans in w/w (d.b.) ratio of 50/50 were also prepared.

### **3.2.4. Measurement of Glass Transition Temperature ( $T_g$ ) by Differential Scanning Calorimetry (DSC)**

Thermal analysis was performed using a TA 4000 Thermal Analysis System with a DSC 30-S Cell/TC11 TA Processor (Mettler Instrument Inc., Highstown, NJ). 40 $\mu\text{l}$ , medium pressure, stainless steel crucibles with O-ring were used for the analysis. An empty crucible was used as a reference. Calibration of the instrument was performed

using indium as a standard. A heating rate of 10°C/min was used throughout the study. Pure dextrans equilibrated at different water activities were scanned between -50°C to 200°C, depending on the  $a_w$  values of the samples. Mixtures obtained by preliminary solubilization and equilibrated at  $a_w=0.33$  were scanned between 30-130°C; mixtures formed by mixing dextran powders and equilibrated at  $a_w=0.33$  were scanned between 0-150°C. Rescans were performed immediately after each scan, in order to erase the thermal history of the samples and to confirm the location of the  $T_g$ , based on the reversibility of this second order transition. The glass transition temperature was determined from the DSC rescans, at the midpoint in the shift of the heat flow baseline, which corresponded to the temperature at which one-half of the change in the heat capacity,  $\Delta C_p$ , occurred. The reported data were the averages of two replicate measurements.

### **3.2.5. Steady Shear Rheological Measurements**

Pure dextran solutions containing 20% and 40% dextrans with molecular weights of 970; 10,800; 43,000; 67,200 and 482,000 were prepared. Steady shear rheological measurements were conducted with shear rates ranging from  $10^{-2}$  to  $10^3 \text{ s}^{-1}$ , at a frequency of 6.28rad/s (1 Hz), using a strain-controlled rheometer, Advanced Rheometric Expansion System (ARES), in conjunction with the Orchestrator data collection and analysis software (Rheometric Scientific, Inc., Piscataway, NJ). Cone and plate geometry (interplaten gap = 0.05mm) with 50mm diameter was used. In order to avoid dehydration during measurements, the samples were thinly coated with mineral oil. Zero-shear

viscosity for each sample was determined by extrapolating the apparent viscosity to low values of shear rate. The reported results are the average of two replicate measurements.

### 3.3. Investigation of the Specific Bonding Interactions and the Possible Mechanism of Miscibility in Dextran Systems

#### 3.3.1. Materials

Two chemically derivatized dextrans, dextran sulfate (DS500) and diethylaminoethyl dextran (DEAE) that are both produced from standard dextran with an average molecular weight of 500,000, were used (pK Chemicals A/S, Denmark). Diethylaminoethyl dextran (DEAE) is a chemically derivatized dextran produced by reacting diethylaminoethyl chloride with standard dextran. It is a polycationic derivative and the degree of substitution corresponds to approximately 1 DEAE substituent per 3 glucose units (0.33 mol DEAE per 1 mol glucose) (Figure 3.3).

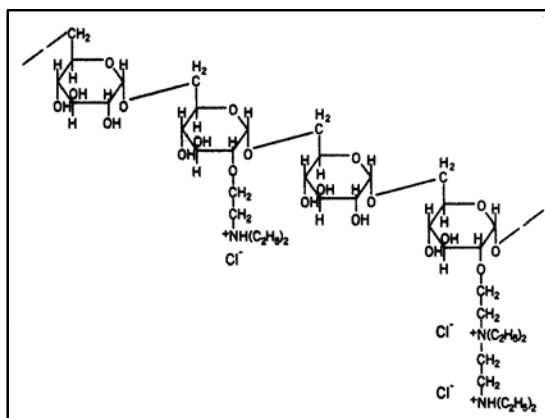


Figure 3.3: Molecular structure of diethylaminoethyl dextran (DEAE)

Dextran sulfate (DS500) is another derivatized dextran that is produced by sulfating standard dextran. It is the polyanionic derivative in which each glucose unit has approximately two sulfate groups, located normally at C2 and C4 of the glucose units (2 mol sulfate per 1 mol glucose) (Figure 3.4).

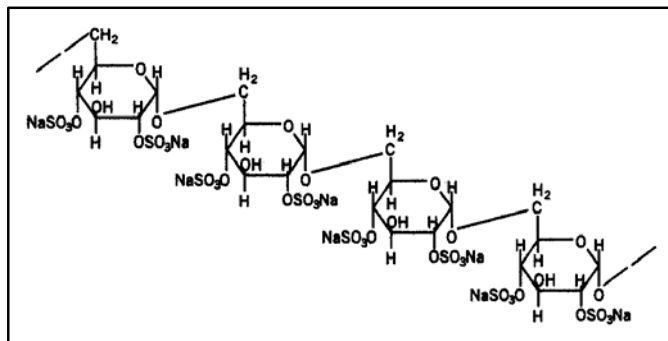


Figure 3.4: Molecular structure of dextran sulfate (DS500)

### 3.3.2. Sample Preparation for DSC and FTIR Spectroscopy Measurements

The samples were prepared at different total polymer concentrations (30%; 50%; and 70% (w/w, w.b.)); and at various component ratios (0/100; 25/75; 50/50; 75/25; and 100/0 (w/w, d.b.)). The powders of the components were first mixed and then solubilized using deionized, distilled water at 45-50°C to ensure complete solubilization of the powders in water, especially at high total polymer concentrations. The effect of salt addition on the miscibility was investigated using NaCl solutions with ionic strengths of 0; 1M; and 2M. The required amount of salt was added to the systems after solubilizing the dextran powders in water. By this way, “salting out effect” of NaCl, where salt competes for the available water resulting in insufficient solubilization of dextran, was

eliminated. The prepared solutions were freeze-dried in a bench top freeze dryer (The Virtis Company Inc., Gardiner, NY). Dried samples were grinded using a mortar and a pestle. These ground samples were then equilibrated at a specific water activity to ensure that all samples analyzed were in similar conditions (at  $a_w=0.33$  over saturated  $\text{MgCl}_2$  solution). After equilibration, the powder samples were directly used for analysis.

### **3.3.3. Moisture Content of Samples**

The moisture content of samples was measured following the same procedure in Section 3.2.2. Two replicate measurements were performed for each analysis.

### **3.3.4. Methods of Analysis**

#### **3.3.4.1. Differential Scanning Calorimetry (DSC)**

Thermal analysis was performed using the same procedure as in Section 3.2.4. Scans ranges were between 0°C and 150°C. The reported data are the averages of at least two replicate measurements.

#### **3.3.4.2. Fourier Transform Infrared (FTIR) Spectroscopy**

A Bruker Equinox 55 FTIR-Attenuated Total Reflectance (ATR) (SensIR Durascope<sup>TM</sup>) spectrometer (Bruker Optics Inc., Billerica, MA), available in Chemistry Department at Rutgers, The State University of New Jersey, was used for the analysis. Approximately 10mg of powder samples was placed on the ATR crystal and the measurements were done by co-adding 100 scans with a resolution of  $4\text{cm}^{-1}$ .

### 3.4. Quantitative Prediction of Miscibility in Carbohydrate Polymer Systems

All systems under investigation for predictive miscibility were two component systems (i.e. low and high  $M_w$  dextrans) at limited moisture contents. The quantitative predictions developed were compared to the experimental data, where two component systems were obtained by mixing in solution and removing the solvent by freeze-drying as described in Section 3.2.3.2. For experimental analysis, all two component systems were equilibrated at a particular water activity to keep all materials at limited moisture environment.

#### 3.4.1. Determination of Volume Fractions in Dextran Mixtures

The molecular weight of the monomeric (repeating) unit of dextran is 162g/mol (Figure 3.5). Equation 2.6 was used to calculate the volume fractions in the two-component dextran systems using moles of the two polymers in the blend ( $n_A$  and  $n_B$ ) and the number of segments in each polymer chain ( $M_A$  and  $M_B$ ). As an example, the calculated volume fractions of dextran with  $M_w=1,000$  ( $\Phi_B$ ) as a function of % weight/weight ratio ( $m_B$ ) is shown in Figure 3.6. For the dextran systems under investigation, for example, 40/60% ratio of the two component  $M_w=1,000/M_w=2,000,000$  had volume fractions as  $\Phi_B=0.4$  ( $M_w=1,000$ ) and  $\Phi_A=0.6$  ( $M_w=2,000,000$ ), respectively. The details of the calculations are shown in Appendix B.



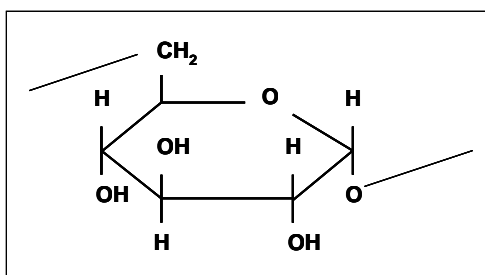


Figure 3.5: Monomer (repeating unit) of dextran

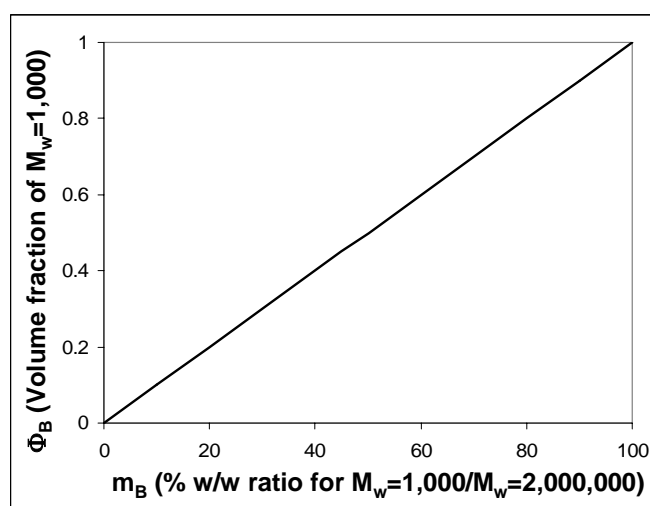


Figure 3.6: Calculated volume fractions in the system of two dextrans with  $M_w=1,000$  and  $M_w=2,000,000$  as a function of % w/w ratio ( $m_B$ )

### 3.4.2. Application of Original Flory-Huggins Theory to Predict Miscibility in Dextran Systems

#### 3.4.2.1. Determination of Solubility Parameter of Monomeric Unit of Dextran

Solubility parameter ( $\delta$ ) for the monomer (repeating unit) of dextran was calculated through the atomic groups that conform the molecule using Equation 2.9 and Equation 2.10, respectively.  $\delta_{\text{monomer}}$  was calculated as  $19.8(\text{cal}/\text{cm}^3)^{1/2}$  using Equation 2.9

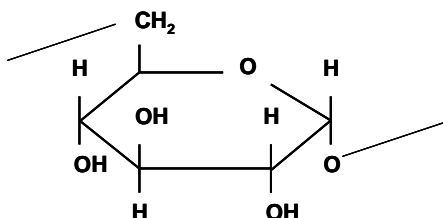
(Figure 3.7). Using the second predictive equation for the solubility parameter (Equation 2.10),  $\delta$  for the monomer unit of dextran was recalculated as  $22.6(\text{cal/cm}^3)^{1/2}$  (Figure 3.8), which was relatively different from the one calculated in Figure 3.7. In Equation 2.9, only dispersive forces were included in the solubility parameter prediction, whereas in Equation 2.10, a rough estimation due to polar and hydrogen bonding forces were included together with dispersive forces, resulting in the difference between the two predicted values. In the next section, a predictive methodology to calculate the solubility parameters of dextrans with different molecular weights are presented, making use of the solubility parameters of monomer calculated in Figure 3.6 and Figure 3.7. Further, it was investigated which  $\delta$  approximation gave better results for prediction of miscibility in dextran systems and the results are presented in Section 4.3.1.

#### **3.4.2.2. A Predictive Methodology to Determine the Solubility Parameters of Dextrans with Different $M_w$ as a Function of Their Glass Transition Temperatures**

Hayes (1961) has suggested that molar cohesive energy of a polymer can be written directly proportional to the molar rotational energy of the polymer and suggested a relationship between rotational energy and the glass transition temperature using a number of different synthetic polymers with known structures and  $T_g$  values. During cooling, the rotation of various atoms and groups in a polymer becomes less and at  $T_g$ , this rotation is finally inhibited due to lack of enough rotational energy to overcome the forces holding the molecules together (Hayes, 1961). At  $T_g$ ;

$$E_{\text{coh}} = E_R + C.n \quad (3.4)$$

where  $E_{\text{coh}}$  is the molar cohesive energy;  $E_R$  is the molar rotational energy;  $n$  is the



GROUP	Number of group	$E_{coh}$ (J/mol)	$\Sigma E_{coh}$ (J/mol)	$V_m$ (cm <sup>3</sup> /mol)	$\Sigma V_m$ (cm <sup>3</sup> /mol)
— CH <sub>2</sub>	1	4,950	4,950	16.1	16.1
>CH—	5	3,430	17,150	-1.0	-5.0
— OH	3	21,850	65,550	13.0	39.0
— O —	2	3,350	6,700	3.8	7.6

$$\delta_{monomer of dextran} = \left( \frac{\Sigma E_{coh}}{\Sigma V_m} \right)^{1/2} = \left( \frac{94,350}{57.7} \right)^{1/2} \left( \frac{J}{cm^3} \right)^{1/2} = 40.4 \left( \frac{J}{cm^3} \right)^{1/2} = 19.8 \left( \frac{cal}{cm^3} \right)^{1/2}$$

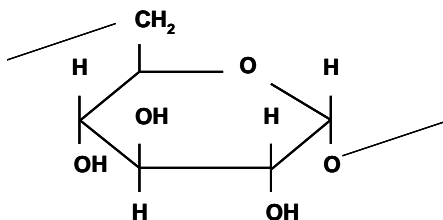
Figure 3.7: Calculation of the solubility parameter for monomer of dextran ( $E_{coh}$  and  $V_m$  values for different atomic groups were obtained from Van Krevelen and Hoftyzer (1976))

degrees of freedom that is related to the ability of atoms to rotate; and  $C$  is a constant.  $E_R$  can be written as a function of  $T_g$  as (Hayes, 1961);

$$E_R = (0.5).n.R.T_g \quad (3.5)$$

where  $R$  is the gas constant.

The rules to determine “ $n$ ”, in Equation 3.4 and Equation 3.5 are; “1” is assigned for each atom or group that can rotate without causing any chain motion; “6” is assigned for each atom or group that causes chain motion when it rotates; an additional “2” is



GROUP	Number of group	$F_{di}$ (J.cm <sup>3</sup> /mol) <sup>1/2</sup>	$F_{pi}$ (J.cm <sup>3</sup> /mol) <sup>1/2</sup>	$F_{pi}^2$ (J.cm <sup>3</sup> /mol)	$E_{hi}$ (J/mol)
— CH <sub>2</sub>	1	(270)*1	0	(0)*1	(0)*1
>CH—	5	(80)*5	0	(0)*5	(0)*5
— OH	3	(210)*3	500	(250,000)*3	(20,000)*3
— O —	2	(100)*2	400	(160,000)*2	(3,000)*2

$$\delta_{\text{monomer of dextran}} = \left( 26^2 + 17.9^2 + 33.8^2 \right)^{1/2} = 46.3 \left( \frac{J}{cm^3} \right)^{1/2} = 22.6 \left( \frac{cal}{cm^3} \right)^{1/2}$$

Figure 3.8: A second method for calculation of the solubility parameter for monomer of dextran ( $F_{di}$ ,  $F_{pi}$  and  $E_{hi}$  values for different atomic groups were obtained from Van Krevelen and Hoftyzer (1976))

assigned when any branch group cannot rotate without bumping into the polymer chain due to its size; when a double bond or phenyl group prevents the rotation of a particular atom or group of atoms, the group that is restricted is counted as one atom (Hayes, 1961). Based on these rules, “n” for the monomeric unit of dextran was calculated as follows: 7 H atoms connected to C atoms that can rotate without causing any chain motion ( $7 \times 1 = 7$ ); 3 H atoms on OH groups that can rotate without causing any chain motion ( $3 \times 1 = 3$ ); 3 O atoms on OH groups that can cause chain motion when they rotate ( $3 \times 6 = 18$ ); 2 individual O atoms that can cause chain motion when they rotate ( $2 \times 6 = 12$ ); 6 C atoms that can

cause chain motion when they rotate ( $6 \times 6 = 36$ ). Therefore, the total number of “n” for the monomeric unit of dextran was calculated to be  $n=76$ .

Inserting Equation 3.5 into Equation 3.4 and dividing both sides of the resulting equation by molar volume of the monomer ( $V_m$ ), Equation 3.6 would be obtained following Equation 2.8:

$$\frac{E_{coh}}{V_m} = CED = \delta^2 = \frac{(0.5).n.R.T_g + C.n}{V_m} \quad (3.6)$$

where CED is the cohesive energy density. As mentioned earlier, CED is related to the energy changes needed to separate molecules from each other during mixing or solution process and in fact it is the energy required to completely vaporize a mole of a molecule thus estimating all of the forces that are holding the molecule together. According to Equation 3.6, CED would increase with  $T_g$ . For a polymer of different molecular weights, it has been shown that  $T_g$  increases as  $M_w$  increases (Cowie, 1975; Aklonis and MacKnight, 1983; Slade and Levine, 1991a, 1991b; Ruan et al., 1999; Sperling, 2001, Gropper et al., 2002). So, according to Equation 3.6, CED would increase with  $M_w$ . However, there should be an inverse relationship between CED and  $M_w$ , because as the molecule gets larger at higher molecular weights, lower energy per unit volume would be sufficient to separate the molecules from each other (easier separation). For example, for simple liquids, CED is inversely related to  $M_w$  and given as (Lide, 2004);

$$CED = \frac{\Delta H_v - R.T}{M_w / \rho} \quad (3.7)$$

where  $\Delta H_v$  is the heat of vaporization;  $R$  is the gas constant;  $T$  is the temperature; and  $\rho$  is the density. Moreover, Patnaik and Pachter (1999) and (2002) have shown the inverse relationship between CED and  $M_w$  of poly(methyl methacrylate) (PMMA) using

molecular dynamics simulations. The researchers have calculated the cohesive energy density for PMMA with 100 monomeric units as  $150\text{J}/\text{cm}^3$ , whereas the cohesive energy density for PMMA with 6, 3, 1 monomeric units as  $225\text{J}/\text{cm}^3$ ,  $276\text{J}/\text{cm}^3$ ,  $415\text{J}/\text{cm}^3$ , respectively. This shows that as the molecule gets larger at higher molecular weights, the energy needed to separate all contacts per unit volume gets smaller (Patnaik and Pachter, 1999, 2002). The reason why there is a direct relationship between cohesive energy and  $T_g$  according to Hayes (1961) (Equation 3.6) would possibly be because the researcher did not focus on the polymers with different  $M_w$ , but polymers with different  $T_g$  values. A polymer with a high  $T_g$  value would not necessarily mean that it would have a higher  $M_w$  for different polymers in Hayes (1961) study. Since solubility parameters as a function of  $M_w$  for one type of polymer (dextran, in our study) was needed, we have done a modification on the suggested relation by Hayes (1961), following the molecular dynamic simulations by Patnaik and Pachter (1999) and (2002), described as follows: Using the data points reported in Patnaik and Pachter (2002), a logarithmic relationship between CED and number of monomers was fitted with an acceptable regression coefficient (Figure 3.9 and Equation 3.8).

$$\text{CED} = (-44.69) \cdot \ln(\# \text{ of monomers}) + 356.93 \quad R^2 = 0.85 \quad (3.8)$$

where  $\# \text{ of monomers} = \frac{Mw_{\text{polymer}}}{Mw_{\text{monomer}}}$ . As a more generalized form, Equation 3.8 can be

written as;

$$\text{CED} = (-A) \cdot \ln(Mw_{\text{polymer}}) + B \quad (3.9)$$

where A and B are constants, showing the inverse relationship between CED and  $M_w$  of the polymer. In order to obtain a similar relationship between solubility parameters and

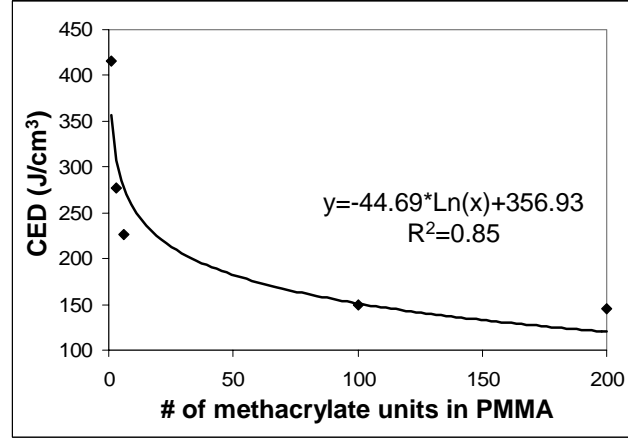


Figure 3.9: Variation of cohesive energy density (CED) as a function of number of methacrylate units in poly(methyl methacrylate) - redrawn from the figure reported by Patnaik and Pachter (2002)

$M_w$  of the dextrans, the  $T_g$ - $M_w$  relationships reported by Icoz et al. (2005) were used. The regression lines for  $T_g$ - $M_w$  relations for dextrans at  $a_w=0.00$  was given as;

$$M_w < \sim 27,000$$

$$T_g = (13.30) \cdot \ln(Mw_{\text{polymer}}) + 39.82 \quad R^2 = 0.92 \quad (3.10)$$

$$M_w > \sim 27,000$$

$$T_g = (0.98) \cdot \ln(Mw_{\text{polymer}}) + 165.58 \quad R^2 = 0.97 \quad (3.11)$$

(Icoz et al., 2005). So when Equation 3.10 and Equation 3.11 were inserted into Equation 3.6, keeping in mind that CED would be inversely related to  $M_w$  following Patnaik and Pachter (1999) and (2002), a modification of inserting (-) sign in front of rotational energy term was needed. This would result in a relationship similar to Equation 3.9 as;

$$CED = (-D) \cdot \ln(Mw_{\text{polymer}}) + E \quad (3.12)$$

where D and E are constants specific to the system of interest.

Rewriting Equation 3.12 in the form of Equation 3.13, the solubility parameters of dextrans with different  $M_w$  could be calculated.

$$CED = \delta^2 = \frac{(-0.5).n.R.T_g + C.n}{V_m} \quad (3.13)$$

First, the constant “C” was obtained calculating  $T_g$  of the monomeric unit from Equation 3.10 and knowing the solubility parameter (Figure 3.7 and Figure 3.8),  $n$  and  $V_m$  of monomer of dextran. Then, using this calculated constant “C” and the  $T_g$  of dextrans with different  $M_w$  (Icoz et al., 2005), solubility parameter of dextran with different  $M_w$  were calculated using Equation 3.13. In these calculations,  $n$  and  $V_m$  of monomer were used, because  $n$  and  $V_m$  for a polymer would be ( $n \times \#$  of monomers) and ( $V_m \times \#$  of monomers), where ( $\#$  of monomers) would be cancelled as it would be present in both numerator and denominator of Equation 3.13.

Accordingly, using  $T_{g,1000}=124.6^\circ\text{C}$ ,  $T_{g,5000}=158.9^\circ\text{C}$ ,  $T_{g,10000}=168.8^\circ\text{C}$ , and  $T_{g,20000000}=179.5^\circ\text{C}$  (Icoz et al., 2005); and  $\delta_{\text{monomer of dextran}}=19.8 \text{ (cal/cm}^3)^{1/2}$  (Figure 3.7); solubility parameters for dextrans with various  $M_w$  were calculated as;

$$\begin{aligned} \delta_{1000} &= 19.2 \text{ (cal/cm}^3)^{1/2} \\ \delta_{5000} &= 18.0 \text{ (cal/cm}^3)^{1/2} \\ \delta_{10000} &= 17.6 \text{ (cal/cm}^3)^{1/2} \\ \delta_{20000000} &= 17.2 \text{ (cal/cm}^3)^{1/2} \end{aligned} \quad (3.14)$$

In the similar way, using  $\delta_{\text{monomer of dextran}}=22.6 \text{ (cal/cm}^3)^{1/2}$  (Figure 3.8);

$$\begin{aligned} \delta_{1000} &= 22.1 \text{ (cal/cm}^3)^{1/2} \\ \delta_{5000} &= 21.1 \text{ (cal/cm}^3)^{1/2} \\ \delta_{10000} &= 20.7 \text{ (cal/cm}^3)^{1/2} \end{aligned}$$



$$\delta_{2000000}=20.4 \text{ (cal/cm}^3\text{)}^{1/2} \quad (3.15)$$

The details of the calculations are shown in Appendix C. Equation 3.14 and Equation 3.15 show that as  $M_w$  of dextrans increased, the solubility parameter decreased, as expected. The individual values of solubility parameters may not provide much information, because solubility that is in interest here is solubility/miscibility of a material in another, such as with a solvent or with another molecule. Sperling (2001) reports the solubility parameter of water as  $23.4 \text{ (cal/cm}^3\text{)}^{1/2}$ . We can compare the solubility parameter of water to those calculated for dextrans with different molecular weights in Equation 3.14 and Equation 3.15, because as shown in Equation 2.7, square of the difference between the solubility parameters of two components is related to the Flory-Huggins interaction parameter, whose magnitude is important in predicting miscibility of mixture systems. The larger the difference between two solubility parameters, the larger will be their square, and thereof Flory-Huggins interaction parameter. Larger interaction parameter will result in higher positive values of enthalpy of mixing in Equation 2.5, which would be unfavorable for mixing. For instance, the difference between  $\delta_{1000}=22.1 \text{ (cal/cm}^3\text{)}^{1/2}$  (Equation 3.15) and  $\delta_{\text{water}}=23.4 \text{ (cal/cm}^3\text{)}^{1/2}$  is less compared to the difference between  $\delta_{2000000}=20.4 \text{ (cal/cm}^3\text{)}^{1/2}$  (Equation 3.15) and  $\delta_{\text{water}}=23.4 \text{ (cal/cm}^3\text{)}^{1/2}$ . Similarly, the difference between  $\delta_{1000}=19.2 \text{ (cal/cm}^3\text{)}^{1/2}$  (Equation 3.14) and  $\delta_{\text{water}}=23.4 \text{ (cal/cm}^3\text{)}^{1/2}$  is less compared to the difference between  $\delta_{2000000}=17.2 \text{ (cal/cm}^3\text{)}^{1/2}$  (Equation 3.14) and  $\delta_{\text{water}}=23.4 \text{ (cal/cm}^3\text{)}^{1/2}$ . These indicate that lower molecular weight dextrans would be more miscible with water compared to higher molecular weight dextrans, because the unfavorable enthalpy of mixing will be less in the case of low molecular weight dextrans compared to the case of high molecular weight

dextrans. This is also in agreement with the general observation that smaller sugar based molecules are much more soluble in water than their higher molecular weight counterparts (such as glucose vs. amylopectin). Solubility parameter of complex carbohydrates, such as amylopectin, can also be calculated in a similar knowing the  $T_g$  of amylopectin, since the repeating unit of amylopectin is the same as that of dextran.

Molecular dynamics simulations could also be used to obtain the relationships, between solubility parameters and molecular weight of polymers as in the studies by Patnaik and Pachter (1999) and (2002); however, if computational tools are not available, the methodology of using CED- $T_g$  relationship (Equation 3.13) in combination with  $T_g$ - $M_w$  relationships (those similar to Equation 3.10 and Equation 3.11) would provide an acceptable alternative.

### **3.4.2.3. Prediction of Thermodynamics of Mixing using Original Flory-Huggins Theory in Dextran Systems**

Thermodynamics of mixing for dextran systems using the Flory-Huggins theory was calculated using Equation 2.5. In Equation 2.5, the left-hand-side is the free energy of mixing ( $\Delta G_{\text{mix}}$ ), the first two terms on the right-hand-side gives entropy of mixing ( $-T\Delta S_{\text{mix}}$ ), and the last term on the right-hand-side gives the enthalpy of mixing ( $\Delta H_{\text{mix}}$ ). Volume fractions were calculated from Equation 2.6, which is also shown in Figure 3.6 at different component ratios. Flory-Huggins interaction parameter ( $\chi_{AB}$ ) in Equation 2.5 was calculated from Equation 2.7. Solubility parameters ( $\delta$ ) in Equation 2.7 of dextrans with different  $M_w$  was given in Equation 3.14 and Equation 3.15, depending on the two predictive methods of calculating  $\delta$  of monomeric unit of dextran (as calculated in Figure

3.7 and Figure 3.8, respectively).  $V_r$  in Equation 2.7 is the molar volume of monomeric unit ( $V_m$ ) of dextrans and was calculated as shown in Figure 3.6. The details of the calculations are shown in Appendix D.

### **3.4.3. Application of Painter-Coleman Association Model to Predict Miscibility in Dextran Systems**

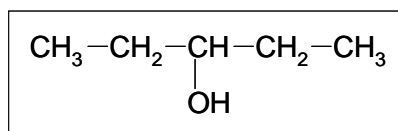
“Miscibility Guide and Phase Calculator” (MG&PC) Software, which was originally introduced by Coleman et al. (1991) (Equation 2.12) and then modified by inclusions of intra-molecular screening parameter (Coleman et al., 1999) (Equation 2.39) was used to calculate the thermodynamics of mixing through Painter-Coleman association model. This modified version of the software was kindly provided by Prof. Paul Painter of the Material Science and Engineering Department at Pennsylvania State University. The software has the capabilities to calculate free energy of mixing ( $\Delta G_{\text{mix}}$ ) and its second derivative, entropy of mixing ( $-T.\Delta S_{\text{mix}}$ ), enthalpy of mixing ( $\Delta H_{\text{mix}}$ ), free energy of hydrogen bonding ( $\Delta G_H$ ) as a function of volume fraction ( $\Phi_B$ ).

#### **3.4.3.1. Approximations Allowing Utilization of the Painter-Coleman Association Model for Carbohydrate Polymers**

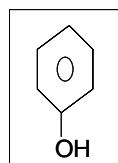
Analogue compounds can be used to approximate the hydrogen bonding of the OH groups on the repeating units of carbohydrates. These analogue compounds would be the small molecular weight molecules that have hydroxyl groups with similar chemical environments to the repeating unit of the polymer in interest. In other words, they are model with similar chemical structure to the repeating unit of the polymer in interest. The

focus of this dissertation was quantitative prediction of miscibility in two component carbohydrate (i.e. dextran) systems. Three analogue compounds (pentanol, phenol, and dimethylphenol) (Figure 3.10) were identified whose hydrogen bonding through OH groups (in terms of parameters describing self-association and inter-association) were previously reported by Painter-Coleman group (Coleman and Painter, 2006); and that have the closest available hydrogen bonding structures to the hydrogen bonding groups of the repeating unit of dextrans (Figure 3.5). In pentanol, hydroxyl group is connected to a linear molecule (Figure 3.10a). On the repeating unit of dextran (Figure 3.5), the hydroxyl groups are connected to a linear structure, too. Therefore, pentanol forms an excellent analogue compound to approximate hydrogen bonding in dextrans. In phenol, hydroxyl group is connected to a ring structure (Figure 3.10b), which would be very interesting to study as the model compound that will provide a valuable comparison between the effectiveness of a linear structure (pentanol) vs. a ring structure (phenol) on predicting miscibility in carbohydrates. In dimethylphenol, hydroxyl group is connected to a ring structure, similar to phenol, to which two methyl groups are also connected (Figure 3.10c). These methyl groups would provide more steric hindrance to the molecule and will provide a good comparison between effectiveness of phenol vs. dimethylphenol on predicting miscibility in carbohydrates.

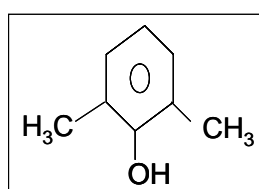
In order to be able to use the MG&PC software and make quantitative predictions of miscibility, dextran with lower  $M_w$  (for example,  $M_w=1,000$  in  $M_w=1,000+M_w=2,000,000$  system) was defined as the self-associating component (component denoted as 'B'), whereas the dextran with highest  $M_w$  was defined not to



(a)



(b)



(c)

Figure 3.10: Analogue compounds whose hydrogen bonding was approximated to the hydrogen bonding of dextrans (model carbohydrate polymers) (a) pentanol; (b) phenol; (c) dimethylphenol

self-associate (component denoted as ‘A’), but form inter-molecular hydrogen bonds with dextran of low  $M_w$ . Selecting dextran with  $M_w=1,000$  as the self-associating component in the system is a reasonable choice, because it would be expected that the small molecular weight component would more easily self-associate since the low molecular weight component would be far more mobile. In addition to this, Section 4.3.2.3 presents miscibility predictions where  $M_w=2,000,000$  was selected as the self-associating polymer in the  $M_w=1,000+M_w=2,000,000$  system, which provides comparison for the selection of self-associating component on the miscibility predictions. Moreover, it was assumed that the multiple OH groups in repeating unit of dextran did not significantly affect the overall

hydrogen bond distribution in the system. This was a necessary assumption so that it would be possible to utilize the analogue compounds with single hydrogen bonding groups to approximate the hydrogen bonding in dextrans. The MG&PC software does not handle inclusion of multiple hydrogen bonding groups to affect the overall hydrogen bonding distribution.

### **3.4.3.2. Association Equilibrium Constants of Dextrans Approximated from Those of the Selected Analogue Compounds**

Self-association and inter-association equilibrium constants are the two required parameters necessary in the MG&PC Software to calculate the  $\Delta G_H$  in Equation 2.39. For molecules that self-associate, the equilibrium constants describing “di-mer” formation (Figure 2.6) (two repeating units (mers) making hydrogen bonds and forming “di-mers”) is different from that describing subsequent “multi-mer” formation (Figure 2.6) (multiple repeating units (mers) making hydrogen bonds and forming hydrogen-bonded chains (“multi-mers”)) (Coleman et al., 1991). Therefore, in a particular system, three equilibrium constants are needed: two for self-association ( $K_2$  and  $K_B$  for di-mer and multi-mer formation, respectively) and one for inter-association ( $K_A$ ). Table 3.1 shows the ‘standard’ self-association equilibrium constants (determined by Painter-Coleman group utilizing IR spectroscopy using the procedures presented in Section 2.3.3.1) for hydrogen bond formation of the analogue compounds selected in Figure 3.10 (Coleman and Painter, 2006). ‘Standard’ self-association constants indicate values determined for standard molar volume ( $V_m^{\text{std}}$ ) of  $100\text{cm}^3/\text{mol}$  and at temperature of  $25^\circ\text{C}$ .

Table 3.1: Standard self-association equilibrium constants for hydrogen bond formation of OH group in pentanol, phenol and dimethylphenol

	$K_2^{std}$	$K_B^{std}$
Pentanol OH	26.6	44.1
Phenol OH	21.0	66.8
Dimethylphenol OH	6.7	24.5

$K_2^{std}$ : self-association equilibrium constant for di-mer formation

$K_B^{std}$ : self-association equilibrium constant for multi-mer formation

If equilibrium constants for a molecule with different molar volumes are needed, then the actual values are calculated using a conversion as;

$$K^{std} \cdot V_m^{std} = K^{actual} \cdot V_m^{actual} \quad (3.16)$$

Molar volume of repeating unit of dextrans using group contributions (Coleman et al., 1991), was calculated as 51.5cm<sup>3</sup>/mol using the MG&PC Software (Appendix E). Moreover, since the system of interest in this dissertation was the mixture of two carbohydrate molecules (i.e. dextrans) that have the same repeating unit (specifically, glucose), inter-association equilibrium constant was taken to be equal to the self-association equilibrium constant describing multi-mer formation ( $K_A=K_B$ ). In a self-associating polymer, there is a distribution of “free” and “H-bonded” mers (repeating units) at a particular concentration as illustrated in Figure 2.6. When the two components in a mixed system have similar repeating units (as in the case of two dextrans/two carbohydrates), the inter-association between two components will be similar to the self-association for multi-mer formation in the self-associating component (as illustrated in Figure 2.6). That is why  $K_A$  was set to be equal to  $K_B$  for dextran mixtures since the functional groups of the two components were the same. It should be noted that for components with two different functional groups (as in Figure 2.9),  $K_A$  will not be equal

to  $K_B$ . The actual equilibrium constants for self-association and inter-association in dextrans approximated using H-bond formation of different analogue compounds using Equation 3.16 are given in Table 3.2.

Table 3.2: Actual self- and inter-association equilibrium constants for hydrogen bond formation of dextran when approximated through hydrogen bond formation of pentanol OH, phenol OH and dimethylphenol OH

	$K_2$	$K_B$	$K_A$
Pentanol OH	51.6	85.6	85.6
Phenol OH	40.7	129.6	129.6
Dimethylphenol OH	13.0	47.6	47.6

$K_2$ : self-association equilibrium constant for di-mer formation in dextrans

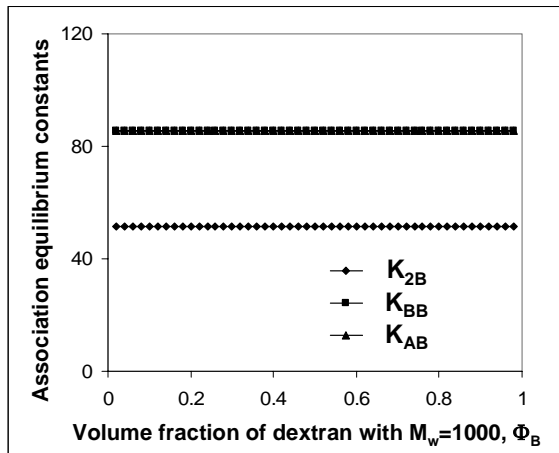
$K_B$ : self-association equilibrium constant for multi-mer formation in dextrans

$K_A$ : inter-association equilibrium constant between dextrans

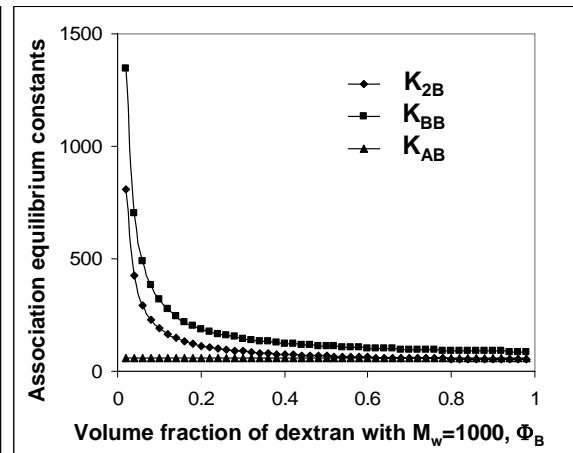
The association equilibrium constants in Table 3.2 were calculated where there were no intra-molecular screening effects ( $\gamma=0.00$ ). In Figure 3.11a-c-e, the values of association constants as a function of volume fraction of dextran with  $M_w=1,000$  ( $\Phi_B$ ) shows constant values independent on the volume fraction. In the case of inclusion of intra-molecular screening effects ( $\gamma=0.30$ ), association constants are modified using Equations 2.40-2.42. Figure 3.11b-d-f shows the volume fraction dependent  $K_{2B}$  and  $K_{BB}$  (Equations 2.40-2.41) and volume fraction independent  $K_{AB}$  (Equation 2.42). Comparing the figures, it can be seen that when intra-molecular screening effect were taken into account by using  $\gamma=0.30$ , the self-association constants ( $K_{2B}$  and  $K_{BB}$ ) were calculated to be larger, especially at low volume fractions of  $M_w=1,000$ , than the values when screening effect was not taken into account with  $\gamma=0.00$ . On the other hand,  $K_{AB}$  values



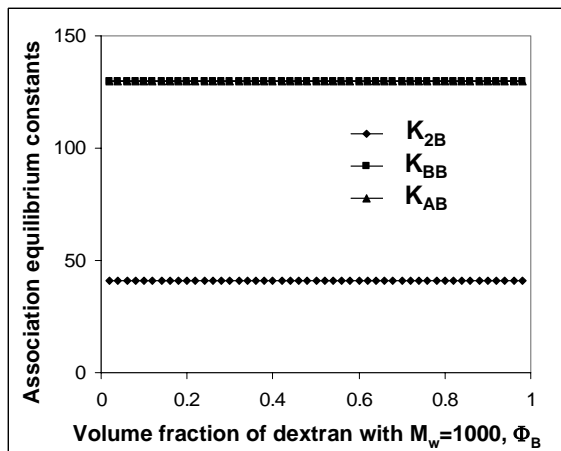
were slightly smaller when screening effects was included compared to the case where screening effects were not included. Higher  $K_{2B}$  and  $K_{BB}$  and lower  $K_{AB}$  with screening effects indicate that the relative favorability of self-association vs. inter-association were increased. This would have unfavorable effect on miscibility calculations of two polymers, however, it should also be kept in mind that the enthalpy of mixing term ( $\chi_{AB} \cdot \Phi_A \cdot \Phi_B \cdot (1-\gamma)$ ) in Equation 2.39 also changes when intra-molecular screening is taken into account. This term gets a lower positive value, so the free energy of hydrogen bonding term in Equation 2.39 would need to overcome a lower positive valued term. Therefore, the free energy of mixing ( $\Delta G_{\text{mix}}$ ) is, then, determined depending on the relative values of enthalpy of mixing ( $\Delta H_{\text{mix}}$ ) and free energy of H-bonding ( $\Delta G_H$ ), which are both modified due to the intra-molecular screening.



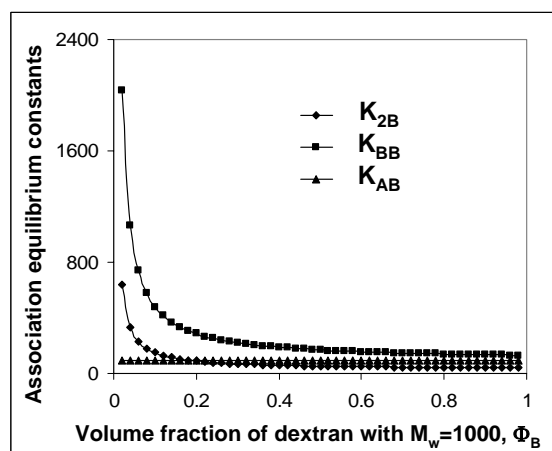
(a)



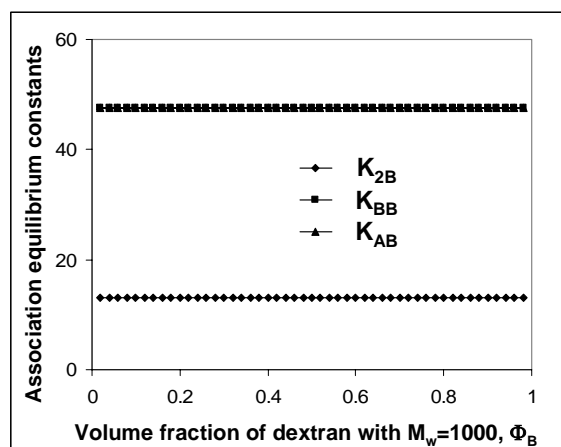
(b)



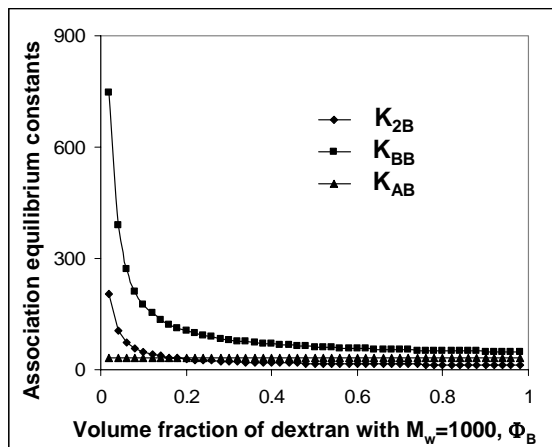
(c)



(d)



(e)



(f)

Figure 3.11: Self- and inter-association equilibrium constants as a function of volume fraction for hydrogen bond formation of dextran when approximated through hydrogen bond formation of pentanol OH (a-b); phenol OH (c-d); and dimethylphenol OH (e-f) ( $\gamma=0.00$  for a-c-e; and  $\gamma=0.30$  for b-d-f)

### 3.4.3.3. Calculation of Non-hydrogen-bonded Solubility Parameters of Dextrans (Solubility Parameters that Exclude the Effect of Hydrogen Bonding)

According to the Painter-Coleman association model,  $\chi_{AB} \cdot \Phi_A \cdot \Phi_B$  term of Equation 2.12 should only include dispersive forces, since the effect of any specific interactions, such as hydrogen bonding) are included in  $\Delta G_H / R.T$  term of Equation 2.12. Therefore,  $\chi_{AB}$  in Equation 2.7 needs to be calculated as a function of non-hydrogen-bonded solubility parameters. Non-hydrogen-bonded solubility parameter of the repeating unit of dextran was calculated using Equation 2.14 and groups contributions specifically designed to exclude any effect of specific interaction (Table 2.1). A value of  $14.00 \text{ (cal/cm}^3\text{)}^{0.5}$  was calculated by dividing total molar attraction constants that exclude hydrogen bonding effects to total molar volume of the repeating unit of the molecule ( $V_m=51.5\text{cm}^3/\text{mol}$ ) (Appendix E). Then, non-hydrogen-bonded solubility parameters of dextrans with different molecular weights were determined as described in Section 3.4.2.2 using Equations 3.10-3.11 and Equation 3.13 (Appendix F). Calculated values are given in Table 3.3, showing decrease in non-hydrogen-bonded solubility parameters as  $M_w$  increased, as discussed in section 3.4.2.2.

Table 3.3: Non-hydrogen bonded solubility parameters of dextrans with different molecular weights

Dextrans with different $M_w$	Non-hydrogen-bonded solubility parameters ( $\delta$ ) ( $\text{cal/cm}^3$ ) <sup>0.5</sup>
$M_w=1,000$	13.10
$M_w=5,000$	10.96
$M_w=10,000$	10.27
$M_w=2,000,000$	9.40

### 3.4.3.4. Individual Enthalpic and Entropic Contributions of Hydrogen Bonding on Overall Free Energy of Hydrogen Bonding ( $\Delta G_H$ )

Free energy of hydrogen bonding ( $\Delta G_H$ ) is a combination of entropic and enthalpic contributions. Enthalpy of hydrogen bonding ( $\Delta H_H$ ) per mole of lattice site is calculated as (Coleman et al., 1991);

$$\Delta H_H = n_B \cdot \left[ \left( \frac{\Gamma_1^0}{\Gamma_2^0} \right) - \left( \frac{\Gamma_1}{\Gamma_2} \right) \right] h_{BB,ave} + n_B \cdot \left[ \left( \frac{\Gamma_1}{\Gamma_2} \right) \left( \frac{X}{1+X} \right) \right] h_{AB} \quad (3.17)$$

where  $n_B$  is the number of moles of B molecules (self-associating polymer) at a particular volume fraction;  $h_{BB,ave}$  and  $h_{AB}$  are the enthalpies of individual B-B and A-B type of hydrogen bond formation (cal/mol);  $\Gamma_1$ ,  $\Gamma_2$ ,  $X$ ,  $\Gamma_1^0$ ,  $\Gamma_2^0$  are determined following Equations 2.34-2.38 and including the effect of intra-molecular screening parameter as in Equation 2.40-2.42;

$$\Gamma_1 = \left( 1 - \frac{K_{2B}}{K_{BB}} \right) + \frac{K_{2B}}{K_{BB}} \cdot \left[ \frac{1}{(1 - K_{BB} \cdot \Phi_{B1})} \right] \quad (3.18)$$

$$\Gamma_2 = \left( 1 - \frac{K_{2B}}{K_{BB}} \right) + \frac{K_{2B}}{K_{BB}} \cdot \left[ \frac{1}{(1 - K_{BB} \cdot \Phi_{B1})^2} \right] \quad (3.19)$$

$$X = \frac{K_{AB} \cdot \Phi_{A1}}{r} \quad (3.20)$$

$$\Gamma_1^0 = \left( 1 - \frac{K_{2B}}{K_{BB}} \right) + \frac{K_{2B}}{K_{BB}} \cdot \left[ \frac{1}{(1 - K_{BB} \cdot \Phi_{B1}^0)} \right] \quad (3.21)$$

$$\Gamma_2^0 = \left( 1 - \frac{K_{2B}}{K_{BB}} \right) + \frac{K_{2B}}{K_{BB}} \cdot \left[ \frac{1}{(1 - K_{BB} \cdot \Phi_{B1}^0)^2} \right] \quad (3.22)$$

A couple of important points to mention for the calculation of  $\Delta H_H$  are;

- Self-association equilibrium constants calculated through Equations 2.40-2.42 ( $K_{2B}$  and  $K_{BB}$ ) were functions of volume fraction ( $\Phi_B$ ) (Figure 3.11b-d-f), which means that for each volume fraction,  $K_{2B}$  and  $K_{BB}$  changed from the values calculated in Table 3.2. The significance of this change in terms of miscibility is discussed at the end of Section 2.3.5 and once again in Section 3.4.3.2. During calculation of  $\Gamma_1^0$ ,  $\Gamma_2^0$ , which is for the conditions in pure B (where  $\Phi_B=1$ ),  $K_{2B}$  and  $K_{BB}$  took the values when  $\Phi_B=1$ , which was equal to the values in Table 3.2.
- $h_{BB,ave}$  was approximated as an average of  $h_{2B}$  and  $h_{BB}$ .  $h_{2B}$ ,  $h_{BB}$  and  $h_{AB}$  were used as reported in Coleman et al. (1991) (Table 3.4).

Table 3.4: Enthalpy of individual B-B and A-B type hydrogen bond formation of dextran when approximated through hydrogen bonding of pentanol OH, phenol OH and dimethylphenol OH

	<b><math>h_{2B}</math> (cal/mol)</b>	<b><math>h_{BB}</math> (cal/mol)</b>	<b><math>h_{AB}</math> (cal/mol)</b>
Pentanol OH	-5000	-5000	-5000
Phenol OH	-5600	-5200	-5200
Dimethylphenol OH	-5600	-5200	-5200

$h_{2B}$ : enthalpy of individual B-B type of hydrogen bond formation (for di-mer formation)

$h_{BB}$ : enthalpy of individual B-B type of hydrogen bond formation (for multi-mer formation)

$h_{AB}$ : enthalpy of individual A-B type of hydrogen bond formation

- The MG&PC Software calculates fraction of the free (non-hydrogen-bonded) OH groups in the self-associating polymer ( $f_m^{OH}$ ) (Equation 3.23) and fraction of the free functional group in the non-self-associating polymer ( $f_F^A$ ) (Equation 3.24) as a function of volume fraction;

$$f_m^{OH} = \frac{\Phi_{B1}}{\Phi_B} \quad (3.23)$$

$$f_F^A = \frac{\Phi_{A1}}{\Phi_A} \quad (3.24)$$

where  $\Phi_{A1}$  and  $\Phi_{B1}$  are the volume fractions of non-hydrogen bonded (free) ‘A’ and ‘B’ species. Therefore, using Equation 3.23 and Equation 3.24 together with the calculated values given by the software,  $\Phi_{B1}$ ,  $\Phi_{A1}$  were calculated as a function of volume fraction.  $\Phi_{B1}^0$  is the volume fraction of non-hydrogen bonded (free) ‘B’ in pure state, which was also calculated from Equation 3.23 with  $\Phi_B=1$ .

- Calculated  $\Delta H_H$  in Equation 3.17 had a unit of ‘cal’, which then needs to be divided by V (ml) (volume of the system at a particular volume fraction).

$$V = V_A \cdot n_A \cdot M_A + V_B \cdot n_B \cdot M_B \quad (3.25)$$

- Contribution of entropy of hydrogen bonding was then calculated by subtracting enthalpy of hydrogen bonding from free energy of hydrogen bond formation, following Coleman et al. (1991) and Painter et al. (1991).

#### **3.4.4. Validation of the Predictive Miscibility Approximations for Dextran on ‘Real’ Carbohydrate Polymers: Testing Miscibility in Inulin/Amylopectin Systems**

Amylopectin is a glucose polymer, close to dextran structurally (Figure 3.5), with  $\alpha$ -D-(1-4) linkages together with some  $\alpha$ -D-(1-6) linked branches (Jacobs and Delcour, 1998; Parker and Ring, 2001). Therefore, non-hydrogen-bonded solubility parameter of amylopectin with  $M_w=400,000,000$  (Gluck-Hirsch, 1998) with  $T_g$  of 185.6°C (Zimeri and Kokini, 2003a) was determined using Equation 3.13 and as described in Section 3.4.3.3.

The calculated non-hydrogen-bonded solubility parameter of amylopectin was 8.99 (cal/cm<sup>3</sup>)<sup>0.5</sup> which followed the same trend of having lower solubility parameters at higher M<sub>w</sub> of glucose (Table 3.3).

Inulin is an oligo-fructose with a M<sub>w</sub>=6,000. Non-hydrogen-bonded solubility parameter of its repeating unit (Figure 3.12) was determined as described in Coleman et al. (1991) from group contributions. A value of 14.4 (cal/cm<sup>3</sup>)<sup>0.5</sup> was calculated by dividing total molar attraction constants that exclude hydrogen bonding effects to the corresponding total molar volume of the repeating unit (V<sub>m</sub>=49.4cm<sup>3</sup>/mol). The resulting non-hydrogen-bonded solubility parameter of inulin with M<sub>w</sub>=6,000 was calculated as 14.26 (cal/cm<sup>3</sup>)<sup>0.5</sup>. The solubility parameters of amylopectin (8.99 (cal/cm<sup>3</sup>)<sup>0.5</sup>) and inulin (14.26 (cal/cm<sup>3</sup>)<sup>0.5</sup>) are far apart from each other. Actually, the solubility parameter of repeating unit of amylopectin (glucose) and repeating unit of inulin (fructose) are quite close to each other (14.0 and 14.4 (cal/cm<sup>3</sup>)<sup>0.5</sup>, respectively) because the chemical structure of glucose and fructose are composed of very similar groups (Figure 3.5 and Figure 3.12, respectively). However, the solubility parameter of amylopectin, which is a very high molecular weight polymer of glucose (M<sub>w</sub>=400,000,000), is much lower than that of its repeating unit, as calculated from Equation 3.13 and as described in Section 3.4.3.3.

Painter-Coleman association model was used to make a case study of testing prediction of miscibility/immiscibility in inulin-amylopectin systems. As mentioned before, the solubility parameters of amylopectin (8.99 (cal/cm<sup>3</sup>)<sup>0.5</sup>) and inulin (14.26 (cal/cm<sup>3</sup>)<sup>0.5</sup>) are far apart from each other, which will result in a large positive valued enthalpy of mixing, which will be unfavorable for free energy of mixing. Entropy

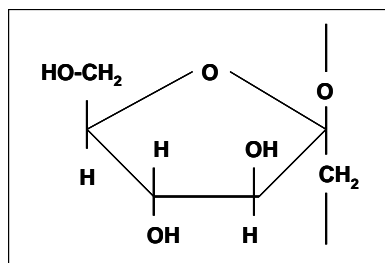


Figure 3.12: Monomer (repeating unit) of inulin

of mixing, which is always favorable to free energy of mixing with negative values, will have a very small contribution to the overall free energy due to the very high molecular weight of amylopectin. Now, we are interested in to see if the favorable negative valued hydrogen bonding contribution, determined using the approximations with analogue compounds, will be enough to overcome the large positive value of enthalpy of mixing (Equation 2.39); and if the predicted miscibility/immiscibility is parallel to experimentally observed miscibility behavior.

MG&PC software was used to make the calculations of free energy and second derivative of free energy of mixing in inulin+amylopectin systems at limited moisture contents, where it is approximated that there were two components in the system (inulin and amylopectin) as in the case of dextran systems. Model analogue compounds shown in Figure 3.10 and similar approximations described in Section 3.4.3.1 were used to approximate the hydrogen bonding in these real carbohydrate systems. As the lower molecular weight polymer, inulin was set to be the self-associating component unless otherwise stated, following the selection that dextran with lower molecular weight was chosen as the self-associating component. Intra-molecular screening parameter was set as  $\gamma=0.30$  unless otherwise stated. The quantitative miscibility predictions in inulin and



amylopectin systems were compared to the experimental miscibility/immiscibility reported by Zimeri and Kokini (2003a).

According to Zimeri and Kokini (2003a), mixed systems of waxy maize starch (WMS), which is composed of 98% amylopectin, and inulin were prepared as follows: (a) 10.5% inulin, 24.5% WMS and 65% water (w/w, w.b.), corresponding to an inulin to WMS ratio of 30:70 (% d.b.), and (b) 20% inulin, 15% WMS and 65% water (w/w, w.b.), corresponding to an inulin to WMS ratio of 60:40 (% d.b.) were mixed, dried and milled into a fine powder. Details of the sample preparation procedures can be found in Zimeri and Kokini (2003a). The 30:70 and 60:40 (% d.b.) ratios of inulin-amylopectin corresponds to volume fractions of inulin at  $\Phi_B=0.3$  and  $\Phi_B=0.6$ , respectively. [The molecular weight of the repeating unit of inulin and amylopectin are the same (Figures 3.12 and Figure 3.5) and is equal to 162g/mol. Volume fractions in the two-component inulin-amylopectin system were calculated from Equation 2.6, similar to that in dextran-dextran system, so their volume fraction vs. %w/w component ratio was calculated to be same as given in Figure 3.6.

The samples used to experimentally determine miscibility in Zimeri and Kokini (2003a), which were compared to the predictive miscibility in this current paper, were obtained by equilibrating the mixed inulin-amylopectin blends at  $a_w=0.33$  and miscibility was experimentally measured by DSC through glass transition temperature determination. At this water activity (limited moisture environments with approximately 10% moisture content), it is approximated that there were only two components in the system (inulin and amylopectin, only). This rough approximation was needed because the

inclusion of water into predictive miscibility framework is not possible at this point due to its complicated H-bonding capacity.

## 4. RESULTS AND DISCUSSION

### 4.1. Investigation of Miscibility in Dextran Systems with Different $M_w$

#### 4.1.1. Moisture Sorption Properties of Individual Dextrans

The moisture sorption isotherms (at room temperature) of dextrans with  $M_w=970$ ;  $M_w=10,800$ ;  $M_w=43,000$  and  $M_w=2,000,000$  showed sigmoidal shape (Figure 4.1), which is typical of most food systems (Roos, 1995; Serris and Biliaderis, 2001) and was well predicted by the Guggenheim-Anderson-de Boer (GAB) model (lines in Figure 4.1). At the same  $a_w$ , the moisture content increased with  $M_w$  (Figure 4.1), indicating higher moisture sorption capacity for the higher  $M_w$  dextrans, which was also reflected by the values of the “monolayer moisture content” ( $M_o$ ) calculated with the GAB model. As can be seen from the data (5.13%, 7.03%, 7.73%, and 8.73% for the dextrans with  $M_w=970$ ;  $M_w=10,800$ ;  $M_w=43,000$ ; and  $M_w=2,000,000$ , respectively) the  $M_o$  values increased as molecular weight increased. This was likely caused by the larger number of available sites for water binding in the higher  $M_w$  dextrans. The only exception to this trend was noted at  $a_w>0.7$  for the dextran with lowest molecular weight ( $M_w=970$ ), whose sorption isotherm exhibits a sharper slope at high  $a_w$  values (Figure 4.1). The sharp increase in moisture content at high  $a_w$  values is characteristic of molecules with a crystalline behavior, which indicates a relatively organized structure of the molecule. At low  $M_w$ , dextrans would probably have a better structural organization, which is actually consistent with the report of the “rod-like” molecular organization reported by Gekko (1981) for dextrans with  $M_w<2,000$  (Icoz et al., 2005).

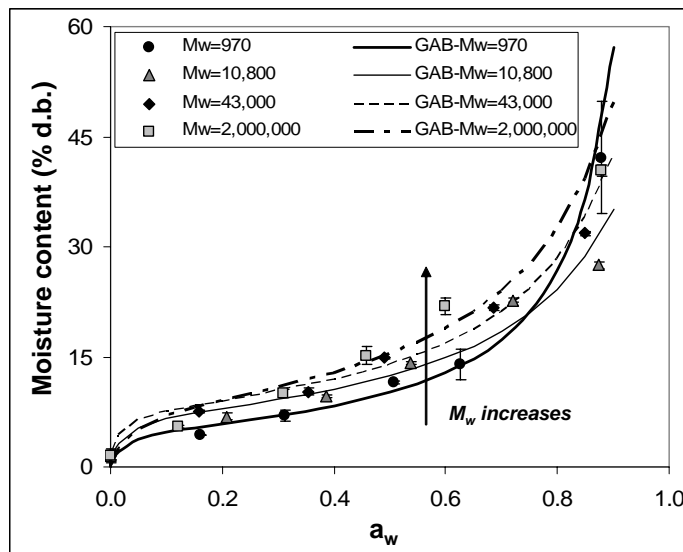


Figure 4.1: Moisture sorption isotherms of pure dextrans with  $M_w=970$ ;  $M_w=10,800$ ;  $M_w=43,000$ ; and  $M_w=2,000,000$

#### 4.1.2. Effect of $M_w$ on $T_g$ of Pure Dextrans

Since at high water activities,  $T_g$ s were difficult to identify accurately due to the proximity of the ice melting transition, only the  $T_g$  values measured at  $a_w < 0.5$  were used further in this analysis. As shown in Figure 4.2, the  $T_g$  increased sharply with  $M_w$  up to a critical molecular weight, which was very close for all four data sets (Figure 4.2 and Table 4.1). Above this critical molecular weight,  $T_g$  was relatively independent of molecular weight, as demonstrated by the very small slopes of the  $T_g$  vs.  $M_w$  plots, which confirms the earlier findings of Gropper et al. (2002). In Figure 4.2, the value of  $M_w$  that marked the change in behavior was estimated from the intersection of the regression lines to be approximately between 23,000 and 30,000 (Table 4.1) (Icoz et al., 2005).

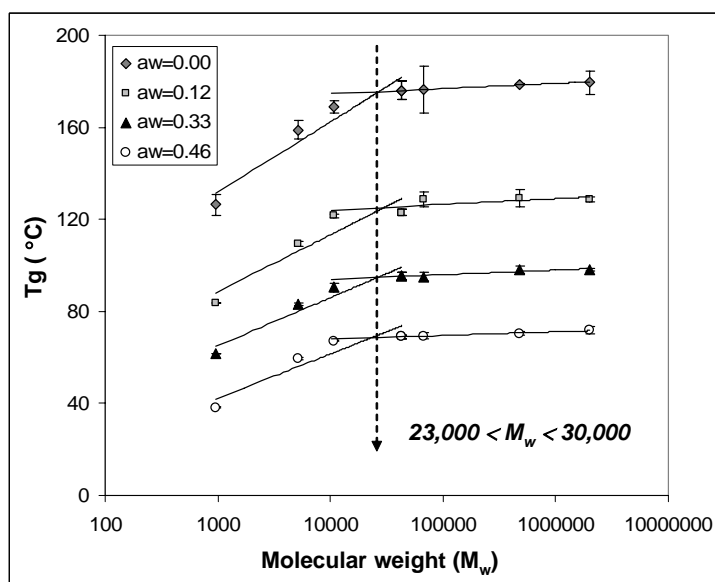


Figure 4.2: Effect of  $M_w$  on  $T_g$  of pure dextrans at different water activities

Table 4.1: Quantitative glass transition temperature vs. molecular weight correlations for dextrans at various water activities

$a_w$	$M_w \leq 43,000$		$M_w \geq 43,000$		Intersection	
	$T_g$ vs. $M_w$	$R^2$	$T_g$ vs. $M_w$	$R^2$	$M_w$	No. glucose residues
<b>0.00</b>	$y = 13.30\ln(x) + 39.82$	0.92	$y = 0.98\ln(x) + 165.58$	0.97	27013	150
<b>0.12</b>	$y = 10.77\ln(x) + 14.08$	0.88	$y = 1.06\ln(x) + 114.29$	0.40*	30368*	169*
<b>0.33</b>	$y = 9.07\ln(x) + 2.49$	0.93	$y = 0.89\ln(x) + 85.71$	0.87	26256	146
<b>0.46</b>	$y = 8.37\ln(x) - 15.51$	0.88	$y = 0.68\ln(x) + 61.80$	0.99	23269	129

(\* weak correlation)

This  $M_w$  range was also confirmed by steady shear rheological measurements, in which the shear rate dependence of apparent viscosity was determined for different molecular weights at two different concentrations. Zero-shear viscosity ( $\eta_0$ ) vs.  $M_w$  of dextrans at 20% and 40% concentrations (Figure 4.3) showed an increase in  $\eta_0$  with  $M_w$

as expected (Aklonis and MacKnight, 1983). The dependency became stronger (i.e. a steeper slope of the regression line) at  $M_w$  around 22,000, which was very close to the critical molecular weight estimated from the  $T_g$  vs.  $M_w$  plots in Figure 4.2 (Icoz et al., 2005).

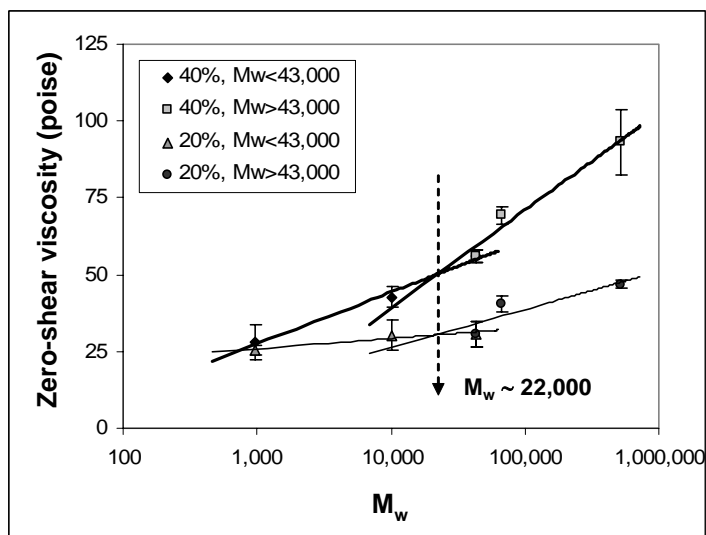


Figure 4.3: Zero-shear viscosity behavior for 20% and 40% dextran solutions with different molecular weights

The results were also consistent with the findings of Cowie (1975), who reported that the  $T_g$  dependence on molecular size for polystyrene, polybutadiene, polyisoprene and poly( $\alpha$ -methylstyrene) exhibited three different regions: A region of pronounced increase in  $T_g$  with molecular size, defined as the region where oligomers reach sufficiently long chain lengths to assume polymeric properties; followed by a region characterized by a lower, but steady increase in  $T_g$  with molecular size; and a plateau region, at very high chain length (Figure 4.4).

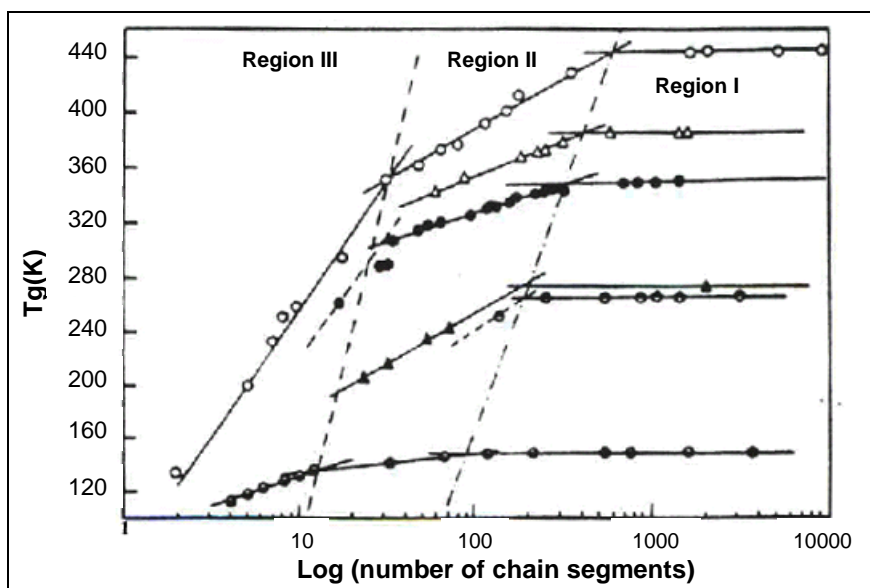


Figure 4.4: Effect of molecular size of polystyrene, polybutadiene, polyisoprene and poly( $\alpha$ -methlstyrene) on glass transition temperature (Cowie, 1975)

Figure 4.2 have demonstrated that the glass transition temperature of pure dextrans decreased with increased water activity.  $T_g$  of bone-dry ( $a_w=0.00$ ) dextrans with  $M_w=970$  and  $M_w=2,000,000$  were determined as  $124.6^\circ\text{C}$  and  $179.5^\circ\text{C}$ , respectively. The  $T_g$  of the highest  $M_w$  dextran was close to, but slightly smaller, when compared to the  $T_g$  of amylopectin from waxy maize starch ( $M_w=400,000,000$  (Gluck-Hirsch, 1998)), which was reported to be at  $185.6^\circ\text{C}$  by Zimeri and Kokini (2003a). Amylopectin is a glucose polymer as dextran, with  $\alpha$ -D-(1-4) linkages that result in the formation of the linear chain together with some  $\alpha$ -D-(1-6) linked branches (Jacobs and Delcour, 1998; Parker and Ring, 2001). When the  $T_g$  vs.  $M_w$  relationship for dextrans at  $a_w=0.00$  (Table 4.1) was applied for amylopectin using a molecular weight of 400,000,000, a  $T_g$  value of  $185^\circ\text{C}$  was obtained, which is stunningly close to  $185.6^\circ\text{C}$ , the experimental  $T_g$  value

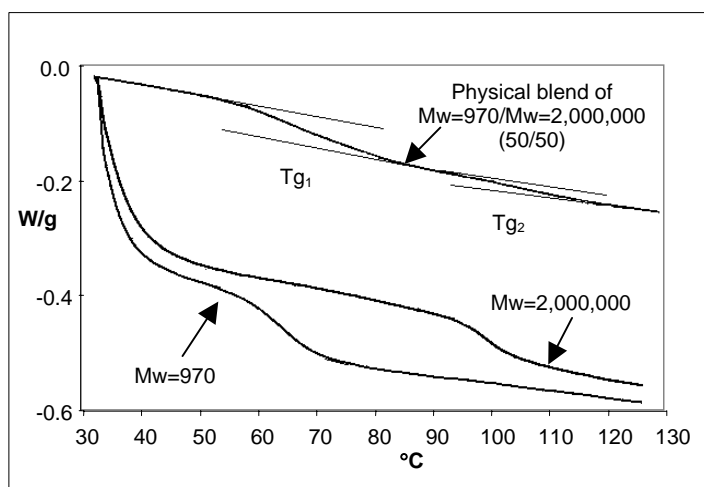
determined by Zimeri and Kokini (2003a). This clearly shows validation of the  $T_g$  vs.  $M_w$  relationship for glucose polymers, including starch (Icoz et al., 2005).

#### **4.1.3. Influence of Mixture Preparation Method on Miscibility of Dextran Systems**

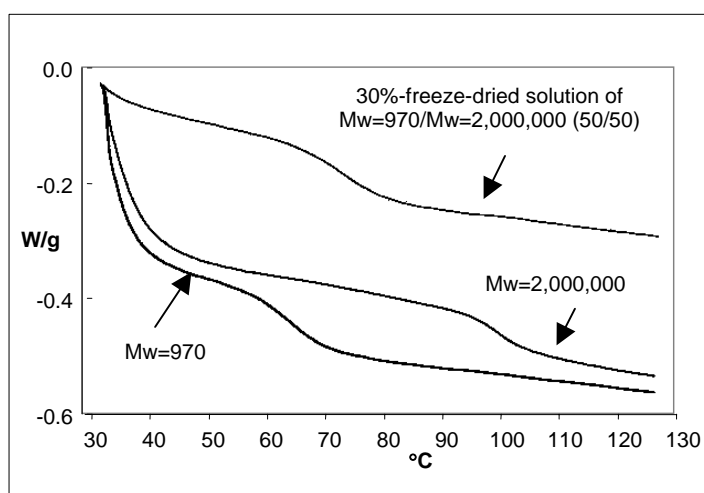
The first part of the miscibility study was to examine the effect of physical blending with solubilization in water on mixing efficiency. These studies were conducted using dextran systems equilibrated at  $a_w=0.33$ . When dextrans with  $M_w=970$  and  $M_w=2,000,000$  were physically blended in equal amounts in powder form, two separate  $T_g$ s, very close to the  $T_g$ s of the two individual components of the blend, were obtained (Figure 4.5a). The lower  $T_g$  of the blend was  $63.7^\circ\text{C}$ , close to the  $T_g$  of pure  $M_w=970$  ( $T_g=61.7^\circ\text{C}$ ), and the higher  $T_g$  of the blend was  $101.7^\circ\text{C}$ , close to the  $T_g$  of the pure  $M_w=2,000,000$  ( $T_g=98.2^\circ\text{C}$ ). The blends were then subjected to successive heating and cooling cycles by rescanning multiple times in the DSC. After this treatment, two separate  $T_g$ s were still observed (Figure 4.6). This was due to a diffusion barrier in dry blends in dry and melt phases and the limited free volume in the highly concentrated amorphous mixtures that did not allow rearrangement and interpenetration of the long dextran molecules. Branching of the high  $M_w$  dextran might also prevent molecular interpenetration, through steric hindrance. Thus, the two molecular species retain their separate phase behavior within the time of the experiment (Icoz et al., 2005).

The miscibility behavior was quite different when mixtures were obtained after a preliminary solubilization step. The samples prepared by mixing 50/50 (d.b.) ratios of 30% (w.b.) dextran solutions of  $M_w=970$  and  $M_w=2,000,000$ , followed by freeze-drying, exhibited a single  $T_g$ , located between the  $T_g$  of the two individual components at around





(a)



(b)

Figure 4.5: Influence of mixture preparation method ( $M_w=970/M_w=2,000,000$ ) (50/50);  
 (a) Physical blend of powder dextrans; (b) 30% concentrated, freeze-dried solution of dextrans

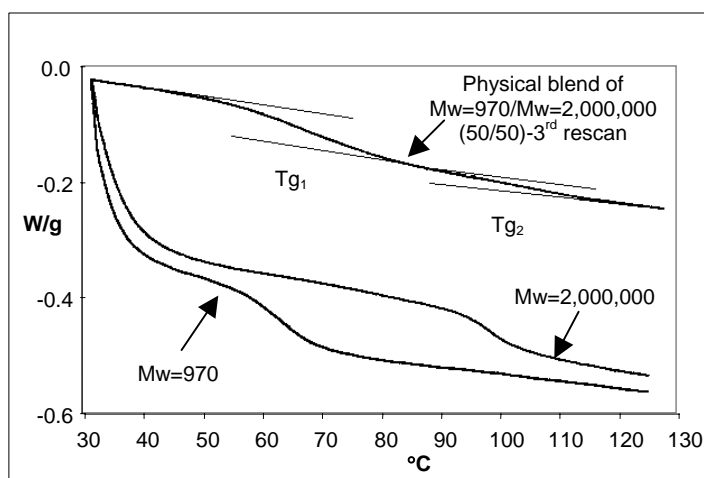
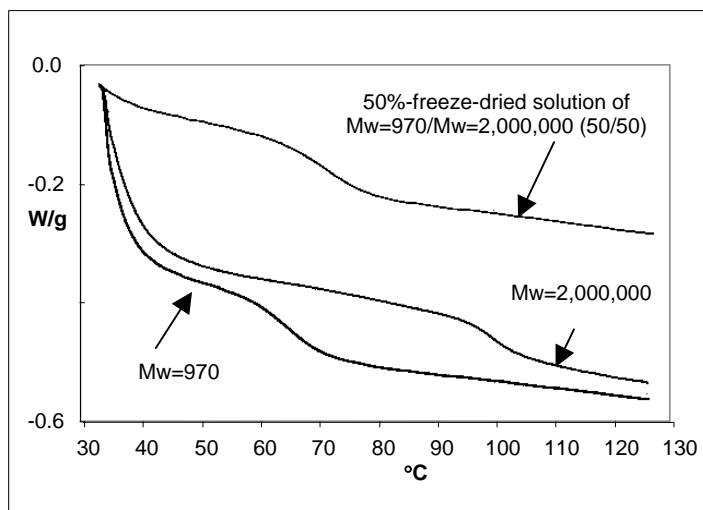


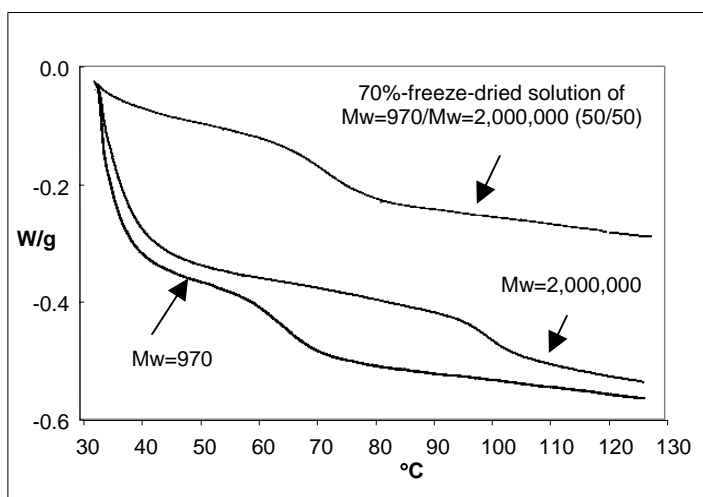
Figure 4.6: 3<sup>rd</sup> DSC rescan of physical blend of dextran mixture of  $M_w=970/M_w=2,000,000$  (50/50)

68.2°C (Figure 4.5b). This demonstrated the presence of a single phase and molecular miscibility of the two dextrans. The same mixing behavior was observed for mixtures obtained by mixing 50% and 70% dextran solutions and a  $T_g$  value of 69°C was obtained for both concentrations (Figure 4.7), indicating miscibility even at higher total polymer concentrations just as long as dextran could be solubilized. Similar dependence of phase behavior on method of preparation was obtained for the mixtures of dextrans with  $M_w=5,200+M_w=2,000,000$  and  $M_w=10,800+M_w=2,000,000$  (Icoz et al., 2005).

In solution, small dextrans come close to the backbone and side branches of the larger dextran molecules and intimately inter-disperse with them to the high free volume and entropy of the system. Upon removal of the solvent (water) by freeze-drying, the dextrans remained interwoven as a single phase and exhibit a single  $T_g$ . Figure 4.8 shows a conceptual model of the two types of mixed dextran systems (Icoz et al., 2005).



(a)



(b)

Figure 4.7: Thermal behavior of freeze-dried dextran solutions of  $M_w=970/M_w=2,000,000$  (50/50): (a) 50% concentrated solutions; (b) 70% concentrated solutions

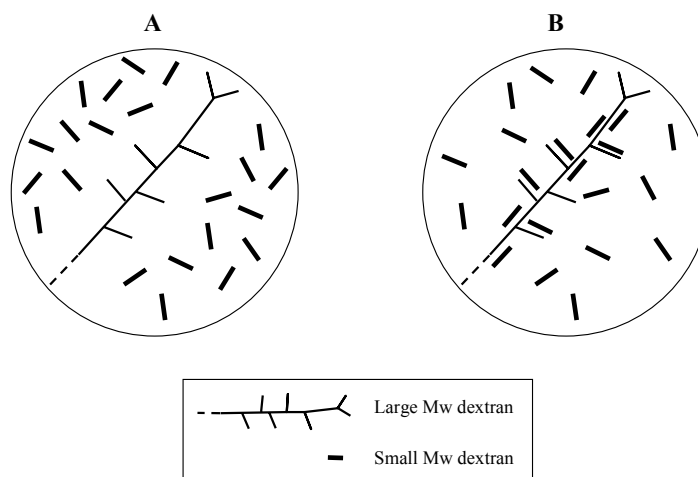


Figure 4.8: Conceptual model of the mixed dextran systems; (A) Without prior solubilization; (B) With prior solubilization

An interesting observation in the dextran systems under investigation was that when dextran with  $M_w=970$  was mixed in equal weight proportions with dextran of  $M_w=2,000,000$ , the  $T_g$  of the equal-mixture was closer to the  $T_g$  of the low  $M_w$  component (Figure 4.5b). Since the two dextrans were mixed in equal amounts, the mixtures contained a much larger number of small dextran molecules; roughly 2,000 molecules of  $M_w=970$  per 1 molecule of  $M_w=2,000,000$ . This clearly suggests that the operating  $M_w$  in predicting  $T_g$  is the number average molecular weight. As shown in Figure 4.9, even in the presence of a small amount of low  $M_w$  dextran (10/90 ratio), the  $T_g$  of the mixture was closer to the  $T_g$  of the low  $M_w$  dextrans which introduced a significant free volume in the system, leading to significant increase in molecular mobility and had a significant effect on the  $T_g$  of the mixtures. This indicated that the  $T_g$  of the mixed dextran systems were better predicted by their number-average molecular weight ( $M_n$ ), which is related to the length (number) of the polymer chains, rather than

their weight-average molecular weight ( $M_w$ ), which is related to the weight of the chains.

The calculated values of the blends'  $M_n$  are shown in Table 4.2 (Icoz et al., 2005).

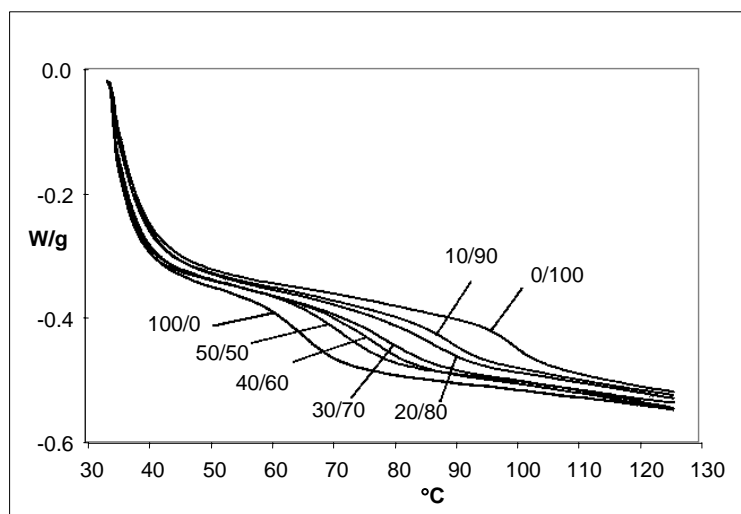


Figure 4.9: Effect of dextran with  $M_w=970$  on the  $T_g$  of 30% concentrated, freeze-dried solutions of dextran mixtures. The numbers indicate the  $M_w=970/M_w=2,000,000$  ratio (w/w, d.b.)

The results were consistent with the reports of Wang and Jane (1994), Lourdin et al. (1997), and Gabarra and Hartel (1998), who observed strong effect of small amounts of low molecular weight components on the properties of large molecular weight molecular species. Kalichevsky and Blanshard (1993) showed that in mixtures of fructose and amylopectin at fructose concentrations above 20%, the mechanical properties of the mixture were dominated by fructose. The small molecular weight component acts as a plasticizer for the large polymeric molecule. However, these authors did not mention the significance of the number of low molecular weight species quantitatively.

Table 4.2: Molecular size characteristics of the dextran blends obtained after solubilization

Blend composition (%M <sub>w</sub> 1 / %M <sub>w</sub> 2)	Equivalent M <sub>n</sub> of blend	Polydispersity index (M <sub>w</sub> /M <sub>n</sub> ) of blend
A. M <sub>w</sub> =970/M <sub>w</sub> =2,000,000		
50/50	1,939	516
40/60	2,423	495
30/70	3,230	434
20/80	4,841	331
10/90	9,658	186
B. M <sub>w</sub> =5,200/M <sub>w</sub> =2,000,000		
50/50	10,373	97
40/60	12,949	93
30/70	17,229	81
20/80	25,732	62
10/90	50,811	35
C. M <sub>w</sub> =10,800/M <sub>w</sub> =2,000,000		
50/50	21,484	47
40/60	26,783	45
30/70	35,552	39
20/80	52,858	30
10/90	102,994	17

The change in  $T_g$  with  $M_n$  for miscible dextran blends is shown in Figure 4.10. A log-linear relationship between  $T_g$  and  $M_n$  for all mixtures under investigation was observed.

For dextran mixtures of  $M_w=970$  and  $M_w=2,000,000$ ;

$$T_g = (10.91) \ln (M_n) - 12.90 \quad (4.1)$$

For mixtures of  $M_w=5,200$  and  $M_w=2,000,000$ ;

$$T_g = (2.55) \ln (M_n) + 61.14 \quad (4.2)$$

For mixtures of  $M_w=10,800$  and  $M_w=2,000,000$ ;

$$T_g = (1.41) \ln (M_n) + 74.84 \quad (4.3)$$

At  $M_n > 10,000$ , the sharp increase of  $T_g$  with increasing  $M_n$  started to level off and for mixtures of 10,800/2,000,000 blends, the  $T_g$  values of mixtures with different component ratios were not significantly different from one another. According to Billmeyer (1984),  $T_g$  of glass-forming polymers increases with increasing  $M_n$  up to a plateau where entanglement coupling of the high molecular weight polymers lead to an entangled network of infinite molecular weight. In case of the dextran mixtures investigated in this work, the leveling off could also be due to the fact that, as the  $M_n$  increased, the homogeneity of the system also increased, as demonstrated by the polydispersity index values shown in Table 4.2, and the  $T_g$  values tend asymptotically to the  $T_g$  of the largest dextran (Icoz et al., 2005).

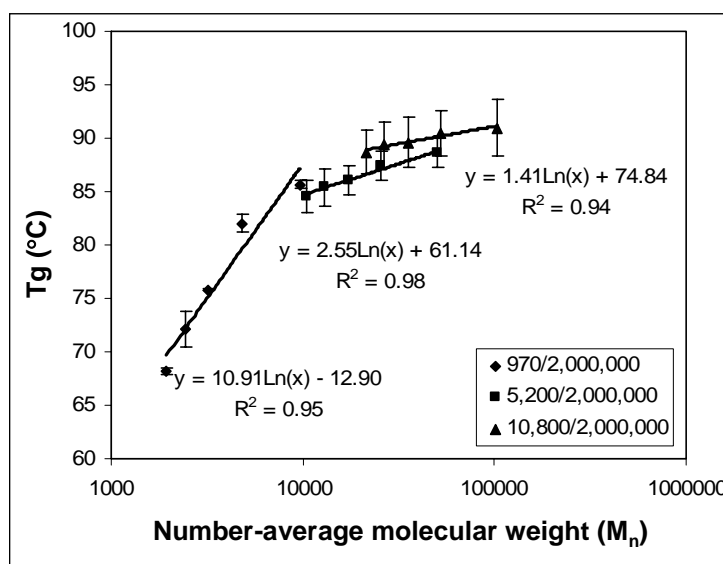


Figure 4.10: Effect of  $M_n$  on  $T_g$  of the 30% concentrated, freeze-dried solutions of dextran mixtures

#### 4.1.4. Relationship between $T_g$ and Composition of Dextran Systems

The dextran mixtures prepared from 30% dextran solutions displayed a single  $T_g$ , located between the  $T_g$ s of the individual components (Figure 4.5b). The relationship between the glass transition temperature and the composition of a compatible polymer blend is typically described by the Couchman-Karasz equation (Equation 2.50) (Couchman and Karasz, 1978). Yet, in practice many deviations from this additivity equation have been observed. For example, the experimental  $T_g$  values can be either smaller or larger than the predicted ones (Schneider, 1997). In case of the miscible dextran blends analyzed in this study, the experimental  $T_g$  values were lower than the  $T_g$  values predicted by the Couchman-Karasz equation using  $T_g$  and  $\Delta C_p$  of the individual components at  $a_w=0.33$  (Figure 4.11). According to Schneider (1997), this is typical of polymer blends characterized by interaction energies mostly involving non-polar interactions, hydrogen bonds. Such blends show less or no local ordering due to hetero-contacts which lead to enhanced conformational mobility and higher free volume as compared to the additivity based predictions (Icoz et al., 2005).

So far, the major question that was being investigated was: “Are there barriers to miscibility of dextrans with different molecular weights?” The results have demonstrated that when mutual diffusion limited miscibility, even polymers with the same chemistry/molecular structure with different molecular weights exhibited immiscibility. When the polymers were dissolved in a common solvent, the same materials become completely miscible at all component ratios.



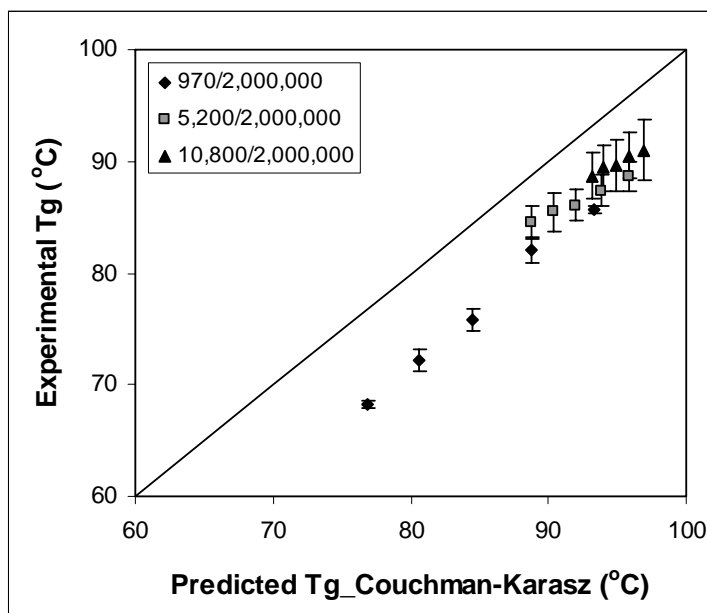


Figure 4.11: Comparison of  $T_g$  predictions by Couchman-Karasz equation with experimental  $T_g$  values for 30% concentrated, freeze-dried solutions of dextran mixtures

The next question to be investigated was; “What can be the molecular mechanism of miscibility in dextran systems?” and “Are there specific bonding interactions that affect miscibility?” The next section focuses on providing answers to these questions.

## 4.2. Investigation of the Specific Bonding Interactions and the Possible Mechanism of Miscibility in Dextran Systems

### 4.2.1. Glass Transition Temperature ( $T_g$ ) of Derivatized Dextrans

This section presents the glass transition temperatures of individual derivatized dextrans (diethylaminoethyl dextran (DEAE) and dextran sulfate (DS500)). These chemically derivatized dextrans, which are commercially obtained, are both produced from standard dextran with an average molecular weight of 500,000.  $T_g$  of pure DEAE

dextran (Figure 3.3) prepared from solutions at different polymer concentrations equilibrated at  $a_w=0.33$  were determined to be between 56-57°C (Figure 4.12). The  $T_g$  of the standard dextran with an average molecular weight of 500,000 equilibrated at  $a_w=0.33$  was 98.1°C (Figure 4.2). The difference in  $T_g$ s between the standard dextran of  $M_w \sim 500,000$  and DEAE dextran produced from a similar molecular weight indicated the effect of the added side chains on the mobility of the dextrans. The addition of DEAE-subunits (0.33 mol DEAE/1 mol glucose) increased the mobility of dextran molecule significantly. A decrease in the  $T_g$  from 98.1°C to 56-57°C is quite significant and shows the effect of side branches on mobility. On the other hand, the  $T_g$  for DS500 (Figure 3.4) at similar conditions was 106°C (Figure 4.12), which was slightly higher than the  $T_g$  of standard dextran with  $M_w \sim 500,000$ . Even though the substitution of sulfate groups in DS500 (2 mol sulfate/1 mol glucose) was significantly higher than the substitution in DEAE dextran (0.33 mol DEAE/1 mol glucose), they did not contribute to the mobility of the system. The reason for obtaining slightly higher  $T_g$  with DS500 than that with standard dextran would possibly be due to having slightly higher molecular weight of DS500 compared to standard dextran because of the high number of added side chains. Longer side chains even with lower degree of substitution (as in the case of DEAE dextran) promoted flexibility of the molecule and enhanced the mobility in the system resulting in lower  $T_g$  as compared to the  $T_g$  of standard dextran with similar  $M_w$ ; and as compared to another similar  $M_w$  derivatized dextran with short side chains even with higher degree of substitution (as in the case of DS500). The comparison between the  $T_g$  of derivatized dextrans and standard dextran showed that even small changes in the

chemistry of a carbohydrate polymer changed the behavior of the system significantly (Icoz and Kokini, 2007a).

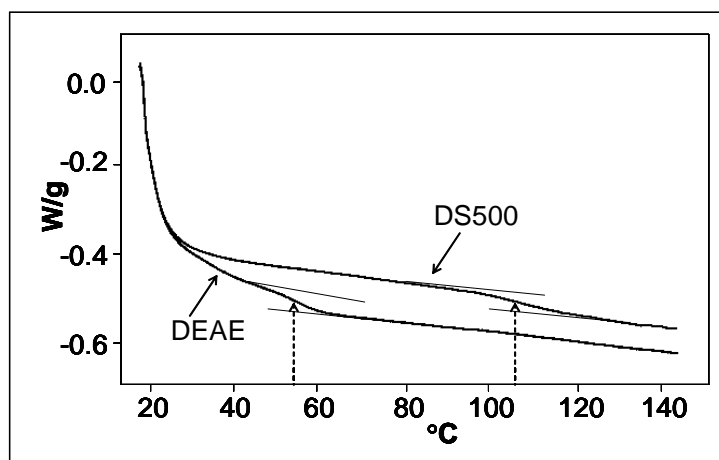


Figure 4.12: DSC thermograms of DEAE and DS500 prepared from 30% polymer concentrated solutions in the absence of NaCl [IS(NaCl)=0]

#### 4.2.2. Miscibility in Derivatized Dextrans Prepared from Different Polymer Concentrations and Added NaCl

In the previous section, the glass transition temperatures of individual derivatized dextrans were discussed. In this current section, the miscibility behavior of these dextrans with each other in the presence of salt and without salt are presented. Salt is an electrolyte that screens the repulsive forces between the polyelectrolytes and would result in a change in the miscibility behavior of these charged polymers. In the absence of NaCl [IS(NaCl)=0], the  $T_g$  of DEAE prepared from 30%, 50%; and 70% polymer concentrated solutions were determined as  $56.1 \pm 0.28^\circ\text{C}$ ;  $56.9 \pm 0.14^\circ\text{C}$ ; and  $56.3 \pm 0.35^\circ\text{C}$ , respectively (Table 4.3). Similarly,  $T_g$  of DS500 prepared from different concentrated solutions were

106.7±0.28°C; 105.7±0.64°C; and 105.4±0.21°C, respectively (Table 4.3). Samples prepared from different polymer concentrations in the absence of NaCl resulted in similar glass transition temperatures, as would be expected. The moisture contents of these samples [IS(NaCl)=0] were also very comparable to each other (Table 4.4) (Icoz and Kokini, 2007a).

Table 4.3:  $T_g$  of DS500 and DEAE systems prepared from 30%; 50%; and 70% polymer concentrations with added NaCl of IS=0; IS=1M; and IS=2M

	$T_g$ (°C)	$T_g$ (°C)	$T_g$ (°C)
	IS(NaCl)=0	IS(NaCl)=1M	IS(NaCl)=2M
DS500 - 30%	106.7 ± 0.28	100.8 ± 0.35	101.1 ± 0.21
DS500+DEAE - 30% - 50/50	82.9 ± 0.71	41.7 ± 0.14 / 103.8 ± 0.35	41.6 ± 0.35 / 113.7 ± 0.85
DEAE - 30%	56.1 ± 0.28	47.0 ± 0.71	46.8 ± 1.06
	IS(NaCl)=0	IS(NaCl)=1M	IS(NaCl)=2M
	IS(NaCl)=0	IS(NaCl)=1M	IS(NaCl)=2M
DS500 - 50%	105.7 ± 0.64	100.1 ± 0.14	100.8 ± 0.35
DS500+DEAE - 50% - 50/50	82.1 ± 0.57		40.7 ± 0.21 / 111.9 ± 0.28
DEAE - 50%	56.9 ± 0.14	52.5 ± 0.71	50.1 ± 0.64
	IS(NaCl)=0	IS(NaCl)=1M	IS(NaCl)=2M
	IS(NaCl)=0	IS(NaCl)=1M	IS(NaCl)=2M
DS500 - 70%	105.4 ± 0.21	102.7 ± 1.20	102.4 ± 1.20
DS500+DEAE - 70% - 50/50	80 ± 0.71	79.0 ± 1.41	78.6 ± 0.14
DEAE - 70%	56.3 ± 0.35	55.2 ± 0.07	51.3 ± 3.96

$T_g$  values of mixtures prepared only at 50/50 ratio were reported, since sensitivity of DSC to monitor multiple  $T_g$  behavior in 25/75 and 75/25 ratios, if any, would be limited. As one of the component ratios gets smaller, as in the case of 25/75 or 75/25, the heat flow also gets smaller at a similar ratio, which makes  $T_g$  identification difficult. In the absence of NaCl [IS(NaCl)=0], samples prepared from 30%, 50% and 70% total polymer concentrated solutions showed a single  $T_g$  (Figure 4.13) (82.9±0.71°C;

Table 4.4: Moisture content (% d.b.) of DS500 and DEAE systems prepared from 30%; 50%; and 70% polymer concentrations with added NaCl of IS=0; IS=1M; and IS=2M

	% Moisture (d.b.)	% Moisture (d.b.)	% Moisture (d.b.)
	IS(NaCl)=0	IS(NaCl)=1M	IS(NaCl)=2M
DS500 - 30%	13.71 ± 0.52	12.54 ± 0.02	11.43 ± 0.08
DS500+DEAE - 30% - 50/50	11.93 ± 0.72	11.36 ± 0.04	11.05 ± 0.00
DEAE - 30%	11.09 ± 0.74	11.79 ± 1.23	9.91 ± 0.03
	IS(NaCl)=0	IS(NaCl)=1M	IS(NaCl)=2M
DS500 - 50%	13.68 ± 0.90	13.48 ± 0.10	13.00 ± 0.20
DS500+DEAE - 50% - 50/50	12.41 ± 0.93	12.48 ± 0.42	12.49 ± 0.01
DEAE - 50%	10.85 ± 0.02	11.59 ± 0.08	11.13 ± 0.11
	IS(NaCl)=0	IS(NaCl)=1M	IS(NaCl)=2M
DS500 - 70%	13.64 ± 0.45	13.58 ± 0.06	13.92 ± 0.27
DS500+DEAE - 70% - 50/50	12.48 ± 0.31	12.06 ± 0.02	12.84 ± 0.85
DEAE - 70%	10.85 ± 0.21	11.26 ± 0.42	12.06 ± 1.88

82.1±0.57°C; and 80±0.71°C, respectively) (Table 4.3), indicating miscible systems. In Section 4.1.3 we showed that the  $T_g$  of the mixed dextrans depended on their number-average molecular weight, rather than weight-average molecular weights. When a small molecular weight dextran was mixed in equal weight proportions (50/50) with a high molecular weight dextran, the single  $T_g$  of the mixed system was closer to the  $T_g$  of the small molecular weight component. When the two dextrans of different molecular weights were mixed in equal amounts, the mixture had higher number of small molecular weight dextran than high molecular weight dextran resulting in higher free volume in the system and causing the significant effect on the  $T_g$  of the mixture. In the mixture of DS500 and DEAE, since the two components in the blend have similar molecular weights (around 500,000), the  $T_g$  of the 50/50 ratio mixtures were approximately at the midpoint of the  $T_g$ s of the individual components (Table 4.3) (Icoz and Kokini, 2007a).

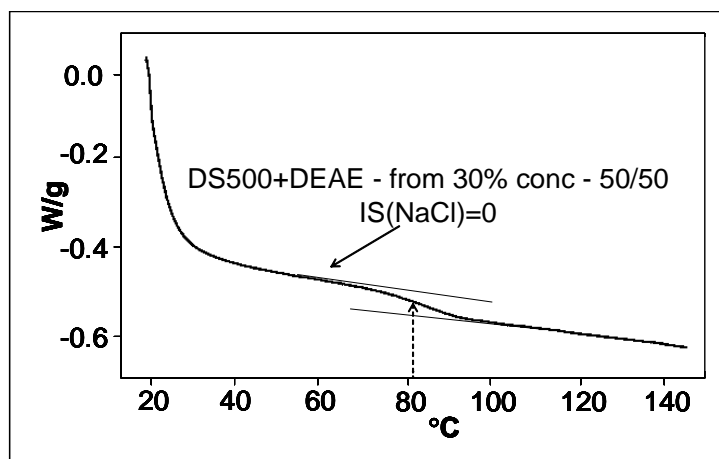


Figure 4.13: Single  $T_g$  in 50/50 ratio of DS500+DEAE prepared from 30% polymer concentrated solutions in the absence of NaCl [IS(NaCl)=0]

$T_g$  of both DS500 and DEAE prepared from 30% polymer concentration in the presence of NaCl [IS(NaCl)=1M or IS(NaCl)=2M] were lower than  $T_g$  of samples prepared from 30% concentrated samples in the absence of NaCl ( $100.8 \pm 0.35^\circ\text{C}$  and  $47.0 \pm 0.71^\circ\text{C}$  at IS(NaCl)=1M;  $101.1 \pm 0.71^\circ\text{C}$  and  $46.8 \pm 1.06^\circ\text{C}$  at IS(NaCl)=2M compared to  $106.7 \pm 0.28^\circ\text{C}$  and  $56.1 \pm 0.28^\circ\text{C}$  at IS(NaCl)=0) (Table 4.3). Both DEAE and DS500 are charged polymers (poly-electrolytes). There are strong repulsive forces between similarly charged monomers of a polyelectrolyte that results in highly swollen and stretched conformation of the molecule (Shinoda, 1978; Dobrynin et al., 1996; Jousset et al., 1998; Lauten and Nystrom, 2000; Walstra, 2003). These strong repulsive interactions have shown to be screened by the addition of an electrolyte (such as salt) to the aqueous solution of charged polymer molecules (Figure 2.18) (Demetriades and McClements, 1998; Lauten and Nystrom, 2000; Basak et al., 2003; Hellebust et al., 2004). Due to electrostatic screening effects in the presence of an electrolyte, flexibility

of the polyelectrolyte increases favoring intra-molecular interactions, and leads to more compact and less expanded structure that occupies less volume (Basak et al., 2003). According to this, both DEAE and DS500 became more flexible upon addition of NaCl; and as the  $T_g$  data showed, the mobility in the polymers increased, resulting in lower  $T_g$  in the presence of added NaCl compared to polymers without NaCl (Table 4.3). Moisture contents of these samples were slightly different from each other; for example, moisture content of DS500 prepared from 30% solutions at IS(NaCl)=0; 1M; and 2M were 13.71; 12.54; 11.43% (d.b.), respectively (Table 4.4). Lower moisture content at IS(NaCl)=2M than IS(NaCl)=1M resulted in slightly similar  $T_g$  value of the two samples. If these two samples had closer moisture contents, then  $T_g$  of sample with IS(NaCl)=2M would be slightly lower than the reported value due to plasticization effect of water, which would more clearly show the effect of more addition of NaCl (1M vs. 2M) on the  $T_g$  behavior of the samples (Icoz and Kokini, 2007a).

In the 50/50 mixture of the same polymer mixture, there were 2  $T_g$  values (Table 4.3) ( $41.7 \pm 0.14^\circ\text{C}$  and  $103.8 \pm 0.35^\circ\text{C}$  at IS(NaCl)=1M (Figure 4.14);  $41.6 \pm 0.35^\circ\text{C}$  and  $113.7 \pm 0.85^\circ\text{C}$  at IS(NaCl)=2M), representing the  $T_g$  of the individual components in the blend, indicating immiscibility between the components. The explanation of immiscibility of two poly-electrolytes in the presence of added salt would be due to “preferable” intra-molecular interactions in the components rather than inter-molecular interactions between the components. At IS(NaCl)=0, both poly-electrolytes had intra-molecular repulsive forces so when these poly-electrolytes came together, they got involved in inter-molecular interactions, resulting in miscible polymers with 1  $T_g$ . However, in the presence of NaCl, the repulsive forces were screened and the intra-

molecular interactions were enabled, decreasing the possible inter-molecular interactions and resulting in immiscible systems with 2  $T_g$ s (Icoz and Kokini, 2007a).

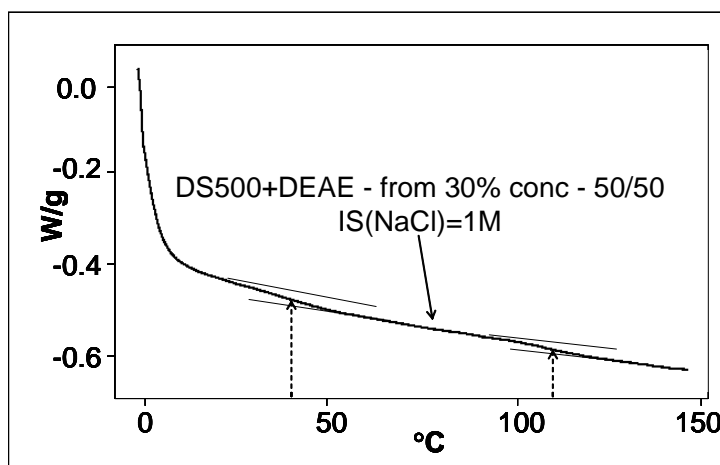


Figure 4.14: Two  $T_g$ s in 50/50 ratio of DS500+DEAE prepared from 30% polymer concentrated solutions with IS(NaCl)=1M

Similar behavior was observed for samples prepared from 50% total polymer concentrated solutions and their blends (Table 4.3). On the other hand, for samples prepared at 70% polymer concentration, the effect of added NaCl (1M and 2M) on reducing the  $T_g$  of pure components was less compared to samples prepared at lower polymer concentrations (Table 4.3). The  $T_g$  of the individual components prepared at 70% concentration in the presence of NaCl were closer to the  $T_g$ s in the absence of NaCl. There was also a single  $T_g$  in the mixed systems. Because at high polymer concentrations, the concentration of the counter-ions in the poly-electrolyte was also high, so the presence of NaCl did not significantly affect the mobility and miscibility in the systems. Therefore, the polyelectrolyte at high polymer concentration, even in the presence of added NaCl, behaved closer to the system in the absence of salt (Icoz and Kokini, 2007a).



#### **4.2.3. FTIR Spectroscopy for Miscible/Immiscible Derivatized Dextrans to Probe Specific Bonding Interactions**

DSC analyses of blends with two derivatized dextrans have shown miscible or immiscible system depending on the ionic strength through addition of NaCl. This current section investigates the possible mechanism of these miscibility/immiscibility through FTIR spectroscopy, which provides information on specific interaction between molecules. Molecules containing hydroxyl groups can self-associate and can form intramolecular interactions through formation of hydrogen bonds between their hydroxyl groups, forming di-mers and higher multi-mers (Figure 2.6). Hydrogen bonds are dynamic in nature, so they continuously break and reform by thermal motion. At any instant of time, a number of free (non-hydrogen bonded) monomers, hydrogen bonded dimers and multi-mers exist; and the change in concentration and temperature affects their distribution (Coleman et al., 1991; Coleman and Painter, 1995). Coleman and Painter (1995) have analyzed the infrared spectra of the hydroxyl stretching region of 2-propanol, a small molecule with a hydroxyl group that can form hydrogen bonds, in cyclohexane, an inert solvent that can not make any hydrogen bonds with 2-propanol, at different concentrations (Figure 2.7). Bands at 3630, 3530 and 3350 $\text{cm}^{-1}$  are assigned to non-hydrogen bonded hydroxyl groups, hydrogen bonded dimers and hydrogen bonded multimers, respectively (Coleman and Painter, 1995); and the reasoning behind the changes in these bands at different concentrations are discussed in Section 2.3.3.1. These assigned bands would form the basis for the observed bands in hydroxyl stretching regions of dextran systems in this study.

Hydroxyl stretching regions of FTIR spectra ( $\sim 4000\text{--}2700\text{cm}^{-1}$ ) for DS500+DEAE blends prepared from 30% polymer concentration in the absence of NaCl is given in Figure 4.15. Based on the band assignments of Coleman and Painter (1995) described above and also in Section 2.8.2, Figure 4.15 was interpreted as follows: Individual DEAE showed a broad band at  $3286\text{cm}^{-1}$  due to high number of hydrogen bonded OH groups (in the form of multi-mers). Individual DS500 had a shoulder in the similar region (at  $3250\text{cm}^{-1}$ ) due to a number of hydrogen bonded OH groups (in the form of multi-mers). DS500 (Figure 3.4) has one hydroxyl group per glucose molecule that can make intra-molecular hydrogen bonds and these groups are much less than those in DEAE (Figure 3.3), which was confirmed in the spectra as a shoulder rather than a broad band at  $3250\text{cm}^{-1}$ . DS500 has also showed a broad band at  $3450\text{cm}^{-1}$  due to hydrogen bonded OH (in the form of di-mers); and a shoulder around  $3600\text{cm}^{-1}$  due to free OH groups. The shoulder of DS500 around  $3600\text{cm}^{-1}$  for free OH groups disappeared as DEAE was introduced into the system, because free OH groups participated in hydrogen bonding with DEAE (Figure 4.16). The shoulder of DS500 at  $3250\text{cm}^{-1}$  was still present in the blends although its magnitude was getting smaller. The broad band of DS500 at  $3450\text{cm}^{-1}$  and the broad band of DEAE at  $3286\text{cm}^{-1}$  shifted towards each other in mixtures, indicating that the components were forming inter-molecular hydrogen bonds with each other. This was shown by the broad bands at  $3420\text{cm}^{-1}$ ;  $3381\text{cm}^{-1}$ ; and  $3323\text{cm}^{-1}$  for 75/25, 50/50 and 25/75 blends, respectively (Figure 4.15) (Icoz and Kokini, 2007a).

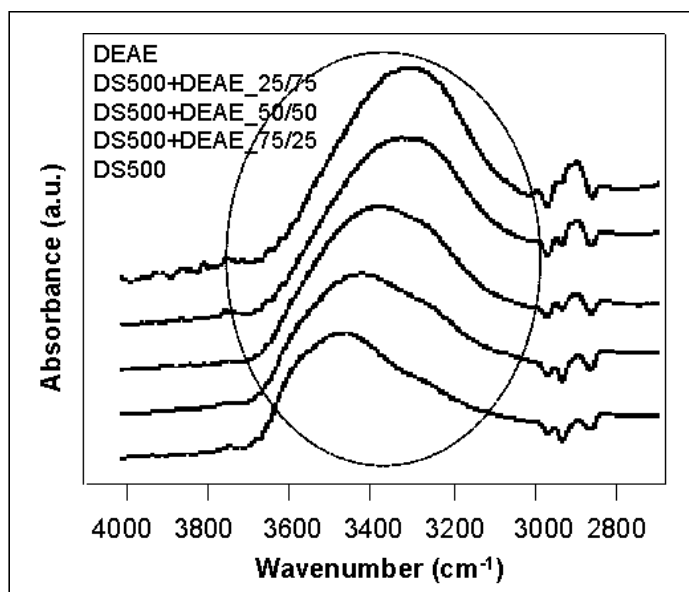


Figure 4.15: Hydroxyl stretching regions of FTIR spectra for DS500+DEAE blends prepared from 30% polymer concentration in the absence of NaCl [IS(NaCl)=0]

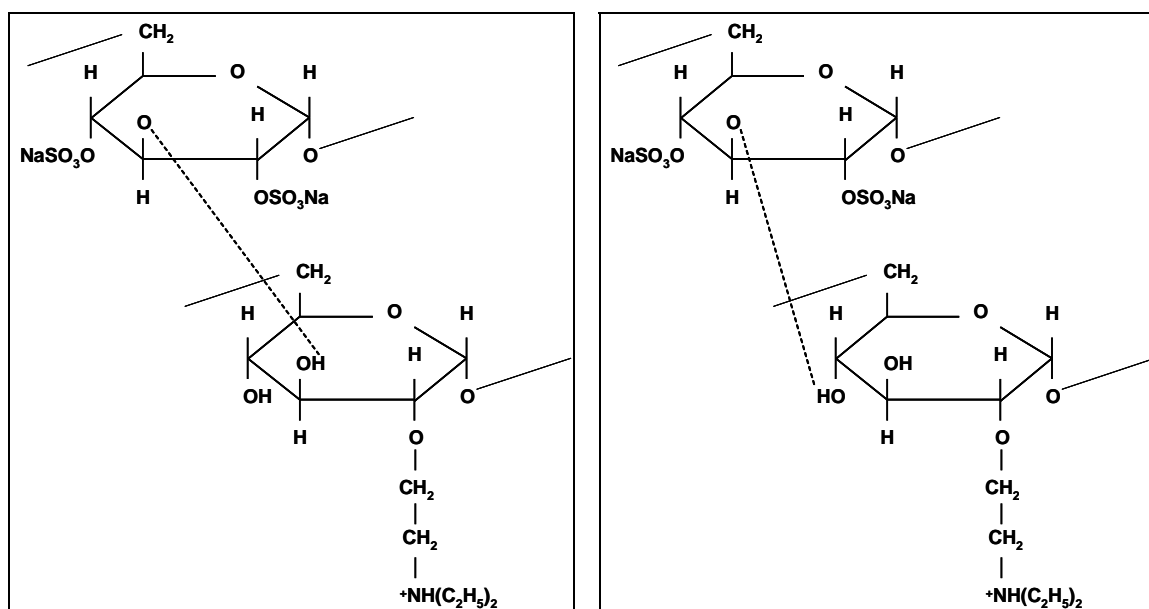


Figure 4.16: Schematics of possible hydrogen bonding between DS500 and DEAE

Another significant region that can be analyzed in terms of interactions in dextran systems was the C-OH stretching region of FTIR spectra ( $\sim 990\text{-}1060\text{cm}^{-1}$ ). Because when a hydroxyl group next to a carbon atom was involved in hydrogen bond formation, the bond between C and OH would also be affected. C-OH stretching vibrations of DS500+DEAE blends prepared at 30% polymer concentration in the absence of NaCl is shown in Figure 4.17. DEAE had a single peak around  $1003\text{cm}^{-1}$ . DS500 had two peaks at  $1010\text{cm}^{-1}$  and  $976\text{cm}^{-1}$ , respectively. In the blends, as DS500 was introduced into DEAE, the following shifts in the bands occurred: A peak around  $1005\text{cm}^{-1}$  and a shoulder around  $990\text{cm}^{-1}$  in DS500+DEAE(25/75) blend; two peaks around  $1007\text{cm}^{-1}$  and  $985\text{cm}^{-1}$  in DS500+DEAE(50/50) blend; two peaks around  $1009\text{cm}^{-1}$  and  $978\text{cm}^{-1}$  in DS500+DEAE(75/25) blend. The systematic shifts/changes in the bands of mixtures were also an indicative of the switches in bands from intra-molecular hydrogen bonds to inter-molecular hydrogen bonds between components that affected the C-OH vibrations. These blends have shown a single  $T_g$  behavior determined by DSC (Table 4.3). Therefore, the formation of sufficient hydrogen bonds facilitates miscibility, as observed by thermal analysis. Other blends that showed a single  $T_g$  behavior had similar FTIR spectra (Icoz and Kokini, 2007a).

Hydroxyl stretching regions of FTIR spectra for DS500+DEAE blends prepared from 30% polymer concentration and at NaCl added [ $\text{IS}(\text{NaCl})=1\text{M}$ ] is given in Figure 4.18. FTIR spectra of these blends, which showed 2  $T_g$ s with DSC, did not show such systematic change in the bands compared to those with a single  $T_g$ . IR spectrum of the pure components, DEAE and DS500, showed similar bands as those in Figure 4.15. The bands of the mixtures got broader rather than any kind of shifts or changes in

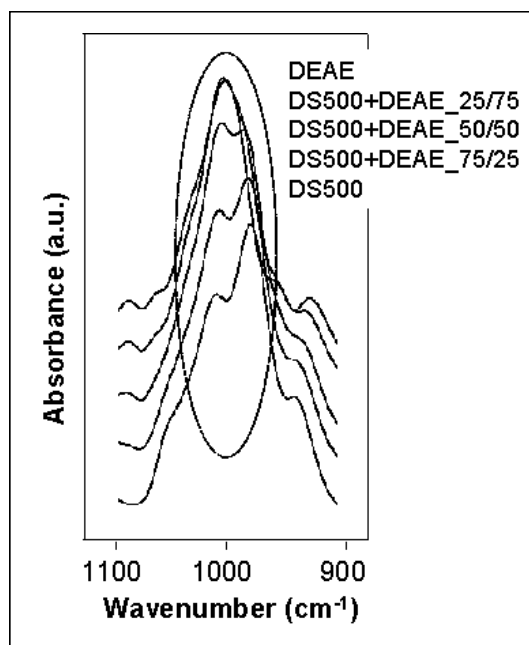


Figure 4.17: C-OH stretching region of FTIR spectra for DS500+DEAE blends prepared from 30% polymer concentration in the absence of NaCl [IS(NaCl)=0]

the bands. Similarly, C-OH vibrations for this system did not show the systematic change in the bands of the mixtures (Figure 4.19). For example, DEAE showed a peak around  $1002\text{cm}^{-1}$ ; DS500+DEAE(25/75) blend had a single peak around  $1004\text{cm}^{-1}$ ; DS500+DEAE(50/50) blend also had a single peak around  $1005\text{cm}^{-1}$ ; DS500 shows two peaks around  $1010\text{cm}^{-1}$  and  $977\text{cm}^{-1}$ ; and DS500+DEAE(75/25) blend has two peaks similar to pure DS500, around  $1007\text{cm}^{-1}$  and  $995\text{cm}^{-1}$ . These results can be interpreted as the “appropriate addition” of IR spectra of pure components (Chalmers and Overall, 1993; Dong and Ozaki, 1997). Other blends that showed 2  $T_g$ s with thermal analysis had similar FTIR spectra (Icoz and Kokini, 2007a).

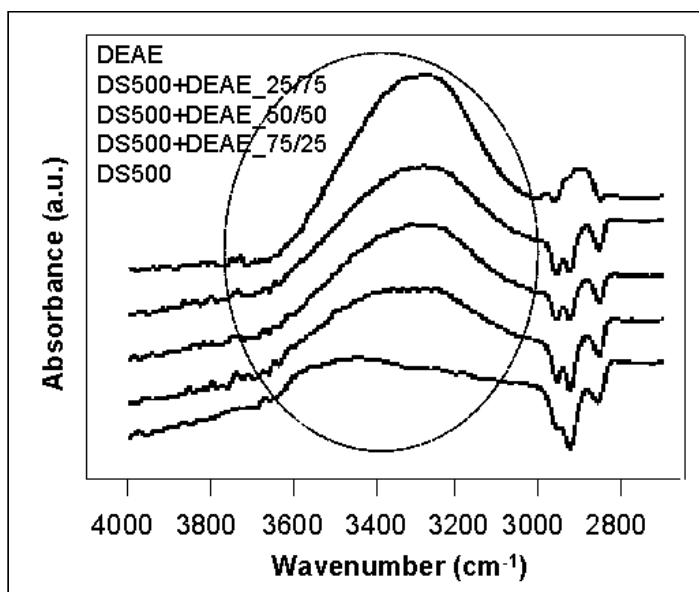


Figure 4.18: Hydroxyl stretching regions of FTIR spectra for DS500+DEAE blends prepared from 30% polymer concentration with IS(NaCl)=1M

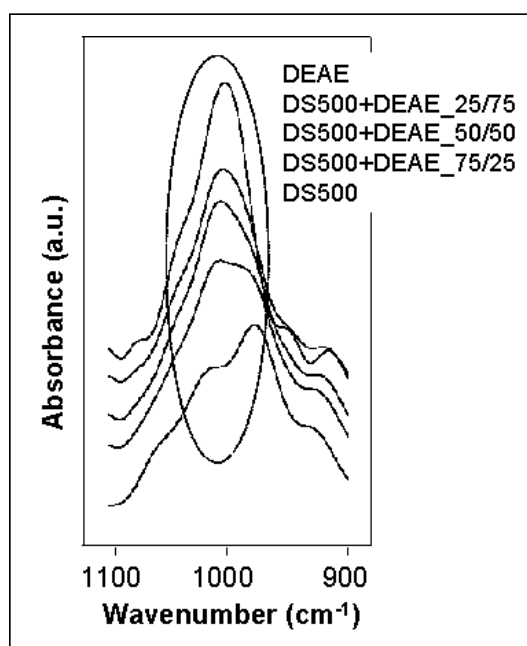


Figure 4.19: C-OH stretching region of FTIR spectra for DS500+DEAE blends prepared from 30% polymer concentration with IS(NaCl)=1M

As a summary, the analysis in this section has shown that there were changes in hydrogen bonding distribution of pure components in the miscible dextran systems, due to changes in intra- and inter-molecular interactions as the components were mixed. For instance, free OH bonds in DS500 participated in hydrogen bonding with DEAE; intra-molecular hydrogen bonding got lesser in DEAE as it was mixed with DS500 forming inter-molecular bonds. In the immiscible systems, similar clear changes were not observed, indicating that sufficient hydrogen bonding was not present to form miscible systems. Overall, FTIR spectroscopy was shown to probe the specific bonding interactions in dextrans as model carbohydrate polymers, which was combined with the DSC results, suggesting the possible mechanism of miscible systems through sufficient hydrogen bonding interactions in the blend (Icoz and Kokini, 2007a).

### **4.3. Quantitative Prediction of Miscibility in Carbohydrate Polymer Systems**

#### **4.3.1. Examination of the Original Flory-Huggins Theory to Predict Miscibility in Dextran Systems**

This part of the dissertation deals with quantitative prediction of miscibility/immiscibility in carbohydrate polymers using thermodynamic rules of mixing. First, the quantitative predictions using Flory-Huggins theory, which is a thermodynamic model based on the role of the number of configurational arrangements and quantitative measures based on dispersive interactions, is presented to show its ability to predict miscibility in dextran systems. Figure 4.20 and Figure 4.21 show free energy and 2<sup>nd</sup> derivative of free energy of mixing for two dextrans of  $M_w=1,000+M_w=2,000,000$  using Flory-Huggins equation (Equation 2.5), calculated using the solubility parameters in

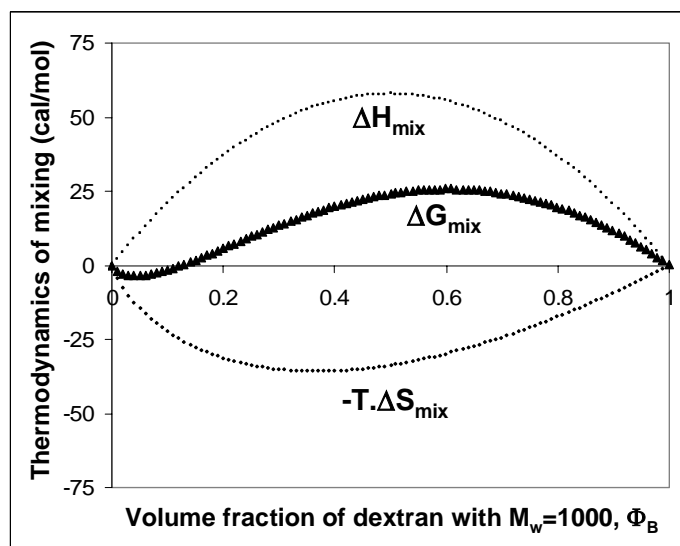
Equation 3.14 (from Figure 3.7) and Equation 3.15 (from Figure 3.8), respectively. The contributions from both entropic ( $-T.\Delta S_{\text{mix}}$ ) and enthalpic ( $\Delta H_{\text{mix}}$ ) terms are also illustrated as a function of volume fraction of  $M_w=1,000$  ( $\Phi_B$ ) on each figure (Appendix D). Both Figure 4.20a and Figure 4.21a showed negative (-) valued contribution from  $-T.\Delta S_{\text{mix}}$  (favorable for mixing) over the entire volume fraction range of dextrans, since the volume fractions in Equation 2.5 were smaller than 1 and logarithm of a number smaller than 1 always gives a negative (-) value. The calculation of the entropic term was independent of two different versions of calculating solubility parameters; and was only dependent on the volume fractions and the size of the polymers; as a result both Figure 4.20a and Figure 4.21a had same  $-T.\Delta S_{\text{mix}}$  values (Icoz and Kokini, 2007b).

On the other hand, contribution from enthalpy of mixing ( $\Delta H_{\text{mix}}$ ) was calculated to be positive (+) over the entire composition range, opposing mixing, since enthalpic term was determined through the square of the difference between solubility parameters of components. Slightly different  $\Delta H_{\text{mix}}$  values were calculated in Figure 4.20a and Figure 4.21a due to the difference in calculating solubility parameters from Equation 2.9 (Figure 3.7) and Equation 2.10 (Figure 3.8) (Icoz and Kokini, 2007b). In the calculation of solubility parameter from group contributions using Equation 2.9, only weak dispersive forces were included, whereas the calculation of solubility parameter using Equation 2.10 also includes a rough estimation of groups contributions due to polar and hydrogen bonding forces. The calculation of  $\Delta H_{\text{mix}}$  involves the square difference of component solubility parameters (Equation 2.7 and Equation 2.5). Using Equation 2.9, solubility parameters of dextran with  $M_w=1,000$  and  $M_w=2,000,000$  were calculated as  $\delta_{1000}=19.2 \text{ (cal/cm}^3)^{1/2}$  and  $\delta_{2000000}=17.2 \text{ (cal/cm}^3)^{1/2}$ , resulting in a factor from the square

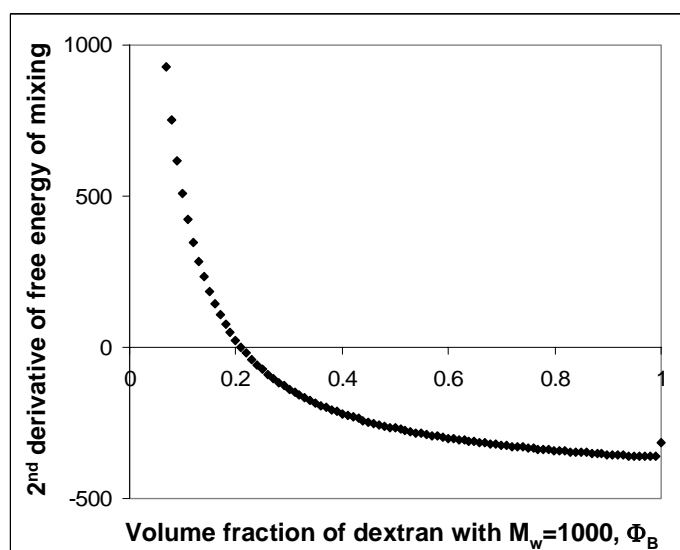


of the solubility parameter difference as “4”. Using Equation 2.10,  $\delta_{1000}=22.1 \text{ (cal/cm}^3\text{)}^{1/2}$  and  $\delta_{2000000}=20.4 \text{ (cal/cm}^3\text{)}^{1/2}$  was obtained, resulting in a factor from the square of the solubility parameter difference as “2.89”. So, the difference between “4” and “2.89” inserted in Equation 2.7 to calculate the Flory-Huggins interaction parameter ( $\chi_{AB}$ ), which is then inserted in Equation 2.5 to calculate the  $\Delta H_{\text{mix}}$  is the reason for obtaining slightly different values for  $\Delta H_{\text{mix}}$  in Figure 4.20a and Figure 4.21a.

The requirement for miscibility is having negative (-) valued  $\Delta G_{\text{mix}}$  (Equation 2.1) and positive (+) valued second derivative of  $\Delta G_{\text{mix}}$  (Equation 2.3). In Figure 4.20 and Figure 4.21, the overall free energy of mixing ( $\Delta G_{\text{mix}}$ ), which is the summation of entropic and enthalpic terms (Equation 2.2 and Equation 2.5), and the second derivative of free energy of mixing gave partial positive and partial negative values over the entire composition range, depending on the contribution from enthalpic term ( $\Delta H_{\text{mix}}$ ). This indicated prediction of partially miscible systems. If negative (-)  $\Delta G_{\text{mix}}$  had been obtained over the entire volume fraction range with a concave upwards plot (Figure 2.1a), then dextran with  $M_w=1,000$  and  $M_w=2,000,000$  would be predicted to be completely miscible for all compositions. Blends of dextran with  $M_w=1,000+M_w=2,000,000$  were shown to be miscible (Figure 4.9 and Figure 4.10) due to their compatible nature with same repeating unit structure. However, the free energy and its second derivative calculated using the original Flory-Huggins theory in Figure 4.20 and Figure 4.21 were unsatisfactory in predicting the actual miscibility in these systems. The Flory Huggins theory predicted that dextrans would be immiscible which is not supported by experimental data (Icoz and Kokini, 2007b).



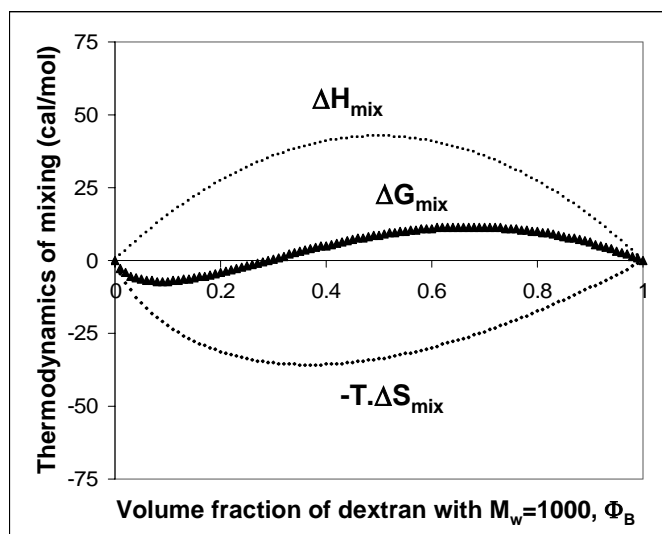
(a)



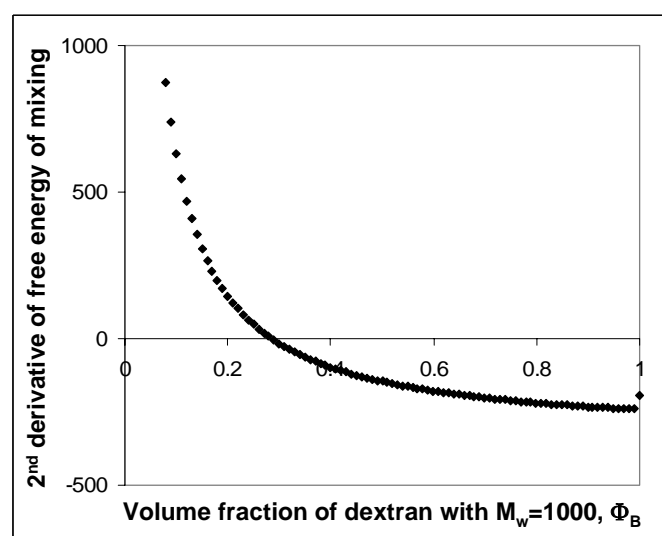
(b)

Figure 4.20: Flory-Huggins miscibility predictions for two dextrans with  $M_w=1,000$  and  $M_w=2,000,000$  at  $25^\circ\text{C}$ ; (a) Free energy ( $\Delta G_{\text{mix}}$ ), enthalpy ( $\Delta H_{\text{mix}}$ ), and entropy ( $-T\Delta S_{\text{mix}}$ ) of mixing; (b) 2<sup>nd</sup> derivative of free energy of mixing

[using solubility parameters calculated from group contributions as  $\delta = \left( \frac{\sum E_{\text{coh}}}{\sum V_m} \right)^{1/2}$ ]



(a)



(b)

Figure 4.21: Flory-Huggins miscibility predictions for two dextrans with  $M_w=1,000$  and  $M_w=2,000,000$  at  $25^\circ\text{C}$ ; (a) Free energy ( $\Delta G_{\text{mix}}$ ), enthalpy ( $\Delta H_{\text{mix}}$ ), and entropy ( $-T\Delta S_{\text{mix}}$ ) of mixing; (b) 2<sup>nd</sup> derivative of free energy of mixing

[using solubility parameters calculated from group contributions as  $\delta^2 = \delta_d^2 + \delta_p^2 + \delta_h^2$ ]

In Figure 4.20, the volume fraction ( $\Phi_B$ ) of  $M_w=1,000$  where the change from negative  $\Delta G_{\text{mix}}$  (and positive 2<sup>nd</sup> derivative) to positive  $\Delta G_{\text{mix}}$  (and negative 2<sup>nd</sup> derivative) occurred (i.e. *from miscible to immiscible system predictions*) was around  $\Phi_B=0.13$  (13/87 % component ratio of  $M_w=1,000+M_w=2,000,000$ ). In Figure 4.21 the same volume fraction for transition from miscibility to immiscibility was determined to be about  $\Phi_B=0.29$  (29/71 % component ratio of  $M_w=1,000+M_w=2,000,000$ ), showing a larger range of volume fraction region where the two polymers are miscible (Figure 4.20). The reason for this was due to the difference in calculation of the solubility parameter ( $\delta$ ) of the repeating unit of dextran (Figure 3.7 and Figure 3.8) and therefore calculation of  $\delta$  for dextran with different  $M_w$ . Calculation of solubility parameter in Figure 3.7 was done by considering only the dispersive forces through group contribution methods. The calculation of the solubility parameter in Figure 3.8 has also very roughly included the effect of the polar and the hydrogen bonding forces in addition to dispersive forces. Since the repeating unit of dextran is a glucose molecule with a number of hydroxyl groups, it has high capacity to participate in hydrogen bonding interactions. The difference between solubility parameters of dextran with  $M_w=1,000$  and  $M_w=2,000,000$  given in Equation 3.14 was larger than that in Equation 3.15, resulting in higher enthalpic contribution through Equation 2.7 and resulting in a smaller range of volume fractions to obtain miscibility between the two dextrans of different molecular weights (Figure 4.20 vs. Figure 4.21). In other words, although Figure 4.21 showed more regions where the two components were predicted to be miscible compared to Figure 4.20, it was still not successful enough to predict the experimentally observed miscibility (Icoz and Kokini, 2007b).

These results have shown that the original Flory-Huggins theory was not able to predict miscibility in dextran blends as model carbohydrate polymers. Its inability to adequately predict miscibility was due to the lack of inclusion of specific bonding interactions and in particular due to its limitation of underestimating the contribution of hydrogen bonds to mixing of dextrans. In other words, calculating enthalpy of mixing using interaction parameters determined from the square of the difference between solubility parameters of the two components underestimated the presence of strong hydrogen bonding between the components, which would actually enhance their miscibility by creating sufficient thermodynamics of interactions.

#### **4.3.2. Application of Painter-Coleman Association Model to Predict Miscibility in Dextran Systems**

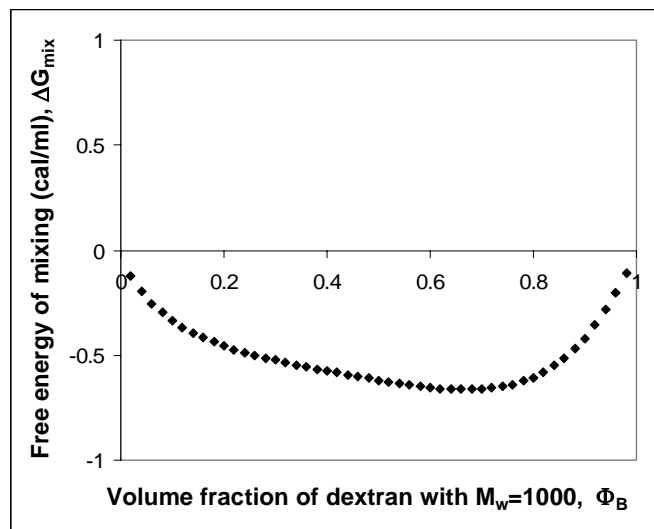
Previous section has shown that thermodynamic theories based solely on conformational and configurational theories (Flory-Huggins theory) is not capable of predicting miscibility in carbohydrates. As most carbohydrate polymers have structural groups that can form a large number of hydrogen bonds, prediction of their molecular mixing would require advanced thermodynamic models that can include the effect of hydrogen bonding. Painter-Coleman association model is one such quantitative thermodynamic model that can improve the miscibility predictions, which handles the specific hydrogen bonding interactions separately by inserting a free energy of hydrogen bond formation term to the right-hand side of the original Flory-Huggins equation (Equation 2.12, Equation 2.39).

#### 4.3.2.1. Effect of Analogue Compound Selected to Approximate Hydrogen Bonding in Carbohydrates on Thermodynamic Calculations of Miscibility

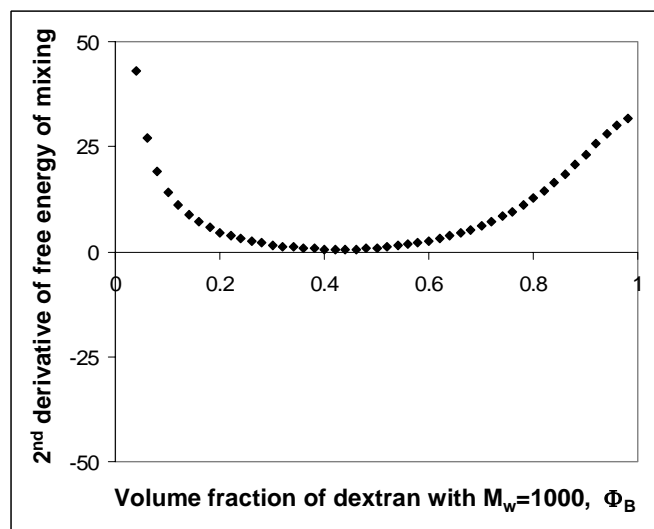
In order to be able to utilize Painter-Coleman association model, one of the approximations to be made is the use of analogue compounds to simulate the hydrogen bonding of the OH groups on the repeating units of carbohydrates. These analogue compounds are small molecular weight molecules that have hydroxyl groups with similar chemical environments to the repeating unit of the polymer in interest. In other words, they are model with similar chemical structure to the repeating unit of the polymer in interest. As described in Section 3.4.3.1, pentanol, phenol and dimethylphenol (Figure 3.10) were identified as the analogue compounds which hydrogen bonding through OH groups were approximated for hydrogen bonding in dextrans. Figures 4.22-4.24 show the calculated free energy (Equation 2.39) and second derivative of free energy of mixing for two dextrans with  $M_w=1,000$  and  $M_w=2,000,000$  as a function of volume fraction of dextran with  $M_w=1,000$  ( $\Phi_B$ ). Negative free energy of mixing ( $\Delta G_{\text{mix}}$ ) coupled with positive 2<sup>nd</sup> derivative is the quantitative indication for miscible polymers. According to this, when H-bonding of dextrans was approximated using H-bond formation of pentanol OH through self- and inter-association equilibrium constants ( $K_2=51.6$ ;  $K_B=85.6$ ;  $K_A=85.6$ , Table 3.2),  $\Delta G_{\text{mix}}$  was calculated to be negative (Figure 4.22a) and 2<sup>nd</sup> derivative of  $\Delta G_{\text{mix}}$  gave positive values for all volume fractions ( $\Phi_B$ ) (Figure 4.22b), satisfying the two required thermodynamic conditions for miscibility. This new calculation predicted miscibility at all component volume ratios in this polymer system. When H-bonding of dextrans was approximated with H-bond formation of phenol OH through self- and inter-association equilibrium constants ( $K_2=40.7$ ;  $K_B=129.6$ ;  $K_A=129.6$ ,

Table 3.2),  $\Delta G_{\text{mix}}$  was determined to be negative at all  $\Phi_B$  (Figure 4.23a), but 2<sup>nd</sup> derivative of  $\Delta G_{\text{mix}}$  gave negative values at  $\Phi_B=0.33-0.71$  (Figure 4.23b), predicting immiscible systems in this range. On the other hand, when H-bonding of dextrans was approximated with H-bond formation of dimethylphenol OH through self- and inter-association equilibrium constants ( $K_2=13.0$ ;  $K_B=47.6$ ;  $K_A=47.6$ , Table 3.2),  $\Delta G_{\text{mix}}$  gave positive values at  $\Phi_B=0.36-0.91$  (Figure 4.24a), and 2<sup>nd</sup> derivative was negative at  $\Phi_B=0.32-0.82$  (Figure 4.24b), predicting immiscibility between  $\Phi_B=0.32-0.91$  in the system. These two dextrans with  $M_w=1,000$  and  $M_w=2,000,000$  were experimentally miscible at all proportions with single  $T_g$  behavior. They basically have the same repeating groups and the same chemical structure and form miscible systems due to their compatible nature. Figures 4.22-4.24 demonstrates that using “pentanol” as the analogue model compound for H-bond formation of dextrans enabled miscible system predictions over the entire composition range, whereas the use of phenol and dimethylphenol as the analogue compounds did not. This helped us calibrate the value of the predictions with different hydrogen bond forming molecules and groups. Clearly the only useful system helping us predict miscibility is the “pentanol” system (Icoz and Kokini, 2007c).

In order to clearly demonstrate what causes the difference between miscibility predictions of dextrans using the three analogue compounds (Figures 4.22-4.24), individual contributions of entropy, enthalpy and H-bonding on total free energy of mixing (Equation 2.39) were plotted in Figure 4.25. Both enthalpic and entropic contributions had the same values in Figures 4.25a, 4.25b, 4.25c. Entropic contributions were calculated from the first two terms on the right hand side of Equation 2.39 using



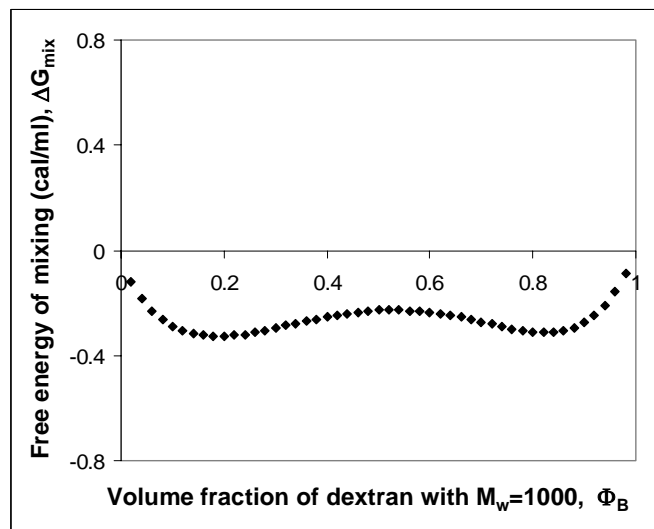
(a)



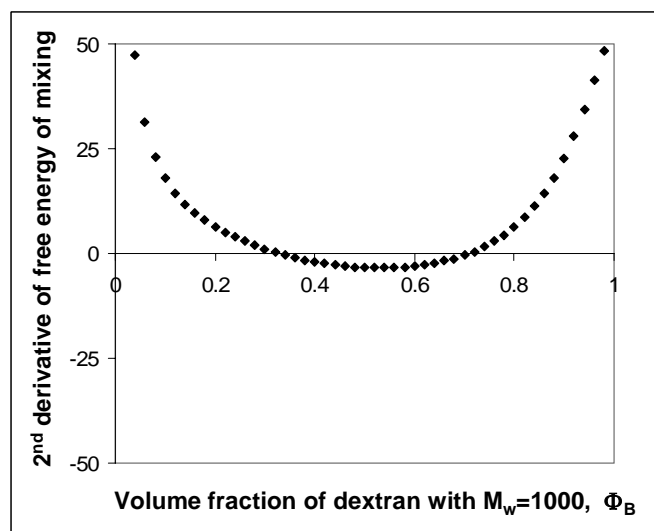
(b)

Figure 4.22: Predicted miscibility of two dextrans with  $M_w=1,000$  and  $M_w=2,000,000$  at  $25^\circ\text{C}$  when H-bonding of *pentanol OH* was used to simulate H-bonding in dextrans; (a) Free energy of mixing; (b) 2<sup>nd</sup> derivative of free energy of mixing [ $\gamma=0.30$ ]



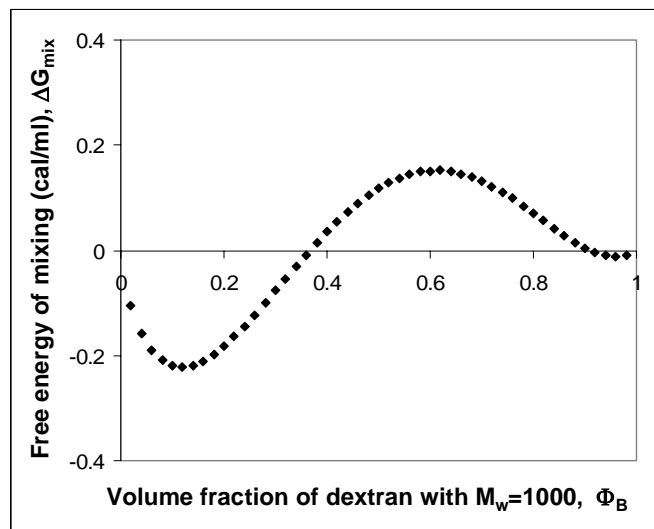


(a)

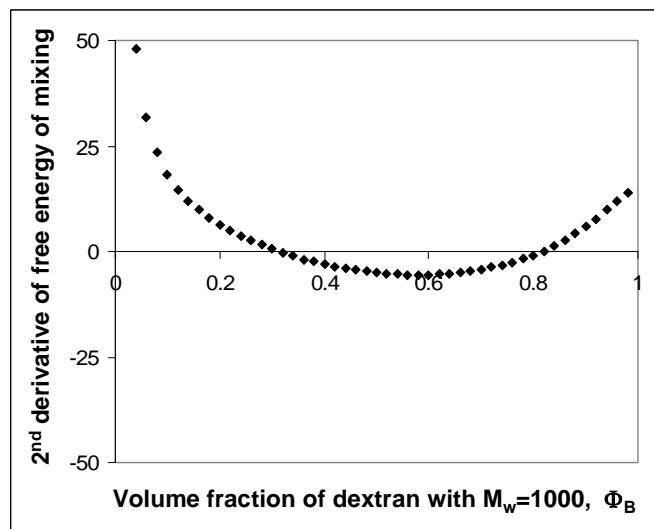


(b)

Figure 4.23: Predicted miscibility of two dextrans with  $M_w=1,000$  and  $M_w=2,000,000$  at  $25^\circ\text{C}$  when H-bonding of *phenol OH* was used to simulate H-bonding in dextrans; (a) Free energy of mixing; (b) 2<sup>nd</sup> derivative of free energy of mixing [ $\gamma=0.30$ ]



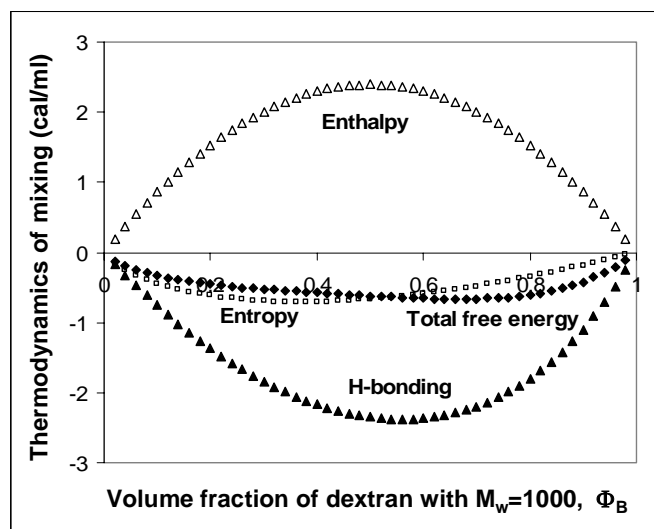
(a)



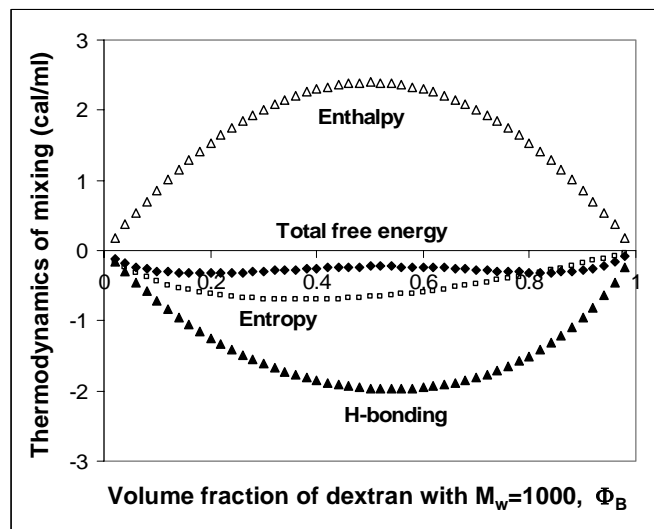
(b)

Figure 4.24: Predicted miscibility of two dextrans with  $M_w=1,000$  and  $M_w=2,000,000$  at  $25^\circ\text{C}$  when H- bonding of dimethylphenol OH was used to simulate H-bonding in dextrans; (a) Free energy of mixing; (b) 2<sup>nd</sup> derivative of free energy of mixing [ $\gamma=0.30$ ]

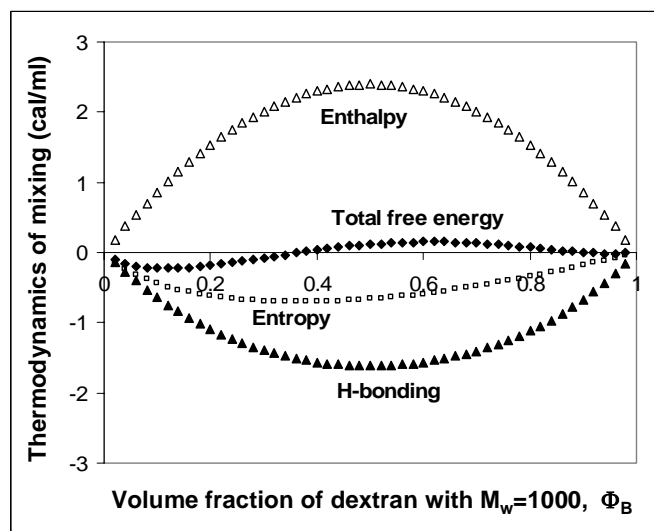
volume fractions and degree of polymerization of dextrans themselves, and were favorable to mixing with negative values (Figure 4.25). Enthalpic contributions were calculated from the 3<sup>rd</sup> term on the right hand side of Equation 2.39 using non-hydrogen-bonded solubility parameters of dextrans (Table 3.3), and were unfavorable to mixing with positive values (Figure 4.25). H-bonding contributions (last term on the right hand side of Equation 2.39) were calculated to be negative (Figure 4.25), showing strong favorable contribution to mixing. These contributions were calculated as a function of self- and inter-association equilibrium constants of dextrans (Table 3.2) that were approximated from H-bonding in pentanol, phenol and dimethylphenol. H-bonding contribution decreased in the order of the use of pentanol, phenol and dimethylphenol as the analogue compound (Figure 4.25) (Icoz and Kokini, 2007c).



(a)



(b)



(c)

Figure 4.25: Entropic, enthalpic, and H-bonding contributions to the total free energy of mixing two dextrans with  $M_w=1,000$  and  $M_w=2,000,000$  at  $25^\circ\text{C}$  when H-bonding of; (a) pentanol OH; (b) phenol OH; (c) dimethylphenol OH was used to simulate H-bonding in dextrans [ $\gamma=0.30$ ]

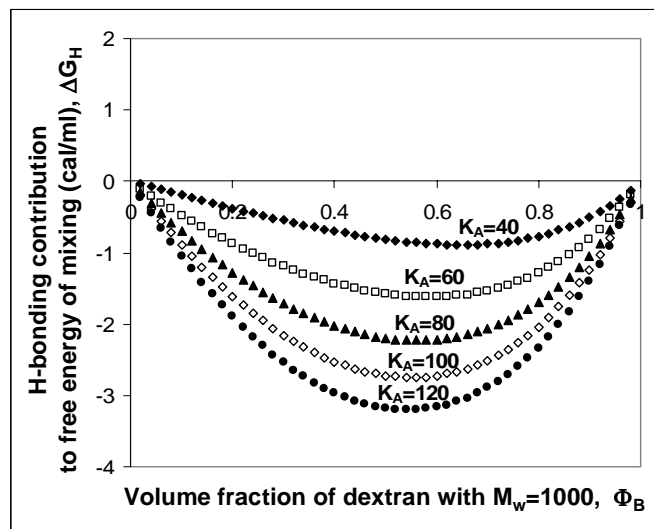
Since entropic and enthalpic contributions to total free energy of mixing were the same (Figures 4.25a, 4.25b, 4.25c), the difference in total free energy of mixing was only due to the differences in H-bonding approximations. The structure of pentanol is the closest to the repeating unit of dextran with its linearly bonded carbon atoms (Figure 4.25a). Phenol, on the other hand, has a double bonded ring structure which creates steric hindrance in the structure making it less possible for its OH group to be involved in H-bonding (Figure 4.25b). Dimethylphenol has two additional methyl groups on phenol that causes even more steric hindrance and, therefore, less H-bonding capability demonstrated by the smallest H-bonding contribution (Figure 4.25c). Overall the results demonstrated that pentanol was the most suitable analogue model for H-bonding in the carbohydrate systems leading to better miscibility predictions (Icoz and Kokini, 2007c).

#### **4.3.2.2. Effect of Relative Values of Self-association and Inter-association Equilibrium Constants on Thermodynamic Calculations of Miscibility**

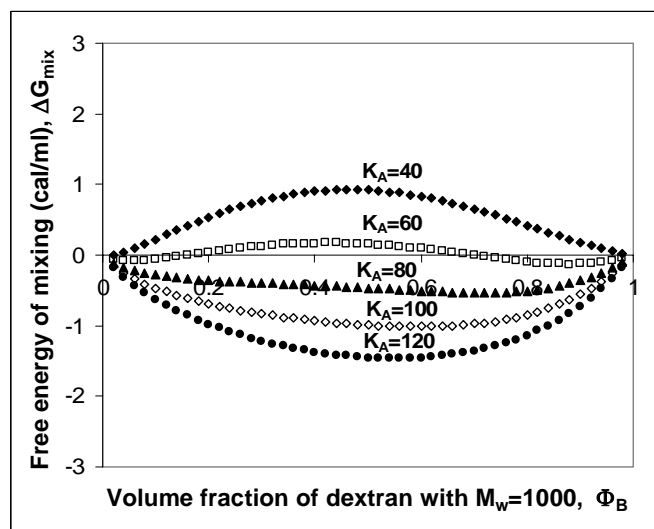
Self-association vs. inter-association in a system is an important factor in determining the extent of hydrogen bonding contribution to free energy of mixing. If self-association is more pronounced than inter-association (i.e. higher self-association equilibrium constant than inter-association equilibrium constant), it is expected that will be unfavorable for mixing in a two component system. Because the self-associating component will preferably be interacting with itself rather than forming inter-molecular bonds with the other component. On the other hand, if inter-association is more pronounced than self-association, then this will result in favorable mixing. Therefore, the

relative values of the equilibrium constants are the determinant factor for the extent of overall H-bonding and the free energy of mixing.

In order to demonstrate these ideas quantitatively, Figures 4.26-4.28 show the hypothetical hydrogen bonding contribution and the resulting free energy of mixing when the relative values of self-association and inter-association equilibrium constants were changed. Only H-bonding contribution and total free energy of mixing are shown in Figures 4.26-4.28, because entropic and enthalpic contributions to free energy of mixing would be the same for all cases (Equation 2.39 and Figure 4.25). When pentanol was used as the analogue compound for H-bonding of dextrans, the self-association equilibrium constants for di-mer and multi-mer formations were  $K_2=51.6$  and  $K_B=85.6$ , whereas inter-association equilibrium constant was  $K_A=85.6$  (Table 3.2). When  $K_A$  was hypothetically selected smaller than  $K_2$  or  $K_B$  (i.e. when  $K_A=40$  or  $K_A=60$ ), H-bonding contribution was small (Figure 4.26a), and was not enough to overcome the positive valued, unfavorable enthalpic contribution in Figure 4.25a, resulting in positive valued  $\Delta G_{\text{mix}}$  (immiscibility) (Figure 4.26b). As  $K_A$  values were chosen to be higher than  $K_2$  and  $K_B$  (i.e. when  $K_A=100$  or  $K_A=120$ ), the resulting negative valued H-bonding contribution was sufficient enough to overcome the positive valued, unfavorable enthalpic contribution. Thereby, negative valued  $\Delta G_{\text{mix}}$  (Figure 4.26b), in other words, miscibility in these systems, could be obtained. Similar hypothetical results are shown in Figure 4.27 and Figure 4.28, where phenol and dimethylphenol were used as the analogue compound for H-bonding of dextrans (Icoz and Kokini, 2007c).

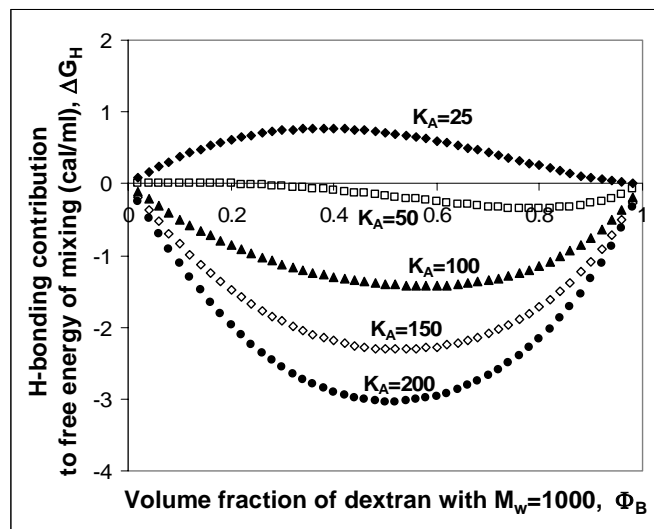


(a)

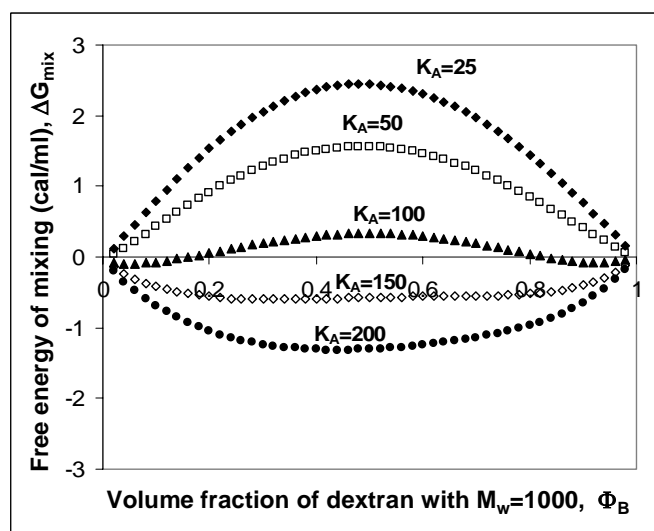


(b)

Figure 4.26: Effect of the value of inter-association equilibrium constant ( $K_A$ ) relative to self-association equilibrium constants ( $K_2$  and  $K_B$ ) on; (a) H-bonding contribution; (b) total free energy of mixing two dextrans with  $M_w=1,000$  and  $M_w=2,000,000$  at 25°C [H-bonding of pentanol OH was approximated for H-bonding in dextrans; and  $\gamma=0.30$ ]



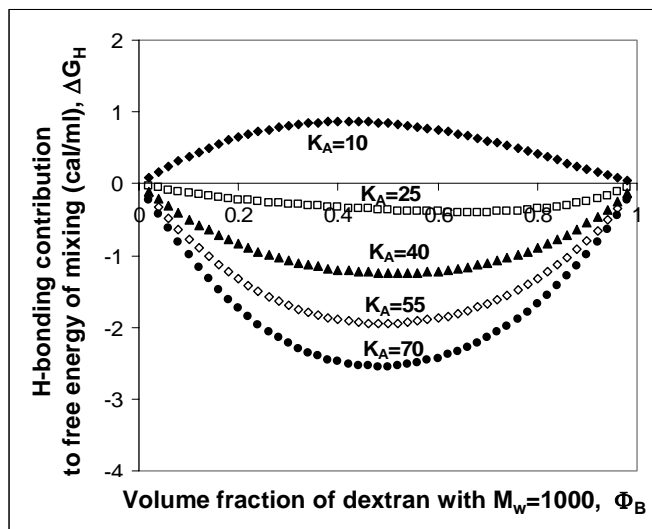
(a)



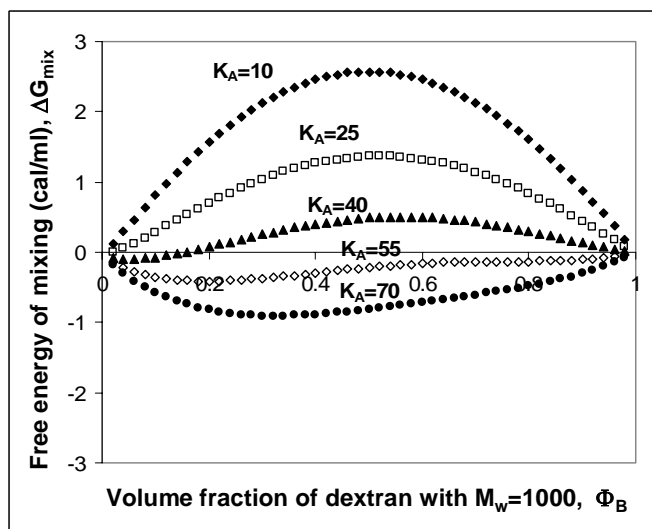
(b)

Figure 4.27: Effect of the value of inter-association equilibrium constant ( $K_A$ ) relative to self-association equilibrium constants ( $K_2$  and  $K_B$ ) on; (a) H-bonding contribution; (b) total free energy of mixing two dextrans with  $M_w=1,000$  and  $M_w=2,000,000$  at  $25^\circ\text{C}$  [H-bonding of phenol OH was approximated for H-bonding in dextrans; and  $\gamma=0.30$ ]





(a)



(b)

Figure 4.28: Effect of the value of inter-association equilibrium constant ( $K_A$ ) relative to self-association equilibrium constants ( $K_2$  and  $K_B$ ) on; (a) H-bonding contribution; (b) Total free energy of mixing two dextrans with  $M_w=1,000$  and  $M_w=2,000,000$  at  $25^\circ\text{C}$  [H-bonding of dimethylphenol OH was approximated for H-bonding in dextrans; and  $\gamma=0.30$ ]

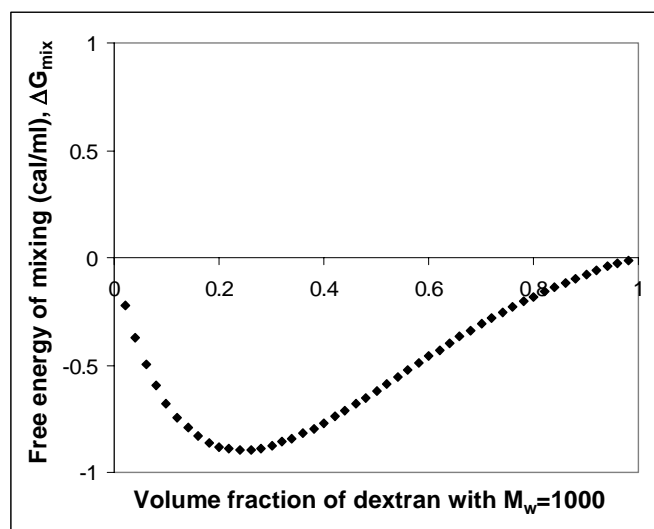
#### **4.3.2.3. Effect of Selection of the Self-associating Component in the System on Thermodynamic Calculations of Miscibility**

In order to use the Miscibility Guide & Phase Calculator (MG&PC) Software, one of the approximations needed was to define one of the dextran molecules as the self-associating component. Results up to now (Section 4.3.2.1 and Section 4.3.2.2) showed the results when dextran with  $M_w=1,000$  was chosen as the self-associating component in  $M_w=1,000 + M_w=2,000,000$  system. This is reasonable because it would be expected that the small molecular weight component would more easily self associate since the low molecular weight component would be far more mobile. In the current section, thermodynamics of mixing when dextran with  $M_w=2,000,000$  was selected as the self-associating component. This is needed to create a contrast between the self association of the low molecular weight and high molecular weight component in affecting miscibility predictions.

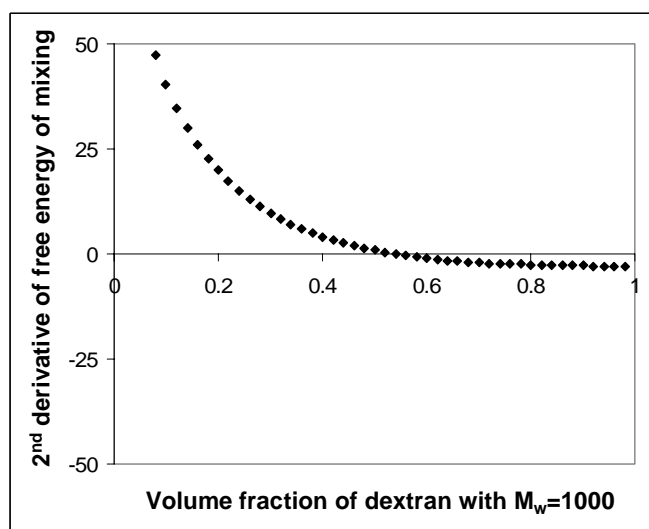
In the MG&PC Software, the self-associating component is always denoted as “B”. When the thermodynamics of mixing are calculated, the values of the x-axis in the resulting plots are the volume fractions of the self-associating component (B). In this section, the self-associating polymer is selected as dextran with  $M_w=2,000,000$ . For the results presented in this section, the x-axis was re-calculated as the volume fraction of  $M_w=1,000$  (by subtracting volume fraction of  $M_w=2,000,000$  from 1) in order to be able to compare these results with those when  $M_w=1,000$  was selected as the self-associating component (Figures 4.22-4.25).

Figures 4.29-4.31 illustrate free energy and 2<sup>nd</sup> derivative of free energy of mixing when dextran with  $M_w=2,000,000$  was selected as the self-associating component rather than  $M_w=1,000$ . When pentanol was used as the analogue compound, negative  $\Delta G_{\text{mix}}$  was calculated for all volume fractions (Figure 4.29a) and 2<sup>nd</sup> derivative of  $\Delta G_{\text{mix}}$  was negative at volume fractions  $> 0.54$  (Figure 4.29b) (immiscibility at volume fractions = 0.54-0.99). Selection of  $M_w=2,000,000$  as the self-associating component resulted in significantly smaller component ratios where the two dextrans are miscible when compared to the case of  $M_w=1,000$  as the self-associating component (Figure 4.22a and Figure 4.22b). On the other hand, when dimethylphenol was used as the analogue compound,  $\Delta G_{\text{mix}}$  was calculated to have positive values at volume fractions = 0.36-0.99 (Figure 4.31a); and 2<sup>nd</sup> derivative of  $\Delta G_{\text{mix}}$  had negative values at volume fractions = 0.30-0.82 (Figure 4.31b). There is not significant difference when miscibility prediction in Figure 4.24 (immiscibility between  $\Phi_B=0.32$ -0.91) were compared to that in Figure 4.31 (immiscibility at volume fraction = 0.30-0.99). H-bonding contribution was the least with dimethylphenol as the analogue compound (Figure 4.25c) and thermodynamic calculations showed that selecting dextran with low or high  $M_w$  as the self-associating component did not significantly change the miscibility predictions with this analogue compound. Similarly, when phenol was used as the analogue compound, negative  $\Delta G_{\text{mix}}$  was calculated for all volume fractions (Figure 4.30a) and 2<sup>nd</sup> derivative of  $\Delta G_{\text{mix}}$  was negative at volume fractions = 0.36-0.84 (Figure 4.30b) (immiscibility prediction at volume fraction = 0.36-0.84). Figure 4.25 and Figures 4.29-4.31 collectively demonstrated that the possibility of the components being involved in self-associated H-bonding ( $M_w=1,000$  vs.  $M_w=2,000,000$ ) affected the miscibility calculations as in the case

of using pentanol vs. dimethylphenol as the analogue compound (Icoz and Kokini, 2007c).

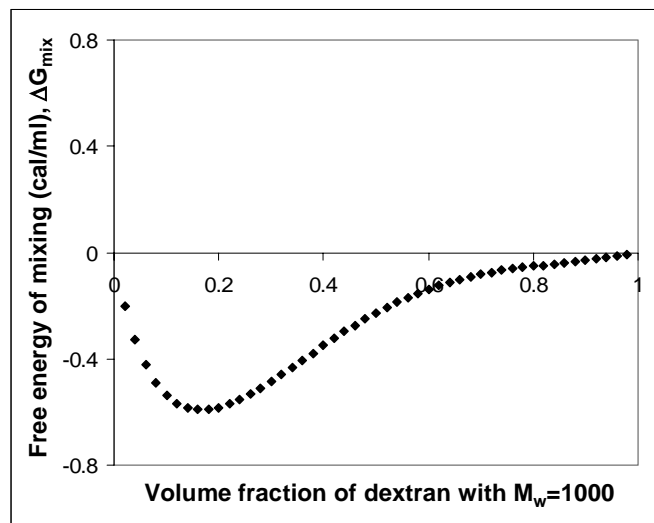


(a)

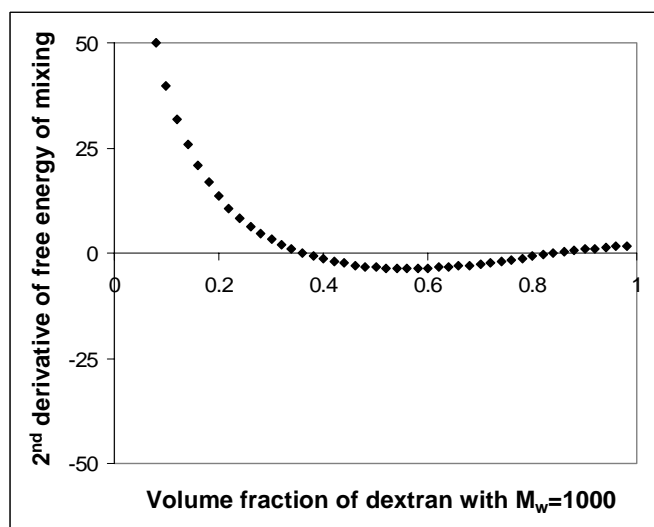


(b)

Figure 4.29: Predicted miscibility [ (a) free energy and (b) 2<sup>nd</sup> derivative of free energy of mixing) ] of two dextrans with  $M_w=1,000$  and  $M_w=2,000,000$  at 25°C when dextran with  $M_w=2,000,000$  was selected as the self-associating component [H-bonding of pentanol OH was approximated for H-bonding in dextrans; and  $\gamma=0.30$ ]

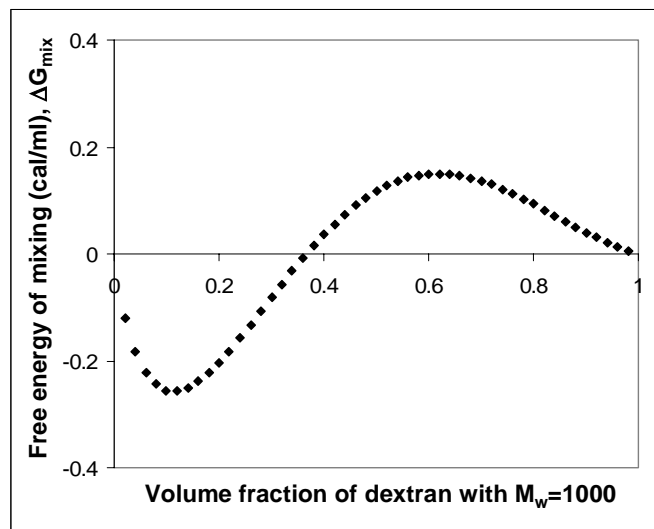


(a)

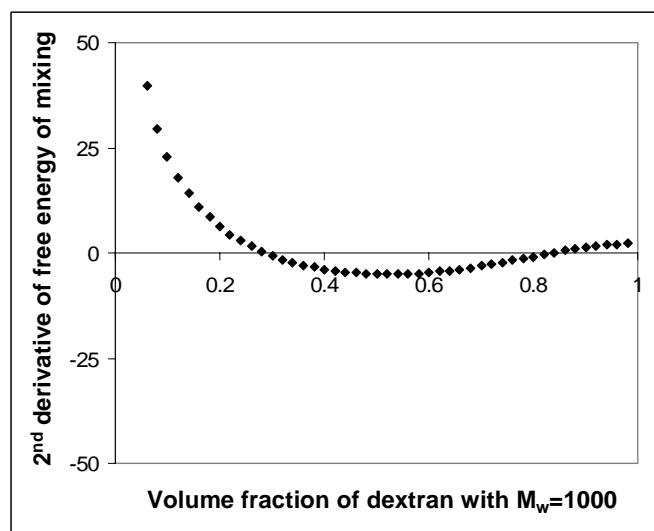


(b)

Figure 4.30: Predicted miscibility [ (a) free energy and (b) 2<sup>nd</sup> derivative of free energy of mixing ] of two dextrans with  $M_w=1,000$  and  $M_w=2,000,000$  at 25°C when dextran with  $M_w=2,000,000$  was selected as the self-associating component [H-bonding of phenol OH was approximated for H-bonding in dextrans; and  $\gamma=0.30$ ]



(a)



(b)

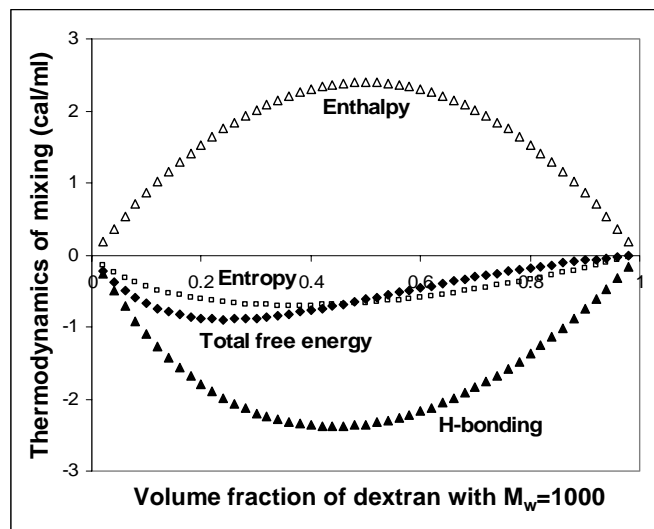
Figure 4.31: Predicted miscibility [ (a) free energy and (b) 2<sup>nd</sup> derivative of free energy of mixing ) ] of two dextrans with  $M_w=1,000$  and  $M_w=2,000,000$  at 25°C when dextran with  $M_w=2,000,000$  was selected as the self-associating component [H-bonding of dimethylphenol OH was approximated for H-bonding in dextrans; and  $\gamma=0.30$ ]

In order to understand the origins of the difference between the thermodynamics of mixing when dextran with  $M_w=1,000$  (Figures 4.22-4.24) or  $M_w=2,000,000$  (Figures 4.29-4.31) was selected as the self-associating component, individual contributions from entropy, enthalpy and H-bonding were plotted in Figure 4.32. Regardless of which analogue model compound was used for the hydrogen bonding in dextrans, enthalpic contributions had the same positive (+) values in Figure 4.32 and in Figure 4.25 (when  $M_w=1,000$  was selected as the self-associating component). This was because enthalpic contribution was calculated by inserting Equation 2.7 into Equation 2.39, where  $\chi$  was determined as a function of the square of the difference between non-hydrogen-bonded solubility parameters of components. Since there was a square of the difference, it did not make any difference if solubility parameter of  $M_w=1,000$  was subtracted from solubility parameter of  $M_w=2,000,000$  or the reverse. Moreover, enthalpic term in Equation 2.39 involved multiplication of volume fractions of components ( $\Phi_A$  and  $\Phi_B$ ) and since  $\Phi_A+\Phi_B=1$ , the multiplication of volume fractions did not change when the self-associating component changed. Similarly, entropic contributions in Figure 4.32 had the same negative (-) values compared to those in Figure 4.25, calculated from the first two terms on the right hand side of Equation 2.39 using volume fractions and degree of polymerization.

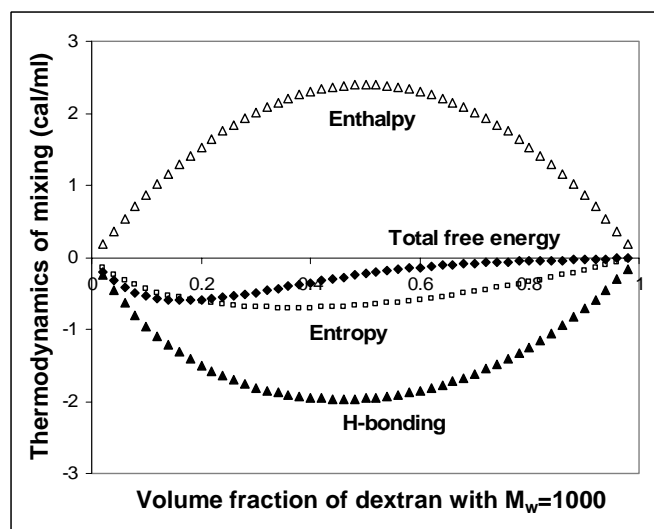
So, the difference between Figures 4.22-4.24 and Figures 4.29-4.31 was due to the slight difference in overall H-bonding contribution (last term on the right hand side of Equation 2.39) when either  $M_w=1,000$  or  $M_w=2,000,000$  was selected as the self-associating component. Although the association equilibrium constants used were exactly the same, the cause of this difference can be explained as follows: H-bonding

contribution does not have a symmetric convex shape with respect to volume fraction of 0.5 (Figure 4.25 and Figure 4.32). Rather, it shows a shift in the minimum point of the convex curve towards higher volume fractions of the self-associating component (around volume fraction of 0.6 of  $M_w=1,000$  and 0.4 of  $M_w=2,000,000$  in Figure 4.25; and around volume fraction of 0.6 of  $M_w=2,000,000$  and 0.4 of  $M_w=1,000$  in Figure 4.32). So, this shows that whichever self-associating component was selected, the overall H-bonding contribution was the most favorable (the highest negative values) at volume fraction of approximately 0.6 of the self-associating component; that is when the self-associating component was slightly more than the other component in the blend. On the other hand, for instance, at volume fraction of 0.2 of the self-associating component, there would be much less of self-associating component than the other component (0.2 vs. 0.8), so although the other component is at high volume fraction, there aren't enough self-associating components to participate in hydrogen bonding with it. Similarly, at volume fraction of 0.8 of the self-associating component (0.8 vs. 0.2), there would be much less of the other component, so similarly again not enough to participate in hydrogen bonding with the self-associating component. Note again that in Figure 4.32, the X-axis shows volume fraction of  $M_w=1,000$ ; and “(1-volume fraction of  $M_w=1,000$ )” would give volume fraction of  $M_w=2,000,000$ , which was the self-associating component in that figure. As volume fraction of  $M_w=1,000$  was low, volume fraction of  $M_w=2,000,000$  was high. This difference in the effect of volume fractions on the H-bonding contribution caused the difference in overall free energy in Figures 4.25 and Figure 4.32. Overall results demonstrated that selecting the component with the lower  $M_w$  resulted in better miscibility predictions.

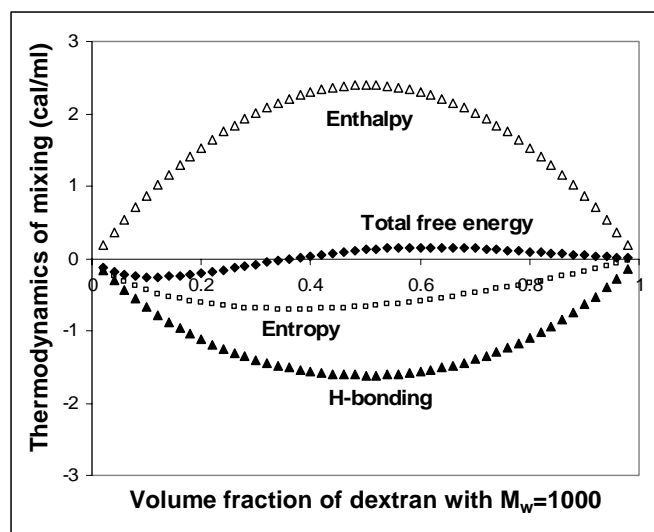




(a)



(b)



(c)

Figure 4.32: Entropic, enthalpic, and H-bonding contributions to the total free energy of mixing two dextrans with  $M_w=1,000$  and  $M_w=2,000,000$  at  $25^\circ\text{C}$  when dextran with  $M_w=2,000,000$  was selected as the self-associating component [H-bonding of; (a) pentanol OH; (b) phenol OH; (c) dimethylphenol OH was approximated for H-bonding in dextrans; and  $\gamma=0.30$ ]

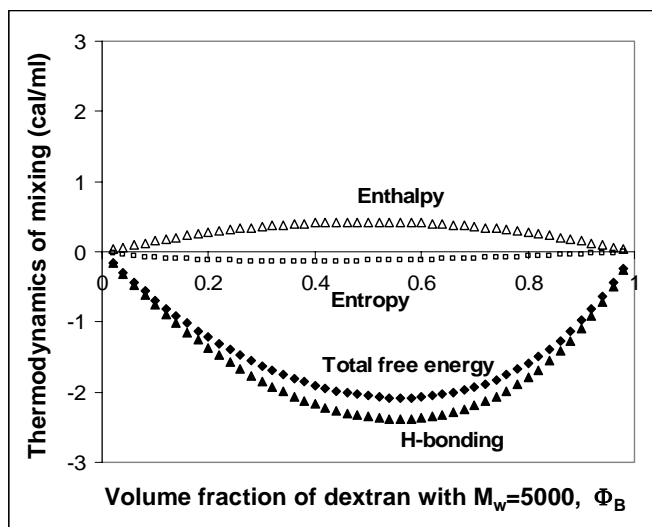
#### 4.3.2.4. Effect of Molecular Weight of Components on Thermodynamic Calculations of Miscibility

Figure 4.33a and Figure 4.33b show the individual thermodynamic contributions when dextran with  $M_w=1,000$  in the system was replaced with higher  $M_w$  dextrans ( $M_w=5,000$  and  $M_w=10,000$ , respectively) with pentanol being the analogue compound. These systems ( $M_w=5,000 + M_w=2,000,000$  and  $M_w=10,000 + M_w=2,000,000$ ) have also shown to be miscible with single  $T_g$  behavior (Figure 4.10). Enthalpic contributions decreased significantly as  $M_w$  of the components increased (Figure 4.25a, Figure 4.33a

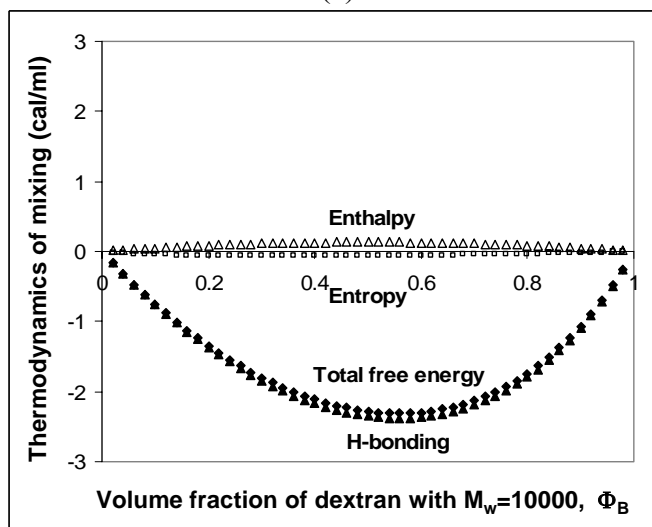
and Figure 4.33b), which was favorable for mixing. They were calculated from the square of the difference between the non-hydrogen-bonded solubility parameters of the two components (Equation 2.7 and equation 2.39), which got closer as the  $M_w$  of the components in the system got closer (Table 3.3), resulting in smaller enthalpic contribution. Entropic contributions also decreased as  $M_w$  of the components increased (Figure 4.25a, Figure 4.33a and Figure 4.33b), because the value of the first two terms in Equation 2.39 decreased as 'M' (number of segments in each polymer chain) got larger values with higher  $M_w$ , and this behavior was unfavorable for mixing. H-bonding contribution in all cases was calculated the same way (Figure 4.25a, Figure 4.33a and Figure 4.33b), which were approximated from H-bonding of pentanol as the analogue compound (Icoz and Kokini, 2007c).

Total free energy of mixing is the summation of entropic, enthalpic and H-bonding contributions (Equation 2.39). Since the entropic and, especially, enthalpic contributions decreased significantly with increased  $M_w$  of the components, total free energy of mixing resulted in higher negative values (Figure 4.25a, Figure 4.33a and Figure 4.33b). This indicated more spontaneous miscibility as the components had  $M_w$  that were closer in magnitude (for instance,  $M_w=1,000+M_w=2,000,000$  vs.  $M_w=10,000+M_w=2,000,000$ ). The total free energy of mixing significantly depended on H-bonding contribution, which became even more important in the systems with high  $M_w$  components (Figure 4.25a, Figure 4.33a and Figure 4.33b), as contributions from entropy and enthalpy vanished (Icoz and Kokini, 2007c). Similar results were obtained when phenol and dimethylphenol were used as the analogue compounds for H-bonding in dextrans (Figure 4.34 and Figure 4.35, respectively). Overall results demonstrated that as

$M_w$  of the components were closer to each other, the free energy of mixing, thereby miscibility, was mostly controlled by H-bonding contribution.

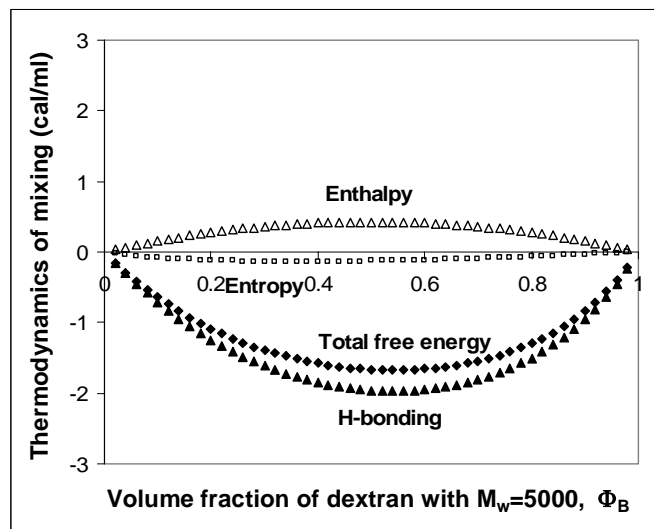


(a)

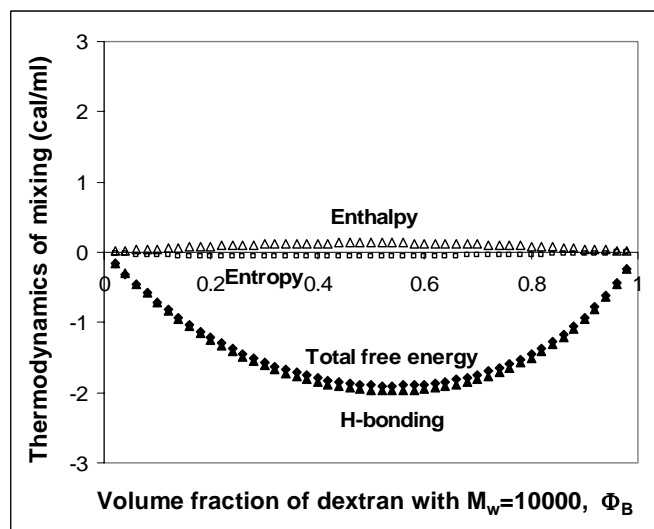


(b)

Figure 4.33: Effect of component molecular weight on entropic, enthalpic, and H-bonding contributions to the total free energy of mixing two dextrans at 25°C; Systems of (a)  $M_w=5,000$  and  $M_w=2,000,000$ ; (b)  $M_w=10,000$  and  $M_w=2,000,000$  [H-bonding of pentanol OH was approximated for H-bonding in dextrans; and  $\gamma=0.30$ ]

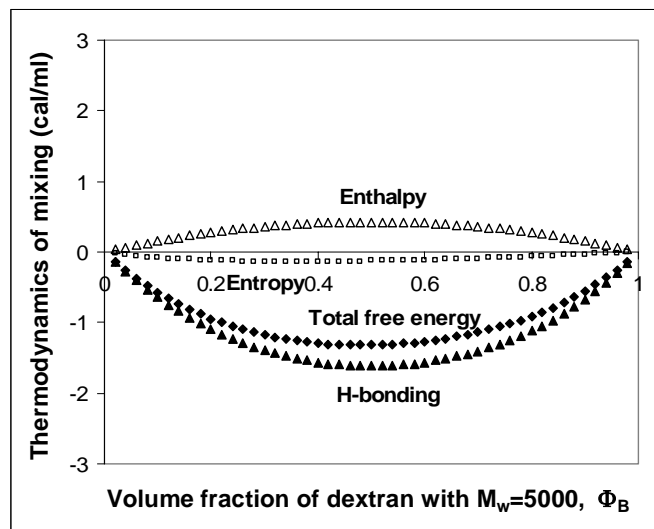


(a)

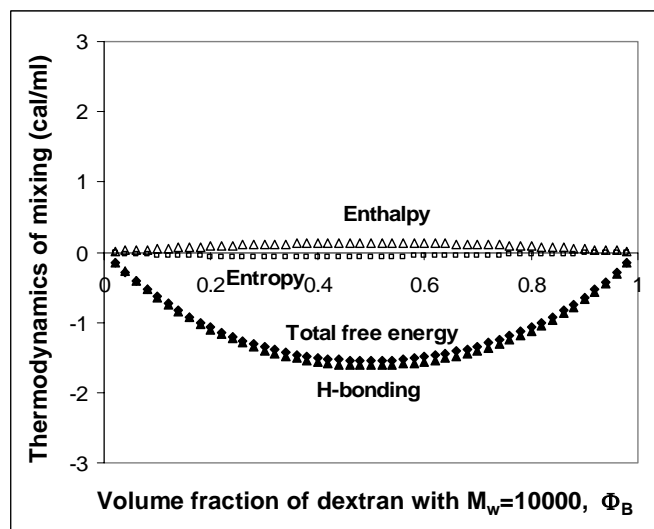


(b)

Figure 4.34: Effect of component molecular weight on entropic, enthalpic, and H-bonding contributions to the total free energy of mixing two dextrans at 25°C; Systems of (a)  $M_w=5,000$  and  $M_w=2,000,000$ ; (b)  $M_w=10,000$  and  $M_w=2,000,000$  [H-bonding of phenol OH was approximated for H-bonding in dextrans; and  $\gamma=0.30$ ]



(a)



(b)

Figure 4.35: Effect of component molecular weight on entropic, enthalpic, and H-bonding contributions to the total free energy of mixing two dextrans at 25°C; Systems of (a)  $M_w=5,000$  and  $M_w=2,000,000$ ; (b)  $M_w=10,000$  and  $M_w=2,000,000$  [H-bonding of dimethylphenol OH was approximated for H-bonding in dextrans; and  $\gamma=0.30$ ]

#### 4.3.2.5. Effect of the Value of Intra-molecular Screening Parameter ( $\gamma$ ) on Thermodynamic Calculations of Miscibility

The quantitative miscibility predictions so far have used Equation 2.39 with a constant intra-molecular screening parameter of  $\gamma=0.30$ , which has been accepted as an average value for most polymer systems (Coleman et al., 1998; Coleman and Painter, 2006). In order to demonstrate the effect of intra-molecular screening affects, Figures 4.36-4.38 using  $\gamma=0.00$  were compared to Figures 4.22-4.24 where  $\gamma=0.30$ . As discussed in Section 2.3.5 with Figure 2.14, Painter-Coleman group have looked into different  $\gamma$  values and determined the best realistic value comparing the experimental fraction of carbonyl groups ( $f_F^{C=O}$ ) obtained directly from IR spectra using the free carbonyl bands to the best predictive fit of Equation 2.32 for various synthetic polymer systems. The model with  $\gamma=0.00$  can not reproduce the experimental data, whereas using  $\gamma=0.25$ -0.35 provides the best comparison with the experimental data. That is how an average value of  $\gamma=0.30$  is being accepted for most polymer systems (Coleman et al., 1998; Coleman and Painter, 2006). Using models with  $\gamma$  values higher than 0.30, such as 0.50 or 0.70, would not result in realistic miscibility predictions based on Painter-Coleman's extensive experimental vs. model prediction of miscibility using various polymers.

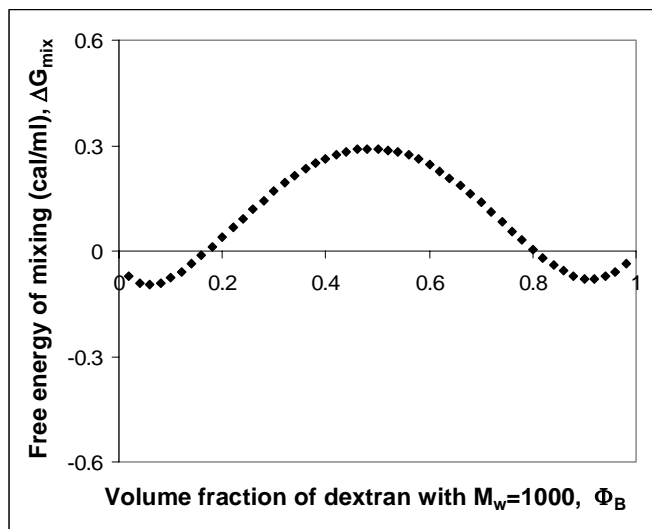
According to Figure 4.36, Figure 4.37, and Figure 4.38, when  $\gamma=0.00$ , the regions where dextrans with  $M_w=1,000 + M_w=2,000,000$  were predicted to be immiscible were determined as  $\Phi_B=0.17$ -0.81,  $\Phi_B=0.18$ -0.96, and  $\Phi_B>0.13$ , respectively (H-bonding of pentanol OH, phenol OH and dimethylphenol OH approximated to that in dextrans, respectively). The predictions gave much larger regions of immiscibility (almost entire

volume fraction ranges) resulting in inadequate predictions. For instance, when pentanol was used and when  $\gamma=0.30$ , Figure 4.22 showed completely miscible systems over the entire composition range, whereas when  $\gamma=0.00$ , only a small range of component ratios were predicted to be miscible (Figure 4.36).

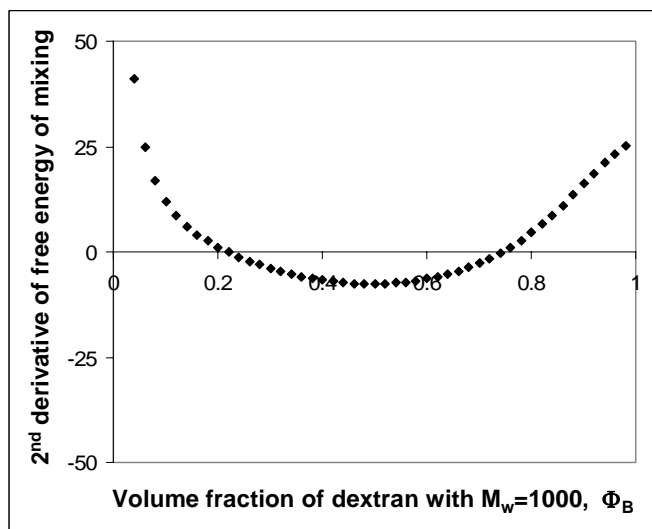
Figure 4.39 shows the individual thermodynamic contributions to overall free energy of mixing when  $\gamma=0.00$ . Entropic contribution had the same values as those in Figure 4.25 (when  $\gamma=0.30$ ), because entropic contribution was calculated from the first two terms on the right-hand-side of Equation 2.39 regardless of the  $\gamma$  value. Enthalpic contributions were calculated to have higher positive (+) values when  $\gamma=0.00$  (Figure 4.39) compared to enthalpic values when  $\gamma=0.30$  (Figure 4.25). Because in Equation 2.39, intra-molecular screening parameter affected the third term on the right-hand-side with a factor of  $(1-\gamma)$  (i.e. in case of  $\gamma=0.00$ , the numbers were multiplied with “ $1-0=1$ ”, whereas in case of  $\gamma=0.30$ , the numbers were multiplied with “ $1-0.3=0.7$ ”, which is smaller than 1). Having higher positive (+) enthalpic contribution when  $\gamma=0.00$  was more unfavorable to mixing than the case when  $\gamma=0.30$ .

However, as explained in Section 3.4.3.2 with Figure 3.11,  $\gamma$  does not only affect enthalpy of mixing, but it also modifies the  $\Delta G_H$  term in Equation 2.39 through modification of self-association and inter-association equilibrium constants (Equation 2.40-2.42) as described in Section 3.4.3.2 with Figure 3.11. When this effect is not included into miscibility predictions ( $\gamma=0.00$ ), then Equations 2.40-2.42 directly result in the self-association equilibrium constants calculated in Table 3.2 (Figure 3.11). According to this, calculated H-bonding contributions took slightly higher negative (-)



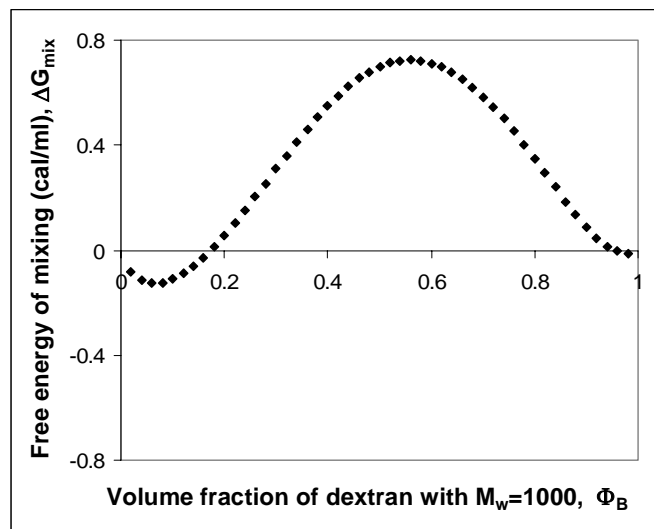


(a)

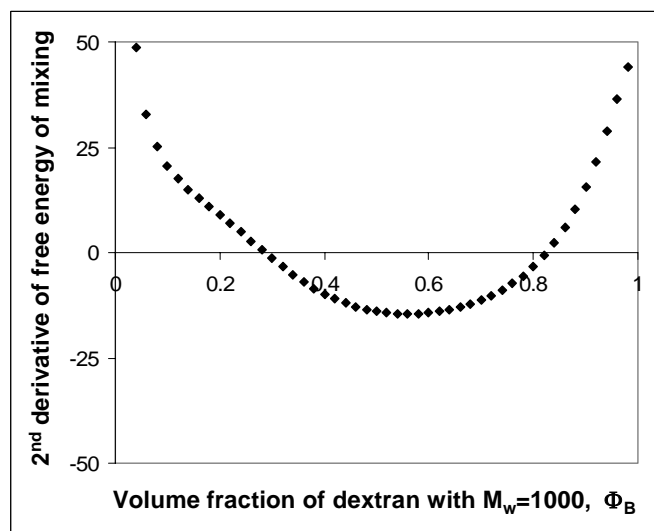


(b)

Figure 4.36: Predicted miscibility [ (a) Free energy of mixing; (b) 2<sup>nd</sup> derivative of free energy of mixing) ] of two dextrans with  $M_w=1,000$  and  $M_w=2,000,000$  at 25°C when  $\gamma=0.00$  [H-bonding of pentanol OH was approximated for H-bonding in dextrans]

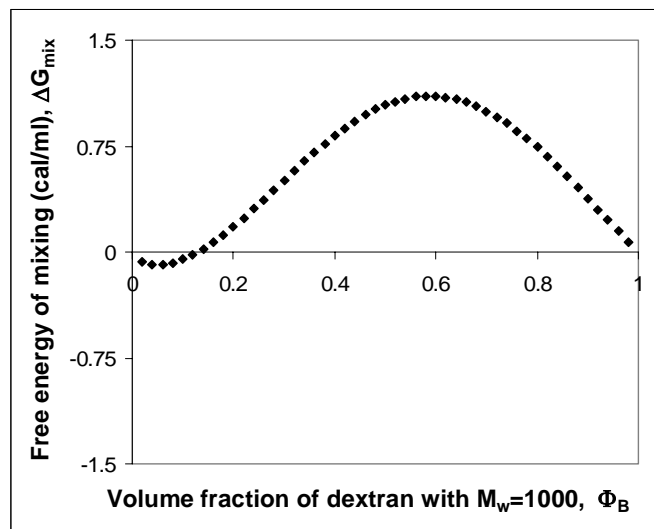


(a)

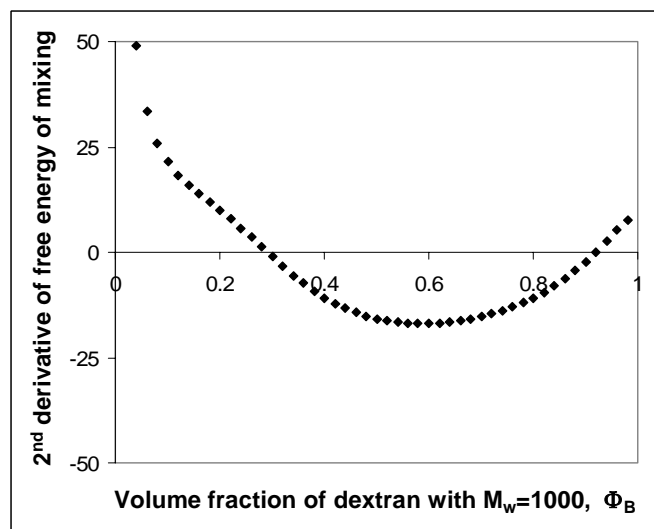


(b)

Figure 4.37: Predicted miscibility [ (a) Free energy of mixing; (b) 2<sup>nd</sup> derivative of free energy of mixing) ] of two dextrans with  $M_w=1,000$  and  $M_w=2,000,000$  at 25°C when  $\gamma=0.00$  [H-bonding of phenol OH was approximated for H-bonding in dextrans]



(a)

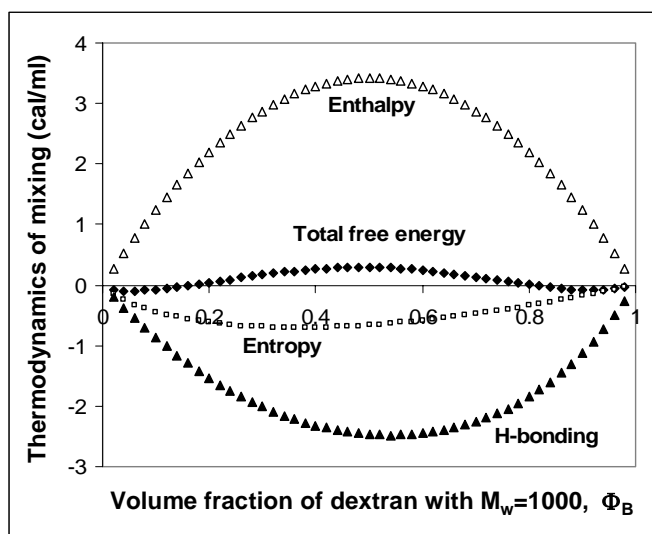


(b)

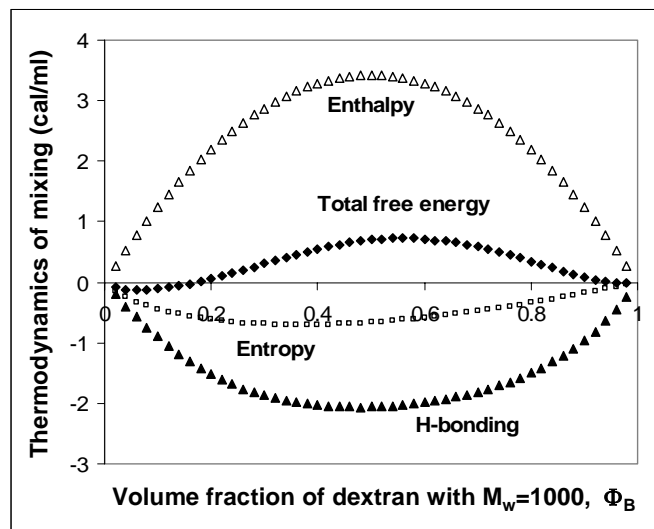
Figure 4.38: Predicted miscibility [ (a) Free energy of mixing; (b) 2<sup>nd</sup> derivative of free energy of mixing) ] of two dextrans with  $M_w=1,000$  and  $M_w=2,000,000$  at 25°C when  $\gamma=0.00$  [H-bonding of dimethylphenol OH was approximated for H-bonding in dextrans]

values when  $\gamma=0.00$  (Figure 4.39) compared to the case where  $\gamma=0.30$  (Figure 4.25). However, with  $\gamma=0.00$ , the significantly higher positive (+) values for the enthalpic contribution overwhelmed the slightly higher negative (-) values for the H-bonding contribution compared to the case where  $\gamma=0.30$ . This resulted in positive (+)  $\Delta G_{\text{mix}}$  for a large volume fraction range (Figure 4.39 vs. Figure 4.25), predicting immiscibility over a large amount of component ratios when  $\gamma=0.00$ .

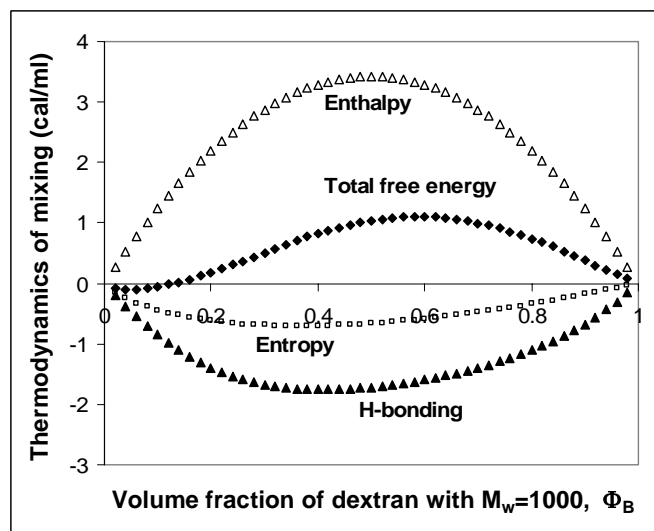
Figure 4.25a and Figure 4.39a have shown the entropic, enthalpic, and H-bonding contributions to the total free energy of mixing two dextrans with  $M_w=1,000$  and  $M_w=2,000,000$  when  $\gamma=0.30$  and  $\gamma=0.00$ , respectively. As discussed above and explained at the beginning of Section 4.3.2.5, the use of  $\gamma=0.30$  provides a realistic miscibility calculation. However, in order to demonstrate how the thermodynamics of mixing would be affected by the use of a  $\gamma$  value higher than 0.30, Figure 4.40 shows the free energy of



(a)



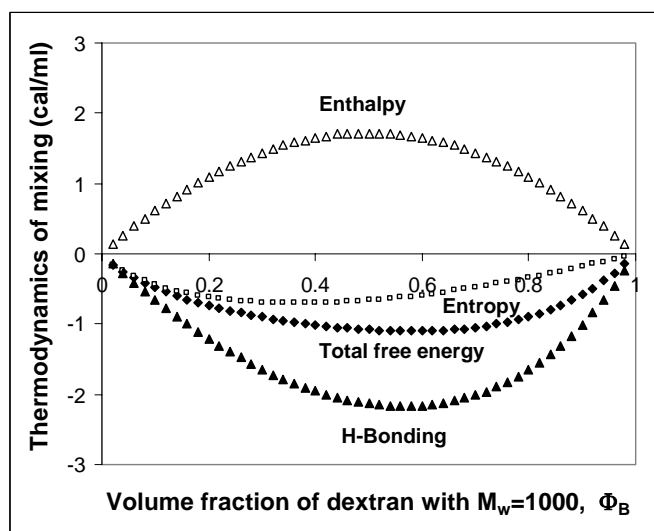
(b)



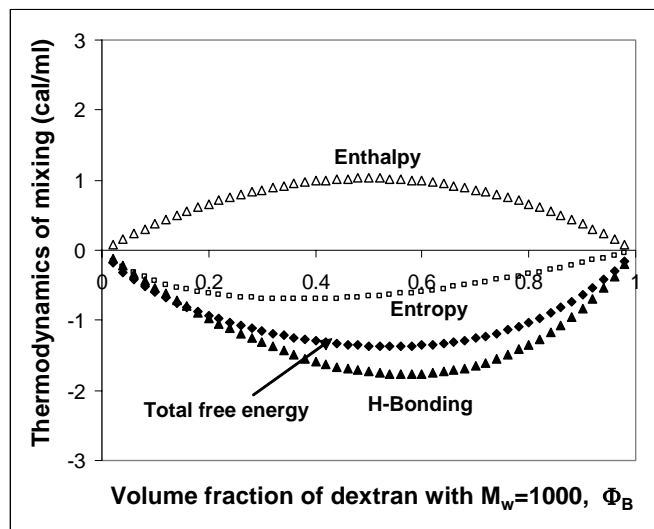
(c)

Figure 4.39: Entropic, enthalpic, and H-bonding contributions to the total free energy of mixing two dextrans with  $M_w=1,000$  and  $M_w=2,000,000$  at  $25^\circ\text{C}$  when  $\gamma=0.00$  [H-bonding of; (a) pentanol OH; (b) phenol OH; (c) dimethylphenol OH was approximated for H-bonding in dextrans]

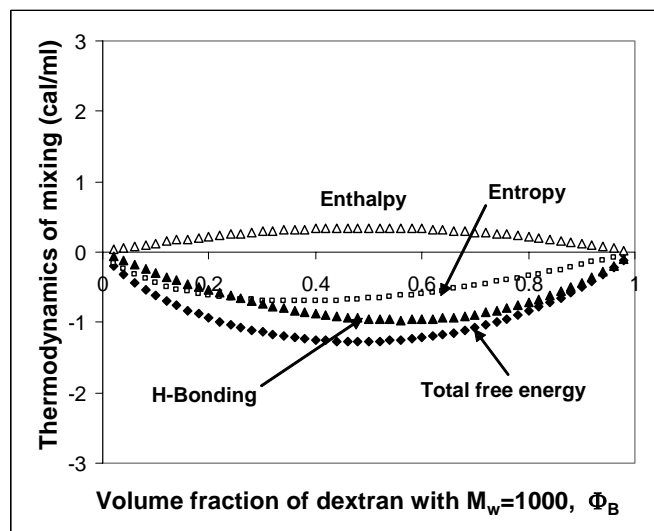
mixing and its individual contributions if  $\gamma=0.50$ ,  $\gamma=0.70$ ,  $\gamma=0.90$  were used. As in Figure 4.25a and Figure 4.39a, the entropy of mixing were calculated independent of the value of  $\gamma$ . As the value of  $\gamma$  got higher, the enthalpy of mixing term  $[\chi_{AB} \cdot \Phi_A \cdot \Phi_B \cdot (1-\gamma)]$ , which is inversely dependent on the  $\gamma$  term, resulted in smaller positive valued unfavorable contribution (Figure 4.40). This was in favor of obtaining negative total free energy of mixing values. Furthermore, higher  $\gamma$  values results in more favorable self-association (through increasing self-association constants) and much less favorable inter-association (through decreasing inter-association constant) (Section 2.3.5), which revealed in less H-bonding contribution (Figure 4.40). Relatively speaking, the decrease in the positive value of enthalpic term was more than the decrease in the negative value of the H-bonding term. When a  $\gamma$  value of 0.90 was used, the overall enthalpic term became even less significant than the entropic term, which is always negligibly small due to its inverse relationship with the molecular size of the polymers.



(a)



(b)



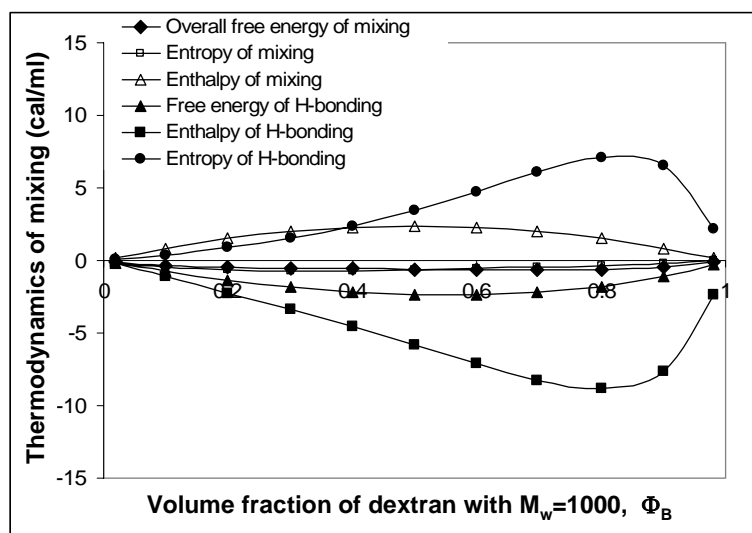
(c)

Figure 4.40: Entropic, enthalpic, and H-bonding contributions to the total free energy of mixing two dextrans with  $M_w=1,000$  and  $M_w=2,000,000$  at  $25^\circ\text{C}$  when; (a)  $\gamma=0.50$ ; (b)  $\gamma=0.70$ ; (c)  $\gamma=0.90$  [H-bonding of pentanol OH was approximated for H-bonding in dextrans]

Overall results demonstrated in this section showed that intra-molecular screening parameter of  $\gamma=0.30$  resulted in the optimum miscibility predictions in carbohydrate systems similar to synthetic polymer systems.

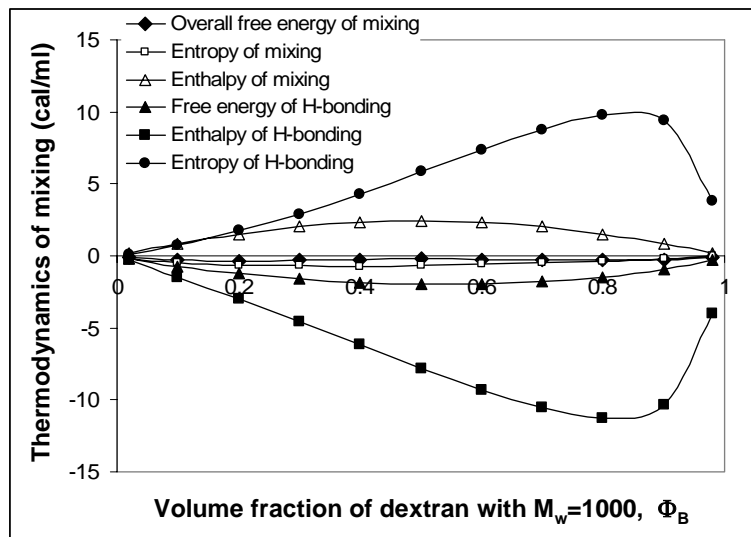
#### 4.3.2.6. Individual Enthalpic and Entropic Contributions of Hydrogen Bonding on Overall Free Energy of Hydrogen Bonding ( $\Delta G_H$ )

Figure 4.41 shows all of the individual contributions to the overall free energy of mixing two dextrans with low and high molecular weights. In Figure 4.25, entropy of mixing, enthalpy of mixing, free energy of H-bonding, and overall free energy of mixing were plotted, whereas in Figure 4.41, additionally, free energy of H-bonding was further dissected into its enthalpic and entropic contributions (enthalpy of H-bonding and entropy of H-bonding) using Equation 3.17. Figure 4.41 illustrates that quantitatively enthalpy and entropy of H-bonding was much higher than other individual contributions.

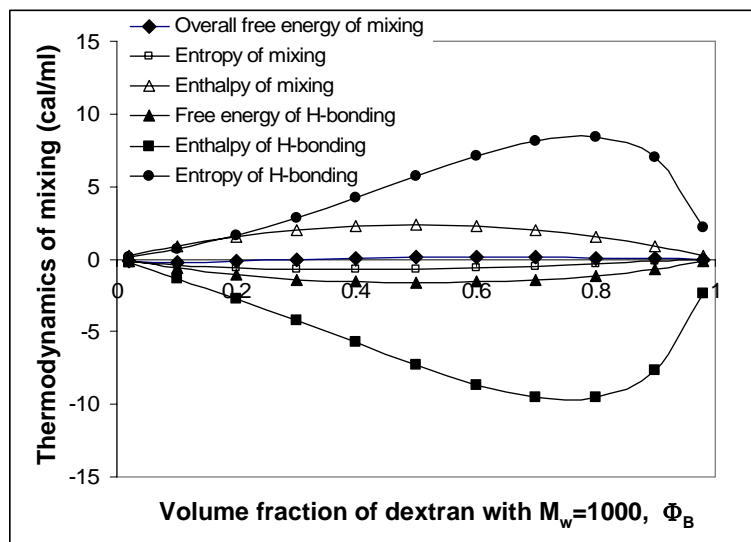


(a)





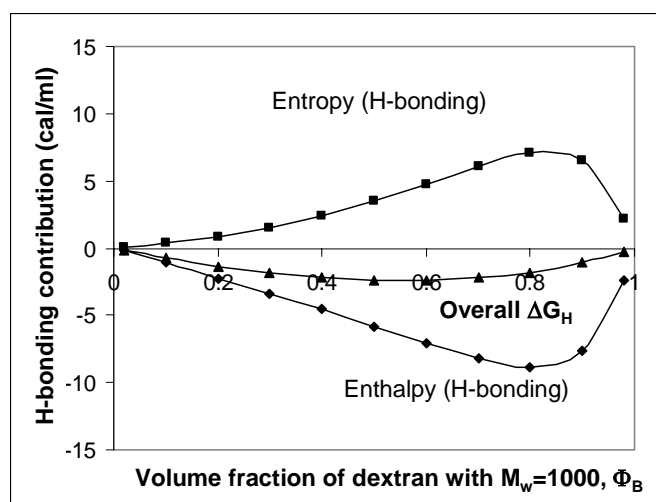
(b)



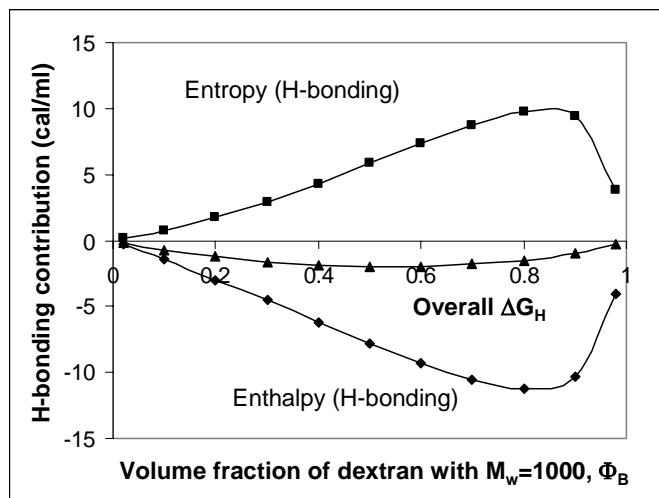
(c)

Figure 4.41: Individual contributions to the overall free energy of mixing, including enthalpy and entropy of H-bonding when (a) pentanol OH; (b) phenol OH; (c) dimethylphenol OH was used as the model analogue compound for H-bonding in dextran systems of  $M_w=1,000+M_w=2,000,000$  at  $25^\circ\text{C}$  [ $\gamma=0.30$ ]

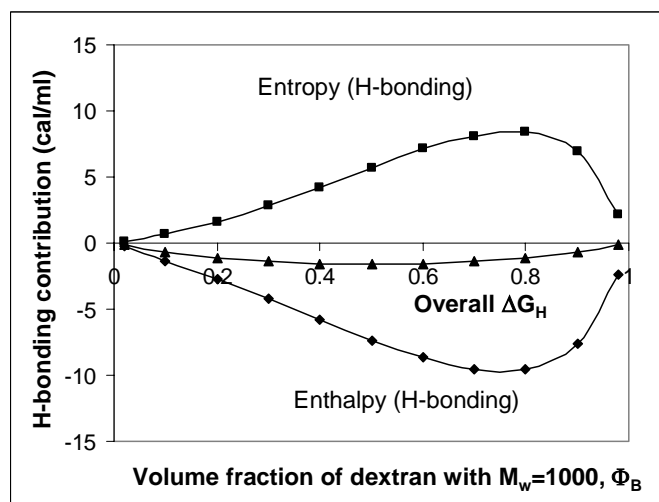
In order to clarify the quantitative calculations, Figure 4.42 only shows the individual enthalpic and entropic contributions of H-bonding together with the overall free energy of H-bonding ( $\Delta G_H$ ) for three model analogue compounds used. Hydrogen bonding contributions were calculated as a function of association equilibrium constants (Table 3.2). There were negative valued enthalpic contributions (showing formation of hydrogen bonds in the system), but there were also positive valued entropic changes occurring due to formation of the same hydrogen bonds (Figure 4.42). In other words, formation of hydrogen bonds in the system created negative valued, favorable energy (enthalpy of H-bonding), but it also caused loss of degrees of internal rotational freedom of segments in the polymeric chain, creating some degree of order. Due to this order, entropy of H-bonding got high positive values (Figure 4.42), which was an unfavorable contribution to mixing.



(a)



(b)



(c)

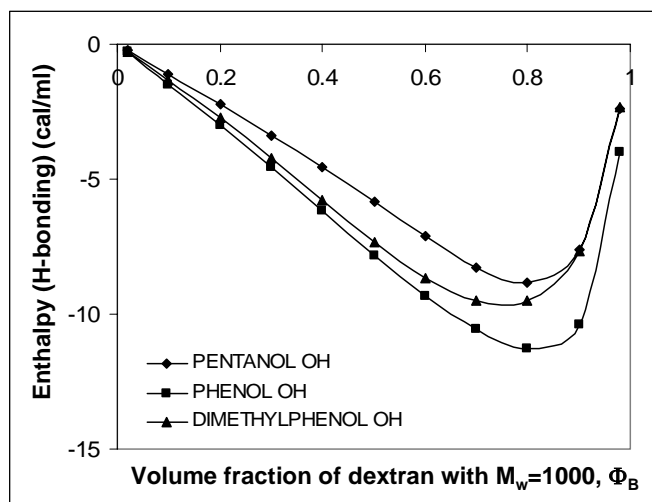
Figure 4.42: Enthalpy and entropy of H-bonding; and overall free energy of H-bonding when (a) pentanol OH; (b) phenol OH; (c) dimethylphenol OH was used as the model analogue compound for H-bonding in dextran systems of  $M_w=1,000+M_w=2,000,000$  at  $25^\circ\text{C}$  [ $\gamma=0.30$ ]

Enthalpy of H-bonding was higher with phenol and dimethylphenol analogue compounds compared to the enthalpy of H-bonding with pentanol (Figure 4.43a). This is due to the relative values of  $K_2$ ,  $K_B$  and  $K_A$  (Table 3.2). Although inter-association (represented by  $K_A$ ) was equal to self-association for multi-mer formation (represented by  $K_B$ ) (i.e. formation of A-B bonds have similar favorability compared to formation of B-B bonds), there was also the effect of self-association for di-mer formation (represented by  $K_2$ ). When  $K_2$ s were compared to  $K_A$ s for each analogue compound, there was a larger difference between  $K_2$  and  $K_A$  with phenol and dimethylphenol (40.7 vs. 129.6 and 13 vs. 47.6, respectively) than that with pentanol (51.6 vs. 85.6), indicating that di-mer self-association was relatively much less than inter-association in phenol and dimethylphenol compared to pentanol. This resulted in higher enthalpy of H-bonding for phenol and dimethylphenol compared to pentanol.

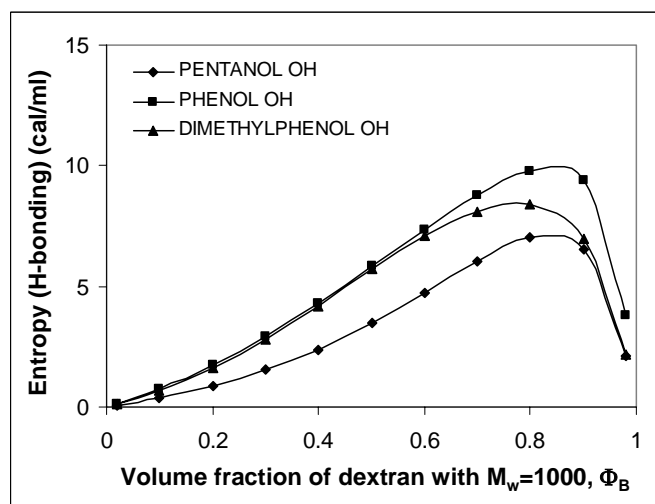
Although enthalpy of H-bonding was higher with phenol and dimethylphenol, there were also higher positive valued entropic contribution with these two model compounds than that with pentanol (Figure 4.43b). This was possibly due to the steric hindrance of the phenol and dimethylphenol structure, because of their double bonded ring structure (Figure 3.10b and Figure 3.10c) compared to pentanol with a linear structure (Figure 3.10a). In other words, the relative values of equilibrium constants forced phenol and dimethylphenol to have higher enthalpy of hydrogen bonding than pentanol, but to achieve those enthalpy, phenol and dimethylphenol resulted in higher entropy to orient themselves in order to be involved in hydrogen bonding.

Overall, free energy of H-bonding, which was the combination of enthalpy and entropy of H-bonding, showed higher negative values when pentanol was used as the

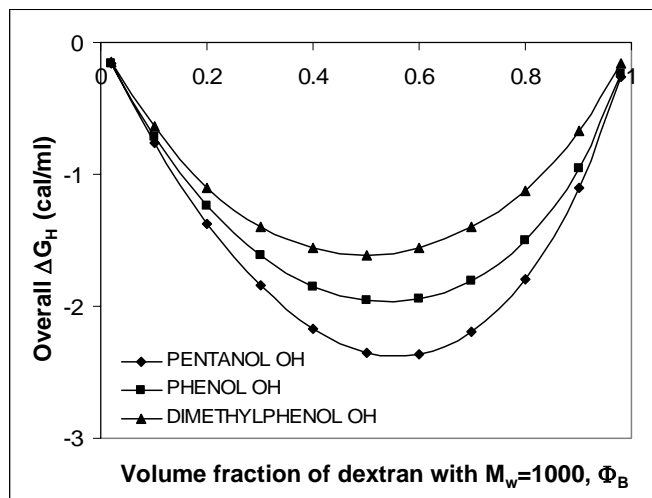
analogue compound (Figure 4.43c) indicating that overall H-bonding with pentanol was more favorable than H-bonding with phenol and dimethylphenol.



(a)



(b)



(c)

Figure 4.43: Comparison of; (a) enthalpy of H-bonding; (b) entropy of H-bonding; (c) overall free energy of H-bonding between pentanol OH, phenol OH and dimethylphenol OH as model analogues for H-bonding in dextran systems of  $M_w=1,000+M_w=2,000,000$  at 25°C [ $\gamma=0.30$ ]

#### 4.3.3. Validation of the Predictive Miscibility Approximations for Dextran on ‘Real’ Carbohydrate Polymers: Testing Miscibility in Inulin/Amylopectin Systems

In this section, this dissertation aims to validate all the calculations and predictive capabilities developed through the Painter-Coleman model and dextran molecules utilizing an inulin-amylopectin system. Figure 4.44 shows the predicted miscibility in inulin and amylopectin systems as a validation of the quantitative prediction approximations and learning with dextran systems in Section 4.3.2. In Figure 4.44, H-bonding of pentanol, which was shown to be the most accurate model analogue for hydrogen bonding in dextran (Section 4.3.2.1), was used for calculation of H-bonding

contribution in inulin-amylopectin system to calculate enthalpy, entropy and free energy of mixing. Entropy of mixing (negative valued, favorable to mixing) calculated from the first two terms on the right-hand-side of Equation 2.39 had very small values, almost equal to zero (Figure 4.44a), over the entire volume fraction range due to the very high molecular weight of amylopectin. Enthalpy of mixing, calculated from the third term on the right-hand-side of Equation 2.39, took large positive values (Figure 4.44a), which was unfavorable to mixing. It was calculated from the square of the difference between the non-hydrogen bonded solubility parameters ( $\delta$ ) (Equation 2.7). The difference between  $\delta$  of inulin and amylopectin [ $14.26$  and  $8.99$  ( $\text{cal}/\text{cm}^3$ )<sup>0.5</sup>, respectively] (Section 3.4.4) was higher than the difference between  $\delta$  of dextrans with  $M_w=1,000$  and  $M_w=2,000,000$  [ $13.10$  and  $9.40$  ( $\text{cal}/\text{cm}^3$ )<sup>0.5</sup>, respectively] (Table 3.3). Therefore, a higher positive valued enthalpic contribution was calculated for inulin-amylopectin systems compared to that for dextran systems (Figure 4.25a).

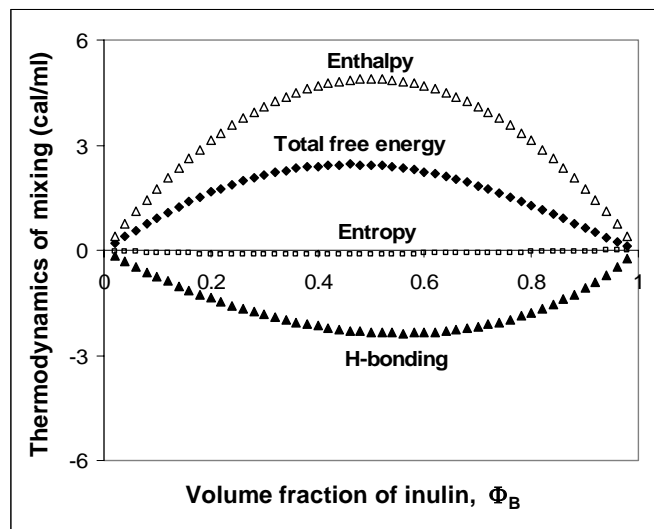
H-bonding contribution was determined to be negative (Figure 4.44) and had values similar to that calculated for H-bonding in mixing two dextrans (Figure 4.25a), because it was approximated from the same analogue compound, pentanol (Icoz and Kokini, 2008). Negative H-bonding contribution was calculated, as shown in Figure 4.44a. However, positive valued, unfavorable enthalpic contribution overwhelmed the negative valued, favorable H-bonding contribution. As an overall summation of all these individual contributions, the total free energy of mixing was calculated to be positive over the entire volume fraction range for inulin-amylopectin systems (Figure 4.44a). 2<sup>nd</sup> derivative of free energy of mixing also had negative values for volume fraction of inulin

at  $\Phi_B < 0.9$  (Figure 4.44b); overall indicating immiscibility predictions in inulin-amylopectin systems at all compositions in limited moisture contents.

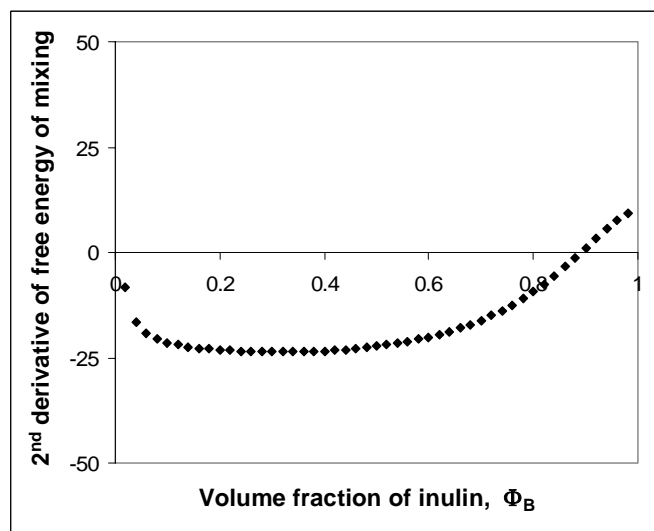
These predictive results were compared to the experimental miscibility result presented in Zimeri and Kokini (2003a). Figure 4.45 shows the DSC thermograms of mixed inulin-amylopectin systems with 30:70 and 60:40 (% d.b.) ratios of components. In the thermograms, there were two independent reversible endothermic transitions (Figure 4.45). Figure 4.46 shows glass transition temperature ( $T_g$ ) vs. moisture content for inulin-amylopectin systems stored at  $a_w=0.33$  (~11% moisture) and  $a_w=0.52$  (~14% moisture) that were mixed at 30:70 and 60:40 ratios of inulin:amylopectin. In Figure 4.46, the lines are the Gordon-Taylor plots for pure inulin and pure amylopectin, whereas the data points of double  $T_g$ s in mixed inulin-amylopectin systems are shown with symbols. Figure 4.46 shows that transition 1 ( $T_{g1}$ ) occurred at the same temperature as  $T_g$  of pure inulin, whereas transition 2 ( $T_{g2}$ ) occurred at the same temperature as  $T_g$  of pure amylopectin. Overall, these results experimentally indicated that there was double glass transition temperature behavior in mixed inulin-amylopectin systems at limited moisture environments, indicating immiscible systems.

30:70 ( $\Phi_B=0.3$ ) and 60:40 ( $\Phi_B=0.6$ ) ratios of inulin:amylopectin systems were the only two data points reported in Zimeri and Kokini (2003a) in limited environments that would be suitable to compare miscibility predictions to experimental miscibility values. Together with the overall results presented in Zimeri and Kokini (2003a), these specific data provided information that inulin and amylopectin systems were experimentally immiscible at limited moisture contents.





(a)



(b)

Figure 4.44: Predicted miscibility of inulin and amylopectin at 25°C when H-bonding of pentanol OH was approximated for H-bonding in carbohydrates; (a) Entropic, enthalpic, and H-bonding contributions to the total free energy of mixing; (b) 2<sup>nd</sup> derivative of free energy of mixing [ $\gamma=0.30$ ]

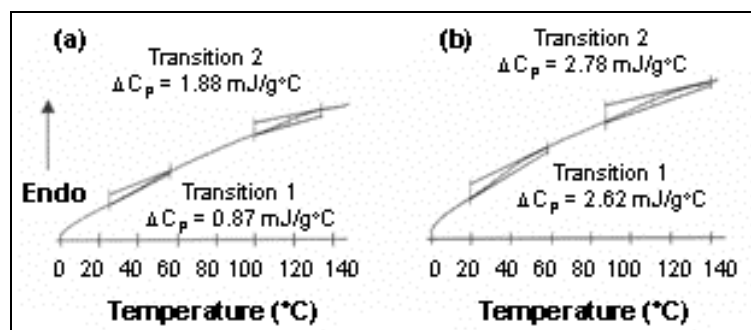
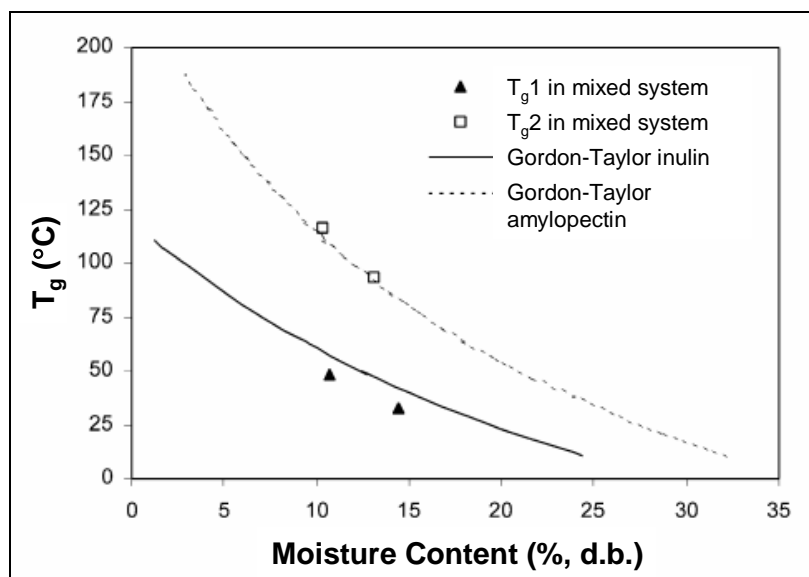
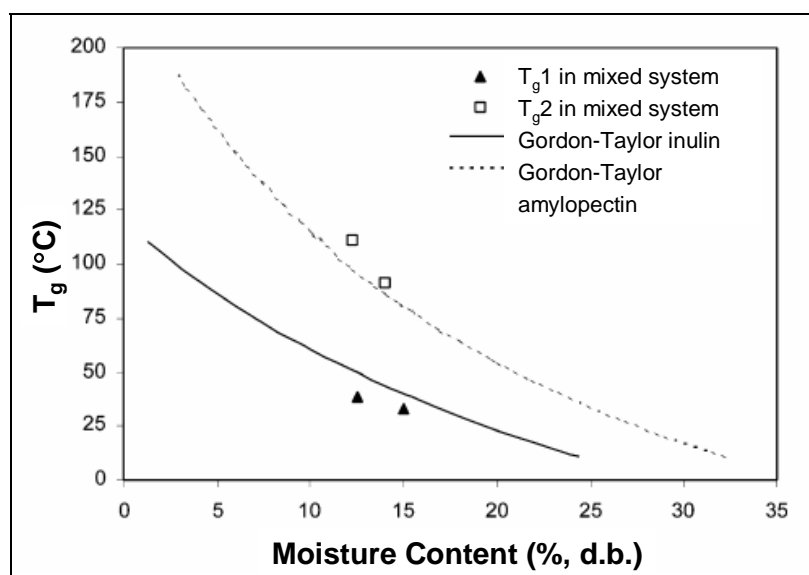


Figure 4.45: DSC rescans of mixed inulin-amylopectin systems stored at  $a_w = 0.33$  for inulin to amylopectin ratio of; (a) 30:70; and (b) 60:40 (% , d.b.) (Zimeri and Kokini, 2003a)

These results indicates that the approximate prediction rules set with dextran systems (model carbohydrates) using Painter-Coleman association model (i.e. use of pentanol as the analogue compound; accepting a value of  $\gamma=0.30$  for intra-molecular screening; and selecting low  $M_w$  polymer as the self-associating component) were also suitable to approximately predict miscibility/immiscibility in inulin-amylopectin systems as an example for real carbohydrate blends. Because theoretical predictions show immiscibility at all component ratios for inulin-amylopectin systems, and experimental miscibility results (Zimeri and Kokini, 2003a) also show immiscibility for the same system.



(a)



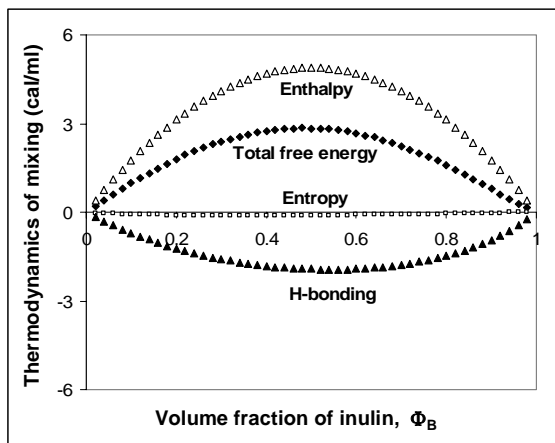
(b)

Figure 4.46: Two glass transition temperatures in mixed samples containing inulin to amylopectin ratio of (a) 30:70 and (b) 60:40 (% d.b.) (Zimeri and Kokini, 2003a)

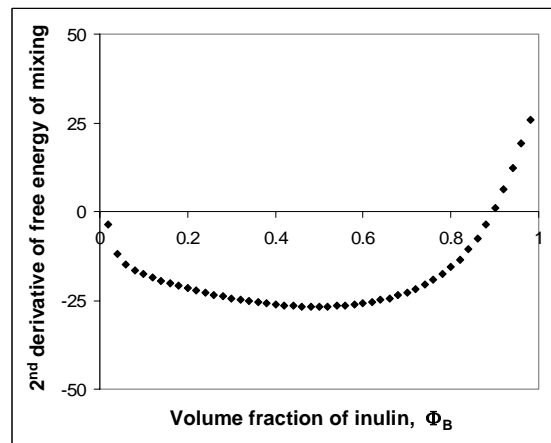
Figure 4.47 shows similar predictions when phenol and dimethylphenol were used as the model analogue compound for hydrogen bonding in carbohydrates. These calculations also show immiscibility over the entire volume fraction range. Because the very large positive contribution from the enthalpic term also overwhelms H-bonding contributions when these analogue compounds were used (Icoz and Kokini, 2008).

Figure 4.48 shows predictions in inulin+amylopectin systems when amylopectin was selected as the self-associating component instead of inulin; and Figure 4.49 shows predictions when intra-molecular screening effects were neglected ( $\gamma=0.00$ ). Both these figures show positive free energy of mixing over the entire composition ranges in inulin+amylopectin systems.

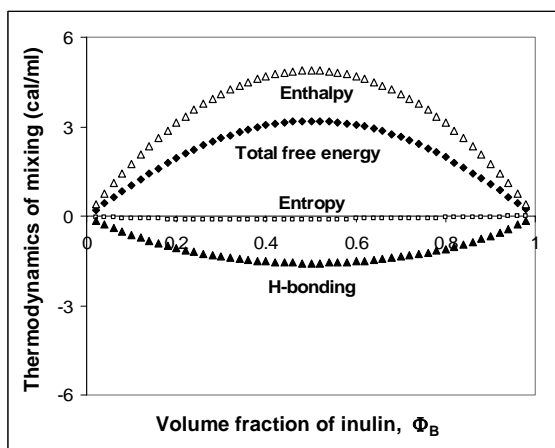
In order to hypothetically demonstrate in what hydrogen bonding extent inulin and amylopectin would be predicted to be miscible, Figure 4.50 shows the effect of the value of inter-association equilibrium constant ( $K_A$ ) relative to self-association equilibrium constants ( $K_2$  and  $K_B$ ) on H-bonding contribution and the resulting overall free energy of mixing. Similar to Figures 4.26-4.28, only H-bonding contribution and total free energy were demonstrated in Figure 4.44a and Figure 4.44b, since entropic and enthalpic contributions to free energy would be the same for all cases (Equation 2.39 and Figure 4.44a). In Figure 4.50, pentanol was used as the best available model analogue compound for describing H-bonding in carbohydrates with  $K_2=51.6$ ,  $K_B=85.6$  and  $K_A=85.6$  (Table 3.2). When  $K_A$  was hypothetically given values of  $K_A=100$  and  $K_A=150$  (which were much higher than the actual value of  $K_A=85.6$ , which also means much higher inter-association than self-association), free energy of mixing and its 2<sup>nd</sup> derivative



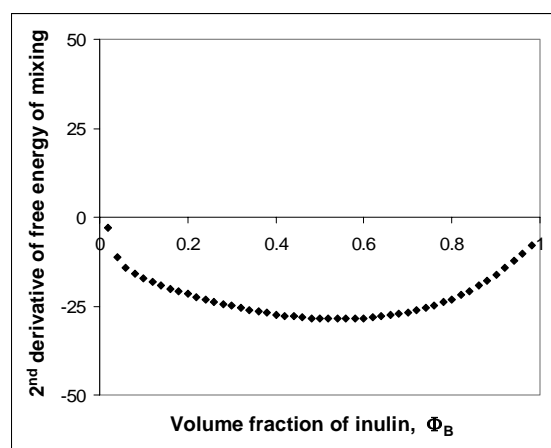
(a)



(b)

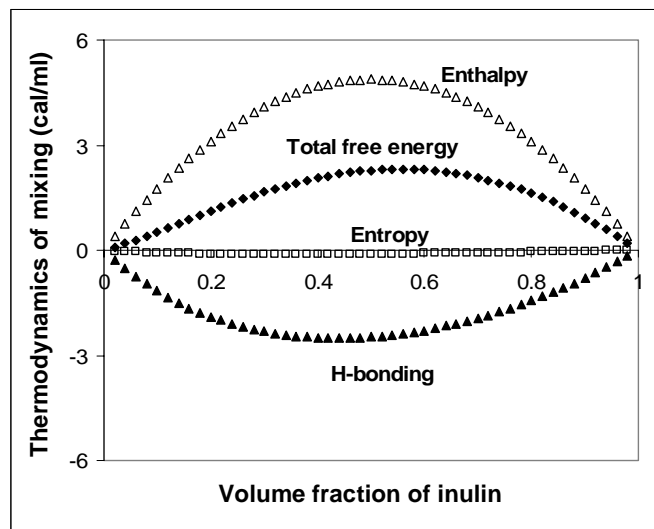


(c)

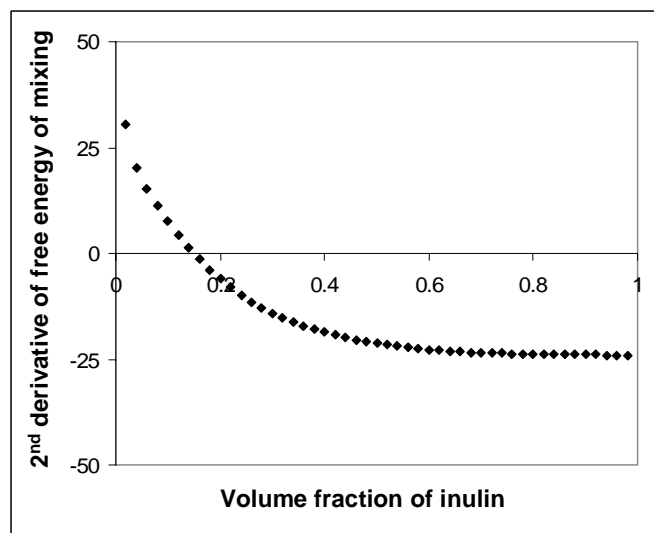


(d)

Figure 4.47: Predicted miscibility of inulin and amylopectin at 25°C when H-bonding of (a-b) phenol OH; (c-d) dimethylphenol OH was approximated for H-bonding in carbohydrates [ (a-c) Entropic, enthalpic, and H-bonding contributions to the total free energy of mixing; (b-d) 2<sup>nd</sup> derivative of free energy of mixing; and  $\gamma=0.30$  ]

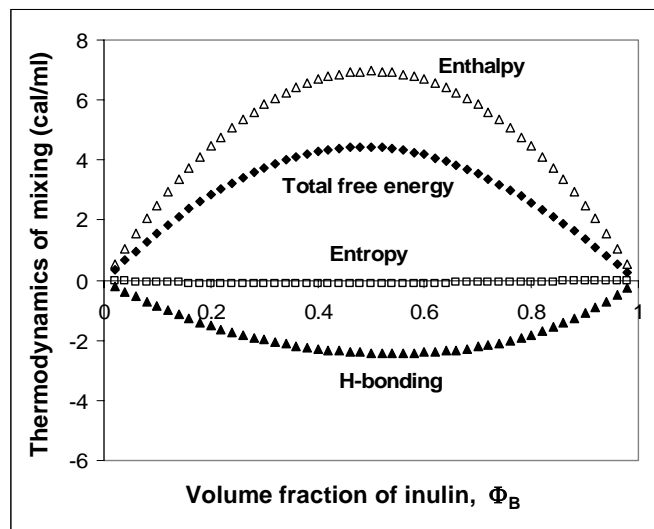


(a)

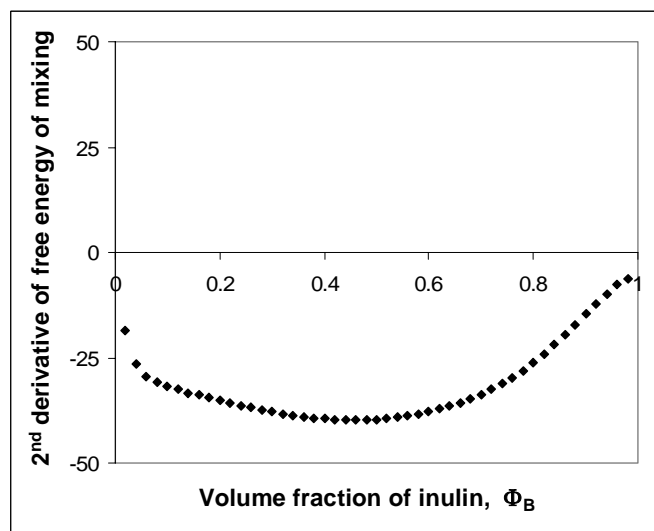


(b)

Figure 4.48: Predicted miscibility [ (a) Entropic, enthalpic, and H-bonding contributions to the total free energy of mixing; (b) 2<sup>nd</sup> derivative of free energy of mixing) ] of inulin and amylopectin at 25°C when amylopectin was selected as the self-associating component [H-bonding of pentanol OH was approximated for H-bonding in carbohydrates; and  $\gamma=0.30$ ]



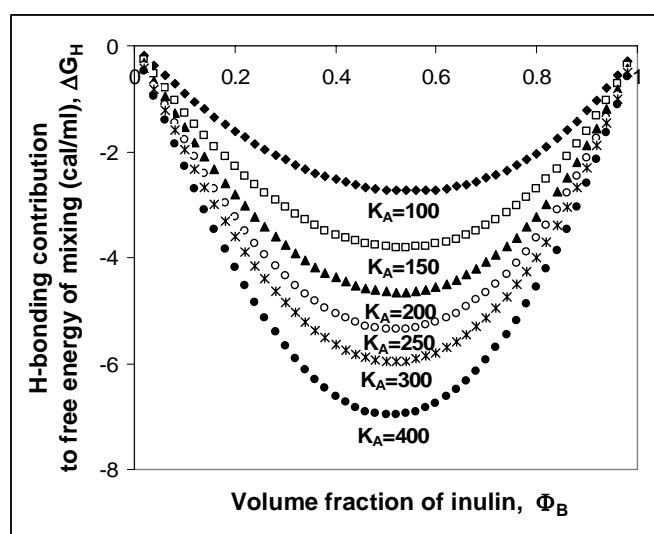
(a)



(b)

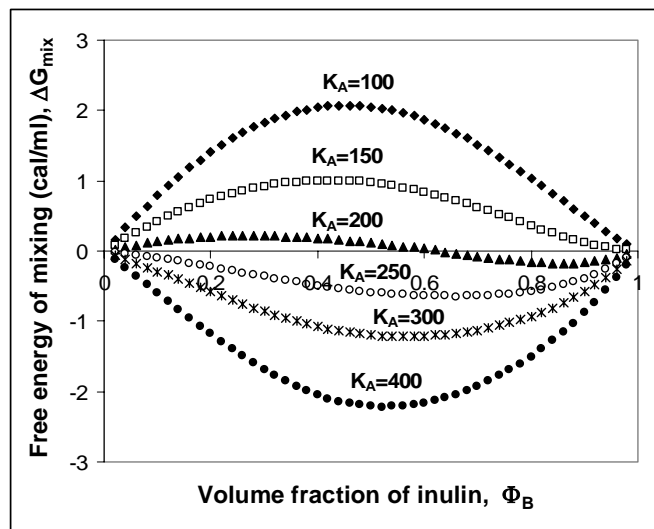
Figure 4.49: Predicted miscibility [ (a) Entropic, enthalpic, and H-bonding contributions to the total free energy of mixing and (b) 2<sup>nd</sup> derivative of free energy of mixing ] of inulin and amylopectin at 25°C when  $\gamma=0.00$  [H-bonding of pentanol OH was approximated for H-bonding in carbohydrates]

were calculated to be negative (Figure 4.50b) and positive (Figure 4.50c), respectively, still predicting completely immiscible systems. When hypothetically  $K_A=200$ , some miscibility prediction (partial positive and negative free energy of mixing and its second derivative) was started to be observed over the composition range. When hypothetically  $K_A>250$ , H-bonding contribution could partially overcome the positive valued, unfavorable enthalpic contribution (Figure 4.44a), resulting in mostly miscible systems (Figure 4.50b and Figure 4.50c). When hypothetically  $K_A=400$  (when inter-association was chosen to be almost five times higher than self-association), then miscible inulin+amylopectin systems were predicted over the entire volume fraction range (Figure 4.50b and Figure 4.50c). This hypothetical analysis demonstrates that the thermodynamics from negative valued (favorable) H-bonding needs to be very high to overcome the large positive valued (unfavorable) enthalpy of mixing contribution (Icoz and Kokini, 2008).

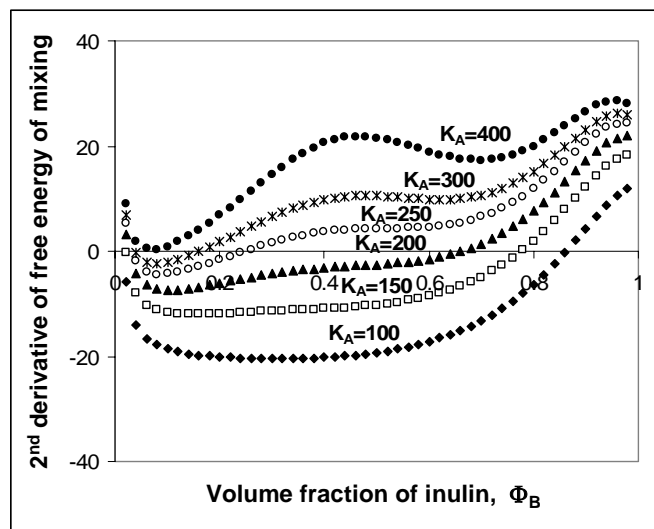


(a)





(b)



(c)

Figure 4.50: Effect of the value of inter-association equilibrium constant ( $K_A$ ) relative to self-association equilibrium constants ( $K_2$  and  $K_B$ ) on; (a) H-bonding contribution; (b) Total free energy of mixing; (c) 2<sup>nd</sup> derivative of free energy of mixing inulin and amylopectin at 25°C [H-bonding of pentanol OH was approximated for H-bonding in carbohydrates; and  $\gamma=0.30$ ]

## 5. CONCLUSIONS

This dissertation investigated the molecular and thermodynamic basis of miscibility in carbohydrate blends. Miscibility of carbohydrate polymers with similar chemistry at low water activity ( $a_w$ ) was studied using dextran mixtures as structurally compatible model systems. First, the barriers for miscibility of dextrans with different molecular weights ( $M_w$ ) were investigated. Through thermal analysis, it was shown that the physical blend of dextrans in powder form resulted in immiscibility due to the diffusion barrier, whereas miscibility was achieved for dextrans pre-solubilized in a common solvent and freeze-dried.

Second, the possible molecular mechanism of miscibility in dextran systems was investigated using mixtures of chemically derivatized dextrans with added side chains. Miscible systems were obtained for samples prepared at low, medium and high polymer concentrations in the absence of NaCl; and at high concentrations in the presence of NaCl. Immiscible systems were obtained for samples prepared at low and medium polymer concentrations in the presence of NaCl. FTIR spectroscopy showed significantly different behavior for miscible and immiscible systems, capturing the specific bonding interactions in carbohydrate polymers. The systematic changes in the FTIR spectra of miscible blends were assigned to the changes in hydrogen bonding distribution of the pure components in the mixture, resulting from changes in the distribution of intra-molecular and inter-molecular interactions. No such significant systematic change was observed in the FTIR spectra of immiscible systems. The combined analysis of FTIR

spectroscopy and thermal analysis indicated the possible mechanism of miscibility through formation of hydrogen bonding interactions in the blends, which demonstrated the importance of hydrogen bonds in affecting miscibility in carbohydrate mixtures.

In order to quantitatively predict miscibility in carbohydrate polymers, theoretical thermodynamic models were examined. The solubility parameter of the monomeric unit of dextran was calculated from two different group contribution methods using the molecular structure. A predictive methodology to calculate the solubility parameters of dextrans with different molecular weights as a function of their glass transition temperatures was presented, with an inverse relationship between molecular weight and solubility parameter. Molecular dynamics simulations could also be used to obtain similar relationships between solubility parameters and molecular weight of polymers as long as the computational tools are available. Otherwise, the methodology demonstrated in this research provides an exceptional alternative for polymers.

The solubility parameters were then used to predict miscibility of two dextrans with low and high molecular weights using the Flory-Huggins theory, which is based on the number of configurational arrangements and quantitative measure of dispersive interactions. The original theory was shown to be unsatisfactory for predicting miscibility due to its limitation to account for specific interactions in the blends. This demonstrated its restriction for carbohydrate systems with monomeric units consisting of multiple hydroxyl groups. The more advanced thermodynamic model by Painter-Coleman group with its capability to account for strong hydrogen bonding interactions demonstrated that hydrogen bonding significantly contributed to quantitatively miscibility in carbohydrate blends. By approximating hydrogen bond formation of model analogue compounds to the

hydrogen bonding in dextrans, Painter-Coleman association model improved the miscibility predictions with original Flory-Huggins theory. With the inclusion of hydrogen bonding contributions into the predictions, sufficient thermodynamics was achieved, which was not only through inter-molecular bonds but also through intra-molecular bonds. Moreover, the formation of hydrogen bonds not only provided favorable enthalpic energy but also resulted in unfavorable entropic changes in the mixtures and the resulting hydrogen bonding energy was a combination of these two contributions. Pentanol was shown to be the most suitable analogue model for hydrogen bonding in the carbohydrate systems leading to better miscibility predictions. It was also shown that as the  $M_w$  of the components were closer to each other; miscibility was significantly controlled by hydrogen bonding contribution, which again shows the importance of these specific interactions in carbohydrate blends.

The overall understanding and learning with dextrans were then validated by testing miscibility in real carbohydrate systems of inulin and amylopectin at limited moisture conditions. The approximate prediction rules set with dextran systems using Painter-Coleman association model (i.e. use of pentanol as the analogue compound;  $\gamma=0.30$ ; and selecting low  $M_w$  polymer as the self-associating component) was shown to predict immiscibility in inulin-amylopectin systems as an example for real carbohydrate blends.

Although Painter-Coleman association model has its own limitations to be totally accurately applicable to carbohydrate polymer blends, the understanding gained in this dissertation is a significant step towards choosing which ingredients in a food formulation would form the desired miscible/immiscible systems on a predictive basis. The generated

knowledge will speed up the new product development process and increase the utilization of alternative agricultural ingredients in novel food products with new/improved functionalities.

## 6. FUTURE WORK

Although the application of the Painter-Coleman association model to carbohydrate polymers that was demonstrated in this dissertation resulted in significant understanding of the thermodynamic basis of miscibility and enabled approximate miscibility predictions, the current form of the Painter-Coleman hydrogen bonding association model for carbohydrate systems has still limitations. Because the current form of the model assumes that the repeating unit of the first polymer has a single functional group that can self-associate, and the repeating unit of the second polymer has one functional group that can form bonds with the first polymer but can not self-associate. However, in the mixture of two carbohydrates, both components have the ability to self-associate. Moreover, in most carbohydrates the monomeric units have multiple functional groups that can be involved in hydrogen bonding. The same is true for systems involving water since water has the ability to make strong hydrogen bonds. However, in these systems, calculating the exact hydrogen bonding contributions to the free energy are much more complicated, and the available association model can not directly deal with such systems. An alternative theoretical method that uses a combinatorial approach introduced by Veytsman (1990, 1993) is more suitable for these kinds of multiple associating systems. This combinatorial approach counts the number of hydrogen bonds that are distributed between donor and acceptor groups in the mixture and the original model can be expanded to account for multiple associations.

Future work would involve the development of a new theoretical thermodynamic model using Veytsman's combinatorial approach to describe the exact interactions between the components in carbohydrate blends that can accurately account for the structural complexities of carbohydrates, including the presence of multiple hydrogen bonding groups and the fact that both components can self-associate. Theoretical expressions describing the number of ways of distributing hydrogen bonds between all multiple donors and acceptor groups in a typical carbohydrate mixture are needed to be developed. The exact interactions between carbohydrates are needed to be quantitatively characterized by specially designed FTIR spectroscopy. However, the analysis will be complicated because of the multiple hydrogen bonding groups in carbohydrates which would overload the hydroxyl stretching regions in FTIR spectra. Also for systems with high water contents, where water should be counted as the third component, multiple component expression should be developed and the interactions of carbohydrates with water also needs to be described and included into the model.

These advances will further the state-of-art in carbohydrate polymer science.

## **APPENDIX A**

### **Guggenheim-Anderson-De Boer (GAB) Fit of Moisture Sorption Isotherms of Dextrans with Different Molecular Weights**



### GAB MODEL FOR DEXTRANS WITH MW=970

$$\frac{a_w}{M} = \frac{k}{M_o} \left( \frac{1}{C_G} - 1 \right) a_w^2 + \frac{1}{M_o} \left( 1 - \frac{2}{C_G} \right) a_w + \frac{1}{k M_o C_G}$$

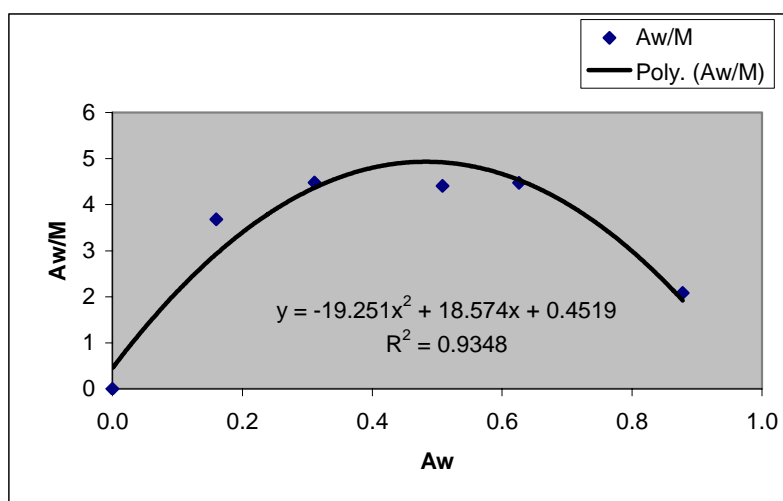
M: moisture content (dry basis)  
 Mo: monolayer moisture content  
 k: correction factor for multilayer  
 Cg: Guggenheim constant  
 aw: water activity

aw	measured aw	moisture % (d.b.)
0	0.000	1.541
0.12	0.160	4.350
0.33	0.311	6.938
0.52	0.508	11.530
0.75	0.626	13.995
0.93	0.878	42.137

Mw=970

Point	a <sub>w</sub>	M (kg/kg d.b.)
1	0.000	0.015
2	0.160	0.044
3	0.311	0.069
4	0.508	0.115
5	0.626	0.140
6	0.878	0.421

a <sub>w</sub>	a <sub>w</sub> /M
0.000	0.000000
0.160	3.678161
0.311	4.482560
0.508	4.405898
0.626	4.473026
0.878	2.083679



Coefficients from regression:

$\alpha$	-19.251
$\beta$	18.574
$\gamma$	0.4519
$R^2$	0.9348

Coefficients of the GAB equation:

$C_G$	42.63256
k	1.011554
$M_o$	5.13%

Coefficients from regression:

$\alpha$	-19.251
$\beta$	18.574
$\gamma$	0.4519
$R^2$	0.9348

Coefficients of the GAB equation:

$C_G$	42.63256
$k$	1.011554
$M_0$	5.13%

<b>Aw</b>	<b><math>\alpha * Aw^2</math></b>	<b><math>\beta * Aw</math></b>	<b><math>\gamma</math></b>	<b>Aw/M</b>	<b>M</b>	<b>M*100</b>
0	0	0	0.4519	0.4519	0	0
0.001	-1.93E-05	0.018574	0.4519	0.470455	0.002126	0.212560295
0.005	-0.000481	0.09287	0.4519	0.544289	0.009186	0.918630089
0.006	-0.000693	0.111444	0.4519	0.562651	0.010664	1.066380471
0.011	-0.002329	0.204314	0.4519	0.653885	0.016823	1.68225395
0.016	-0.004928	0.297184	0.4519	0.744156	0.021501	2.150087549
0.05	-0.048128	0.9287	0.4519	1.332473	0.037524	3.752422658
0.1	-0.19251	1.8574	0.4519	2.11679	0.047241	4.724134184
0.15	-0.433148	2.7861	0.4519	2.804853	0.053479	5.347874799
0.2	-0.77004	3.7148	0.4519	3.39666	0.058881	5.88813717
0.25	-1.203188	4.6435	0.4519	3.892213	0.064231	6.423081987
0.3	-1.73259	5.5722	0.4519	4.29151	0.069905	6.990546451
0.35	-2.358248	6.5009	0.4519	4.594553	0.076177	7.617716851
0.4	-3.08016	7.4296	0.4519	4.80134	0.08331	8.331007594
0.45	-3.898328	8.3583	0.4519	4.911873	0.091615	9.161475588
0.5	-4.81275	9.287	0.4519	4.92615	0.101499	10.14991423
0.55	-5.823428	10.2157	0.4519	4.844173	0.113538	11.35384836
0.6	-6.93036	11.1444	0.4519	4.66594	0.128591	12.85914521
0.65	-8.133548	12.0731	0.4519	4.391453	0.148015	14.80148083
0.7	-9.43299	13.0018	0.4519	4.02071	0.174099	17.40986045
0.75	-10.82869	13.9305	0.4519	3.553713	0.211047	21.10468981
0.8	-12.32064	14.8592	0.4519	2.99046	0.267517	26.75173719
0.85	-13.90885	15.7879	0.4519	2.330953	0.364658	36.46577955
0.9	-15.59331	16.7166	0.4519	1.57519	0.57136	57.13596455

### GAB MODEL FOR DEXTRANS WITH MW=10,800

$$\frac{a_w}{M} = \frac{k}{M_o} \left( \frac{1}{C_G} - 1 \right) a_w^2 + \frac{1}{M_o} \left( 1 - \frac{2}{C_G} \right) a_w + \frac{1}{k M_o C_G}$$

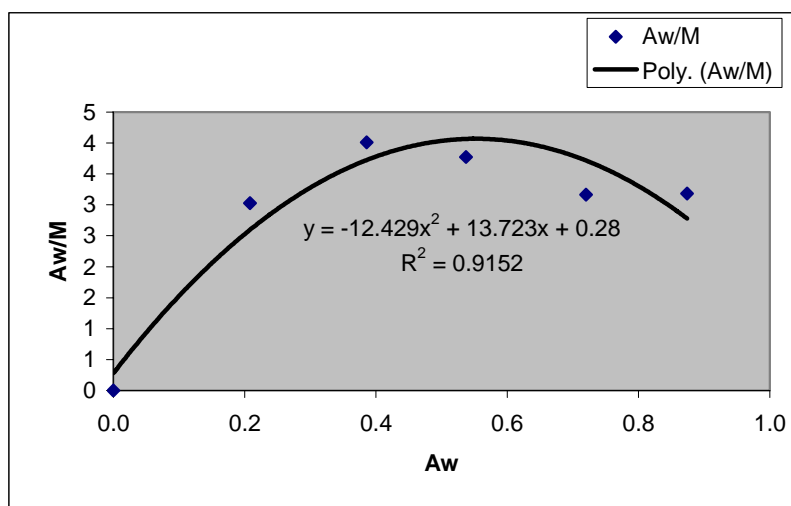
M: moisture content (dry basis)  
 Mo: monolayer moisture content  
 k: correction factor for multilayer  
 Cg: Guggenheim constant  
 aw: water activity

aw	measured aw	moisture % (d.b.)
0	0.000	1.594
0.12	0.208	6.864
0.33	0.386	9.629
0.52	0.537	14.227
0.75	0.720	22.733
0.93	0.874	27.466

Mw=10,800

Point	aw	M (kg/kg d.b.)
1	0.000	0.016
2	0.208	0.069
3	0.386	0.096
4	0.537	0.142
5	0.720	0.227
6	0.874	0.275

aw	aw/M
0.000	0.000000
0.208	3.030303
0.386	4.008724
0.537	3.774513
0.720	3.167202
0.874	3.182116



Coefficients from regression:

$\alpha$	-12.429
$\beta$	13.723
$\gamma$	0.28
$R^2$	0.9152

Coefficients of the GAB equation:

$C_G$	57.09546
k	0.88956
$M_o$	7.03%

Coefficients from regression:

$\alpha$	-12.429
$\beta$	13.723
$\gamma$	0.28
$R^2$	0.9152

Coefficients of the GAB equation:

$C_G$	57.09546
$k$	0.88956
$M_0$	7.03%

$A_w$	$\alpha * A_w^2$	$\beta * A_w$	$\gamma$	$A_w/M$	$M$	$M*100$
0	0	0	0.28	0.28	0	0
0.001	-1.24E-05	0.013723	0.28	0.293711	0.003405	0.340471232
0.005	-0.000311	0.068615	0.28	0.348304	0.014355	1.435526452
0.006	-0.000447	0.082338	0.28	0.361891	0.01658	1.657959817
0.011	-0.001504	0.150953	0.28	0.429449	0.025614	2.561421186
0.016	-0.003182	0.219568	0.28	0.496386	0.032233	3.223296855
0.05	-0.031073	0.68615	0.28	0.935078	0.053472	5.34715037
0.1	-0.12429	1.3723	0.28	1.52801	0.065445	6.544459788
0.15	-0.279653	2.05845	0.28	2.058798	0.072858	7.285806399
0.2	-0.49716	2.7446	0.28	2.52744	0.079131	7.913145317
0.25	-0.776813	3.43075	0.28	2.933938	0.08521	8.520972243
0.3	-1.11861	4.1169	0.28	3.27829	0.091511	9.151112318
0.35	-1.522553	4.80305	0.28	3.560498	0.098301	9.830086947
0.4	-1.98864	5.4892	0.28	3.78056	0.105804	10.58044311
0.45	-2.516873	6.17535	0.28	3.938478	0.114257	11.42573494
0.5	-3.10725	6.8615	0.28	4.03425	0.123939	12.39387742
0.55	-3.759773	7.54765	0.28	4.067878	0.135206	13.52056447
0.6	-4.47444	8.2338	0.28	4.03936	0.148538	14.85383823
0.65	-5.251253	8.91995	0.28	3.948698	0.164611	16.46112421
0.7	-6.09021	9.6061	0.28	3.79589	0.18441	18.44099803
0.75	-6.991313	10.29225	0.28	3.580938	0.209442	20.94423597
0.8	-7.95456	10.9784	0.28	3.30384	0.242142	24.21424766
0.85	-8.979953	11.66455	0.28	2.964598	0.286717	28.67168309
0.9	-10.06749	12.3507	0.28	2.56321	0.351122	35.11222256

### GAB MODEL FOR DEXTRANS WITH MW=43,000

$$\frac{a_w}{M} = \frac{k}{M_o} \left( \frac{1}{C_G} - 1 \right) a_w^2 + \frac{1}{M_o} \left( 1 - \frac{2}{C_G} \right) a_w + \frac{1}{k M_o C_G}$$

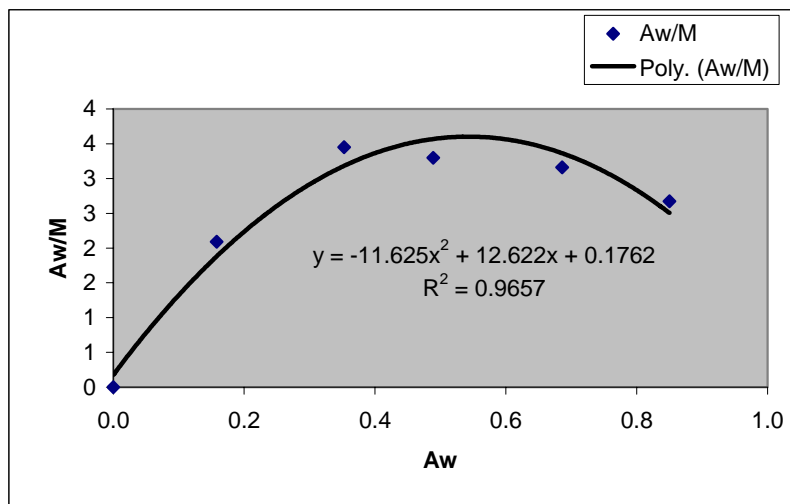
M: moisture content (dry basis)  
 Mo: monolayer moisture content  
 k: correction factor for multilayer  
 Cg: Guggenheim constant  
 aw: water activity

Mw=43,000

aw	measured aw	moisture % (d.b.)
0	0.000	1.560
0.12	0.158	7.551
0.33	0.353	10.229
0.52	0.489	14.821
0.75	0.686	21.693
0.93	0.850	31.803

Point	a <sub>w</sub>	M (kg/kg d.b.)
1	0.000	0.016
2	0.158	0.076
3	0.353	0.102
4	0.489	0.148
5	0.686	0.217
6	0.850	0.318

a <sub>w</sub>	a <sub>w</sub> /M
0.000	0.000000
0.158	2.092438
0.353	3.450973
0.489	3.299373
0.686	3.162310
0.850	2.672704



Coefficients from regression:

$\alpha$	-11.625
$\beta$	12.622
$\gamma$	0.1762
$R^2$	0.9657

Coefficients of the GAB equation:

$C_G$	80.76559
k	0.909464
$M_o$	7.73%

Coefficients from regression:

$\alpha$	-11.625
$\beta$	12.622
$\gamma$	0.1762
$R^2$	0.9657

Coefficients of the GAB equation:

$C_G$	80.76559
$k$	0.909464
$M_0$	7.73%

<b>Aw</b>	<b><math>\alpha * Aw^2</math></b>	<b><math>\beta * Aw</math></b>	<b><math>\gamma</math></b>	<b>Aw/M</b>	<b>M</b>	<b>M*100</b>
0	0	0	0.1762	0.1762	0	0
0.001	-1.16E-05	0.012622	0.1762	0.18881	0.005296	0.529631912
0.005	-0.000291	0.06311	0.1762	0.239019	0.020919	2.091880627
0.006	-0.000419	0.075732	0.1762	0.251514	0.023856	2.385557833
0.011	-0.001407	0.138842	0.1762	0.313635	0.035073	3.507257432
0.016	-0.002976	0.201952	0.1762	0.375176	0.042647	4.264665117
0.05	-0.029063	0.6311	0.1762	0.778238	0.064248	6.424773928
0.1	-0.11625	1.2622	0.1762	1.32215	0.075634	7.563438339
0.15	-0.261563	1.8933	0.1762	1.807938	0.082967	8.296746984
0.2	-0.465	2.5244	0.1762	2.2356	0.089461	8.946144212
0.25	-0.726563	3.1555	0.1762	2.605138	0.095964	9.596422454
0.3	-1.04625	3.7866	0.1762	2.91655	0.102861	10.28612573
0.35	-1.424063	4.4177	0.1762	3.169838	0.110416	11.04157548
0.4	-1.86	5.0488	0.1762	3.365	0.118871	11.88707281
0.45	-2.354063	5.6799	0.1762	3.502038	0.128497	12.84966252
0.5	-2.90625	6.311	0.1762	3.58095	0.139628	13.96277524
0.55	-3.516563	6.9421	0.1762	3.601738	0.152704	15.27040769
0.6	-4.185	7.5732	0.1762	3.5644	0.168331	16.8331276
0.65	-4.911563	8.2043	0.1762	3.468938	0.187377	18.73772589
0.7	-5.69625	8.8354	0.1762	3.31535	0.211139	21.11390954
0.75	-6.539063	9.4665	0.1762	3.103638	0.241652	24.16519326
0.8	-7.44	10.0976	0.1762	2.8338	0.282306	28.23064436
0.85	-8.399063	10.7287	0.1762	2.505838	0.339208	33.92079494
0.9	-9.41625	11.3598	0.1762	2.11975	0.424578	42.45783701

### GAB MODEL FOR DEXTRANS WITH MW=2,000,000

$$\frac{a_w}{M} = \frac{k}{M_o} \left( \frac{1}{C_G} - 1 \right) a_w^2 + \frac{1}{M_o} \left( 1 - \frac{2}{C_G} \right) a_w + \frac{1}{k M_o C_G}$$

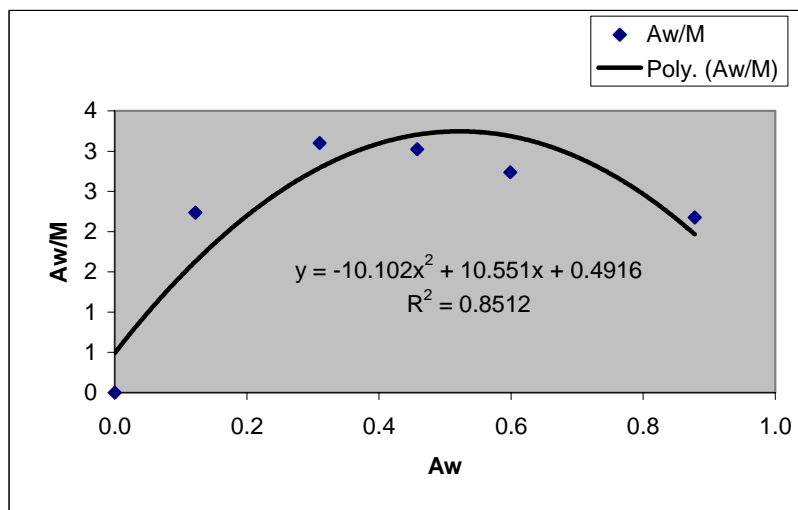
M: moisture content (dry basis)  
 Mo: monolayer moisture content  
 k: correction factor for multilayer  
 Cg: Guggenheim constant  
 aw: water activity

aw	measured aw	moisture % (d.b.)
0	0.000	1.541
0.12	0.122	4.350
0.33	0.310	6.938
0.52	0.458	11.530
0.75	0.599	13.995
0.93	0.878	42.137

Mw=2,000,000

Point	a <sub>w</sub>	M (kg/kg d.b.)
1	0.000	0.015
2	0.122	0.055
3	0.310	0.100
4	0.458	0.152
5	0.599	0.219
6	0.878	0.403

a <sub>w</sub>	a <sub>w</sub> /M
0.000	0.000000
0.122	2.234432
0.310	3.100620
0.458	3.022903
0.599	2.735784
0.878	2.176500



Coefficients from regression:

$\alpha$	-10.102
$\beta$	10.551
$\gamma$	0.4916
$R^2$	0.8512

Coefficients of the GAB equation:

$C_G$	25.37549
$k$	0.918166
$M_o$	8.73%

Coefficients from regression:

$\alpha$	-10.102
$\beta$	10.551
$\gamma$	0.4916
$R^2$	0.8512

Coefficients of the GAB equation:

$C_G$	25.37549
$k$	0.918166
$M_0$	8.73%

$A_w$	$\alpha * A_w^2$	$\beta * A_w$	$\gamma$	$A_w/M$	$M$	$M*100$
0	0	0	0.4916	0.4916	0	0
0.001	-1.01E-05	0.010551	0.4916	0.502141	0.001991	0.199147292
0.005	-0.000253	0.052755	0.4916	0.544102	0.009189	0.918944585
0.006	-0.000364	0.063306	0.4916	0.554542	0.01082	1.081973313
0.011	-0.001222	0.116061	0.4916	0.606439	0.018139	1.813868535
0.016	-0.002586	0.168816	0.4916	0.65783	0.024322	2.432239746
0.05	-0.025255	0.52755	0.4916	0.993895	0.050307	5.0307125
0.1	-0.10102	1.0551	0.4916	1.44568	0.069172	6.917160091
0.15	-0.227295	1.58265	0.4916	1.846955	0.081215	8.121475618
0.2	-0.40408	2.1102	0.4916	2.19772	0.091003	9.100340353
0.25	-0.631375	2.63775	0.4916	2.497975	0.100081	10.00810657
0.3	-0.90918	3.1653	0.4916	2.74772	0.109181	10.91814304
0.35	-1.237495	3.69285	0.4916	2.946955	0.118767	11.87666591
0.4	-1.61632	4.2204	0.4916	3.09568	0.129212	12.92123217
0.45	-2.045655	4.74795	0.4916	3.193895	0.140894	14.0893799
0.5	-2.5255	5.2755	0.4916	3.2416	0.154245	15.42448174
0.55	-3.055855	5.80305	0.4916	3.238795	0.169816	16.98162434
0.6	-3.63672	6.3306	0.4916	3.18548	0.188355	18.83546593
0.65	-4.268095	6.85815	0.4916	3.081655	0.210926	21.09256228
0.7	-4.94998	7.3857	0.4916	2.92732	0.239127	23.91265731
0.75	-5.682375	7.91325	0.4916	2.722475	0.275485	27.54846234
0.8	-6.46528	8.4408	0.4916	2.46712	0.324265	32.42647297
0.85	-7.298695	8.96835	0.4916	2.161255	0.39329	39.32900097
0.9	-8.18262	9.4959	0.4916	1.80488	0.498648	49.86481096



## **APPENDIX B**

### **Calculation of Volume Fractions in Dextran Mixtures**

**Mw (1,000) + Mw (2,000,000)**

$$Mwt_B := 1000 \quad Mwt_A := 2000000 \quad Mwt_{mer} := 162$$

$$m_A(m_B) := 100 - m_B$$

$$n_B(m_B, Mwt_B) := \frac{m_B}{Mwt_B}$$

$$n_A(m_B, Mwt_A) := \frac{m_A(m_B)}{Mwt_A}$$

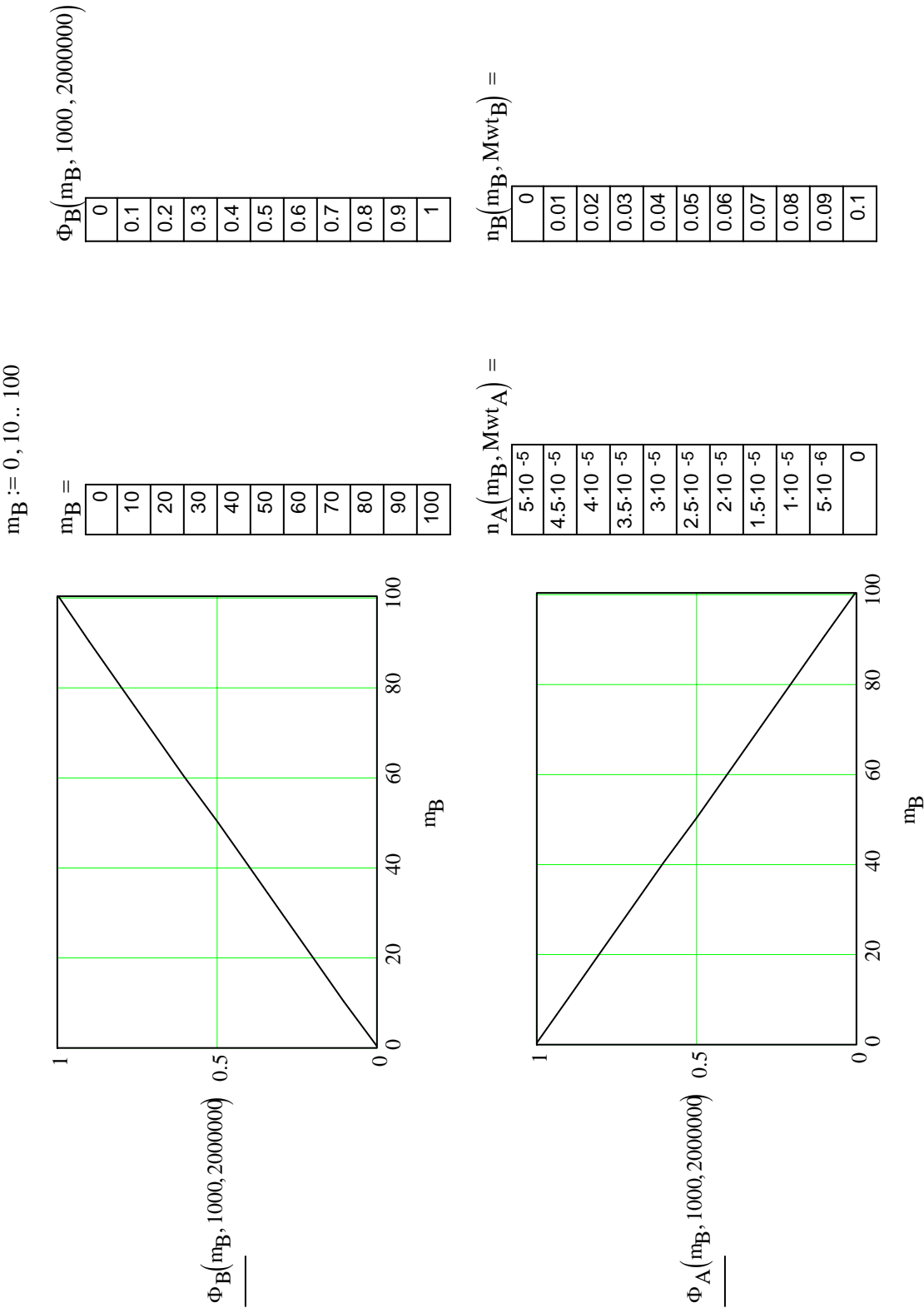
$$M_A(Mwt_A) := \frac{Mwt_A}{Mwt_{mer}}$$

$$M_B(Mwt_B) := \frac{Mwt_B}{Mwt_{mer}}$$

$$\Phi_B(m_B, Mwt_A, Mwt_B) := \frac{n_B(m_B, Mwt_B) \cdot M_B(Mwt_B)}{n_A(m_B, Mwt_A) \cdot M_A(Mwt_A) + n_B(m_B, Mwt_B) \cdot M_B(Mwt_B)}$$

$$\Phi_A(m_B, Mwt_A, Mwt_B) := \frac{n_A(m_B, Mwt_A) \cdot M_A(Mwt_A)}{n_A(m_B, Mwt_A) \cdot M_A(Mwt_A) + n_B(m_B, Mwt_B) \cdot M_B(Mwt_B)}$$

$$\Phi_B(m_B, Mwt_A, Mwt_B) := 1 - \Phi_A(m_B, Mwt_A, Mwt_B)$$



## **APPENDIX C**

### **Calculation of Solubility Parameters of Dextrans with Different Molecular Weights**

$$\delta_B = \left( \frac{E_{coh}}{V_r} \right)^{\frac{1}{2}}$$

1. Using the solubility parameter of monomer calculated from the following equation:

$$\frac{E_{coh}}{V_m} = CED = \delta_B^2 \frac{(-0.5 \cdot n \cdot R \cdot T_g + C \cdot n)}{V_m}$$

$$\delta_{B,monomer} := 19.8 \quad T_{g,monomer} := 107.5 + 273 \quad n := 76$$

$$V_m := 57.7 \quad R := 2$$

$$C := \frac{(\delta_{B,monomer}^2 \cdot V_m)}{n} + 0.5 \cdot R \cdot T_{g,monomer} \quad \rightarrow \quad C = 678.14$$

**Solubility parameter of dextran with Mw=1,000:**

$$T_{g,1000} := 124.6 + 273 \quad R := 2 \quad C = 678.141 \quad n := 76 \quad V_m := 57.7$$

$$\delta_{B,1000} := \left( \frac{-0.5 \cdot n \cdot R \cdot T_{g,1000} + C \cdot n}{V_m} \right)^{\frac{1}{2}}$$

$$\delta_{B,1000} = 19.223 \left( \frac{cal}{cm^3} \right)^{0.5}$$

**Solubility parameter of dextran with Mw=5,000:**

$T_{g,5000} := 158.9 + 273 \qquad R := 2 \qquad C = 678.141 \qquad n := 76 \qquad V_m := 57.7$

$$\delta_{B,5000} := \left( \frac{-0.5 \cdot n \cdot R \cdot T_{g,5000} + C \cdot n}{V_m} \right)^{\frac{1}{2}}$$

$$\delta_{B,5000} = 18.009 \qquad \left( \frac{\text{cal}}{\text{cm}^3} \right)^{0.5}$$

**Solubility parameter of dextran with Mw=10,000:**

$T_{g,10000} := 168.8 + 273 \qquad R := 2 \qquad C = 678.141 \qquad n := 76 \qquad V_m := 57.7$

$$\delta_{B,10000} := \left( \frac{-0.5 \cdot n \cdot R \cdot T_{g,10000} + C \cdot n}{V_m} \right)^{\frac{1}{2}}$$

$$\delta_{B,10000} = 17.644 \qquad \left( \frac{\text{cal}}{\text{cm}^3} \right)^{0.5}$$

**Solubility parameter of dextran with Mw=2,000,000:**

$$T_{g,2000000} := 180 + 273 \quad R := 2 \quad C = 678.141 \quad n := 76 \quad V_m := 57.7$$

$$\delta_{B,2000000} := \left( \frac{-0.5 \cdot n \cdot R \cdot T_{g,2000000} + C \cdot n}{V_m} \right)^{\frac{1}{2}}$$

$$\delta_{B,2000000} = 17.221 \left( \frac{\text{cal}}{\text{cm}^3} \right)^{0.5}$$

$$\delta_B = \left( \delta_d^2 + \delta_p^2 + \delta_h^2 \right)^{\frac{1}{2}}$$

**2. Using the solubility parameter of monomer calculated from the following equation:**

$$\frac{E_{coh}}{V_m} = CED = \delta_B^2 = \frac{(-0.5 \cdot n \cdot R \cdot T_g + C \cdot n)}{V_m}$$

$$\delta_{B,monomer} := 22.6 \quad T_{g,monomer} := 107.5 + 273 \quad n := 76$$

$$V_m := 57.7 \quad R := 2$$

$$C := \frac{(\delta_{B,monomer}^2 \cdot V_m)}{n} + 0.5 \cdot R \cdot T_{g,monomer} \quad \rightarrow C = 768.274$$

**Solubility parameter of dextran with Mw=1,000:**

$T_{g,1000} := 124.6 + 273$        $R := 2$        $C = 768.274$        $n := 76$        $V_m := 57.7$

$$\delta_{B,1000} := \left( \frac{-0.5 \cdot n \cdot R \cdot T_{g,1000} + C \cdot n}{V_m} \right)^{\frac{1}{2}}$$

$$\delta_{B,1000} = 22.096 \left( \frac{\text{cal}}{\text{cm}^3} \right)^{0.5}$$

**Solubility parameter of dextran with Mw=5,000:**

$T_{g,5000} := 158.9 + 273$        $R := 2$        $C = 768.274$        $n := 76$        $V_m := 57.7$

$$\delta_{B,5000} := \left( \frac{-0.5 \cdot n \cdot R \cdot T_{g,5000} + C \cdot n}{V_m} \right)^{\frac{1}{2}}$$

$$\delta_{B,5000} = 21.049 \left( \frac{\text{cal}}{\text{cm}^3} \right)^{0.5}$$



**Solubility parameter of dextran with Mw=10,000:**

$T_{g,10000} := 168.8 + 273$        $R := 2$        $C = 768.274$        $n := 76$        $V_m := 57.7$

$$\delta_{B,10000} := \left( \frac{-0.5 \cdot n \cdot R \cdot T_{g,10000} + C \cdot n}{V_m} \right)^{\frac{1}{2}}$$

$$\delta_{B,10000} = 20.737 \left( \frac{\text{cal}}{\text{cm}^3} \right)^{0.5}$$

**Solubility parameter of dextran with Mw=2,000,000:**

$T_{g,2000000} := 180 + 273$        $R := 2$        $C = 768.274$        $n := 76$        $V_m := 57.7$

$$\delta_{B,2000000} := \left( \frac{-0.5 \cdot n \cdot R \cdot T_{g,2000000} + C \cdot n}{V_m} \right)^{\frac{1}{2}}$$

$$\delta_{B,2000000} = 20.378 \left( \frac{\text{cal}}{\text{cm}^3} \right)^{0.5}$$

## **APPENDIX D**

### **Predictions of Thermodynamics of Mixing Dextran with $M_w=1,000$ and $M_w=2,000,000$ Using Flory-Huggins Equation**

**Mixing Dextrans with Mw=1,000 + Mw=2,000,000**

$$\Delta G_{\text{mix}} = \left[ \frac{\Phi_A}{M_A} \cdot \ln(\Phi_A) + \frac{\Phi_B}{M_B} \cdot \ln(\Phi_B) + \left[ \frac{V_r}{R \cdot T} \cdot (\delta_A - \delta_B)^2 \right] \cdot \Phi_A \cdot \Phi_B \right] \cdot R \cdot T$$

Flory-Huggins Equation

**1. Using the solubility parameter of monomer calculated from the following equation:**

$$\delta_{\text{monomer}} = \left( \frac{E_{\text{coh}}}{V_r} \right)^{\frac{1}{2}}$$

$$\delta_{1000} := 19.223$$

$$\delta_{2000000} := 17.221$$

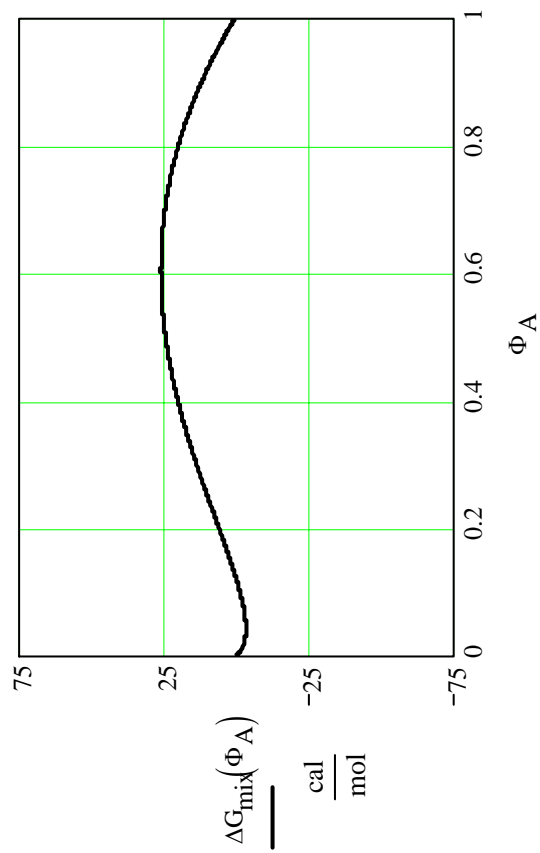
$$V_r := 57.7 \quad R := 2 \quad T := 300$$

$$\chi_{AB} := \frac{V_r}{R \cdot T} \cdot (\delta_{1000} - \delta_{2000000})^2$$

$$M_A := \frac{1000}{162} \quad M_B := \frac{2000000}{162}$$

$$\Phi_B(\Phi_A) := 1 - \Phi_A$$

$$\Delta G_{\text{mix}}(\Phi_A) := R \cdot T \cdot \left( \frac{\Phi_A}{M_A} \cdot \ln(\Phi_A) + \frac{\Phi_B(\Phi_A)}{M_B} \cdot \ln(\Phi_B(\Phi_A)) + \chi_{AB} \cdot \Phi_A \cdot \Phi_B(\Phi_A) \right)$$



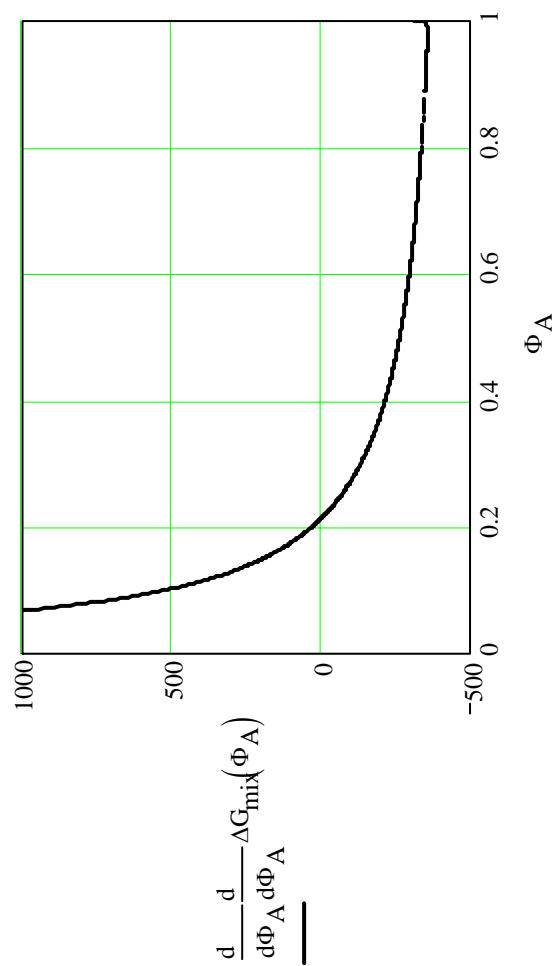
$$\Delta G_{\text{mix}}(\Phi_A) = R \cdot T \cdot \left( \frac{\Phi_A}{M_A} \cdot \ln(\Phi_A) + \frac{\Phi_B(\Phi_A)}{M_B} \cdot \ln(\Phi_B(\Phi_A)) + \chi_{AB} \cdot \Phi_A \cdot \Phi_B(\Phi_A) \right)$$

1st derivative:

$$\frac{d}{d\Phi_A} \Delta G_{\text{mix}}(\Phi_A) = R \cdot T \cdot \left( \frac{1}{M_A} \cdot \ln(\Phi_A) + \frac{1}{M_A} + \frac{\frac{d}{d\Phi_A} \Phi_B(\Phi_A)}{M_B} \cdot \ln(\Phi_B(\Phi_A)) + \frac{1}{M_B} \cdot \frac{d}{d\Phi_A} \Phi_B(\Phi_A) + \chi_{AB} \cdot \Phi_A + \chi_{AB} \cdot \Phi_A \cdot \frac{d}{d\Phi_A} \Phi_B(\Phi_A) \right)$$

2nd derivative:

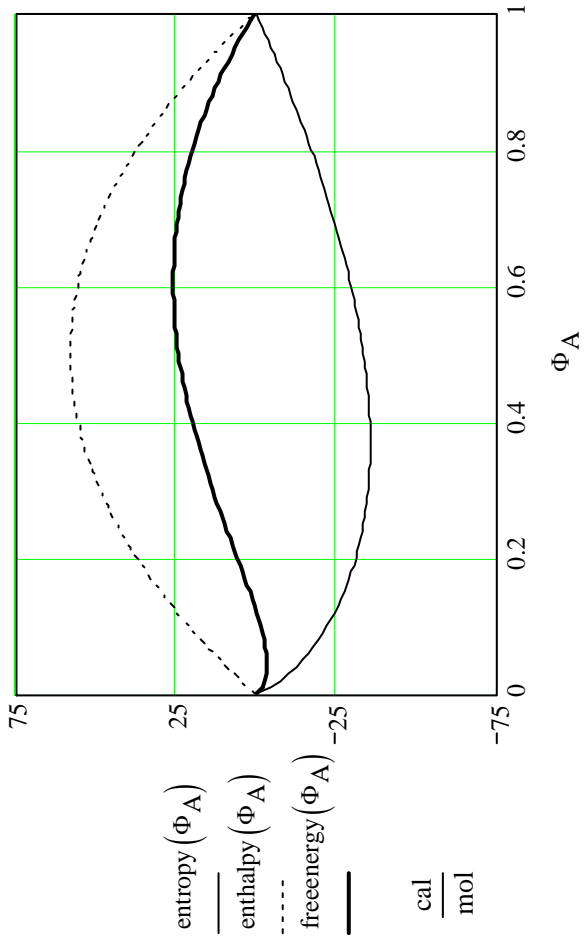
$$\begin{aligned} \frac{d}{d\Phi_A} \frac{d}{d\Phi_A} \Delta G_{\text{mix}}(\Phi_A) = R \cdot T \cdot & \left[ \frac{1}{M_A \cdot \Phi_A} + \frac{\frac{d}{d\Phi_A} \frac{d}{d\Phi_A} \Phi_B(\Phi_A)}{M_B} - \ln(\Phi_B(\Phi_A)) + \frac{\left( \frac{d}{d\Phi_A} \Phi_B(\Phi_A) \right)^2}{M_B \cdot \Phi_B(\Phi_A)} + \frac{\frac{d}{d\Phi_A} \frac{d}{d\Phi_A} \Phi_B(\Phi_A)}{M_B} \right] \\ & + R \cdot T \cdot \left( 2 \cdot \chi_{AB} \cdot \frac{d}{d\Phi_A} \Phi_B(\Phi_A) + \chi_{AB} \cdot \Phi_A \cdot \frac{d}{d\Phi_A} \frac{d}{d\Phi_A} \Phi_B(\Phi_A) \right) \end{aligned}$$



$$\text{entropy}(\Phi_A) := \left( \frac{\Phi_A}{M_A} \cdot \ln(\Phi_A) + \frac{\Phi_B(\Phi_A)}{M_B} \cdot \ln(\Phi_B(\Phi_A)) \right) \cdot R \cdot T$$

$$\text{enthalpy}(\Phi_A) := (\chi_{AB} \cdot \Phi_A \cdot \Phi_B(\Phi_A)) \cdot R \cdot T$$

$$\text{freenergy}(\Phi_A) := \text{entropy}(\Phi_A) + \text{enthalpy}(\Phi_A)$$



$$\delta_B = \frac{1}{2} \left( \delta_d^2 + \delta_p^2 + \delta_h^2 \right)$$

2. Using the solubility parameter of monomer calculated from the following equation:

$$\delta_{1000} := 22.096$$

$$\delta_{2000000} := 20.378$$

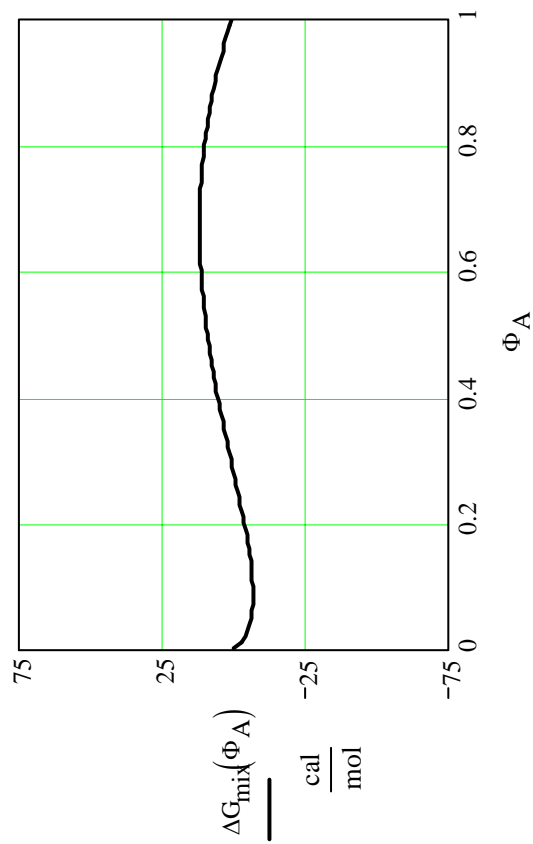
$$V_r := 57.7 \quad R := 2 \quad T := 300$$

$$\chi_{AB} := \frac{V_r}{R \cdot T} \cdot \left( \delta_{1000} - \delta_{2000000} \right)^2$$

$$M_A := \frac{1000}{162} \quad M_B := \frac{2000000}{162}$$

$$\Phi_B(\Phi_A) := 1 - \Phi_A$$

$$\Delta G_{\text{mix}}(\Phi_A) := R \cdot T \cdot \left( \frac{\Phi_A}{M_A} \cdot \ln(\Phi_A) + \frac{\Phi_B(\Phi_A)}{M_B} \cdot \ln(\Phi_B(\Phi_A)) + \chi_{AB} \cdot \Phi_A \cdot \Phi_B(\Phi_A) \right)$$



$$\Delta G_{\text{mix}}(\Phi_A) = R \cdot T \cdot \left( \frac{\Phi_A}{M_A} \cdot \ln(\Phi_A) + \frac{\Phi_B(\Phi_A)}{M_B} \cdot \ln(\Phi_B(\Phi_A)) + \chi_{AB} \cdot \Phi_A \cdot \Phi_B(\Phi_A) \right)$$

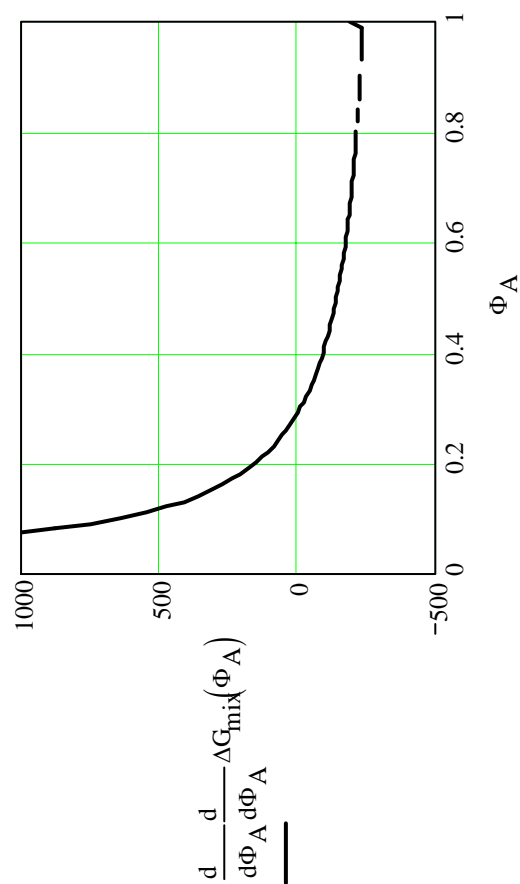
1st derivative:

$$\frac{d}{d\Phi_A} \Delta G_{\text{mix}}(\Phi_A) = R \cdot T \cdot \left( \frac{1}{M_A} \cdot \ln(\Phi_A) + \frac{1}{M_A} + \frac{\frac{d}{d\Phi_A} \Phi_B(\Phi_A)}{M_B} \cdot \ln(\Phi_B(\Phi_A)) + \frac{1}{M_B} \cdot \frac{d}{d\Phi_A} \Phi_B(\Phi_A) \cdot \frac{d}{d\Phi_A} \Phi_A \right)$$



2nd derivative:

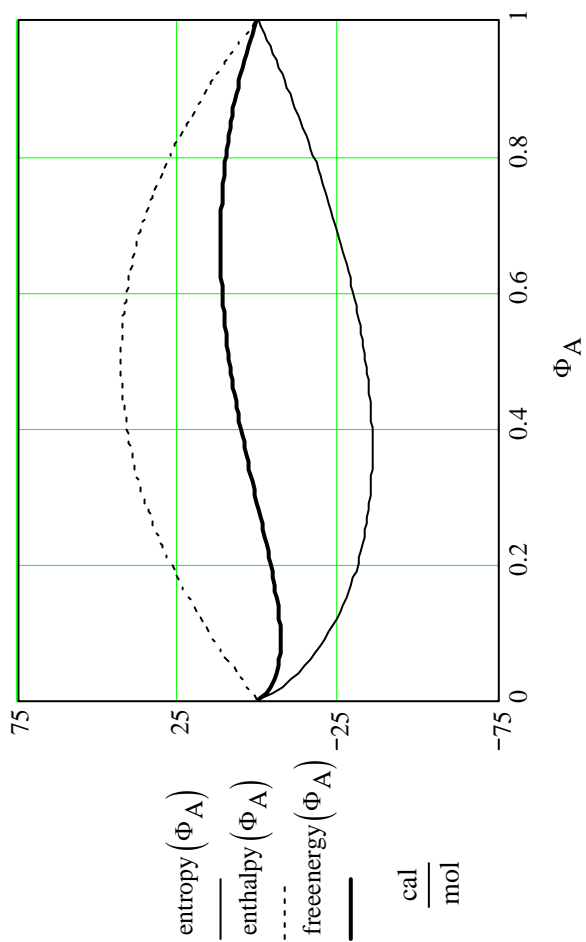
$$\begin{aligned} \frac{d}{d\Phi_A} \frac{d}{d\Phi_A} \Delta G_{\text{mix}}(\Phi_A) = R \cdot T \cdot & \left[ \frac{1}{M_A \cdot \Phi_A} + \frac{\frac{d}{d\Phi_A} \frac{d}{d\Phi_A} \Phi_B(\Phi_A)}{M_B} \cdot \ln(\Phi_B(\Phi_A)) + \frac{\left( \frac{d}{d\Phi_A} \Phi_B(\Phi_A) \right)^2}{M_B \cdot \Phi_B(\Phi_A)} + \frac{\frac{d}{d\Phi_A} \frac{d}{d\Phi_A} \Phi_B(\Phi_A)}{M_B} \right] \\ & + R \cdot T \cdot \left( 2 \cdot \chi_{AB} \cdot \frac{d}{d\Phi_A} \Phi_B(\Phi_A) + \chi_{AB} \cdot \Phi_A \cdot \frac{d}{d\Phi_A} \frac{d}{d\Phi_A} \Phi_B(\Phi_A) \right) \end{aligned}$$



$$\text{entropy}(\Phi_A) := \left( \frac{\Phi_A}{M_A} \cdot \ln(\Phi_A) + \frac{\Phi_B(\Phi_A)}{M_B} \cdot \ln(\Phi_B(\Phi_A)) \right) \cdot R \cdot T$$

$$\text{enthalpy}(\Phi_A) := (\chi_{AB} \cdot \Phi_A \cdot \Phi_B(\Phi_A)) \cdot R \cdot T$$

$$\text{freenergy}(\Phi_A) := \text{entropy}(\Phi_A) + \text{enthalpy}(\Phi_A)$$


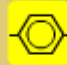

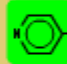







## **APPENDIX E**

**Non-Hydrogen Bonded Solubility Parameter and Molar Volume Calculation of the  
Repeating Unit (Mer) of Dextran Using the Miscibility Guide and Phase Calculator  
(MG&PC) Software**

### Solubility Parameter Calculator

1  $\text{CH}_2$ 
5  $\text{-CH-}$ 
5  $\text{-O-}$

$\text{-CH}_3$	$\text{CH}_2$	$\text{-CH-}$	$\text{-C-}$	$\text{=CH}_2$	$\text{-CH=}$	$\text{-C=}$	$\text{-CN}$
			$\text{-O-}$	$\text{-N-}$	$\text{-NH-}$	$\text{-NH}_2$	$\text{-Cl}$
$\text{-C(=O)-}$	$\text{-C(=O)O-}$	$\text{-O-C(=O)-}$					$\text{-C}\equiv\text{C-}$
$\text{-F}$	$\text{-Br}$	$\text{-I}$	$\text{-S-}$			$\text{-CF}_3$	$\text{CF}_2$
$\text{-NCO}$	$\text{-NO}_2$	$\text{-SO}_2$	$\text{-Si-}$	$\text{-COOH}$	$\text{-OH}$	$\text{-CONH-}$	$\text{-OCONH-}$

CLEAR
Mer-Dextran

**Molar Volume** ( $\text{cm}^3/\text{mol}$ )

**Molecular Weight** ( $\text{g/mol}$ )

**Solubility Parameter** ( $\text{cal}/\text{cm}^3)^{0.5}$ )

51.5

159

14

Figure A.E: Screen snapshot of the software

## **APPENDIX F**

### **Calculation of Non-Hydrogen Bonded Solubility Parameter of Dextrans with Different Molecular Weights and Amylopectin**

**Using the non-hydrogen bonded solubility parameter of monomer calculated from the MG&PC software**

$$\frac{E_{\text{coh}}}{V_{\text{m}}} = \text{CED} = \delta_{\text{B}}^2 = \frac{(-0.5 \cdot n \cdot R \cdot T_{\text{g}} + C \cdot n)}{V_{\text{m}}}$$

$$\delta_{\text{B,monomer}} := 14 \quad T_{\text{g,monomer}} := 107.5 + 273 \quad n := 76$$

$$V_{\text{m}} := 51.5 \quad R := 2$$

$$C := \frac{(\delta_{\text{B,monomer}}^2 \cdot V_{\text{m}})}{n} + 0.5 \cdot R \cdot T_{\text{g,monomer}} \quad \rightarrow \quad C = 513.32$$

***Non-hydrogen bonded solubility parameter of dextran with Mw=1,000:***

$$T_{\text{g},1000} := 124.6 + 273 \quad R := 2 \quad C = 513.32 \quad n := 76 \quad V_{\text{m}} := 51.5$$

$$\delta_{\text{B},1000} := \left( \frac{-0.5 \cdot n \cdot R \cdot T_{\text{g},1000} + C \cdot n}{V_{\text{m}}} \right)^{\frac{1}{2}}$$

$$\delta_{\text{B},1000} = 13.068 \left( \frac{\text{cal}}{\text{cm}^3} \right)^{0.5}$$

**Non-hydrogen bonded solubility parameter of dextran with Mw=5,000:**

$T_{g,5000} := 158.9 + 273$        $R := 2$        $C = 513.32$        $n := 76$        $V_m := 51.5$

$$\delta_{B,5000} := \left( \frac{-0.5 \cdot n \cdot R \cdot T_{g,5000} + C \cdot n}{V_m} \right)^{\frac{1}{2}}$$

$$\delta_{B,5000} = 10.961 \left( \frac{\text{cal}}{\text{cm}^3} \right)^{0.5}$$

**Non-hydrogen bonded solubility parameter of dextran with Mw=10,000:**

$T_{g,10000} := 168.8 + 273$        $R := 2$        $C = 513.32$        $n := 76$        $V_m := 51.5$

$$\delta_{B,10000} := \left( \frac{-0.5 \cdot n \cdot R \cdot T_{g,10000} + C \cdot n}{V_m} \right)^{\frac{1}{2}}$$

$$\delta_{B,10000} = 10.273 \left( \frac{\text{cal}}{\text{cm}^3} \right)^{0.5}$$

**Non-hydrogen bonded solubility parameter of dextran with Mw=2,000,000:**

$T_{g,2000000} := 180 + 273 \qquad R := 2 \qquad C = 513.32 \qquad n := 76 \qquad V_m := 51.5$

$$\delta_{B,2000000} := \left( \frac{-0.5 \cdot n \cdot R \cdot T_{g,2000000} + C \cdot n}{V_m} \right)^{\frac{1}{2}}$$

$$\delta_{B,2000000} = 9.434 \left( \frac{\text{cal}}{\text{cm}^3} \right)^{0.5}$$

**Non-hydrogen bonded solubility parameter of Amylopectin with Mw=400,000,000:**

$T_{g,amylopectin} := 185.6 + 273 \qquad R := 2 \qquad C = 513.32 \qquad n := 76 \qquad V_m := 51.5$

$$\delta_{B,amylopectin} := \left( \frac{-0.5 \cdot n \cdot R \cdot T_{g,amylopectin} + C \cdot n}{V_m} \right)^{\frac{1}{2}}$$

$$\delta_{B,amylopectin} = 8.986 \left( \frac{\text{cal}}{\text{cm}^3} \right)^{0.5}$$



## REFERENCES

- Ahmad, F. B., and Williams, P. A. (2001). Effect of galactomannans on the thermal and rheological properties of sago starch. *Journal of Agricultural and Food Chemistry*, 49, 1578-1586.
- Aklonis, J. J., and MacKnight, W. J. (1983). Introduction to Polymer Viscoelasticity. New York: John Wiley and Sons, Inc.
- Albertsson, P. A. (1986). Partition of Cell Particles and Macromolecules. 3<sup>rd</sup> Edition. New York: John Wiley and Sons, Inc.
- Antipova, A. S., and Semenova, M. G. (1995). Effect of sucrose on the thermodynamic incompatibility of different biopolymers. *Carbohydrate Polymers*, 28, 359-365.
- Basak, P., Nisha, C. K., Manorama, S. V., Maiti, S., and Jayachandran, K. N. (2003). Probing the association behavior of poly(ethylene glycol)-based amphiphilic comb-like polymer in NaCl solution. *Journal of Colloid and Interface Science*, 262, 560-565.
- Batzer, H., and Kreibich, U. T. (1981). Influence of water on thermal transitions in natural polymers and synthetic polyamides. *Polymer Bulletin*, 5, 585.
- Bell, L. N. and Labuza, T. P. (2000). Moisture Sorption: Practical Aspects of Isotherm Measurement and Use. 2<sup>nd</sup> Edition. St. Paul, MN: AACC, Inc.
- Biliaderis, C. G. (1991). The structure and interactions of starch with food constituents. *Canadian Journal of Physiology and Pharmacology*, 69, 60-78.
- Billmeyer, F. W. (1984). Polymer structure and physical properties. In F. W. Billmeyer (Ed.). *Textbook of Polymer Science* (pp. 330-357). New York: Wiley-Interscience.
- Blondiaux, N., Jeney, S., Liley, M., Pugin, R., Sigrist, H., Heinzelmänn, H., and Spencer, N. D. (2001). Structured peg-dextran surfaces for bio-applications. *European Cells and Materials*, 6(1), 62.
- Cascone, M. G., Polacco, G., Lazzeri, L., and Barbani, N. (1997). Dextran/poly(acrylic acid) mixtures as miscible blends. *Journal of Applied Polymer Science*, 66, 2089-2094.
- Chalmers, J. M., and Everall, N. J. (1993). Vibrational Spectroscopy. In B. J. Hunt, and M. I. James (Eds.). *Polymer Characterization* (pp. 69-114). London: Chapman and Hall.

- Closs, C. B., Conde-Petit, B., Roberts, I. D., Tolstoguzov, V. B., and Escher, F. (1999). Phase separation and rheology of aqueous starch/galactomannan systems. *Carbohydrate Polymers*, 39, 67-77.
- Cocero, A. M., and Kokini, J. L. (1991). The study of the glass transition of glutenin using small amplitude oscillatory rheological measurements and differential scanning calorimetry. *Journal of Rheology*, 35(2), 257-270.
- Coleman, M. M., and Painter, P. C. (1990). Infrared-Absorption Spectroscopy. In J. I. Kroschwitz (Ed.). *Polymers: Polymer Characterization and Analysis* (pp. 371-403). New York: John Wiley and Sons, Inc.
- Coleman, M. M., and Painter, P. C. (1995). Hydrogen Bonded Polymer Blends. *Progress in Polymer Science*, 20, 1-59.
- Coleman, M. M., and Painter, P. C. (2006). Miscible Polymer Blends: Background and Guide for Calculations and Design. Lancaster, PA: DEStech Publications, Inc.
- Coleman, M. M., Graf, J. F., and Painter, P. C. (1991). Specific Interactions and the Miscibility of Polymer Blends. Lancaster, PA: Technomic Publishing, Co.
- Coleman, M. M., Pehlert, G. J., and Painter, P. C. (1996). Functional group accessibility in hydrogen bonded polymer blends. *Macromolecules*, 29, 6820-6831.
- Coleman, M. M., Narvett, L.A., Park, Y. H., and Painter, P. C. (1991). Further experimental evidence for intramolecular screening in polymer blends. *Journal of Macromolecular Science. Physics*, B37, 283-299.
- Coleman, M. M., Guigley, K. S., and Painter, P. C. (1999). The prediction of hydrogen bonded polymer blend phase behavior using equilibrium constants determined from low molar mass analogues. *Macromolecular Chemistry and Physics*, 200, 1167-1173.
- Coleman, M. M., Serman, C. J., Bahgwagner, D. E., and Painter, P. C. (1990). A practical guide to polymer miscibility. *Polymer*, 31, 1187-1203.
- Couchman, P. R., and Karasz, F. E. (1978). Classical thermodynamic discussion of the effect of composition on glass transition temperatures. *Macromolecules*, 11, 117-119.
- Cowie, J. M. G. (1975). Some general features of  $T_g$ -M relations for oligomers and amorphous polymers. *European Polymer Journal*, 11, 297-300.
- De Graaf, E.M., Madeka, H., Cocero, A.M., and Kokini, J.L. (1993). Determination of the effect of moisture on gliadin glass transition using mechanical spectroscopy and differential scanning calorimetry. *Biotechnology Progress*, 9, 210-213.
- Demetriades, K., and McClements, D. J. (1998). Influence of dextran sulfate and NaCl on the flocculation of oil-in-water emulsions stabilized by a nonionic surfactant. *Journal of Agricultural and Food Chemistry*, 46(10), 3929-3935.

- Dobrynin, A. V, Rubinstein, M., and Obukhov, S. P. (1996). Cascade of transitions of polyelectrolytes in poor solvents. *Macromolecules*, 29(8), 2974-2979.
- Dong, J., and Ozaki, Y. (1997). FTIR and FT-Raman studies of partially miscible poly(methylmethacrylate)/poly(4-vinylphenol) blends in solid states. *Macromolecules*, 30(2), 286-292.
- Ferry, J. D. (1980). *Viscoelastic Properties of Polymers*. 3<sup>rd</sup> Edition. New York: John Wiley and Sons, Inc.
- Flory, P. J. (1952). *Principles of Polymer Chemistry*. Ithaca, NY: Cornell University Press.
- Forssell, P. M., Mikkila, J. M., Moates, G. K., and Parker, R. (1997). Phase and glass transition behavior of concentrated barley starch-glycerol-water mixtures, a model for thermoplastic starch. *Carbohydrate Polymers*, 34, 275-282.
- Fox, T. G., and Flory, P. J. (1950). Second order transition temperatures and related properties of polystyrene. I. Influence of molecular weight. *Journal of Applied Physics*, 21, 581-591.
- Fu, D., Weller, C. L., and Wehling, R. L. (1999). Zein: Properties, preparations and applications. *Food Science and Biotechnology*, 8, 1-10.
- Furuya, T., Iwai, Y., Tanaka, Y., Uchida, H., Yamada, S., and Arai, Y. (1995). Measurement and correlation of liquid-liquid equilibria for dextran-poly(ethylene glycol)-water aqueous two-phase systems at 20°C. *Fluid Phase Equilibria*, 103, 119-141.
- Gabarra, P., and Hartel, R. W. (1998). Corn syrup solids and their saccharide fractions affect crystallization of amorphous sucrose. *Journal of Food Science*, 63(3), 523-528.
- Garnier, C., Schorsch, C., and Doublier, J. L. (1995). Phase separation in dextran/locust bean gum mixtures. *Carbohydrate Polymers*, 28, 313-317.
- Gaudin, S., Lourdun, D., Le Botlan, D., Ilari, J. L., and Colonna, P. (1999). Plasticization and mobility in starch-sorbitol films. *Journal of Cereal Science*, 29, 273-284.
- Gekko, K. (1981). Solution properties of dextran and its ionic derivatives. In D. A. Brant (Ed.). *Solution Properties of Polysaccharides* (pp. 415-438). Washington, DC: American Chemistry Society Symposium Series 150.
- German, M. L., Blumenfeld, A. L., Guenin, Y. V., Yuryev, V. P., and Tolstoguzov, V. B. (1992). Structure formation in systems containing amylose, amylopectin, and their mixtures. *Carbohydrate Polymers*, 18, 27-34.

- Gioia, L., and Guilbert, S. (1999). Corn protein-based thermoplastic resins: Effect of some polar and amphiphilic plasticizers. *Journal of Agricultural and Food Chemistry*, 47, 1254-1261.
- Gluck-Hirsch, J. B. (1998). Quantification of Crosslink Induced Physicochemical Changes in Waxy Maize Starch using Rheological and Chemical Methods. Ph.D. Dissertation, Rutgers University, New Brunswick.
- Gordon, M., and Taylor, J. S. (1952). Ideal copolymers and the second-order transitions of synthetic rubbers. I. Non-crystalline copolymers. *Journal of Applied Chemistry*, 2, 493-500.
- Greenhalgh, D. J., Williams, A. C., Timmins, P., and York, P. (1999). Solubility parameters as predictors of miscibility in solid dispersions. *Journal of Pharmaceutical Sciences*, 88(11), 1182-1190.
- Grinberg, V. Y., and Tolstoguzov, V. B. (1997). Thermodynamic incompatibility of proteins and polysaccharides in solutions. *Food Hydrocolloids*, 11(2), 145-158.
- Gropper, M., Moraru, C. I., and Kokini, J. L. (2002). Effect of specific mechanical energy on properties of extruded protein-starch mixtures. *Cereal Chemistry*, 79(3), 429-433.
- Hartikainen, J., Lehtonen, O., Harmia, T., Lindner, M., Valkama, S., Ruokolainen, J., and Friedrich, K. (2004). Structure and morphology of polyamide 66 and oligomeric phenolic resin blends: Molecular modeling and experimental investigations. *Chemistry of Materials*, 16(16), 3032-3039.
- Hayes, R. A. (1961). The relationship between glass temperature, molar cohesion, and polymer structure. *Journal of Applied Polymer Science*, V(15), 318-321.
- He, Y., Zhu, B., and Inoue, Y. (2004). Hydrogen bonds in polymer blends. *Progress in Polymer Science*, 29, 1021-1051.
- Hellebust, S., Nilsson, S., and Blokhuis, A. M. (2003). Phase behavior of anionic polyelectrolyte mixtures in aqueous solution: Effects of molecular weights, polymer charge density, and ionic strength of solution. *Macromolecules*, 36(14), 5372-5382.
- Hellebust, S., Blokhuis, A. M., and Nilsson, S. (2004). Associative and segregative phase behavior of a mixed aqueous cationic surfactant and anionic hydrophilic polymer system. *Colloids and Surfaces A*, 243, 133-138.
- Hildebrand, J., and Scott, R. (1950). The Solubility of Non-electrolytes. 3<sup>rd</sup> Edition. Reinhold, NY.
- Hoeve, C.A.J., and Hoeve, M.B. (1978). The glass point of elastin as a function of diluent concentration. *Organic Coatings and Plastics Chemistry*, 39, 441-443.

- Hoseney, R.C., Zeleznak, K., and Lai, C.S. (1986). Wheat gluten: A glassy polymer. *Cereal Chemistry*, 63, 285-286.
- Icoz, D. Z., Moraru, C. I., and Kokini, J. L. (2005). Polymer-polymer interactions in dextran systems using thermal analysis. *Carbohydrate Polymers*, 62(2), 120-129.
- Icoz, D. Z., and Kokini, J. L. (2007a). Probing the boundaries of miscibility in model carbohydrates consisting of chemically derivatized dextrans using DSC and FTIR spectroscopy. *Carbohydrate Polymers*, 68(1), 68-76.
- Icoz, D. Z., and Kokini, J. L. (2007b). Examination of the validity of the Flory-Huggins solution theory in terms of miscibility in dextran systems. *Carbohydrate Polymers*, 68(1), 59-67.
- Icoz, D. Z., and Kokini, J. L. (2007c). Quantitative prediction of molecular miscibility in dextran systems as model carbohydrate polymers. *Carbohydrate Polymers*, 70(2), 181-191.
- Icoz, D. Z., and Kokini, J. L. (2008). Theoretical Analysis of Predictive Miscibility of Carbohydrate Polymers – Software Calculations for Inulin-Amylopectin Systems. *Carbohydrate Polymers*, 72(1), 52-59.
- Ioan, C. E., Aberle, T., and Burchard, W. (2000). Structure properties of dextran: 2. Dilute solution. *Macromolecules*, 33, 5730-5739.
- Jacobs, H. and Delcour, J. A. (1998). Hydrothermal modifications of granular starch, with retention of the granular structure: A review. *Journal of Agricultural and Food Chemistry*, 46(8), 2895-2905.
- Jouppila, K., and Roos, Y. H. (1997). The physical state of amorphous corn starch and its impact on crystallization. *Carbohydrate Polymers*, 32, 95-104.
- Jousset, S., Bellosent, H., and Galin, J. C. (1998). Polyelectrolytes of high charge density in organic solvents: Synthesis and viscosimetric behavior. *Macromolecules*, 31(14), 4520-4530.
- Kakivaya, S. R., and Hoeve, C. A. (1975). The glass transition of elastin. *Proceedings of Natural Academy of Science U.S.A.*, 72, 3505-3507.
- Kalichevsky, M. T., and Ring, S. G. (1987). Incompatibility of amylose and amylopectin in aqueous solution. *Carbohydrate Research*, 162, 323-328.
- Kalichevsky, M. T., and Blanshard, J. M. V. (1993). The effect of fructose and water on the glass transition of amylopectin. *Carbohydrate Polymers*, 20, 107-113.
- Kalichevsky, M. T., Orford, P. D., and Ring, S. G. (1986). The incompatibility of concentrated aqueous solutions of dextran and amylose and its effect on amylose gelation. *Carbohydrate Polymers*, 6, 145-154.

- Kalichevsky, M. T., Jaroszkiewicz, E. M., Ablett, S., Blanshard, J. M., and Lillford, P. J. (1992). The glass transition of amylopectin measured by DSC, DMTA and NMR. *Carbohydrate Polymers*, 18, 77-88.
- Kelly, F.N., and Bueche, F. (1961). Viscosity and glass temperature relations for polymer-diluent systems. *Journal of Polymer Science*, 50, 549-556.
- Kolhe, P., and Kannan, R. M. (2003). Improvement in ductility of chitosan through blending and copolymerization with PEG: FTIR investigation of molecular interactions. *Biomacromolecules*, 4(1), 173-180.
- Kuo, S. W., and Chang, F. C. (2001). Effects of copolymer composition and free volume change on the miscibility of poly(styrene-co-vinylphenol) with poly( $\epsilon$ -caprolactone). *Macromolecules*, 34, 7737-7743.
- Kuo, S. W., and Chang, F. C. (2002). Miscibility behavior and specific interaction of phenolic resin with poly(acetoxystyrene). *Macromolecular Chemistry and Physics*, 203, 868-878.
- Lauten, R. A., and Nystrom, B. (2000). Linear and nonlinear viscoelastic properties of aqueous solutions of cationic polyacrylamides. *Macromolecular Chemistry and Physics*, 201, 677-684.
- Levine, H., and Slade L. (1987). Water as a plasticizer: physicochemical aspects of low moisture polymeric systems. In F. Franks (Ed.). *Water Science Reviews (Vol. 3)* (pp. 79-185). Cambridge: Cambridge University Press.
- Lide, D. R. (2004). Handbook of Chemistry and Physics. 85<sup>th</sup> Edition. Cleveland, OH: CRC Press. pp. 6\_109-6\_125.
- Lourdin, D., Coignard, L., Bizot, H., and Colonna, P. (1997). Influence of equilibrium relative humidity and plasticizer concentration on the water content and glass transition of starch materials. *Polymer*, 38, 5401-5406.
- Madeka, H., and Kokini, J. L. (1994). Changes in rheological properties of gliadin as a function of temperature and moisture: Development of a state diagram. *Journal of Food Engineering*, 22, 241-252.
- Madeka, H., and Kokini, J.L. (1996). Effect of glass transition and aggregation on rheological properties of zein: development of a preliminary state diagram. *Cereal Chemistry*, 73, 433-438.
- Madkour, T. M. (2001). A combined statistical mechanics and molecular dynamics approach for the evaluation of the miscibility of polymers in good, poor and non-solvents. *Chemical Physics*, 274, 187-198.

- Mansfield, M. L. (1993). An Overview of Theories of Glass Transition. In J. M. V. Blanshard, and P. J. Lillford (Eds.). *The Glassy State in Foods* (pp. 103-122). Loughborough, Leicestershire: Nottingham University Press.
- Marshall, A. S., and Petrie, S. E. B. (1980). Thermal transitions in gelatin and aqueous gelatin solutions. *Journal of Photographical Science*, 28, 128-134.
- Medin, A. S., and Janson, J. C. (1993). Studies on aqueous polymer two-phase systems containing agarose. *Carbohydrate Polymers*, 22, 127-136.
- Michon, C., Buvelier, G., Launay, B., Parker, A., and Takerkart, G. (1995). Study of the compatibility/incompatibility of gelatin/iota-carrageenan/water mixtures. *Carbohydrate Polymers*, 28, 333-336.
- Mitsuiki, M., Yamamoto, Y., Mizuno, A., and Motoki, M. (1998). Glass transition properties as a function of water content for various low-moisture galactans. *Journal of Agricultural and Food Chemistry*, 46, 3528-3534.
- Morales-Diaz, A., and Kokini, J. L. (1997). Glass transition of soy globulins using differential scanning calorimetry and mechanical spectrometry. *Biotechnology Progress*, 13, 624-629.
- Morales-Diaz, A. M., and Kokini, J. L. (1998). Understanding phase transitions and chemical complexing reactions in 7S and 11S soy protein fractions. In M. A. Rao, and R.W. Hartel (Eds.). *Phase/State Transitions in Foods*. New York: Marcel Dekker, Inc.
- Moraru, C. I., Lee, T-C., Karwe, M. V., and Kokini, J. L. (2002). Phase behavior of a meat-starch extrudate illustrated on a state diagram. *Journal of Food Science*, 67(8), 3026-3032.
- Nordmeier, E. (1993). Static and dynamic light-scattering solution behavior of pullulan and dextran in comparison. *The Journal of Physical Chemistry*, 97(21), 5770-5785.
- Nyqvist, H. (1983). Saturated salt solutions for maintaining specified relative humidities. *International Journal of Pharmaceutical Technology and Product Manufacture*, 4(2), 47-48.
- Olabisi, O., Robeson, L. M., and Shaw, M. T. (1979). *Polymer-Polymer Miscibility*. New York: Academic Press, Inc.
- Painter, P. C., and Coleman, M. M. (1997). *Fundamentals of Polymer Science: An Introductory Text*. 3<sup>rd</sup> Edition. New York: CRC Press. pp. 307-337.
- Painter, P. C., Graf, J. F., and Coleman, M. M. (1991). Effect of hydrogen bonding on the enthalpy of mixing and the composition dependence of the glass transition temperature in polymer blends. *Macromolecules*, 24, 5630-5638.

- Painter, P. C., Berg, L. P., Veytsman, B., and Coleman, M. M. (1997a). Intra-molecular screening in non-dilute polymer solutions. *Macromolecules*, 30, 7529-7535.
- Painter, P. C., Veytsman, B., Kumar, S., Shenoy, S. Graf, J.F., Xu, Y, and Coleman, M. M. (1997b). Intramolecular screening effects in polymer mixtures. 1. Hydrogen-bonded polymer blends. *Macromolecules*, 30, 932-942.
- Parker, R. and Ring, S. G. (2001). Aspects of the physical chemistry of starch. *Journal of Cereal Science*, 34, 1-17.
- Patnaik, S. S., and Pachter, R. (1999). Anchoring characteristics and interfacial interactions in a polymer dispersed liquid crystal: a molecular dynamics study. *Polymer*, 40, 6507-6519.
- Patnaik, S. S., and Pachter, R. (2002). A molecular simulations study of the miscibility in binary mixtures of polymers and low molecular weight molecules. *Polymer*, 43, 415-424.
- Pauling, L. (1960). The Nature of the Chemical Bond. 3<sup>rd</sup> edition. Ithaca, NY: Cornell University Press.
- Pehlert, G. J., Painter, P. C., and Coleman, M. M. (1998). Functional group accessibility in hydrogen-bonded polymer blends: 3. Steric shielding effects. *Macromolecules*, 31, 8423-8424.
- Reutner, P., Luft, B., and Borchard, W. (1985). Compound formation and glassy solidification in the system gelatin-water. *Colloid and Polymer Science*, 263, 519-529.
- Ribeiro, C., Zimeri, J. E., Yildiz, E., and Kokini, J. L. (2003). Estimation of effective diffusivities and glass transition temperature of polydextrose as a function of moisture content. *Carbohydrate Polymers*, 51, 273-280.
- Roos, Y. H. (1995). Phase Transitions in Foods. San Diego, CA: Academic Press, Inc.
- Roos, Y., and Karel, M. (1991). Phase transitions of mixtures of amorphous polysaccharides and sugars. *Biotechnology Progress*, 7, 49-53.
- Ruan, R., Long, Z., Chen, P., Huang, V., Almaer, S., and Taub, I. (1999). Pulse NMR study of glass transition in maltodextrin. *Journal of Food Science*, 64(1), 6-9.
- Russel, W. B. (1991). Concentrated colloidal dispersions. *MRS Bulletin: Materials Research Society*, 16(8), 27-31.
- Schneider, H. A. (1997). Conformational entropy contributions to the glass temperature of blends of miscible polymers. *Journal of Research of the National Institute of Standards and Technology*, 102(2), 229-248.



- Sears, J. K., and Darby, J. R. (1982). *The Technology of Plasticizers*. New York: John Wiley and Sons, Inc.
- Serris, G. S. and Biliaderis, C. G. (2001). Degradation kinetics of beetroot pigment encapsulated in polymeric matrices. *Journal of the Science of Food and Agriculture*, 81, 691-700.
- Shamblin, S. L., Taylor, L. S., and Zografi, G. (1998). Mixing behavior of colyophilized binary systems. *Journal of Pharmaceutical Sciences*, 76(6), 694-701.
- Shinoda, K. (1978). *Principles of Solution and Solubility*. New York: Marcel Dekker, Inc.
- Singh, R. P. and Heldman D. R. (1993). *Introduction to Food Engineering*. 2<sup>nd</sup> Edition. New York: Academic Press, Inc.
- Slade, L., and Levine, H. (1991a). Beyond water activity: Recent advances based on an alternative approach to the assessment of food quality and safety. *CRC Critical Reviews in Food Science and Nutrition*, 30, 115-360.
- Slade, L., and Levine, H. (1991b). A food polymer science approach to structure-property relationship in aqueous food systems: non-equilibrium behavior of carbohydrate-water systems. In H. Levine, and L. Slade (Eds.). *Water Relationships in Food* (pp. 29-101). New York: Plenum Press.
- Slade, L., and Levine, H. (1993). Water relationships in starch transitions. *Carbohydrate Polymers*, 21, 105-131.
- Slade, L., Levine, H., and Finley, J. W. (1989). Protein-water interactions: Water as a plasticizer of gluten and other protein polymers. In R. D. Phillips, and J. W. Finley (Eds.). *Protein Quality and the Effects of Processing* (pp. 9-124). New York, NY: Marcel Dekker, Inc.
- Slade, L., Levine, H., Ievolella, J., and Wang, M. (1993). The glassy state phenomenon in applications for the food industry: Application of the food polymer science approach to structure-function relationships of sucrose in cookie and cracker systems. *Journal of the Science of Food and Agriculture*, 63, 133-176.
- Sperling, L. H. (2001). *Introduction to Physical Polymer Science*. 3<sup>rd</sup> Edition. New York: John Wiley and Sons, Inc.
- Tadros, T. F. (1996). Correlation of viscoelastic properties of stable and flocculated suspensions with their interparticle interactions. *Advances in Colloid and Interface Science*, 68, 97-200.
- Thuresson, K., Nilsson, S., and Lindman, B. (1996). Effect of hydrophobic modification on phase behavior and rheology in mixtures of oppositely charged polyelectrolytes. *Langmuir*, 12(2), 530-537.

- Tolstoguzov, V. B. (1991). Functional properties of food proteins and role of protein-polysaccharide interaction. *Food Hydrocolloids*, 4(6), 429-468.
- Tolstoguzov, V. B. (1998). Functional properties of protein-polysaccharide mixtures. In S. E. Hill, D. A. Ledward, and J. R. Mitchell (Eds.). *Functional Properties of Food Macromolecules* (pp. 252-277). Maryland: Aspen Publisher.
- Tolstoguzov, V. B. (2000a). Foods as dispersed systems: Thermodynamic aspects of composition-property relationships in formulated food. *Journal of Thermal Analysis and Calorimetry*, 61, 397-409.
- Tolstoguzov, V. B. (2000b). Compositions and phase diagrams for aqueous systems based on proteins and polysaccharides. *International Review of Cytology*, 192, 3-31.
- Tolstoguzov, V. B. (2003). Some thermodynamic considerations in food formulation. *Food Hydrocolloids*, 17(1), 1-23.
- Tvaroska, I., Perez, S., and Marchessault, R. H. (1978). Conformational analysis of (1-6)- $\alpha$ -D-glucan. *Carbohydrate Research*, 61, 97-106.
- Van Krevelen, D. W., and Hoftyzer, P. J. (1976). *Properties of Polymers*. Amsterdam: Elsevier.
- Veytsman, B. A. (1990). Are lattice models valid for fluids with hydrogen bonds? *Journal of Physical Chemistry*, 94, 8499-8500.
- Veytsman, B. A. (1993). Thermodynamics of hydrogen-bonded fluids: Effects of bond cooperativity. *Journal of Physical Chemistry*, 97, 7144-7146.
- Viswanathan, S., and Dadmun, M. D. (2002). Guidelines to creating a true molecular composite: Introducing miscibility in blends by optimizing intermolecular hydrogen bonding. *Macromolecules*, 35, 5049-5060.
- Walsh, D., Arcelli, L., Ikoma, T., Tanaka, J., and Mann, S. (2003). Dextran templating for the synthesis of metallic and metal oxide sponges. *Nature Materials*, 2, 386-390.
- Walstra, P. (2003). *Physical Chemistry of Foods*. New York: Marcel Dekker, Inc. pp. 137-202.
- Wang, Y. J., and Jane, J. (1994). Correlation between glass transition temperature and starch retrogradation in the presence of sugars and maltodextrins. *Carbohydrates*, 71(6), 527-531.
- Yildiz, M. E., and Kokini, J. L. (2001). Determination of Williams-Landel-Ferry constants for a food polymer system: Effect of water activity and moisture content. *Journal of Rheology*, 45(4), 903-912.

- Yildiz, M. E., and Kokini, J. L. (2003). The WLF Equation. In D. Heldman (Ed.). *The Encyclopedia of Agricultural, Food, and Biological Engineering*. NY: Marcel Dekker, Inc.
- Zimeri, J. E., and Kokini, J. L. (2002). The effect of moisture content on the crystallinity and glass transition temperature of inulin. *Carbohydrate Polymers*, 48, 299-304.
- Zimeri, J. E., and Kokini, J. L. (2003a). Phase transitions of inulin-amioca systems in limited moisture environments. *Carbohydrate Polymers*, 51, 183-190.
- Zimeri, J. E., and Kokini, J. L. (2003b). Rheological properties of inulin-waxy maize starch systems. *Carbohydrate Polymers*, 52, 67-85.
- Zimeri, J. E., and Kokini, J. L. (2003c). Morphological characterization of the phase behavior of inulin-waxy maize starch systems in high moisture environments. *Carbohydrate Polymers*, 52, 225-236.

## CURRICULUM VITA

**Didem İçöz**

### Education

- 2008      Ph.D. Food Science  
Rutgers, The State University of New Jersey, New Brunswick NJ
- 2001      M.S. Food Engineering  
Middle East Technical University, Ankara, Turkey
- 1999      B.S. Food Engineering  
Middle East Technical University, Ankara, Turkey

### Work Experience

- 2007-present    Associate Research Scientist  
National Starch and Chemical Company, Bridgewater, NJ
- 2001-2007      Research Assistant, Department of Food Science  
Rutgers, The State University of New Jersey, New Brunswick NJ
- 1999-2001      Teaching Assistant, Department of Food Engineering  
Middle East Technical University, Ankara, Turkey

### Publications

- 2008**      **Icoz, D. Z.** and Kokini, J. L. (2008) Theoretical Analysis of Predictive Miscibility of Carbohydrate Polymers – Software Calculations for Inulin-Amylopectin Systems. *Carbohydrate Polymers*, 72(1): 52-59.
- 2007**      **Icoz, D.Z.** and Kokini, J.L. (2007) Quantitative prediction of molecular miscibility in dextran systems as model carbohydrate polymers. *Carbohydrate Polymers*, 70(2): 181-191.

- 2007**      **Icoz, D.Z.** and Kokini, J.L. (2007) Examination of the validity of the Flory-Huggins solution theory in terms of miscibility in dextran systems. *Carbohydrate Polymers*, 68(1): 59-67.
- 2007**      **Icoz, D.Z.** and Kokini, J.L. (2007) Probing the boundaries of miscibility in model carbohydrates consisting of chemically derivatized dextrans using DSC and FTIR spectroscopy. *Carbohydrate Polymers*, 68(1): 68-76.
- 2007**      **Icoz, D.Z.** and Kokini, J.L. (2007) State Diagrams of Food Materials, in *Food Materials Science, Principles and Practice*, Eds. Aguilera, J.M. and Lillford, P.J., Springer.
- 2005**      **Icoz, D.Z.**, Moraru, C.I. and Kokini, J.L. (2005) Polymer-polymer interactions in dextran systems using thermal analysis. *Carbohydrate Polymers*, 62(2): 120-129.